QA: QA

MDL-WIS-PA-000005 REV00

January 2008

Total System Performance Assessment Model/Analysis for the License Application

Volume III

Prepared for:
U.S. Department of Energy
Office of Civilian Radioactive Waste Management
Office of Repository Development
1551 Hillshire Drive
Las Vegas, Nevada 89134-6321

Prepared by:
Sandia National Laboratories
OCRWM Lead Laboratory for Repository Systems
1180 Town Center Drive
Las Vegas, Nevada 89144

Under Contract Number
DE-AC04-94AL85000

DISCLAIMER

This report was prepared as an account of work sponsored by an agency of the United States Government. Neither the United States Government nor any agency thereof, nor any of their employees, nor any of their contractors, subcontractors or their employees, makes any warranty, express or implied, or assumes any legal liability or responsibility for the accuracy, completeness, or any third party's use or the results of such use of any information, apparatus, product, or process disclosed, or represents that its use would not infringe privately owned rights. Reference herein to any specific commercial product, process, or service by trade name, trademark, manufacturer, or otherwise, does not necessarily constitute or imply its endorsement, recommendation, or favoring by the United States Government or any agency thereof or its contractors or subcontractors. The views and opinions of authors expressed herein do not necessarily state or reflect those of the United States Government or any agency thereof.

Total System Performance Assessment Model/Analysis for the License Application

Volume III

MDL-WIS-PA-000005 REV00

January 2008

CONTENTS

Page

8. POSTCLOSURE PERFORMANCE DEMONSTRATION 8-1
8.1 CONFORMANCE WITH RADIATION PROTECTION STANDARDS 8.1-1
8.1.1 Individual Protection Standard 8.1-2
8.1.2 Groundwater Protection 8.1-12
8.1.3 Human Intrusion Protection 8.1-18
8.2 PROJECTIONS FOR INDIVIDUAL MODELING CASES 8.2-1
8.2.1 Nominal Modeling Case 8.2-2
8.2.2 Early Failure Scenario Class Modeling Cases 8.2-3
8.2.3 Igneous Scenario Class Modeling Cases 8.2-6
8.2.4 Seismic Scenario Class Modeling Cases 8.2-8
8.3 DESCRIPTION OF MULTIPLE BARRIER CAPABILITY 8.3-1
8.3.1 Radionuclides Selected to Demonstrate Multiple Barrier Capability 8.3-2
8.3.2 Identification of Barriers for Yucca Mountain Repository System 8.3-4
8.4 VALIDITY AND DEFENSIBILITY OF PERFORMANCE DEMONSTRATION 8.4-1
8.4.1 Validation of TSPA Model and Component Models 8.4-2
8.4.2 Verification and Validation of TSPA Software and Input Data 8.4-3
8.4.3 Uncertainty Characterization Reviews 8.4-5
8.4.4 Corroboration of TSPA-LA Model Results 8.4-6
8.4.5 Reviews of YMP TSPA Methodology 8.4-10

9. INPUTS AND REFERENCES 9-1
9.1 DOCUMENTS CITED 9-1
9.2 CODES, STANDARDS, REGULATIONS, AND PROCEDURES 9-58
9.3 SOFTWARE CODES 9-60
9.4 SOURCE DATA LISTED BY DATA TRACKING NUMBER 9-62

APPENDIX A—ACRONYMS AND ABBREVIATIONS A-1

APPENDIX B—DATA TRACKING NUMBERS FOR THE TSPA-LA MODEL B-1

APPENDIX C—PERFORMANCE MARGIN ANALYSIS C-1

APPENDIX D—PARAMETER LISTING D-1

APPENDIX E—RESPONSE TO REVIEW COMMENTS FROM THE INTERNATIONAL REVIEW TEAM E-1

APPENDIX F—DYNAMICALLY LINKED LIBRARIES DESCRIPTION AND FEEDS F-1

APPENDIX G—WIRING DIAGRAMS FOR MODEL INFORMATION FEEDS G-1

CONTENTS (Continued)

Page

APPENDIX H—YUCCA MOUNTAIN REVIEW PLAN ACCEPTANCE CRITERIA H-1

APPENDIX I—FEATURES, EVENTS, AND PROCESSES MAPPED TO THE TSPA-LA MODEL I-1

APPENDIX J—CONCEPTUAL STRUCTURE OF THE TSPA-LA J-1

APPENDIX K—UNCERTAINTY AND SENSITIVITY ANALYSIS RESULTS K-1

APPENDIX L—SIMPLIFIED TSPA L-1

APPENDIX M—COMPARISON WITH THE ELECTRIC POWER RESEARCH INSTITUTE MODEL M-1

APPENDIX N—DERIVATION OF IMPLEMENTING EQUATIONS FOR WASTE PACKAGE PARSING AND AVERAGE DAMAGE AREA N-1

APPENDIX O—LOCALIZED CORROSION INITIATION UNCERTAINTY ANALYSIS O-1

APPENDIX P— IMPACT ASSESSMENTS P-1

FIGURES

Page

8-1. Illustration of the Multiple Barriers of Yucca Mountain Repository System.....F8-1

8.1-1. Probabilistic Projections of Total Expected Annual Dose for 10,000 Years after Closure.....F8.1-1
8.1-2. Probabilistic Projections of Total Expected Annual Dose for 1,000,000 Years after Closure.....F8.1-2
8.1-3. Relative Contributions of Scenario Modeling Cases to Total Mean Annual Dose for (a) 10,000 Years and (b) 1,000,000 Years after Repository Closure.....F8.1-3
8.1-4. Histogram of Drip Shield Failure for the Nominal and Seismic Ground Motion Modeling Cases.....F8.1-4
8.1-5. Fraction of (a) CDSP WPs and (b) CSNF WPs Failed for by Seismic Crack Damage as a Function of Time for Percolation Subregion 3.....F8.1-5
8.1-6. Contribution of Individual Radionuclides to Total Mean Annual Dose for 10,000 Years after Repository Closure.....F8.1-6
8.1-7. Contribution of Individual Radionuclides to Total Mean Annual Dose for 1,000,000 Years after Repository Closure.....F8.1-7
8.1-8. Radium Mass Breakthrough Curves (upper) and Median Transport Times (lower) at the RMEI Location.....F8.1-8
8.1-9. Probabilistic Projections of Activity Concentrations Total Radium (^{226}Ra and ^{228}Ra) in Groundwater, Excluding Natural Background, for 10,000 Years after Closure.....F8.1-9
8.1-10. Probabilistic Projections of Activity Concentration of Gross Alpha and ^{226}Ra (Excluding Radon and Uranium) in Groundwater for 10,000 Years after Closure.....F8.1-10
8.1-11. Probabilistic Projections of Annual Drinking Water Doses for Combined Beta and Photon Emitting Radionuclides for 10,000 Years after Closure.....F8.1-11
8.1-12. Probabilistic Projections for Expected Annual Doses for the Human Intrusion Scenario for 1,000,000 Years after Closure with Drilling Event at 200,000 Years.....F8.1-12
8.1-13. Contribution of Individual Radionuclides to Mean Annual Dose for the Human Intrusion Scenario for 1,000,000 Years after Repository Closure.....F8.1-13

8.2-1. Probabilistic Projections of Expected Annual Dose for the Nominal Modeling Case for 1,000,000 Years after Repository Closure.....F8.2-1
8.2-2. Contribution of Individual Radionuclides to Mean Annual Dose for the Nominal Modeling Case for 1,000,000 Years after Repository Closure.....F8.2-2
8.2-3. Probabilistic Projections of Expected Annual Dose for the Drip Shield Early Failure Modeling Case for (a) 10,000 Years and (b) 1,000,000 Years after Repository Closure.....F8.2-3
8.2-4. Contribution of Individual Radionuclides to Mean Annual Dose for Drip Shield Early Failure Modeling Case for (a) 10,000 Years and (b) 1,000,000 Years After Repository Closure.....F8.2-4

FIGURES (Continued)

Page

8.2-5. Probabilistic Projections of Expected Annual Dose for Waste Package Early Failure Modeling Case for (a) 10,000 Years and (b) 1,000,000 Years after Repository Closure....F8.2-5
8.2-6. Contribution of Individual Radionuclides to Mean Annual Dose for Waste Package Early Failure Modeling Case for (a) 10,000 Years and (b) 1,000,000 Years after Repository Closure....F8.2-6
8.2-7. Probabilistic Projections of Expected Annual Dose for the Igneous Intrusion Modeling Case for (a) 10,000 Years and (b) 1,000,000 Years after Repository Closure....F8.2-7
8.2-8. Contribution of Individual Radionuclides to Mean Annual Dose for the Igneous Intrusion Modeling Case for (a) 10,000 Years and (b) 1,000,000 Years After Repository Closure....F8.2-8
8.2-9. Probabilistic Projections of Expected Annual Dose for the Volcanic Eruption Modeling Case for (a) 10,000 Years and (b) 1,000,000 Years after Repository Closure....F8.2-9
8.2-10. Contribution of Individual Radionuclides to Mean Annual Dose for the Volcanic Eruption Modeling Case for (a) 10,000 Years and (b) 1,000,000 Years after Repository Closure....F8.2-10
8.2-11. Probabilistic Projections of Expected Annual Dose for the Seismic Ground Motion Modeling Case for (a) 10,000 Years and (b) 1,000,000 Years after Repository Closure....F8.2-11
8.2-12. Contribution of Individual Radionuclides to Mean Annual Dose for the Seismic Ground Motion Modeling Case for (a) 10,000 Years and (b) 1,000,000 Years after Repository Closure....F8.2-12
8.2-13. Probabilistic Projections of Expected Annual Dose for the Seismic Fault Displacement Modeling Case for (a) 10,000 Years and (b) 1,000,000 Years after Repository Closure....F8.2-13
8.2-14. Contribution of Individual Radionuclides to Mean Annual Dose for the Seismic Fault Displacement Modeling Case for (a) 10,000 Years and (b) 1,000,000 Years After Repository Closure....F8.2-14

8.3-1. Mean Radionuclide Activities in the Nuclear Waste as a Function of Time for (a) 10,000 Years and (b) 1,000,000 Years after Repository Closure....F8.3-1
8.3-2. Mean Radionuclide Contributions to Total Inventory as a Function of Time for (a) 10,000 Years and (b) 1,000,000 Years after Repository Closure....F8.3-2

B-1. Road Map of TSPA-LA Model Data Tracking Numbers.... B-9
B-2. Road Map of Performance Margin Analysis Data Tracking Numbers.... B-10

C6-1. Schematic Illustration of Expected Flow Behavior of Seepage in a Rubble-Filled Collapsed Drift....FC-1
C6-2. Mean Seepage Rate for (a) Intact Drift, (b) Collapsed Drift with Seepage Collected over 11-Meter Wide Drift, and (c) Collapsed Drift with Seepage Collected over 5.5-Meter Wide Center Section of Drift....FC-2

FIGURES (Continued)

Page

C6-3. General Corrosion Rate Distribution Resulting from Fitting of Five-year Exposed Weight-Loss Sample Data FC-3
C6-4. Empirical Cumulative Distribution for General Corrosion Rate of Alloy 22 Weight-Loss and Crevice Samples after Five-Year Exposure in Long-Term Corrosion Test Facility FC-4
C6-5. Schematic Diagram of Modeling System for In-Package Water Balance FC-5
C6-6. Fraction of Water Entering Waste Package Estimated from the Sheet-Flow Model FC-6
C6-7. Temperature Difference between the Inside and Outside of a Waste Package FC-7
C6-8. Illustration of the Approach to Steady State pH and Ionic Strength as a Function of Pore Volumes Flushed FC-8
C6-9. Comparison of Performance Margin Analysis Model for High-Level Waste Glass Dissolution FC-9
C6-10. Plot of Log Transformed PuO_2(am) Solubility vs. pH FC-10
C6-11. Plot of Log Transformed Differences (Log Predicted−Log Observed) for PuO_2(am) Solubility FC-11
C6-12. Comparison of Predicted (EQ3/6) and Observed Values for NpO_2 Solubility along with Uncertainty Bounds FC-12
C6-13. Comparison of Predicted (EQ3/6) and Observed Values for Np_2O_5 Solubility along with Uncertainty Bounds FC-13
C6-14. Comparison of Predicted (EQ3/6) and Observed Values for Na-Boltwoodite Solubility along with Uncertainty Bounds FC-14
C6-15. Comparison of Predicted (EQ3/6) and Observed Values for $Na_4UO_2(CO_3)_3$ Solubility along with Uncertainty Bounds FC-15
C6-16. Decrease in Relative Dissolution Rate as a Function of Critical Reaction-Rind Thickness for Each of Three Values for the Final Reaction Affinity FC-16
C6-17. Colloid Filtration Rate Constants and Fractional Recoveries vs. Unretarded Groundwater Travel Times (Determined from Conservative Solute Tracers) from Tracer Experiments in Saturated Fractured Volcanics FC-17
C6-18. Colloid Detachment Rate Constants and Retardation Factors vs. Unretarded Groundwater Travel Times (Determined from Conservative Solute Tracers) from Tracer Experiments in Saturated Fractured Volcanics FC-18
C6-19. Colloid Filtration Rate Constants and Fractional Recoveries vs. Unretarded Groundwater Travel Times (Determined from Conservative Solute Tracers) from Tracer Experiments in Saturated Alluvium FC-19
C6-20. Colloid Detachment Rate Constants and Retardation Factors vs. Unretarded Groundwater Travel Times (Determined from Conservative Solute Tracers) from Tracer Experiments in Saturated Alluvium FC-20
C6-21. Colloid Filtration Rate Constants and Fractional Recoveries Unretarded Groundwater Travel Times for Saturated Fractured Volcanics (Data Replotted from Figure C6-17) FC-21
C6-22. Colloid Filtration Rate Constants and Fractional Recoveries Unretarded Groundwater Travel Times for Saturated Alluvium (Data Replotted from Figure C6-19) FC-22

FIGURES (Continued)

Page

C6-23. Volcanic and Alluvium Log Fractional Recoveries vs. Log Groundwater Travel Time Plotted Together and Fitted by Linear Regression Separately and Together FC-23
C6-24. Log Fractional Recoveries versus Log Ground Travel Time FC-24
C6-25. Colloid Filtration Rate Constant Cumulative Distribution Functions Associated with (1), (2), and (3) from Figure C6-24 Plotted along with the Actual Cumulative Distribution Function of the Filtration Rate Constants (Data Points) FC-25
C6-26. Minimum, Central, and Maximum Cumulative Distribution Functions of Colloid Retardation Factors Associated with a 100-Year Groundwater Travel Times FC-26
C6-27. Results of Sampling a Discretized Version of the Retardation Factor CDF Two Times to Obtain an Effective Retardation Distribution in the Combined Unsaturated Zone and Saturated Zone FC-27
C6-28. Cumulative Distribution Functions of Uncertainty in Water Table Rise for Individual Workshop Participants FC-28
C6-29. Cumulative Distribution Functions of Uncertainty in Water Table Rise by Consensus FC-29
C6-30. Map Showing Locations of Wells with Oxidizing and Reducing Groundwaters FC-30
C6-31. Saturated Zone Matrix Block Used as a Conduit for Unsaturated Matrix Mass Flux to the Saturated Zone FC-31
C6-32. Schematic Diagram Showing Conceptual Dual-Porosity Model for the Unsaturated Zone to Saturated Zone Mass Flux FC-32
C6-33. Configuration of Unsaturated Zone to Saturated Zone Matrix Diffusion FC-33
C6-34. Structure of the GoldSim Saturated Zone1-D Transport Model Setup for the Compliance Model FC-34
C6-35. Structure of the GoldSim Saturated Zone1-D Transport Model with Modifications for the Reducing Zones Model FC-35
C7-1. Probabilistic Projections of the Performance Margin Analysis Total Dose for 10,000 Years after Repository Closure FC-36
C7-2. Probabilistic Projections of Performance Margin Analysis Total Dose for 1,000,000 Years after Repository Closure FC-37
C7-3. Comparison of the Projected Total Mean Annual Dose for the TSPA-LA Model Relative to the Performance Margin Analysis for 10,000 Years after Repository Closure FC-38
C7-4. Comparison of the Projected Total Mean Annual Dose for the TSPA-LA Relative to the Performance Margin Analysis for 1,000,000 Years after Repository Closure FC-39
C7-5. Contributions of Individual Radionuclides to Total Mean Annual Dose for (a) the TSPA-LA and (b) the Performance Margin Analysis 10,000 Years after Repository Closure FC-40

FIGURES (Continued)

Page

C7-6. Contributions of Individual Radionuclides to Total Mean Annual Dose History for (a) the TSPA-LA and (b) the Performance Margin Analysis for 1,000,000 Years after Repository Closure FC-41
C7-7. Comparison of Scenario Modeling Cases to Projected Total Mean Annual Dose 10,000 Years after Repository Closure for (a) Drip Shield Early Failure, (b) Waste Package Early Failure, (c) Seismic Ground Motion, (d) Seismic Fault Displacement, (e) Igneous Intrusion, and (f) Relative Contributions of Scenario Modeling Cases to the Projected Mean Annual Dose for the Performance Margin Analysis. FC-42
C7-8. Comparison of Scenario Modeling Cases to Projected Total Mean Annual Dose 1,000,000 Years after Repository Closure for (a) Drip Shield Early Failure, (b) Waste Package Early Failure, (c) Seismic Ground Motion, (d) Seismic Fault Displacement, (e) Igneous Intrusion, and (f) Relative Contributions of Scenario Modeling Cases to the Projected Mean Annual Dose for the Performance Margin Analysis..... FC-43
C7-9. PMA Scenario Modeling Cases to Radionuclide Contributions to Projected Total Mean Annual Dose 10,000 Years after Repository Closure for (a) Drip Shield Early Failure, (b) Waste Package Early Failure, (c) Seismic Ground Motion, (d) Seismic Fault Displacement, (e) Igneous Intrusion, and (f) Total Mean Annual Dose for the Performance Margin Analysis..... FC-44
C7-10. PMA Scenario Modeling Cases to Radionuclide Contributions to Projected Total Mean Annual Dose 1,000,000 Years after Repository Closure for (a) Drip Shield Early Failure, (b) Waste Package Early Failure, (c) Seismic Ground Motion, (d) Seismic Fault Displacement, (e) Igneous Intrusion, and (f) Total Mean Annual Dose for the Performance Margin Analysis FC-45
C7-11. TSPA-LA Scenario Modeling Cases Radionuclide Contributions to Projected Total Mean Annual Dose 10,000 Years after Repository Closure for (a) Drip Shield Early Failure, (b) Waste Package Early Failure, (c) Seismic Ground Motion, (d) Seismic Fault Displacement, and (e) Igneous Intrusion..... FC-46
C7-12. TSPA-LA Scenario Modeling Cases Radionuclide Contributions to Projected Total Mean Annual Dose 1,000,000 Years after Repository Closure for (a) Drip Shield Early Failure, (b) Waste Package Early Failure, (c) Seismic Ground Motion, (d) Seismic Fault Displacement, and (e) Igneous Intrusion..... FC-47
C7-13. Comparison of Seismic Ground Motion Modeling Cases to Projected Total Mean Annual Dose 1,000,000 Years after Repository Closure for TSPA-LA, Performance Margin Analysis, and the Performance Margin Analysis, including General Corrosion Weight-Loss Data..... FC-48
C7-14. Comparison of Nominal Modeling Cases to Projected Total Mean Annual Dose History 1,000,000 Years after Repository Closure for TSPA-LA, Performance Margin Analysis, and the Performance Margin Analysis, including General Corrosion Weight-Loss Data..... FC-49

G-1. Illustration of the Transfer of Information between Model Components and Submodels of the TSPA-LA Model for the Nominal Scenario Class G-4

FIGURES (Continued)

Page

G-2. Illustration of the Transfer of Information between Model Components and Submodels of the TSPA-LA Model for the Early Failure Scenario Class G-5
G-3. Illustration of the Transfer of Information between Model Components and Submodels of the TSPA-LA Model for the Igneous Intrusion Modeling Case..... G-6
G-4. Illustration of the Transfer of Information between Model Components and Submodels of the TSPA-LA Model for the Seismic Ground Motion and Fault Displacement Modeling Cases..... G-7
G-5. Illustration of the Transfer of Information between Model Components and Submodels of the TSPA-LA Model for the Human Intrusion Scenario Class G-8
G-6. Illustration of the Transfer of Information on Water Fluxes between Model Components and Submodels of the TSPA-LA Model..... G-9
G-7. Illustration of the Transfer of Information on Radionuclide Fluxes between Model Components and Submodels of the TSPA-LA Model G-10
G-8. Illustration of the Transfer of Information between Model Components and Submodels of the TSPA-LA Model for Factors that Affect Flow through the EBS G-11
G-9. Illustration of the Transfer of Information between Model Components and Submodels of the TSPA-LA Model that affect Radionuclide Transport through the EBS..... G-12
G-10. Illustration of the Transfer of Information between Model Components and Submodels of the TSPA-LA Model, Nominal Scenario Class, for Factors that Affect Waste Form Degradation for CSNF WPs..... G-13
G-11. Illustration of the Transfer of Information between Model Components and Submodels of the TSPA-LA Model, Nominal Scenario Class, for Factors that Affect Waste Form Degradation for CDSP WPs..... G-14

I-1. Implementation of Features, Events, and Processes in the TSPA-LA Model I-3

J3.4-1. Example CCDF: plot of probability $prob_A(c > C)$ that a consequence with a value larger then C will occur. FJ-1
J3.4-2. Approximation of a CCDF with a random sample of size 1,000..... FJ-1
J3.5-1. Different values of CCDF defined by Equation J3.4-5 that derive from different values of e. FJ-2
J3.5-2. Example of an LHS of size $nLHS = 10$ from variables U and V with U normal on [−1, 1] (mean = 0, 0.01 quantile = −1, 0.99 quantile = 1) and V triangular on [0, 4] (mode = 1) (Figure 4, Helton 1999 [DIRS 159042]) FJ-2
J5-1. Estimate obtained with LHS of size $nLHS = 300$ showing epistemic uncertainty in dose $D_N(\tau|\mathbf{a}_N, \mathbf{e}_M)$ to RMEI for $0 \le \tau \le 10^6$ yr that results when only nominal conditions are considered: (a) $D_N(\tau|\mathbf{a}_N, \mathbf{e}_{Mi})$, $i = 1, 2, \ldots, nLHS = 300$, (b) dose $D_N(\tau|\mathbf{a}_N, \mathbf{e}_{Mi})$, $i = 1, 2, \ldots, 50$, (c) exceedance probabilities $pE[D < D_N(\tau|\mathbf{a}_N, \mathbf{e}_M)]$ and quantiles $Q_q[D_N(\tau|\mathbf{a}_N, \mathbf{e}_M)]$, $q =$ 0.05, 0.5, 0.95, for $\tau = 6.0 \times 10^5$ yr, and (d) expected (mean) dose $\bar{\bar{D}}_N(\tau)$ and quantiles $Q_q[D_N(\tau|\mathbf{a}_N, \mathbf{e}_M)]$, $q = 0.05, 0.5, 0.95$..... FJ-3

FIGURES (Continued)

Page

J5-2. Summary of results obtained with LHS of size *nLHS* = 300 showing epistemic uncertainty in dose $D_N(\tau|\mathbf{a}_N, \mathbf{e}_M)$ to RMEI for $0 \le \tau \le 10^6$ yr that results when only nominal conditions are considered. FJ-4

J5-3. Estimate obtained with LHS of size *nLHS* = 300 of epistemic uncertainty in dose $D_{Nr}(\tau|\mathbf{a}_N, \mathbf{e}_M)$ to RMEI for $0 \le \tau \le 10^6$ yr with *r* corresponding to ^{129}I that results when only nominal conditions are considered: (a) dose $D_{Nr}(\tau|\mathbf{a}_N, \mathbf{e}_{Mi})$, $i = 1, 2, \ldots, nLHS = 300$, (b) dose $D_{Nr}(\tau|\mathbf{a}_N, \mathbf{e}_{Mi})$, $i = 1, 2, \ldots, 50$, (c) exceedance probabilities $p_E[D < D_{Nr}(\tau|\mathbf{a}_N, \mathbf{e}_M)]$ and quantiles $Q_q[D_{Nr}(\tau|\mathbf{a}_N, \mathbf{e}_M)]$, $q = 0.05, 0.5$ and 0.95, for $\tau = 6.0 \times 10^5$ yr, and (d) expected (mean) dose $\bar{\bar{D}}_{Nr}(\tau)$ and quantiles $Q_q[D_{Nr}(\tau|\mathbf{a}_N, \mathbf{e}_M)]$, $q = 0.05, 0.5, 0.95$..... FJ-5

J5-4. Estimates obtained with LHS of size *nLHS* = 300 of expected (mean) dose $\bar{\bar{D}}_{Nr}(\tau|\mathbf{a}_N)$ to RMEI for $0 \le \tau \le 10^6$ yr for individual radioactive species that result when only nominal conditions are considered. FJ-6

J5-5. Assessment with replicated sampling of numerical error associated with use of an LHS of size *nLHS* = 300 to determine epistemic uncertainty in dose $D_N(\tau|\mathbf{a}_N, \mathbf{e}_M)$ to RMEI for $0 \le \tau \le 10^6$ yr that results when only nominal conditions are considered: (a) Replicated estimates of expected (mean) dose $\bar{\bar{D}}_N(\tau|\mathbf{a}_N)$ and quantiles $Q_q[D_N(\tau|\mathbf{a}_N, \mathbf{e}_M)]$, $q = 0.05, 0.5, 0.95$, and (b) confidence intervals for estimates of expected (mean) dose $\bar{\bar{D}}_N(\tau|\mathbf{a}_N)$. FJ-7

J6.2-1. Complementary cumulative distribution functions (CCDFs) for number *nEW* of WPs with early failure associated with individual elements of LHS of size *nLHS* = 300 in Equation J.4.9-1: (a) CCDFs for all 300 LHS elements, and (b) CCDFs for first 50 LHS elements. FJ-9

J6.2-2. Summary of results obtained with LHS of size *nLHS* = 300 showing epistemic uncertainty in doses $D_{EW}(\tau|[1, r, 3, t], \mathbf{e}_M)$ for $0 \le \tau \le 20{,}000$ yr: (a) CSNF WP in bin 3 under nondripping conditions (i.e., $D_{EW}(\tau|[1, 1, 3, 0], \mathbf{e}_{Mi})$, $i = 1, 2, \ldots, nLHS = 300$), (b) CSNF WP in bin 3 under dripping conditions (i.e., $D_{EW}(\tau|[1, 1, 3, 1], \mathbf{e}_{Mi})$, $i = 1, 2, \ldots, nLHS = 30$)0, (c) CDSP WP in bin 3 under nondripping conditions (i.e., $D_{EW}(\tau|[1, 2, 3, 0], \mathbf{e}_{Mi})$, $i = 1, 2, \ldots, nLHS = 300$), and (d) CDSP WP in bin 3 under dripping conditions (i.e., $D_{EW}(\tau|[1, 2, 3, 1], \mathbf{e}_{Mi})$, $i = 1, 2, \ldots, nLHS = 300$). FJ-10

FIGURES (Continued)

Page

J6.2-3. Box plots (Description: Box extends from 0.25 to 0.75 quantile; left and right bar and whisker extend to 0.1 and 0.9 quantile, respectively; ×'s represent values outside 0.1 to 0.9 quantile range; median and mean are indicated by light and dark vertical lines, respectively) summarizing results obtained with LHS of size $nLHS = 300$ showing epistemic uncertainty in doses $D_{EW}(\tau|[1, r, s, t], \mathbf{e}_{Mi})$ for selected values of τ, $r = 1, 2$, $s = 1, 2, 3, 4, 5$, $t = 0, 1$, and $i = 1, 2, \ldots, nLHS = 300$: (a, c, e) CSNF WPs at $\tau = 10{,}000$, 15,000 and 20,000 yr, and (b, d, f) CDSP WPs at $\tau = 2000$, 5000 and 10,000 yr. FJ-11

J6.2-4. Estimate of $\bar{D}_{EW}(\tau|\mathbf{e}_1)$ for LHS element $\mathbf{e}_1 = [\mathbf{e}_{A1}, \mathbf{e}_{M1}]$ and $0 \le \tau \le 20{,}000$ yr with integration-based procedure indicated in Equation J6.2-2..... FJ-12

J6.2-5. Estimate obtained with LHS of size $nLHS = 300$ showing epistemic uncertainty in expected dose $\bar{D}_{EW}(\tau|\mathbf{e})$ to RMEI for $0 \le \tau \le 20{,}000$ yr that at results when only early WP failure is considered: (a) expected dose $\bar{D}_{EW}(\tau|\mathbf{e}_i)$, $i = 1, 2, \ldots, nLHS = 300$, (b) expected dose $\bar{D}_{EW}(\tau|\mathbf{e}_i)$, $i = 1, 2, \ldots, 50$, (c) exceedance probabilities $p_E[D < \bar{D}_{EW}(\tau|\mathbf{e})]$ and quantiles $Q_q[\bar{D}_{EW}(\tau|\mathbf{e})]$, $q = 0.05$, 0.5 and 0.95, for $\tau = 10^4$ yr, and (d) expected (mean) dose $\bar{\bar{D}}_{EW}(\tau)$ and quantiles $Q_q[\bar{\bar{D}}_{EW}(\tau|\mathbf{e})]$, $q = 0.05$, 0.5, 0.95. ..... FJ-13

J6.2-6. Summary of results obtained with LHS of size $nLHS = 300$ showing epistemic uncertainty in expected dose $\bar{D}_{EW}(\tau|\mathbf{e})$ to RMEI for $0 \le \tau \le 20{,}000$ yr that results when only early WP failure is considered..... FJ-14

J6.2-7. Estimate obtained with LHS of size $nLHS = 300$ showing epistemic uncertainty in expected dose $\bar{D}_{EW,r}(\tau|\mathbf{e})$ to RMEI for $0 \le \tau \le 20{,}000$ yr with r corresponding to ^{99}Tc that results when only early WP failure is considered: (a) expected dose $\bar{D}_{EW,r}(\tau|\mathbf{e}_i)$, $i = 1, 2, \ldots, nLHS = 300$, (b) expected dose $\bar{D}_{EW,r}(\tau|\mathbf{e}_i)$, $i = 1, 2, \ldots, 50$, (c) exceedance probabilities $p_E[D < \bar{D}_{EW}(\tau|\mathbf{e})]$ and quantiles $Q_q[\bar{D}_{EW,r}(\tau|\mathbf{e})]$, $q = 0.05$, 0.5 and 0.95, for $\tau = 10^4$ yr, and (d) expected (mean) dose $\bar{\bar{D}}_{EW,r}(\tau)$ and quantiles $Q_q[\bar{D}_{EW,r}(\tau|\mathbf{e})]$, $q = 0.05$, 0.5, 0.95..... FJ-15

J6.2-8. Estimates obtained with LHS of size $nLHS = 300$ of expected (mean) dose $\bar{\bar{D}}_{EW,r}(\tau)$ to RMEI for $0 \le \tau \le 20{,}000$ yr for individual radioactive species that result when only early WP failure is considered. FJ-16

J6.2-9. Results associated with $D_{EW}(\tau|\mathbf{a}_{EW}, \mathbf{e}_{M1})$ for LHS element $\mathbf{e}_1 = [\mathbf{e}_{A1}, \mathbf{e}_{M1}]$ obtained with sampling-based (Monte Carlo) procedures: (a) CCDF for $D_{EW}(10^4 \text{ yr}|\mathbf{a}_{EW}, \mathbf{e}_{M1})$ with exceedance probabilities $p_A[D < D_{EW}(10^4 \text{ yr}|\mathbf{a}, \mathbf{e}_{M1})|\mathbf{e}_{A1}]$ defined in Equation (J6.2-12), and (b) expected dose $\bar{D}_{EW}(10^4 \text{ yr}|\mathbf{e}_1)$ associated with $D_{EW}(10^4 \text{ yr}|\mathbf{a}_{EW}, \mathbf{e}_{M1})$ as defined in Equation (J6.2-10)..... FJ-17

FIGURES (Continued)

Page

J6.2-10. Results associated with $D_{EW}(10^4 \text{ yr}|\mathbf{a}_{EW}, \mathbf{e}_M)$ obtained with sampling-based (Monte Carlo) procedures for an LHS of size $nLHS = 300$: (a) CCDFs for $D_{EW}(10^4 \text{ yr}|\mathbf{a}_{EW}, \mathbf{e}_{Mi})$ with exceedance probabilities $p_A[D < D_{EW}(10^4 \text{ yr}|\mathbf{a}, \mathbf{e}_{Mi})|\mathbf{e}_{Ai}]$ defined in Equation J6.2-12 for $i = 1, 2, \ldots, nLHS = 300$, (b) CCDFs for $D_{EW}(10^4 \text{ yr}|\mathbf{a}_{EW}, \mathbf{e}_{Mi})$ with exceedance probabilities $p_A[D < D_{EW}(10^4 \text{ yr}|\mathbf{a}, \mathbf{e}_{Mi})|\mathbf{e}_{Ai}]$ defined in Equation J6.2-13 for $i = 1, 2, \ldots, 50$, and (c) expected (mean) CCDF and quantile curves, $q = 0.05, 0.5, 0.95$, for CCDFs in (a). FJ-18

J6.2-11. Assessment with replicated sampling of numerical error associated with use of an LHS of size $nLHS = 300$ to determine epistemic uncertainty in expected dose $\bar{D}_{EW}(\tau|\mathbf{e})$ to RMEI for $0 \le \tau \le 20{,}000$ yr that results when only early WP failure is considered: (a) Replicated estimates of expected (mean) dose $\bar{\bar{D}}_{EW}(\tau)$ and quantiles $Q_q[\bar{D}_{EW}(\tau|\mathbf{e})]$, $q = 0.05, 0.5, 0.95$, and (b) confidence intervals for estimates of expected (mean) dose $\bar{\bar{D}}_{EW}(\tau)$. FJ-19

J6.2-12. Summary of results obtained with LHS of size $nLHS = 300$ showing epistemic uncertainty in doses $D_{EW}(\tau|[1, r, s, t], \mathbf{e}_M)$ for $0 \le \tau \le 10^6$ yr: (a) CSNF WP in bin 3 under nondripping conditions (i.e., $D_{EW}(\tau|[1, 1, 3, 0], \mathbf{e}_{Mi})$, $i = 1, 2, \ldots, nLHS = 300$), (b) CSNF WP in bin 3 under dripping conditions (i.e., $D_{EW}(\tau|[1, 1, 3, 1], \mathbf{e}_{Mi})$, $i = 1, 2, \ldots, nLHS = 300$), (c) CDSP WP in bin 3 under nondripping conditions (i.e., $D_{EW}(\tau|[1, 2, 3, 0], \mathbf{e}_{Mi})$, $i = 1, 2, \ldots, nLHS = 300$), and (d) CDSP WP in bin 3 under dripping conditions (i.e., $D_{EW}(\tau|[1, 2, 3, 1], \mathbf{e}_{Mi})$, $i = 1, 2, \ldots, nLHS = 300$). FJ-20

J6.2-13. Box plots (see Figure J6.2-3 for description) summarizing results obtained with LHS of size $nLHS = 300$ showing epistemic uncertainty in doses $D_{EW}(\tau|[1, r, s, t], \mathbf{e}_{Mi})$ for $\tau = 5 \times 10^4, 2 \times 10^5, 5 \times 10^5$ yr, $r = 1, 2$, $s = 1, 2, 3, 4, 5$, $t = 0, 1$, and $i = 1, 2, \ldots, nLHS = 300$: (a, c, e) CSNF WPs for $\tau = 5 \times 10^4, 2 \times 10^5, 5 \times 10^5$ yr, and (b, d, f) CDSP WPs for $\tau = 5 \times 10^4, 2 \times 10^5, 5 \times 10^5$ yr. FJ-21

J6.2-14. Estimate of $\bar{D}_{EW}(\tau|\mathbf{e}_1)$ for LHS element $\mathbf{e}_1 = [\mathbf{e}_{A1}, \mathbf{e}_{M1}]$ and $0 \le \tau \le 10^6$ yr with integration-based procedure indicated in Equation (J6.2-2). FJ-22

J6.2-15. Estimate obtained with LHS of size $nLHS = 300$ showing epistemic uncertainty in expected dose $\bar{D}_{EW}(\tau|\mathbf{e})$ to RMEI for $0 \le \tau \le 10^6$ yr that at results when only early WP failure is considered: (a) expected dose $\bar{D}_{EW}(\tau|\mathbf{e}_i)$, $i = 1, 2, \ldots, nLHS = 300$, (b) expected dose $\bar{D}_{EW}(\tau|\mathbf{e}_i)$, $i = 1, 2, \ldots, 50$, (c) exceedance probabilities $p_E[D < \bar{D}_{EW}(\tau|\mathbf{e})]$ and quantiles $Q_q[\bar{D}_{EW}(\tau|\mathbf{e})]$, $q = 0.05, 0.5$ and 0.95, for $\tau = 5 \times 10^5$ yr, and (d) expected (mean) dose $\bar{\bar{D}}_{EW}(\tau)$ and quantiles $Q_q[\bar{D}_{EW}(\tau|\mathbf{e})]$, $q = 0.05, 0.5, 0.95$. FJ-23

FIGURES (Continued)

Page

J6.2-16. Summary of results obtained with LHS of size $nLHS = 300$ showing epistemic uncertainty in expected dose $\bar{D}_{EW}(\tau|\mathbf{e})$ to RMEI for $0 \le \tau \le 10^6$ yr that results when only early WP failure is considered. FJ-24

J6.2-17. Estimate obtained with LHS of size $nLHS = 300$ showing epistemic uncertainty in expected dose $\bar{D}_{EW,r}(\tau|\mathbf{e})$ to RMEI for $0 \le \tau \le 10^6$ yr with r corresponding to ^{242}Pu that results when only early DS failure is considered: (a) expected dose $\bar{D}_{EW,r}(\tau|\mathbf{e}_i)$, $i = 1, 2, \ldots, nLHS = 300$, (b) expected dose $\bar{D}_{EW,r}(\tau|\mathbf{e}_i)$, $i = 1, 2, \ldots, 50$, (c) exceedance probabilities $p_E[D < \bar{D}_{EW,r}(\tau|\mathbf{e})]$ and quantiles $Q_q[\bar{D}_{EW,r}(\tau|\mathbf{e})]$, $q = 0.05$, 0.5 and 0.95, for $\tau = 5 \times 10^5$ yr, and (d) expected (mean) dose $\bar{\bar{D}}_{EW,r}(\tau)$ and quantiles $Q_q[\bar{D}_{EW,r}(\tau|\mathbf{e})]$, $q = 0.05$, 0.5, 0.95 ..... FJ-25

J6.2-18. Estimates obtained with LHS of size $nLHS = 300$ of expected (mean) dose $\bar{\bar{D}}_{EW,r}(\tau)$ to RMEI for $0 \le \tau \le 10^6$ yr for individual radioactive species that result when only early WP failure is considered. FJ-26

J6.2-19. Results associated with $D_{EW}(\tau|\mathbf{a}_{EW}, \mathbf{e}_{M1})$ for LHS element $\mathbf{e}_1 = [\mathbf{e}_{A1}, \mathbf{e}_{M1}]$ obtained with sampling-based (Monte Carlo) procedures: (a) CCDF for $D_{EW}(5 \times 10^5 \text{ yr}|\mathbf{a}_{EW}, \mathbf{e}_{M1})$ with exceedance probabilities $p_A[D < D_{EW}(5 \times 10^5 \text{ yr}|\mathbf{a}, \mathbf{e}_{M1})|\mathbf{e}_{A1}]$ defined in Equation (J6.2-12), and (b) expected dose $\bar{D}_{EW}(5 \times 10^5 \text{ yr}|\mathbf{e}_1)$ associated with $D_{EW}(5 \times 10^5 \text{ yr}|\mathbf{a}_{EW}, \mathbf{e}_{M1})$ as defined in Equation (J6.2-10) FJ-27

J6.2-20. Results associated with $D_{EW}(5 \times 10^5 \text{ yr}|\mathbf{a}_{EW}, \mathbf{e}_M)$ obtained with sampling-based (Monte Carlo) procedures for an LHS of size $nLHS = 300$: (a) CCDFs for $D_{EW}(5 \times 10^5 \text{ yr}|\mathbf{a}_{EW}, \mathbf{e}_{Mi})$ with exceedance probabilities $p_A[D < D_{EW}(5 \times 10^5 \text{ yr}|\mathbf{a}, \mathbf{e}_{Mi})|\mathbf{e}_{Ai}]$ defined in Equation J66.2-12 for $i = 1, 2, \ldots, nLHS = 300$, (b) CCDFs for $D_{EW}(10^4 \text{ yr}|\mathbf{a}_{EW}, \mathbf{e}_{Mi})$ with exceedance probabilities $p_A[D < D_{EW}(5 \times 10^5 \text{ yr}|\mathbf{a}, \mathbf{e}_{Mi})|\mathbf{e}_{Ai}]$ defined in Equation J6.2-20 for $i = 1, 2, \ldots, 50$, and (c) expected (mean) CCDF and quantile curves, $q = 0.05$, 0.5, 0.95, for CCDFs in (a). FJ-28

J6.2-21. Assessment with replicated sampling of numerical error associated with use of an LHS of size $nLHS = 300$ to determine epistemic uncertainty in expected dose $\bar{D}_{EW}(\tau|\mathbf{e})$ to RMEI for $0 \le \tau \le 10^6$ yr that results when only early WP failure is considered: (a) Replicated estimates of expected (mean) dose $\bar{\bar{D}}_{EW}(\tau)$ and quantiles $Q_q[\bar{D}_{EW}(\tau|\mathbf{e})]$, $q = 0.05$, 0.5, 0.95, and (b) confidence intervals for estimates of expected (mean) dose $\bar{\bar{D}}_{EW}(\tau)$. FJ-29

FIGURES (Continued)

Page

J6.3-1. Complementary cumulative distribution functions (CCDFs) for number *nED* of DSs with early failure associated with individual elements of LHS of size *nLHS* = 300 in Equation J4.9-1: (a) CCDFs for all 300 LHS elements, and (b) CCDFs for first 50 LHS elements..... FJ-30

J6.3-2. Summary of results obtained with LHS of size *nLHS* = 300 showing epistemic uncertainty in doses $D_{ED}(\tau|[1, r, s, 1], \mathbf{e}_M)$ for $0 \le \tau \le 20{,}000$ yr: (a) CSNF WP in bin 3 under dripping conditions (i.e., $D_{ED}(\tau|[1, 1, 3, 1], \mathbf{e}_{Mi})$, $i = 1, 2, \ldots, nLHS = 300$), and (b) CDSP WP in bin 3 under dripping conditions (i.e., $D_{ED}(\tau|[1, 2, 3, 1], \mathbf{e}_{Mi})$, $i = 1, 2, \ldots, nLHS = 300$). FJ-31

J6.3-3. Box plots (see Figure J6.2-3 for description) summarizing results obtained with LHS of size *nLHS* = 300 showing epistemic uncertainty in doses $D_{ED}(\tau|[1, r, s, 1], \mathbf{e}_{Mi})$ for $\tau = 2000$, 5000, 10,000 yr, $r = 1, 2$, $s = 1, 2, 3, 4, 5$, $t = 1$, and $i = 1, 2, \ldots, nLHS = 300$: (a, c, e) CSNF WPs at $\tau = 2000$, 5000 and 10,000 yrs, and (b, d, f) CDSP WPs at $\tau = 2000$, 5000 and 10,000 yrs. FJ-32

J6.3-4. Estimate of $\bar{D}_{ED}(\tau|\mathbf{e}_1)$ for LHS element $\mathbf{e}_1 = [\mathbf{e}_{A1}, \mathbf{e}_{M1}]$ and $0 \le \tau \le 20{,}000$ yr with integration-based procedure indicated in Equation (J6.3-2)..... FJ-33

J6.3-5. Estimate obtained with LHS of size *nLHS* = 300 showing epistemic uncertainty in expected dose $\bar{D}_{ED}(\tau|\mathbf{e})$ to RMEI for $0 \le \tau \le 20{,}000$ yr that results when only early DS failure is considered: (a) expected dose $\bar{D}_{ED}(\tau|\mathbf{e}_i)$, $i = 1, 2, \ldots, nLHS = 300$, (b) expected dose $\bar{D}_{ED}(\tau|\mathbf{e}_i)$, $i = 1, 2, \ldots, 50$, (c) exceedance probabilities $p_E[D < \bar{D}_{ED}(\tau|\mathbf{e})]$ and quantiles $Q_q[\bar{D}_{ED}(\tau|\mathbf{e})]$, $q = 0.05$, 0.5 and 0.95, for $\tau = 10^4$ yr, and (d) expected (mean) dose $\bar{\bar{D}}_{ED}(\tau)$ and quantiles $Q_q[\bar{D}_{ED}(\tau|\mathbf{e})]$, $q = 0.05$, 0.5, 0.95. ..... FJ-34

J6.3-6. Summary of results obtained with LHS of size *nLHS* = 300 showing epistemic uncertainty in expected dose $\bar{D}_{ED}(\tau|\mathbf{e})$ to RMEI for $0 \le \tau \le 20{,}000$ yr that results when only early DS failure is considered. FJ-35

J6.3-7. Estimate obtained with LHS of size *nLHS* = 300 showing epistemic uncertainty in expected dose $\bar{D}_{ED,r}(\tau|\mathbf{e})$ to RMEI for $0 \le \tau \le 20{,}000$ yr with r corresponding to ^{99}Tc that results when only early DS failure is considered: (a) expected dose $\bar{D}_{ED,r}(\tau|\mathbf{e}_i)$, $i = 1, 2, \ldots, nLHS = 300$, (b) expected dose $\bar{D}_{ED,r}(\tau|\mathbf{e}_i)$, $i = 1, 2, \ldots, 50$, (c) exceedance probabilities $p_E[D < \bar{D}_{ED,r}(\tau|\mathbf{e})]$ and quantiles $Q_q[\bar{D}_{ED,r}(\tau|\mathbf{e})]$, $q = 0.05$, 0.5 and 0.95, for $\tau = 10^4$ yr, and (d) expected (mean) dose $\bar{\bar{D}}_{ED,r}(\tau)$ and quantiles $Q_q[\bar{D}_{ED,r}(\tau|\mathbf{e})]$, $q = 0.05$, 0.5, 0.95..... FJ-36

J6.3-8. Estimates obtained with LHS of size *nLHS* = 300 of expected (mean) dose $\bar{\bar{D}}_{ED,r}(\tau)$ to RMEI for $0 \le \tau \le 20{,}000$ yr for individual radioactive species that result when only early DS failure is considered. FJ-37

FIGURES (Continued)

Page

J6.3-9. Results associated with $D_{ED}(\tau|\mathbf{a}_{ED}, \mathbf{e}_{M1})$ for LHS element $\mathbf{e}_1 = [\mathbf{e}_{A1}, \mathbf{e}_{M1}]$ obtained with sampling-based (Monte Carlo) procedures: (a) CCDF for $D_{ED}(10^4 \text{ yr}|\mathbf{a}_{ED}, \mathbf{e}_{M1})$ with exceedance probabilities $p_A[D < D_{ED}(10^4 \text{ yr}|\mathbf{a}, \mathbf{e}_{M1})|\mathbf{e}_{A1}]$ defined similarly to $p_A[D < D_{EW}(\tau|\mathbf{a}, \mathbf{e}_{M1})|\mathbf{e}_{A1}]$ in Equation (J6.2-12), and (b) expected dose $\bar{D}_{ED}(10^4 \text{ yr}|\mathbf{e}_1)$ associated with $D_{ED}(10^4 \text{ yr}|\mathbf{a}_{ED}, \mathbf{e}_{M1})$ defined similarly to $\bar{D}_{EW}(\tau|\mathbf{e}_1)$ in Equation (J6.2-10). FJ-38

J6.3-10. Results associated with $D_{ED}(10^4 \text{ yr}|\mathbf{a}_{ED}, \mathbf{e}_M)$ obtained with sampling-based (Monte Carlo) procedures for an LHS of size $nLHS = 300$: (a) CCDFs for $D_{ED}(10^4 \text{ yr}|\mathbf{a}_{ED}, \mathbf{e}_{Mi})$ with exceedance probabilities $p_A[D < D_{ED}(10^4 \text{ yr}|\mathbf{a}, \mathbf{e}_{Mi})|\mathbf{e}_{Ai}]$ defined similarly to $p_A[D < D_{EW}(\tau|\mathbf{a}, \mathbf{e}_{M1})|\mathbf{e}_{A1}]$ in Equation (J6.2-12) for $i = 1, 2, \ldots, nLHS = 300$, (b) CCDFs for $D_{ED}(10^4 \text{ yr}|\mathbf{a}_{ED}, \mathbf{e}_{Mi})$ with exceedance probabilities $p_A[D < D_{ED}(10^4 \text{ yr}|\mathbf{a}, \mathbf{e}_{Mi})|\mathbf{e}_{Ai}]$ defined similarly to $p_A[D < D_{EW}(\tau|\mathbf{a}, \mathbf{e}_{M1})|\mathbf{e}_{A1}]$ in Equation (J6.2-12) for $i = 1, 2, \ldots, 50$, and (c) expected (mean) CCDF and quantile curves, $q = 0.05, 0.5, 0.95$, for CCDFs in (a). FJ-39

J6.3-11. Assessment with replicated sampling of numerical error associated with use of an LHS of size $nLHS = 300$ to determine epistemic uncertainty in expected dose $\bar{D}_{ED}(\tau|\mathbf{e})$ to RMEI for $0 \le \tau \le 20{,}000$ yr that results when only early DS failure is considered: (a) Replicated estimates of expected (mean) dose $\bar{\bar{D}}_{ED}(\tau)$ and quantiles $Q_q[\bar{D}_{ED}(\tau|\mathbf{e})]$, $q = 0.05, 0.5, 0.95$, and (b) confidence intervals for estimates of expected (mean) dose $\bar{\bar{D}}_{ED}(\tau)$. FJ-40

J6.3-12. Summary of results obtained with LHS of size $nLHS = 300$ showing epistemic uncertainty in doses $D_{ED}(\tau|[1, r, s, 1], \mathbf{e}_M)$ for $0 \le \tau \le 10^6$ yr: (a) CSNF WP in bin 3 under dripping conditions (i.e., $D_{ED}(\tau|[1, 1, 3, 1], \mathbf{e}_{Mi})$, $i = 1, 2, \ldots, nLHS = 300$) and (b) CDSP WP in bin 3 under dripping conditions (i.e., $D_{ED}(\tau|[1, 2, 3, 1], \mathbf{e}_{Mi})$, $i = 1, 2, \ldots, nLHS = 300$). FJ-41

J6.3-13. Box plots (see Figure J6.2-3 for description) summarizing results obtained with LHS of size $nLHS = 300$ showing epistemic uncertainty in doses $D_{ED}(\tau|[1, r, s, 1], \mathbf{e}_{Mi})$ for $\tau = 5 \times 10^4, 2 \times 10^5, 5 \times 10^5$ yr, $r = 1, 2$, $s = 1, 2, 3, 4, 5$, $t = 1$, and $i = 1, 2, \ldots, nLHS = 300$: (a, c, e) CSNF WPs at 5×10^4, 2×10^5, 5×10^5 yr, and (b, d, f) CDSP WPs at 5×10^4, 2×10^5, 5×10^5 yr. FJ-42

J6.3-14. Estimate of $\bar{D}_{ED}(\tau|\mathbf{e}_1)$ for LHS element $\mathbf{e}_1 = [\mathbf{e}_{A1}, \mathbf{e}_{M1}]$ and $0 \le \tau \le 10^6$ yr with integration-based procedure indicated in EquationJ6.2-2 ..... FJ-43

J6.3-15. Estimate obtained with LHS of size $nLHS = 300$ showing epistemic uncertainty in expected dose $\bar{D}_{ED}(\tau|\mathbf{e})$ to RMEI for $0 \le \tau \le 10^6$ yr that results when only early DS failure is considered: (a) expected dose $\bar{D}_{ED}(\tau|\mathbf{e}_i)$, $i = 1, 2, \ldots, nLHS = 300$, (b) expected dose $\bar{D}_{ED}(\tau|\mathbf{e}_i)$, $i = 1, 2, \ldots, 50$, (c)

FIGURES (Continued)

Page

exceedance probabilities $p_E[D < \bar{D}_{ED}(\tau|\mathbf{e})]$ and quantiles $Q_q[\bar{D}_{ED}(\tau|\mathbf{e})]$, q = 0.05, 0.5 and 0.95, for $\tau = 5 \times 10^5$ yr, and (d) expected (mean) dose $\bar{\bar{D}}_{ED}(\tau)$ and quantiles $Q_q[\bar{D}_{ED}(\tau|\mathbf{e})]$, q = 0.05, 0.5, 0.95. ..... FJ-44

J6.3-16. Summary of results obtained with LHS of size $nLHS$ = 300 showing epistemic uncertainty in expected dose $\bar{D}_{ED}(\tau|\mathbf{a})$ to RMEI for $0 \le \tau \le 10^6$ yr that results when only early DS failure is considered. FJ-45

J6.3-17. Estimate obtained with LHS of size $nLHS$ = 300 showing epistemic uncertainty in expected dose $\bar{D}_{ED,r}(\tau|\mathbf{e})$ to RMEI for $0 \le \tau \le 10^6$ yr with r corresponding to ^{242}Pu that results when only early DS failure is considered: (a) expected dose $\bar{D}_{ED,r}(\tau|\mathbf{e}_i)$, i = 1, 2, …, $nLHS$ = 300, (b) expected dose $\bar{D}_{ED,r}(\tau|\mathbf{e}_i)$, i = 1, 2, …, 50, (c) exceedance probabilities $p_E[D < \bar{D}_{ED,r}(\tau|\mathbf{e})]$ and quantiles $Q_q[\bar{D}_{ED,r}(\tau|\mathbf{e})]$, q = 0.05, 0.5 and 0.95, for $\tau = 5 \times 10^5$ yr, and (d) expected (mean) dose $\bar{\bar{D}}_{ED,r}(\tau)$ and quantiles $Q_q[\bar{D}_{ED,r}(\tau|\mathbf{e})]$, q = 0.05, 0.5, 0.95 ..... FJ-46

J6.3-18. Estimates obtained with LHS of size $nLHS$ = 300 of expected (mean) dose $\bar{\bar{D}}_{ED,r}(\tau)$ to RMEI for $0 \le \tau \le 10^6$ yr for individual radioactive species that result when only early DS failure is considered. FJ-47

J6.3-19. Results associated with $D_{ED}(\tau|\mathbf{a}_{ED}, \mathbf{e}_{M1})$ for LHS element $\mathbf{e}_1 = [\mathbf{e}_{A1}, \mathbf{e}_{M1}]$ obtained with sampling-based (Monte Carlo) procedures: (a) CCDF for $D_{ED}(5 \times 10^5$ yr$|\mathbf{a}_{ED}, \mathbf{e}_{M1})$ with exceedance probabilities $p_A[D < D_{ED}(5 \times 10^5$ yr$|\mathbf{a}, \mathbf{e}_{M1})|\mathbf{e}_{A1}]$ defined similarly to $p_A[D < D_{EW}(\tau|\mathbf{a}, \mathbf{e}_{M1})|\mathbf{e}_{A1}]$ in Equation (J6.2-12), and (b) expected dose $\bar{D}_{ED}(5 \times 10^5$ yr$|\mathbf{e}_1)$ associated with $D_{ED}(5 \times 10^5$ yr $|\mathbf{a}_{ED}, \mathbf{e}_1)$ defined similarly to $\bar{D}_{EW}(\tau|\mathbf{e}_1)$ in Equation (J6.2-10). FJ-48

J6.3-20. Results associated with $D_{ED}(5 \times 10^5$ yr$|\mathbf{a}_{ED}, \mathbf{e}_M)$ obtained with sampling-based (Monte Carlo) procedures for an LHS of size $nLHS$ = 300: (a) CCDFs for $D_{ED}(5 \times 10^5$ yr$|\mathbf{a}_{ED}, \mathbf{e}_{Mi})$ with exceedance probabilities $p_A[D < D_{ED}(5 \times 10^5$ yr$|\mathbf{a}_{ED}, e_{Mi})|\mathbf{e}_{Ai}]$ defined similarly to $p_A[D < D_{EW}(\tau|\mathbf{a}, \mathbf{e}_{M1})|\mathbf{e}_{A1}]$ in Equation (J6.2-12) for i = 1, 2, …, $nLHS$ = 300, (b) CCDFs for $D_{ED}(10^4$ yr$|\mathbf{a}_{ED}, \mathbf{e}_{Mi})$ with exceedance probabilities $p_A[D < D_{ED}(5 \times 10^5$ yr$|\mathbf{a}_{ED}, e_{Mi})|\mathbf{e}_{Ai}]$ defined similarly to $p_A[D < D_{EW}(\tau|\mathbf{a}, \mathbf{e}_{M1})|\mathbf{e}_{A1}]$ in Equation (J6.2-12) for i = 1, 2, …, 50, and (c) expected (mean) CCDF and quantile curves, q = 0.05, 0.5, 0.95, for CCDFs in (a) FJ-49

J6.3-21. Assessment with replicated sampling of numerical error associated with use of an LHS of size $nLHS$ = 300 to determine epistemic uncertainty in expected dose $\bar{D}_{ED}(\tau|\mathbf{e})$ to RMEI for $0 \le \tau \le 10^6$ yr that results when only early DS

FIGURES (Continued)

Page

failure is considered: (a) Replicated estimates of expected (mean) dose $\bar{\bar{D}}_{ED}(\tau)$ and quantiles $Q_q[\bar{D}_{ED}(\tau|\mathbf{e})]$, q = 0.05, 0.5, 0.95, and (b) confidence intervals for estimates of expected (mean) dose $\bar{\bar{D}}_{ED}(\tau)$. FJ-50

J6.4-1. Estimate obtained with LHS of size $nLHS$ = 300 showing epistemic uncertainty in expected dose $\bar{D}_E(\tau|\mathbf{e})$ to RMEI for $0 \le \tau \le 20{,}000$ yr that results when only early WP and early DS failures are considered: (a) expected dose $\bar{D}_E(\tau|\mathbf{e}_i)$, i = 1, 2, …, $nLHS$ = 300, (b) expected dose $\bar{D}_E(\tau|\mathbf{e}_i)$, i = 1, 2, …, 50, (c) exceedance probabilities $p_E[D < \bar{D}_E(\tau|\mathbf{e})]$ and quantiles $Q_q[\bar{D}_E(\tau|\mathbf{e})]$, q = 0.05, 0.5 and 0.95, for $\tau = 10^4$ yr, and (d) expected (mean) dose $\bar{\bar{D}}_E(\tau)$ and quantiles $Q_q[\bar{D}_E(\tau|\mathbf{e})]$, q = 0.05, 0.5, 0.95 ..... FJ-51

J6.4-2. Estimate obtained with LHS of size $nLHS$ = 300 showing epistemic uncertainty in expected dose $\bar{D}_E(\tau|\mathbf{e})$ to RMEI for $0 \le \tau \le 1{,}000{,}000$ yr that results when only early WP and early DS failures are considered: (a) expected dose $\bar{D}_E(\tau|\mathbf{e}_i)$, i = 1, 2, …, $nLHS$ = 300, (b) expected dose $\bar{D}_E(\tau|\mathbf{e}_i)$, i = 1, 2, …, 50, (c) exceedance probabilities $p_E[D < \bar{D}_E(\tau|\mathbf{e})]$ and quantiles $Q_q[\bar{D}_E(\tau|\mathbf{e})]$, q = 0.05, 0.5 and 0.95, for τ = 500,000 yr, and (d) expected (mean) dose $\bar{\bar{D}}_E(\tau)$ and quantiles $Q_q[\bar{D}_E(\tau|\mathbf{e})]$, q = 0.05, 0.5, 0.95. ..... FJ-52

J6.4-3. Estimate obtained with LHS of size $nLHS$ = 300 showing epistemic uncertainty in expected dose $\bar{D}_{NE}(\tau|\mathbf{e})$ to RMEI for $0 \le \tau \le 1{,}000{,}000$ yr that results when only nominal process failures and early WP and early DS failures are considered: (a) expected dose $\bar{D}_{NE}(\tau|\mathbf{e}_i)$, i = 1, 2, …, $nLHS$ = 300, (b) expected dose $\bar{D}_{NE}(\tau|\mathbf{e}_i)$, i = 1, 2, …, 50, (c) exceedance probabilities $p_E[D < \bar{D}_{NE}(\tau|\mathbf{e})]$ and quantiles $Q_q[\bar{D}_{NE}(\tau|\mathbf{e})]$, q = 0.05, 0.5 and 0.95, for τ = 500,000 yr, and (d) expected (mean) dose $\bar{\bar{D}}_{NE}(\tau)$ and quantiles $Q_q[\bar{D}_{NE}(\tau|\mathbf{e})]$, q = 0.05, 0.5, 0.95. ..... FJ-53

J6.5-1. Box plots (see Figure J6.2-3 for description) summarizing probabilities $p_A(\mathcal{A}_{ED}|\mathbf{e}_{Ai})$, $p_A(\mathcal{A}_{EW}|\mathbf{e}_{Ai})$ and $p_A(\mathcal{A}_E|\mathbf{e}_{Ai})$ for scenario classes $\mathcal{A}_{ED}$, $\mathcal{A}_{EW}$ and $\mathcal{A}_E$ obtained with LHS of size $nLHS$ = 300. ..... FJ-54

J7.2-1. Dose to RMEI $D_{II}(\tau|[1, t_k, nWP], \mathbf{e}_{Mi})$ from igneous intrusive events at times t_k = 10, 600, 2000, 4000, 6000 and 10,000 yr for i = 1, 2, …, $nLHS$ = 300: (a) 10 yr, (b) 600 yr, (c) 2000 yr, (d) 4000 yr, (e) 6000 yr, and (f) 10,000 yr. FJ-55

J7.2-2. Illustration of interpolation procedure used to obtain estimated doses $\hat{D}_{II}(\tau|[1, \hat{t}_k, nWP], \mathbf{e}_{M1})$ from calculated doses $D_{II}(\tau|[1, t_k, nWP], \mathbf{e}_{M1})$ indicated in Equation J7.2-18 for LHS element $\mathbf{e}_1 = [\mathbf{e}_{A1}, \mathbf{e}_{M1}]$ and the time interval [0, 2.0×10^4 yr]: (a) $D_{II}(\tau|[1, t_k, nWP], \mathbf{e}_{M1})$, k = 1, 2, …, 10, (b) interpolated values $\hat{D}_{II}(\tau|[1, \hat{t}_k, nWP], \mathbf{e}_{M1})$ for $\hat{t}_k$ between t_7 = 6000 and t_{8+1} = 10,000,

FIGURES (Continued)

Page

and (c) interpolated values $\hat{D}_{II}(\tau|[1, \hat{t}_k, nWP], \mathbf{e}_{M1})$ for $\hat{t}_k$ between 10 yr and 2.0×10^4 yr. FJ-56

J7.2-3. Determination of $\bar{D}_{II}(\tau|\mathbf{e}_1)$ as indicated in conjunction with Equations J7.2-7, J7.2-9 and J7.2-19 from calculated doses $D_{II}(\tau|[1, t_k, nWP], \mathbf{e}_{M1})$ shown in Equation J7.2-18 for LHS element $\mathbf{e}_1 = [\mathbf{e}_{A1}, \mathbf{e}_{M1}]$ and the time interval [0, 2.0×10^4 yr]. FJ-57

J7.2-4. Estimate obtained with LHS of size $nLHS = 300$ showing epistemic uncertainty in expected dose $\bar{D}_{II}(\tau|\mathbf{e})$ to RMEI for $0 \le \tau \le 20{,}000$ yr that results when only igneous intrusion events are considered: (a) expected dose $\bar{D}_{II}(\tau|\mathbf{e}_i)$, $i = 1, 2, \ldots, nLHS = 300$, (b) expected dose $\bar{D}_{II}(\tau|\mathbf{e}_i)$, $i = 1, 2, \ldots, 50$, (c) exceedance probabilities $p_E[D < \bar{D}_{II}(\tau|\mathbf{e})]$ and quantiles $Q_q[\bar{D}_{II}(\tau|\mathbf{e})]$, $q = 0.05$, 0.5 and 0.95, for $\tau = 10^4$ yr, and (d) expected (mean) dose $\bar{\bar{D}}_{II}(\tau)$ and quantiles $Q_q[\bar{D}_{II}(\tau|\mathbf{e})]$, $q = 0.05$, 0.5, 0.95. ..... FJ-58

J7.2-5. Summary presentation of epistemic uncertainty in expected dose $\bar{D}_{II}(\tau|\mathbf{e})$ to RMEI that results when only igneous intrusion is considered for $0 \le \tau \le 2.0 \times 10^4$ yr. FJ-59

J7.2-6. Estimate obtained with LHS of size $nLHS = 300$ showing epistemic uncertainty in expected dose $\bar{D}_{II,r}(\tau|\mathbf{e})$ to RMEI for $0 \le \tau \le 20{,}000$ yr with r corresponding to ^{99}Tc that results when only igneous intrusive events are considered: (a) expected dose $\bar{D}_{II,r}(\tau|\mathbf{e}_i)$, $i = 1, 2, \ldots, nLHS = 300$, (b) expected dose $\bar{D}_{II,r}(\tau|\mathbf{e}_i)$, $i = 1, 2, \ldots, 50$, (c) exceedance probabilities $p_E[D < \bar{D}_{II,r}(\tau|\mathbf{e})]$ and quantiles $Q_q[\bar{D}_{II,r}(\tau|\mathbf{e})]$, $q = 0.05$, 0.5 and 0.95, for $\tau = 10^4$ yr, and (d) expected (mean) dose $\bar{\bar{D}}_{II,r}(\tau)$ and quantiles $Q_q[\bar{D}_{II,r}(\tau|\mathbf{e})]$, $q = 0.05$, 0.5, 0.95 ..... FJ-60

J7.2-7. Estimates obtained with LHS of size $nLHS = 300$ of expected (mean) dose $\bar{\bar{D}}_{II,r}(\tau)$ to RMEI for $0 \le \tau \le 20{,}000$ yr for individual radioactive species that result when only igneous intrusive events are considered. FJ-61

J7.2-8. Results associated with $\bar{D}_{II}(\tau|\mathbf{e}_1)$ for LHS element $\mathbf{e}_1 = [\mathbf{e}_{A1}, \mathbf{e}_{M1}]$ obtained with sampling-based (Monte Carlo) procedures: (a) CCDF for $D_{II}(10^4$ yr$|\mathbf{a}_{II}, \mathbf{e}_{M1})$ with exceedance probabilities $p_A[D < D_{II}(10^4$ yr$|\mathbf{a}, \mathbf{e}_{M1})|\mathbf{e}_{A1}]$ defined in Equation J7.2-23, and (b) expected dose $\bar{D}_{II}(10^4$ yr$|\mathbf{e}_1)$ associated with $D_{II}(10^4$ yr$|\mathbf{a}_{II}, \mathbf{e}_{M1})$ as defined in Equation J7.2-21 ..... FJ-62

J7.2-9. Results associated with $D_{II}(10^4$ yr$|\mathbf{a}_{II}, \mathbf{e}_M)$ obtained with sampling-based (Monte Carlo) procedures for an LHS of size $nLHS = 300$: (a) CCDFs for $D_{II}(10^4$ yr$|\mathbf{a}_{II}, \mathbf{e}_{Mi})$ with exceedance probabilities $p_A[D < D_{II}(10^4$ yr$|\mathbf{a}, \mathbf{e}_{Mi})|\mathbf{e}_{Ai}]$ defined in Equation J7.2-23 for $i = 1, 2, \ldots, nLHS = 300$, (b)

FIGURES (Continued)

Page

CCDFs for $D_{II}(10^4 \text{ yr}|\mathbf{a}_{II}, \mathbf{e}_{Mi})$ with exceedance probabilities $p_A[D < D_{II}(10^4 \text{ yr}|\mathbf{a}, \mathbf{e}_{Mi})|\mathbf{a}_{Ai}]$ defined in Equation J7.2-23 for $i = 1, 2, \ldots, 50$, and (c) expected (mean) CCDF and quantile curves, $q = 0.05, 0.5, 0.95$, for CCDFs in (a). FJ-63

J7.2-10. Assessment with replicated sampling of numerical error associated with use of an LHS of size $nLHS = 300$ to determine epistemic uncertainty in expected dose $\bar{D}_{II}(\tau|\mathbf{e})$ to RMEI for $0 \le \tau \le 20{,}000$ yr that results when only igneous intrusive events are considered: (a) Replicated estimates of expected (mean) dose $\bar{\bar{D}}_{II}(\tau)$ and quantiles $Q_q[\bar{D}_{II}(\tau|\mathbf{e})]$, $q = 0.05, 0.5, 0.95$, and (b) confidence intervals for estimates of expected (mean) dose $\bar{\bar{D}}_{II}(\tau)$. FJ-64

J7.2-11. Dose to RMEI $D_{II}(\tau|[1, t_k, nWP], \mathbf{e}_{Mi})$ from igneous intrusive events at times $t_k = 10{,}000, 40{,}000, 100{,}000, 200{,}000, 400{,}000$ and $800{,}000$ yr for $i = 1, 2, \ldots, nLHS = 300$: (a) 10,000 yr, (b) 40,000 yr, (c) 100,000 yr, (d) 200,000 yr, (e) 400,000 yr, and (f) 800,000 yr. FJ-65

J7.2-12. Illustration of interpolation procedure used to obtain estimated doses $\hat{D}_{II}(\tau|[1, \hat{t}_k, nWP], \mathbf{e}_{M1})$ from calculated doses $D_{II}(\tau|[1, t_k, nWP], \mathbf{e}_{M1})$ indicated in Equation J7.2-18 for LHS element $\mathbf{e}_1 = [\mathbf{e}_{A1}, \mathbf{e}_{M1}]$ and the time interval $[0, 10^6 \text{ yr}]$: (a) $D_{II}(\tau|[1, t_k, nWP], \mathbf{e}_{M1})$, $k = 1, 2, \ldots, 10$, (b) interpolated values $\hat{D}_{II}(\tau|[1, \hat{t}_k, nWP], \mathbf{e}_{M1})$ for $\hat{t}_k$ between $t_8 = 200{,}000$ yr and $t_9 = 400{,}000$, and (c) interpolated values $\hat{D}_{II}(\tau|[1, \hat{t}_k, nWP], \mathbf{e}_{M1})$ for $\hat{t}_k$ between 250 yr and 10^6 yr. FJ-66

J7.2-13. Determination of $\bar{D}_{II}(\tau|\mathbf{e}_1)$ as indicated in conjunction with Equations J7.2-7, J7.2-9 and J7.2-19 from calculated doses $D_{II}(\tau|[1, t_k, nWP], \mathbf{e}_{M1})$ shown in Equation J7.2-18 for LHS element $\mathbf{e}_1 = [\mathbf{e}_{A1}, \mathbf{e}_{M1}]$ and the time interval $[0, 10^6 \text{ yr}]$ FJ-67

J7.2-14. Estimate obtained with LHS of size $nLHS = 300$ showing epistemic uncertainty in expected dose $\bar{D}_{II}(\tau|\mathbf{e})$ to RMEI for $0 \le \tau \le 10^6$ yr that results when only igneous intrusion is considered: (a) expected dose $\bar{D}_{II}(\tau|\mathbf{e}_i)$, $i = 1, 2, \ldots, nLHS = 300$, (b) expected dose $\bar{D}_{II}(\tau|\mathbf{e}_i)$, $i = 1, 2, \ldots, 50$, (c) exceedance probabilities $p_E[D < \bar{D}_{II}(\tau|\mathbf{e})]$ and quantiles $Q_q[\bar{D}_{II}(\tau|\mathbf{e})]$, $q = 0.05, 0.5$ and 0.95, for $\tau = 5 \times 10^5$ yr, and (d) expected (mean) dose $\bar{\bar{D}}_{II}(\tau)$ and quantiles $Q_q[\bar{D}_{II}(\tau|\mathbf{e})]$, $q = 0.05, 0.5, 0.95$. FJ-68

J7.2-15. Summary presentations of epistemic uncertainty in expected dose $\bar{D}_{II}(\tau|\mathbf{e})$ to RMEI that results when only igneous intrusion is considered for $0 \le \tau \le 10^6$ yr. FJ-69

FIGURES (Continued)

Page

J7.2-16. Estimate obtained with LHS of size $nLHS = 300$ showing epistemic uncertainty in expected dose $\bar{D}_{II,r}(\tau|\mathbf{e})$ to RMEI for $0 \le \tau \le 10^6$ yr with r corresponding to ^{226}Ra that results when only igneous intrusion is considered: (a) expected dose $\bar{D}_{II,r}(\tau|\mathbf{e}_i)$, $i = 1, 2, \ldots, nLHS = 300$, (b) expected dose $\bar{D}_{II,r}(\tau|\mathbf{e}_1)$, $i = 1, 2, \ldots, 50$, (c) exceedance probabilities $p_E[D < \bar{D}_{II,r}(\tau|\mathbf{e})]$ and quantiles $Q_q[\bar{D}_{II,r}(\tau|\mathbf{e})]$, $q = 0.05$, 0.5 and 0.95, for $\tau = 5 \times 10^5$ yr, and (d) expected (mean) dose $\bar{\bar{D}}_{II,r}(\tau)$ and quantiles $Q_q[\bar{D}_{II,r}(\tau|\mathbf{e})]$, $q =$ 0.05, 0.5, 0.95 ..... FJ-70

J7.2-17. Estimates obtained with LHS of size $nLHS = 300$ of expected (mean) dose $\bar{\bar{D}}_{II,r}(\tau)$ to RMEI for $0 \le \tau \le 10^6$ yr for individual radioactive species that result when only igneous intrusive events are considered. FJ-71

J7.2-18. Results associated with $\bar{D}_{II}(\tau|\mathbf{e}_1)$ for LHS elements $\mathbf{e}_1 = [\mathbf{e}_{A1}, \mathbf{e}_{M1}]$ obtained with sampling-based (Monte Carlo) procedures: (a) CCDF for $D_{II}(5 \times 10^5$ yr$|\mathbf{a}_{II}, \mathbf{e}_{M1})$ with exceedance probabilities $p_A[D < D_{II}(5 \times 10^5$ yr$|\mathbf{a}, \mathbf{e}_{M1})|\mathbf{e}_{A1}]$ defined in Equation J7.2-23, and (b) expected dose $\bar{D}_{II}(5 \times 10^5$ yr$|\mathbf{e}_1)$ associated with $D_{II}(5 \times 10^5$ yr$|\mathbf{a}_{II}, \mathbf{e}_{M1})$ as defined in Equation J7.2-21. ..... FJ-72

J7.2-19. Results associated with $D_{II}(5 \times 10^5$ yr$|\mathbf{a}_{II}, \mathbf{e}_M)$ obtained with sampling-based (Monte Carlo) procedures for an LHS of size $nLHS = 300$: (a) CCDFs for $D_{II}(5 \times 10^5$ yr$|\mathbf{a}_{II}, \mathbf{e}_{Mi})$ with exceedance probabilities $p_A[D < D_{II}(5 \times 10^5$ yr$|\mathbf{a}, \mathbf{e}_{Mi})|\mathbf{e}_{Ai}]$ defined in Equation J7.2-23 for $i = 1, 2, \ldots, nLHS = 300$, (b) CCDFs for $D_{II}(5 \times 10^5$ yr$|\mathbf{a}_{II}, \mathbf{e}_{Mi})$ with exceedance probabilities $p_A[D < D_{II}(5 \times 10^5$ yr$|\mathbf{a}, \mathbf{e}_{Mi})|\mathbf{a}_{Ai}]$ defined in Equation J7.2-23 for $i = 1, 2, \ldots, 50$, and (c) expected (mean) CCDF and quantile curves, $q = 0.05$, 0.5, 0.95, for CCDFs in (a). FJ-73

J7.2-20. Assessment with replicated sampling of numerical error associated with use of an LHS of size $nLHS = 300$ to determine epistemic uncertainty in expected dose $\bar{D}_{II}(\tau|\mathbf{e})$ to RMEI for $0 \le \tau \le 10^6$ yr that results when only igneous intrusion is considered: (a) Replicated estimates of expected (mean) dose $\bar{\bar{D}}_{II}(\tau)$ and quantiles $Q_q[\bar{D}_{II}(\tau|\mathbf{e})]$, $q = 0.05$, 0.5, 0.95, and (b) confidence intervals for estimates of expected (mean) dose $\bar{\bar{D}}_{II}(\tau)$. FJ-74

J7.3-1. Dose results $D_{IE}(\tau|[1, t_k, 1, \mathbf{u}_l], \mathbf{e}_{M1})$ obtained for times $t_k = 100$, 1000, 4000, 10,000 yr, igneous eruptive properties $\mathbf{u}_l$, $l = 1, 2, \ldots, nU = 40$, and LHS element $\mathbf{e}_1 = [\mathbf{e}_{A1}, \mathbf{e}_{M1}]$: (a) $t_k = 100$ yr, (b) $t_k = 1000$ yr, (c) $t_k = 4000$ yr, and (d) $t_k = 10{,}000$ yr. FJ-75

FIGURES (Continued)

Page

J7.3-2. Illustration of interpolation procedure used to obtain estimates $\hat{S}(\tau|\hat{t}_k, \mathbf{e}_{M1})$ of conditional expected dose $S(\tau|t, \mathbf{e}_{M1})$ to RMEI (mrem/yr) for LHS element $\mathbf{e}_1 = [\mathbf{e}_{A1}, \mathbf{e}_{M1}]$ and the time interval [0, 20,000 yr]: (a) $S(\tau|t_k, \mathbf{e}_{M1})$, $k = 1, 2, \ldots, 10$, (b) interpolated values $\hat{S}(\tau|\hat{t}_k, \mathbf{e}_{M1})$ for $\hat{t}_k$ between t_7 = 6000 yr and t_8 = 10,000 yr, and (c) interpolated values $\hat{S}(\tau|\hat{t}_k, \mathbf{e}_{M1})$ for $\hat{t}_k$ between 10 yr and 20,000 yr. FJ-76

J7.3-3. Estimate of $\bar{D}_{IE}(\tau|\,\mathbf{e}_1)$ for LHS element $\mathbf{e}_1 = [\mathbf{e}_{A1}, \mathbf{e}_{M1}]$ and $0 \le \tau \le 20{,}000$ yr with integration-based procedure indicated in Equations J7.3-9 and J7.3-16. ..... FJ-77

J7.3-4. Estimate obtained with LHS of size $nLHS = 300$ showing epistemic uncertainty in expected dose $\bar{D}_{IE}(\tau|\mathbf{e})$ to RMEI for $0 \le \tau \le 20{,}000$ yr that results when only igneous eruptive events are considered: (a) expected dose $\bar{D}_{IE}(\tau|\mathbf{e}_i)$, $i = 1, 2, \ldots, nLHS = 300$, (b) expected dose $\bar{D}_{IE}(\tau|\mathbf{e}_i)$, $i = 1, 2, \ldots, 50$, (c) exceedance probabilities $p_E[D < \bar{D}_{IE}(\tau|\mathbf{e})]$ and quantiles $Q_q[\bar{D}_{IE}(\tau|\mathbf{e})]$, $q = 0.05$, 0.5 and 0.95, for $\tau = 10^4$ yr, and (d) expected (mean) dose $\bar{\bar{D}}_{IE}(\tau)$ and quantiles $Q_q[\bar{D}_{IE}(\tau|\mathbf{e})]$, $q = 0.05, 0.5, 0.95$. FJ-78

J7.3-5. Summary of results obtained with LHS of size $nLHS = 300$ showing epistemic uncertainty in expected dose $\bar{D}_{IE}(\tau|\mathbf{e})$ to RMEI for $0 \le \tau \le 20{,}000$ yr that results when only igneous eruptive events are considered. FJ-79

J7.3-6. Estimates obtained with LHS of size $nLHS = 300$ of expected (mean) dose $\bar{\bar{D}}_{IE,r}(\tau)$ to RMEI for $0 \le \tau \le 20{,}000$ yr for individual radioactive species that result when only igneous eruptive events are considered. FJ-80

J7.3-7. Results associated with $D_{IE}(\tau|\mathbf{a}_{IE}, \mathbf{e}_1)$ for LHS element $\mathbf{e}_1 = [\mathbf{e}_{A1}, \mathbf{e}_{M1}]$ obtained with sampling-based (Monte Carlo) procedures: (a) CCDF for $D_{IE}(10^4 \text{ yr}|\mathbf{a}_{IE}, \mathbf{e}_1)$ with exceedance probabilities $p_A[D < D_{IE}(10^4 \text{ yr}|\mathbf{a}, \mathbf{e}_{M1})|\mathbf{e}_{A1}]$ defined in Equation J7.3-20, and (b) expected dose $\bar{D}_{IE}(10^4 \text{ yr}|\mathbf{e}_1)$ associated with $D_{IE}(10^4 \text{ yr}|\mathbf{a}_{IE}, \mathbf{e}_1)$ as defined in Equation J7.3-18. ..... FJ-81

J7.3-8. Results associated with $D_{IE}(10^4 \text{ yr}|\mathbf{a}_{IE}, \mathbf{e}_M)$ obtained with sampling-based (Monte Carlo) procedures for an LHS of size $nLHS = 300$: (a) CCDFs for $D_{IE}(10^4 \text{ yr}|\mathbf{e}_{IE}, \mathbf{e}_{Mi})$ with exceedance probabilities $p_A[D < D_{IE}(10^4 \text{ yr}|\mathbf{a}, \mathbf{e}_{Mi})|\mathbf{e}_{Ai}]$ defined in Equation J7.3-20 for $i = 1, 2, \ldots, nLHS = 300$, (b) CCDFs for $D_{IE}(10^4 \text{ yr}|\mathbf{a}_{IE}, \mathbf{e}_{Mi})$ with exceedance probabilities $p_A[D < D_{IE}(10^4 \text{ yr}|\mathbf{a}, \mathbf{e}_{Mi})|\mathbf{e}_{Ai}]$ defined in Equation J7.3-20 for $i = 1, 2, \ldots, 50$, and (c) expected (mean) CCDF and quantile curves, $q = 0.05, 0.5, 0.95$, for CCDFs in (a). FJ-82

J7.3-9. Assessment with replicated sampling of numerical error associated with use of an LHS of size $nLHS = 300$ to determine epistemic uncertainty in expected

FIGURES (Continued)

Page

dose $\bar{D}_{IE}(\tau)$ to RMEI for $0 \le \tau \le 20{,}000$ yr that results when only igneous eruptive events are considered: (a) Replicated estimates of expected (mean) dose $\bar{D}_{IE}(\tau)$ and quantiles $Q_q[\bar{D}_{IE}(\tau|\mathbf{e})]$, $q = 0.05$, 0.5, 0.95, and (b) confidence intervals for estimates of expected (mean) dose $\bar{\bar{D}}_{IE}(\tau)$. FJ-83

J7.3-10. Dose results $D_{IE}(\tau|[1, t_k, 1, \mathbf{u}_l], \mathbf{e}_{M1})$ obtained for times $t_k = 40{,}000$, 100,000, 200,000, 400,000 yr, igneous eruptive properties $\mathbf{u}_l$, $l = 1, 2, \ldots, nU = 40$, and LHS element $\mathbf{e}_1 = [\mathbf{e}_{A1}, \mathbf{e}_{M1}]$: (a) $t_k = 40{,}000$ yr, (b) $t_k = 100{,}000$ yr, (c) $t_k = 200{,}000$ yr, and (d) $t_k = 400{,}000$ yr. FJ-84

J7.3-11. Illustration of interpolation procedure used to obtain estimates $\hat{S}(\tau|\hat{t}_k, \mathbf{e}_{Mi})$ of conditional expected dose $S(\tau|t, \mathbf{e}_{M1})$ to RMEI (mrem/yr) for LHS element $\mathbf{e}_1 = [\mathbf{e}_{A1}, \mathbf{e}_{M1}]$ and the time interval $[0, 10^6$ yr]: (a) $S(\tau|t_k, \mathbf{e}_{M1})$, $k = 1, 2, \ldots, 10$, (b) interpolated values $\hat{S}(\tau|\hat{t}_k, \mathbf{e}_{M1})$ for $\hat{t}_k$ between $t_8 = 200{,}000$ yr and $t_9 = 400{,}000$ yr, and (c) interpolated values $\hat{S}(\tau|\hat{t}_k, \mathbf{e}_{M1})$ for $\hat{t}_k$ between 250 yr and 10^6 yr. FJ-85

J7.3-12. Estimate of $\bar{D}_{IE}(\tau|\mathbf{e}_1)$ for LHS element $\mathbf{e}_1 = [\mathbf{e}_{A1}, \mathbf{e}_{M1}]$ and $0 \le \tau \le 10^6$ yr with integration-based procedure indicated in Equations J7.3-9 and J7.3-16. ..... FJ-86

J7.3-13. Estimate obtained with LHS of size $nLHS = 300$ showing epistemic uncertainty in expected dose $\bar{D}_{IE}(\tau|\mathbf{e})$ to RMEI for $0 \le \tau \le 10^6$ yr that results when only igneous eruptive events are considered: (a) expected dose $\bar{D}_{IE}(\tau|\mathbf{e}_i)$, $i = 1, 2, \ldots, nLHS = 300$, (b) expected dose $\bar{D}_{IE}(\tau|\mathbf{e}_i)$, $i = 1, 2, \ldots, 50$, (c) exceedance probabilities $p_E[D < \bar{D}_{IE}(\tau|\mathbf{e})]$ and quantiles $Q_q[\bar{D}_{IE}(\tau|\mathbf{e})]$, $q = 0.05$, 0.5 and 0.95, for $\tau = 500{,}000$ yr, and (d) expected (mean) dose $\bar{\bar{D}}_{IE}(\tau)$ and quantiles $Q_q[\bar{D}_{IE}(\tau|\mathbf{e})]$, $q = 0.05$, 0.5, 0.95. ..... FJ-87

J7.3-14. Summary of results obtained with LHS of size $nLHS = 300$ showing epistemic uncertainty in expected dose $\bar{D}_{IE}(\tau|\mathbf{e})$ to RMEI for $0 \le \tau \le 10^6$ yr that results when only igneous eruptive events are considered. FJ-88

J7.3-15. Estimates obtained with LHS of size $nLHS = 300$ of expected (mean) dose $\bar{\bar{D}}_{IE,r}(\tau)$ to RMEI for $0 \le \tau \le 10^6$ yr for individual radioactive species that result when only igneous eruptive events are considered. FJ-89

J7.3-16. Results associated with $D_{IE}(\tau|\mathbf{a}_{IE}, \mathbf{e}_{M1})$ for LHS element $\mathbf{e}_1 = [\mathbf{e}_{A1}, \mathbf{e}_{M1}]$ obtained with sampling-based (Monte Carlo) procedures: (a) CCDF for $D_{IE}(500{,}000$ yr$|\mathbf{a}_{IE}, \mathbf{e}_{M1})$ with exceedance probabilities $p_A[D < D_{IE}(500{,}000$ yr$|\mathbf{a}, \mathbf{e}_{M1})|\mathbf{e}_{A1}]$ defined in Equation J7.3-20, and (b) expected dose $\bar{D}_{IE}(500{,}000$ yr$|\mathbf{e}_1)$ associated with $D_{IE}(500{,}000$ yr$|\mathbf{a}_{IE}, \mathbf{e}_{M1})$ as defined in Equation J7.3-18. ..... FJ-90

J7.3-17. Results associated with $D_{IE}(500{,}000$ yr$|\mathbf{a}_{IE}, \mathbf{e}_M)$ obtained with sampling-based (Monte Carlo) procedures for an LHS of size $nLHS = 300$: (a) CCDFs

FIGURES (Continued)

Page

for $D_{IE}(10^4$ yr$|\mathbf{a}_{IE}, \mathbf{e}_{Mi})$ with exceedance probabilities $p_A[D < D_{IE}(500{,}000$ yr$|\mathbf{a}, \mathbf{e}_{Mi})|\mathbf{e}_{Ai}]$ defined in Equation J7.3-20 for $i = 1, 2, \ldots, nLHS = 300$, (b) CCDFs for $D_{IE}(500{,}000$ yr$|\mathbf{a}_{IE}, \mathbf{e}_{Mi})$ with exceedance probabilities $p_A[D < D_{IE}(500{,}000$ yr$|\mathbf{a}, \mathbf{e}_{Mi})|\mathbf{e}_{Ai}]$ defined in Equation J7.3-20 for $i = 1, 2, \ldots, 50$, and (c) expected (mean) CCDF and quantile curves, $q = 0.05, 0.5, 0.95$, for CCDFs in (a). FJ-91

J7.3-18. Assessment with replicated sampling of numerical error associated with use of an LHS of size $nLHS = 300$ to determine epistemic uncertainty in expected dose $\bar{\bar{D}}_{IE}(\tau)$ to RMEI for $0 \le \tau \le 10^6$ yr that results when only igneous eruptive events are considered: (a) Replicated estimates of expected (mean) dose $\bar{\bar{D}}_{IE}(\tau)$ and quantiles $Q_q[\bar{D}_{IE}(\tau|\mathbf{e})]$, $q = 0.05, 0.5, 0.95$, and (b) confidence intervals for estimates of expected (mean) dose $\bar{\bar{D}}_{IE}(\tau)$. FJ-92

J7.5-1. Box plots summarizing probabilities $p_A[\mathcal{A}_{II}(0, \tau)|\mathbf{e}_{Ai}]$, $p_A[\tilde{\mathcal{A}}_{II}(0, \tau)|\mathbf{e}_{Ai}]$, $p_A[\mathcal{A}_{IE}(0, \tau)|\mathbf{e}_{Ai}]$ and $p_A[\tilde{\mathcal{A}}_{IE}(0, \tau)|\mathbf{e}_{Ai}]$ for scenario classes $\mathcal{A}_{II}(0, \tau)$, $\tilde{\mathcal{A}}_{II}(0, \tau)$, $\mathcal{A}_{IE}(0, \tau)$ and $\tilde{\mathcal{A}}_{IE}(0, \tau)$ defined for the time intervals [0, 20,000 yr] and [0, 1,000,000 yr] obtained with LHS of size $nLHS = 300$. FJ-93

J8.3-1. Summary of results for damage to CDSP WPs obtained with LHS of size $nLHS = 300$ showing epistemic uncertainty in doses $D_{SG}(\tau|[1, t_r, A_S], \mathbf{e}_{Mi})$ for $0 \le \tau \le 20{,}000$ yr damaged area $A_S = (10^{-6})$ (32.6 m^2) and the following values for event time t_r: (a) 200 yr, (b) 1000 yr, (c) 3000 yr, (d) 6000 yr, (e) 12,000 yr, and (f) 18,000 yr. FJ-95

J8.3-2. Box plots (see Figure J6.2-3 for description) summarizing results for damage to CDSP WPs obtained with LHS of size $nLHS = 300$ showing epistemic uncertainty in dose $D_{SG}(\tau|[1, t_r, A_S], \mathbf{e}_{Mi})$ with $t_r = 200$, 1000, 3000, and 6000 yrs, $A_S = 10^{-8+s}$ (32.6 m^2) for $s = 1, 2, 3, 4, 5$, and $i = 1, 2, \ldots, nLHS = 300$, where 32.6 m^2 is the assumed surface area for a CDSP WP: (a) $t_r = 200$ yrs, (b) $t_r = 1000$ yrs, (c) $t_r = 3000$ yrs, and (d) $t_r = 6000$ yrs. FJ-96

J8.3-3. Illustration of interpolation procedure to obtain estimated integrals $\hat{I}_1(\tau|t, \mathbf{e}_{M1})$ from calculated doses $D_{SG}(\tau|[1, t_r, A_S], \mathbf{e}_{M1})$ indicated in Equation J8.3-9 for LHS element $\mathbf{e}_1 = [\mathbf{e}_{A1}, \mathbf{e}_{M1}]$ and the time interval $[0, 2.0 \times 10^4$ yr]: (a) $D_{SG}(\tau|[1, t_r, A_S], \mathbf{e}_{M1})$, $r = 1, 2, \ldots, 6$ and $s = 1, 2, \ldots, 5$, (b) $\hat{I}_1(\tau|t_r, \mathbf{e}_{M1})$, $r = 1, 2, \ldots, 6$, (c) interpolated values $\hat{I}_1(\tau|\hat{t}_k, \mathbf{e}_{M1})$ for $\hat{t}_k$ between $t_4 =$ 6000 yrs and $t_5 = 12{,}000$ yrs, and (d) interpolated values for $\hat{I}_1(\tau|\hat{t}_k, \mathbf{e}_1)$ for $\hat{t}_k$ between = 100 yrs and 20,000 yrs. FJ-97

J8.3-4. Estimate of $\bar{D}_{SG}(\tau|\mathbf{e}_1)$ for LHS element $\mathbf{e}_1 = [\mathbf{e}_{A1}, \mathbf{e}_{M1}]$ and $0 \le \tau \le 20{,}000$ yr with integration-based procedure indicated in Equation J8.3-13. ..... FJ-98

FIGURES (Continued)

Page

J8.3-5. Estimate obtained with LHS of size $nLHS = 300$ showing epistemic uncertainty in expected dose $\bar{D}_{SG}(\tau|\mathbf{e})$ to RMEI for $0 \le \tau \le 20{,}000$ yr that results when only seismic ground motion events are considered: (a) expected dose $\bar{D}_{SG}(\tau|\mathbf{e}_i)$, $i = 1, 2, \ldots, nLHS = 300$, (b) expected dose $\bar{D}_{SG}(\tau|\mathbf{e}_i)$, $i = 1, 2, \ldots, 50$, (c) exceedance probabilities $p_E[D < \bar{D}_{SG}(\tau|\mathbf{e})]$ and quantiles $Q_q[\bar{D}_{SG}(\tau|\mathbf{e})]$, $q = 0.05$, 0.5 and 0.95, for $\tau = 10^4$ yr, and (d) expected (mean) dose $\bar{\bar{D}}_{SG}(\tau)$ and quantiles $Q_q[\bar{D}_{SG}(\tau|\mathbf{e})]$, $q = 0.05$, 0.5, 0.95. ..... FJ-99

J8.3-6. Summary of results obtained with LHS of size $nLHS = 300$ showing epistemic uncertainty in expected dose $\bar{D}_{SG}(\tau|\mathbf{e})$ to RMEI for $0 \le \tau \le 20{,}000$ yr that results when only seismic ground motion events are considered. FJ-100

J8.3-7. Estimate obtained with LHS of size $nLHS = 300$ showing epistemic uncertainty in expected dose $\bar{D}_{SG,r}(\tau|\mathbf{e})$ to RMEI for $0 \le \tau \le 20{,}000$ yr with r corresponding to ^{99}Tc that results when only seismic ground motion events are considered: (a) expected dose $\bar{D}_{SG,r}(\tau|\mathbf{e}_i)$, $i = 1, 2, \ldots, nLHS = 300$, (b) expected dose $\bar{D}_{SG,r}(\tau|\mathbf{e}_i)$, $i = 1, 2, \ldots, 50$, (c) exceedance probabilities $p_E[D < \bar{D}_{SG,r}(\tau|\mathbf{e})]$ and quantiles $Q_q[\bar{D}_{SG,r}(\tau|\mathbf{e})]$, $q = 0.05$, 0.5 and 0.95, for $\tau = 10^4$ yr, and (d) expected (mean) dose $\bar{\bar{D}}_{SG,r}(\tau)$ and quantiles $Q_q[\bar{D}_{SG,r}(\tau|\mathbf{e})]$, $q =$ 0.05, 0.5, 0.95 ..... FJ-101

J8.3-8. Estimates obtained with LHS of size $nLHS = 300$ of expected (mean) dose $\bar{\bar{D}}_{SG,r}(\tau)$ to RMEI for $0 \le \tau \le 20{,}000$ yr for individual radioactive species that result when only seismic ground motion events are considered. FJ-102

J8.3-9. Results associated with $D_{SG}(\tau|\mathbf{a}_{SG}, \mathbf{e}_{M1})$ for LHS element $\mathbf{e}_1 = [\mathbf{e}_{A1}, \mathbf{e}_{M1}]$ obtained with sampling-based (Monte Carlo) procedures: (a) CCDF for $D_{SG}(10^4 \text{ yr}|\mathbf{a}_{SG}, \mathbf{e}_{M1})$ with exceedance probabilities $p_A[D < D_{SG}(10^4 \text{ yr}|\mathbf{a}, \mathbf{e}_{M1})|\mathbf{e}_1]$ defined in Equation J8.3-22, and (b) expected dose $\bar{D}_{SG}(10^4 \text{ yr}|\mathbf{e}_1)$ associated with $D_{SG}(10^4 \text{ yr}|\mathbf{a}_{SG}, \mathbf{e}_{M1})$ defined in Equation J8.3-20. ..... FJ-103

J8.3-10. Results associated with $D_{SG}(10^4 \text{ yr}|\mathbf{a}_{SG}, \mathbf{e}_M)$ obtained with sampling-based (Monte Carlo) procedures for an LHS of size $nLHS = 300$: (a) CCDFs for $D_{SG}(10^4 \text{ yr}|\mathbf{a}_{SG}, \mathbf{e}_{Mi})$ with exceedance probabilities $p_A[D < D_{SG}(10^4 \text{ yr}|\mathbf{a}, \mathbf{e}_{Mi})|\mathbf{e}_{Ai}]$ defined in Equation J4.5-19 for $i = 1, 2, \ldots, nLHS = 300$, (b) CCDFs for $D_{SG}(10^4 \text{ yr}|\mathbf{a}_{SG}, \mathbf{e}_{Mi})$ with exceedance probabilities $p_A[D < D_{SG}(10^4 \text{ yr}|\mathbf{a}, \mathbf{e}_{Mi})|\mathbf{e}_{Ai}]$ defined in Equation J4.5-19 for $i = 1, 2, \ldots, 50$, and (c) expected (mean) CCDF and quantile curves, $q = 0.05$, 0.5, 0.95, for CCDFs in (a). FJ-104

J8.3-11. Assessment with replicated sampling of numerical error associated with use of an LHS of size $nLHS = 300$ to determine epistemic uncertainty in expected dose $\bar{D}_{SG}(\tau|\mathbf{e})$ to RMEI for $0 \le \tau \le 20{,}000$ yr that results when only seismic

FIGURES (Continued)

Page

ground motion events are considered: (a) Replicated estimates of expected (mean) dose $\bar{\bar{D}}_{SG}(\tau)$ and quantiles $Q_q[\bar{D}_{SG}(\tau|\mathbf{e})]$, q = 0.05, 0.5, 0.95, and (b) confidence intervals for estimates of expected (mean) dose $\bar{\bar{D}}_{SG}(\tau)$..... FJ-105

J8.4-1. Doses $D_{SG}(\tau|\mathbf{a}_{SG,ik}, \mathbf{e}_{Mi})$, k = 1, 2, …, nR = 30, and estimated expected doses $\bar{D}_{SG}(\tau|\mathbf{e}_i)$ to the RMEI for $0 \le \tau \le 10^6$ yr for selected LHS elements $\mathbf{e}_i = [\mathbf{e}_{Ai}, \mathbf{e}_{Mi}]$ when only nominal processes and seismic ground motion events are considered: (a) $\mathbf{e}_1$, (b) $\mathbf{e}_2$, (c) $\mathbf{e}_3$, (d) $\mathbf{e}_4$, (e) $\mathbf{e}_5$, and (f) $\mathbf{e}_6$. FJ-106

J8.4-2. Estimate obtained with LHS of size $nLHS$ = 300 showing epistemic uncertainty in expected dose $\bar{D}_{SG}(\tau|\mathbf{e})$ to RMEI for $0 \le \tau \le 10^6$ yr that results when only nominal processes and seismic ground events are considered: (a) expected dose $\bar{D}_{SG}(\tau|\mathbf{e}_i)$, i = 1, 2, …, $nLHS$ = 300, (b) expected dose $\bar{D}_{SG}(\tau|\mathbf{e}_i)$, i = 1, 2, …, 50, (c) exceedance probabilities $p_E[D < \bar{D}_{SG}(\tau|\mathbf{e})]$ and quantiles $Q_q[\bar{D}_{SG}(\tau|\mathbf{e})]$, q = 0.05, 0.5 and 0.95, for τ = 500,000 yr, and (d) expected (mean) dose $\bar{\bar{D}}_{SG}(\tau)$ and quantiles $Q_q[\bar{D}_{SG}(\tau|\mathbf{e})]$, q = 0.05, 0.5, 0.95..... FJ-107

J8.4-3. Summary of results obtained with LHS of size $nLHS$ = 300 showing epistemic uncertainty in expected dose $\bar{D}_{SG}(\tau|\mathbf{e})$ to RMEI for $0 \le \tau \le 10^6$ yr that results when only nominal processes and seismic ground events are considered. FJ-108

J8.4-4. Estimate obtained with LHS of size $nLHS$ = 300 showing epistemic uncertainty in expected dose $\bar{D}_{SG,r}(\tau|\mathbf{e}$ to RMEI for $0 \le \tau \le 10^6$ yr with r corresponding to ^{99}Tc that results when only nominal processes and seismic ground events are considered: (a) expected dose $\bar{D}_{SG,r}(\tau|\mathbf{e}_i)$, i = 1, 2, …, $nLHS$ = 300, (b) expected dose $\bar{D}_{SG,r}(\tau|\mathbf{e}_i)$, i = 1, 2, …, 50, (c) exceedance probabilities $p_E[D < \bar{D}_{SG,r}(\tau|\mathbf{e})]$ and quantiles $Q_q[\bar{D}_{SG,r}(\tau|\mathbf{e})]$, q = 0.05, 0.5 and 0.95, for τ = 500,000 yr, and (d) expected (mean) dose $\bar{\bar{D}}_{SG,r}(\tau)$ and quantiles $Q_q[\bar{D}_{SG,r}(\tau|\mathbf{e})]$, q = 0.05, 0.5, 0.95. ..... FJ-109

J8.4-5. Estimates obtained with LHS of size $nLHS$ = 300 of expected (mean) dose $\bar{\bar{D}}_{SG,r}(\tau)$ to RMEI for $0 \le \tau \le 10^6$ yr for individual radioactive species that result when only nominal proceses and seismic ground events are considered. . FJ-110

J8.4-6. Assessment with replicated sampling of numerical error associated with use of an LHS of size $nLHS$ = 300 to determine epistemic uncertainty in expected dose $\bar{D}_{SG}(\tau|\mathbf{e})$ to RMEI for $0 \le \tau \le 10^6$ yr that results when only nominal processes and seismic ground motion events are considered: (a) Replicated estimates of expected (mean) dose $\bar{\bar{D}}_{SG}(\tau)$ and quantiles $Q_q[\bar{D}_{SG}(\tau|\mathbf{e})]$, q = 0.05, 0.5, 0.95, and (b) confidence intervals for estimates of expected (mean) dose $\bar{\bar{D}}_{SG}(\tau)$. FJ-111

FIGURES (Continued)

Page

J8.6-1. Summary of results for fault displacement damage of CSNF and CDSP WPs obtained with LHS of size $nLHS = 300$ showing epistemic uncertainty in doses $D_{SF,r}(\tau|[1, t_j, 100, A_r/3, \sim]|\mathbf{e}_{Mi})$ for $0 \le \tau \le 20{,}000$ yr, $r = 1, 2$, with 1 ~ CSNF WPs and $r = 2$ ~ CDSP WPs, $A_1 = 2.78$ m^2 and $A_2 = 3.28$ m^2, and $i = 1, 2, \ldots, nLHS = 300$: (a, c, e) CSNF WPs for $t_j = 200$, 2000 and 8000 yrs and (b, d, f) CDSP WPs for $t_j = 200$, 2000 and 8000 yrs. FJ-112

J8.6-2. Box plots (see Figure J6.2-3 for description) summarizing results for fault displacement damage to CSNF and CDSP WPs obtained with LHS of size $nLHS = 300$ showing epistemic uncertainty in dose $D_{SF,r}(10^4$ yr$|[1, t_j, 100, A_{rk}, \sim]|\mathbf{e}_{Mi})$ for $t_j = 200$, 2000, 4000 and 8000 yrs, $r = 1, 2$, with 1 ~ CSNF WPs and $r = 2$ ~ CDSP WPs, $A_{rk} = A_r/3, 2A_r/3, A_r$, with $A_1 = 2.78$ m^2 and $A_2 = 3.28$ m^2, and $i = 1, 2, \ldots, nLHS = 300$: (a) $t_j = 200$ yr, (b) $t_j = 2000$ yr, (c) $t_j = 4000$ yr, and (d) $t_j = 8000$ yr. FJ-113

J8.6-3. Illustration of interpolation procedure to estimate integrals $\hat{I}_r(\tau|t, \mathbf{e}_{Mi})$ and expected dose $\bar{D}_{SF}(\tau|\mathbf{e}_i)$ from calculated doses $D_{SF,r}(\tau|[1, t_j, 100, A_{rk}, 1, \sim], \mathbf{e}_{Mi})$ in Equation J8.6-18 for LHS element $\mathbf{e}_1 = [\mathbf{e}_{A1}, \mathbf{e}_{M1}]$ and the time interval $[0, 2.0 \times 10^4$ yr]: (a) $D_{SF,1}(\tau|[1, t_j, 100, A_{rk}, 1, \sim], \mathbf{e}_{M1})$ for $j = 1, 2, \ldots, 6$ and $k = 1, 2, 3$ (Notes: Results overlay for A_{1k}, $k = 1, 2, 3$, for each t_j, and results for t_1 and t_2 also overlay), (b) Interpolated values $\hat{I}_1(\tau|\hat{t}_k, \mathbf{e}_{M1})$ for $\hat{t}_k$ between $t_4 =$ 4000 yr and $t_5 = 8000$ yr, (c) Interpolated values for $\hat{I}_1(\tau|\hat{t}_k, \mathbf{e}_{M1})$ for $\hat{t}_k$ between 200 and 20,000 yr, and (d) estimates for $\bar{D}_{SF,1}(\tau|\mathbf{e}_i)$ for CSNF WPs, $\bar{D}_{SF,2}(\tau|\mathbf{e}_i)$ for CDSP WPs and $\bar{D}_{SF}(\tau|\mathbf{e}_i)$ for CSNF and CDSP WPs. FJ-114

J8.6-4. Estimate of $\bar{D}_{SF}(\tau|\mathbf{e}_1)$ for LHS element $\mathbf{e}_1 = [\mathbf{e}_{A1}, \mathbf{e}_{M1}]$ and $0 \le \tau \le 20{,}000$ yr with integration-based procedure indicated in Equations J8.6-17 and J8.6-25..... FJ-115

J8.6-5. Estimate obtained with LHS of size $nLHS = 300$ showing epistemic uncertainty in expected dose $\bar{D}_{SF}(\tau|\mathbf{e})$ to RMEI for $0 \le \tau \le 20{,}000$ yr that at results when only fault displacement events are considered: (a) expected dose $\bar{D}_{SF}(\tau|\mathbf{e}_i)$, $i = 1, 2, \ldots, nLHS = 300$, (b) expected dose $\bar{D}_{SF}(\tau|\mathbf{e}_i)$, $i = 1, 2, \ldots, 50$, (c) exceedance probabilities $p_E[D < \bar{D}_{SG}(\tau|\mathbf{e})]$ and quantiles $Q_q[\bar{D}_{SF}(\tau|\mathbf{e})]$, $q = 0.05$, 0.5 and 0.95, for $\tau = 10^4$ yr, and (d) expected (mean) dose $\bar{\bar{D}}_{SF}(\tau)$ and quantiles $Q_q[\bar{D}_{SF}(\tau|\mathbf{e})]$, $q = 0.05$, 0.5, 0.95. ..... FJ-116

J8.6-6. Summary of results obtained with LHS of size $nLHS = 300$ showing epistemic uncertainty in expected dose $\bar{D}_{SF}(\tau|\mathbf{e})$ to RMEI for $0 \le \tau \le 20{,}000$ yr that results when only fault displacement events are considered. FJ-117

J8.6-7. Estimate obtained with LHS of size $nLHS = 300$ showing epistemic uncertainty in expected dose $\bar{D}_{SF,r}(\tau|\mathbf{e})$ to RMEI for $0 \le \tau \le 20{,}000$ yr with r

FIGURES (Continued)

Page

corresponding to ^{99}Tc that results when only fault displacement events are considered: (a) expected dose $\bar{D}_{SF,r}(\tau|\mathbf{e}_i)$, i = 1, 2, …, $nLHS$ = 300, (b) expected dose $\bar{D}_{SF,r}(\tau|\mathbf{e}_i)$, i = 1, 2, …, 50, (c) exceedance probabilities $p_E[D < \bar{D}_{SG,r}(\tau|\mathbf{e})]$ and quantiles $Q_q[\bar{D}_{SF,r}(\tau|\mathbf{e})]$, q = 0.05, 0.5 and 0.95, for $\tau = 10^4$ yr, and (d) expected (mean) dose $\bar{\bar{D}}_{SF,r}(\tau)$ and quantiles $Q_q[\bar{D}_{SF,r}(\tau|\mathbf{e})]$, q = 0.05, 0.5, 0.95 ..... FJ-118

J8.6-8. Estimates obtained with LHS of size $nLHS$ = 300 of expected (mean) dose $\bar{\bar{D}}_{SF,r}(\tau)$ to RMEI for $0 \le \tau \le 20{,}000$ yr for individual radioactive species that result when only seismic ground motion events are considered. FJ-119

J8.6-9. Results associated with $D_{SF}(\tau|\mathbf{a}_{SF}, \mathbf{e}_{M1})$ for LHS element $\mathbf{e}_1 = [\mathbf{e}_{A1}, \mathbf{e}_{M1}]$ obtained with sampling-based (Monte Carlo) procedures: (a) CCDF for $D_{SF}(10^4 \text{ yr}|\mathbf{a}_{SF}, \mathbf{e}_{M1})$ with exceedance probabilities $p_A[D < D_{SF}(10^4 \text{ yr}|\mathbf{a}, \mathbf{e}_{M1})|\mathbf{e}_{A1}]$ defined in Equations J4.5-19 and J8.6-36, and (b) expected dose $\bar{D}_{SF}(10^4 \text{ yr}|\mathbf{e}_1)$ associated with $D_{SF}(10^4|\mathbf{a}_{SF}, \mathbf{e}_{M1})$ as defined in Equation J4.5-20. ..... FJ-120

J8.6-10. Results associated with $D_{SF}(10^4 \text{ yr}|\mathbf{a}_{SF}, \mathbf{e}_M)$ obtained with sampling-based (Monte Carlo) procedures for an LHS of size $nLHS$ = 300: (a) CCDFs for $D_{SF}(10^4 \text{ yr}|\mathbf{a}_{SF}, \mathbf{e}_{Mi})$ with exceedance probabilities $p_A[D < D_{SF}(10^4 \text{ yr}|\mathbf{a}, \mathbf{e}_{Mi})|\mathbf{e}_{Ai}]$ defined in Equation J4.5-19 for i = 1, 2, …, $nLHS$ = 300, (b) CCDFs for $D_{SF}(10^4 \text{ yr}|\mathbf{a}_{SF}, \mathbf{e}_{Mi})$ with exceedance probabilities $p_A[D < D_{SF}(10^4 \text{ yr}|\mathbf{a}, \mathbf{e}_{Mi})|\mathbf{e}_{Ai}]$ defined in Equation J4.5-19 for i = 1, 2, …, 50, and (c) expected (mean) CCDF and quantile curves, q = 0.05, 0.5, 00.95, for CCDFs in (a). FJ-121

J8.6-11. Assessment with replicated sampling of numerical error associated with use of an LHS of size $nLHS$ = 300 to determine epistemic uncertainty in expected dose $\bar{D}_{SF}(\tau|\mathbf{e})$ to RMEI for $0 \le \tau \le 20{,}000$ yr that results when only seismic ground motion events are considered: (a) Replicated estimates of expected (mean) dose $\bar{\bar{D}}_{SF}(\tau)$ and quantiles $Q_q[\bar{D}_{SF}(\tau|\mathbf{e})]$, q = 0.05, 0.5, 0.95, and (b) confidence intervals for estimates of expected (mean) dose $\bar{\bar{D}}_{SF}(\tau)$. FJ-122

J8.6-12. Summary of results for fault displacement damage of CSNF and CDSP WPs obtained with LHS of size $nLHS$ = 300 showing epistemic uncertainty in doses $D_{SF,r}(\tau|[1, t_j, 100, A_r/3, \sim], \mathbf{e}_{Mi})$ for $0 \le \tau \le 20{,}000$ yr, r = 1, 2, with r = 1 ~ CSNF WPs and r = 2 ~ CDSP WPs, A_1 = 2.78 m^2 and A_2 = 3.28 m^2 and i = 1, 2, …, $nLHS$ = 300: (a, c, e) CSNF WPs for t_j = 1000, 80,000 and 200,000 yrs and (b, d, f) CDSP WPs for t_j = 1000, 80,000 and 200,000 yrs. FJ-123

J8.6-13. Box plots (see Figure J6.2-3 for description) summarizing results for fault displacement damage to CSNF and CDSP WPs obtained with LHS of size

FIGURES (Continued)

Page

nLHS = 300 showing epistemic uncertainty in dose $D_{SF,r}(10^4$ yr$|[1, t_j, 100, A_{rk}, \sim], \mathbf{e}_{Mi})$ for t_j =1000, 80,000, 200,000 and 400,000 yrs, r = 1, 2 with r = 1 ~ CSNF WPs and r = 2 ~ CDSP WPs, $A_{rk} = A_r/3, 2A_r/3, A_r$, with A_1 = 2.78 m^2 A_2 = 3.28 m^2, and i = 1, 2, …, *nLHS* = 300: (a) t_j = 1000 yr, (b) t_j = 80,000 yr, (c) t_j = 200,000 yr, and (d) t_j = 400,000 yr..... FJ-124

J8.6-14. Illustration of interpolation procedure to estimate integrals $\hat{I}_r(\tau|t, \mathbf{e}_{M1})$ and expected dose $\bar{D}_{SF}(\tau|\mathbf{e}_i)$ from calculated doses $D_{SF,r}(\tau|[1, t_j, 100, A_{rk}, 1, \sim], \mathbf{e}_{M1})$ in Equation J8.6-18 for LHS element $\mathbf{e}_1 = [\mathbf{e}_{A1}, \mathbf{e}_{M1}]$ and the time interval [0, 1.0 × 10^6 yr]: (a) $D_{SF,1}(\tau|[1, t_j, 100, A_{rk}, 1, \sim], \mathbf{e}_{M1})$ for j = 1, 2, …, 6 and k = 1, 2, 3 (Notes: Results overlay for A_{1k}, k = 1, 2, 3, for each t_j, and results for t_1 and t_2 also overlay), (b) Interpolated values $\hat{I}_1(\tau|\hat{t}_k, \mathbf{e}_{M1})$ for $\hat{t}_k$ between $t_4 = 2.0 \times 10^5$ yr and $t_5 = 4.0 \times 10^5$ yr, (c) Interpolated values for $\hat{I}_1(\tau|\hat{t}_k, \mathbf{e}_{M1})$ for $\hat{t}_k$ between 1000 and 1.0 × 10^6 yr, and (d) estimates for $\bar{D}_{SF,1}(\tau|\mathbf{e}_i)$ for CSNF WPs, $\bar{D}_{SF,2}(\tau|\mathbf{e}_i)$ for CDSP WPs and $\bar{D}_{SF}(\tau|\mathbf{e}_i)$ for CSNF and CDSP WPs. FJ-125

J8.6-15. Estimate of $\bar{D}_{SF}(\tau|\mathbf{e}_1)$ for LHS element $\mathbf{e}_1 = [\mathbf{e}_{A1}, \mathbf{e}_{M1}]$ and $0 \le \tau \le 10^6$ yr with integration-based procedure indicated in Equations J8.6-17 and J8.6-25..... FJ-126

J8.6-16. Estimate obtained with LHS of size *nLHS* = 300 showing epistemic uncertainty in expected dose $\bar{D}_{SF}(\tau|\mathbf{e})$ to RMEI for $0 \le \tau \le 10^6$ yr that at results when only fault displacement events are considered: (a) expected dose $\bar{D}_{SF}(\tau|\mathbf{e}_i)$, i = 1, 2, …, *nLHS* = 300, (b) expected dose $\bar{D}_{SF}(\tau|\mathbf{e}_i)$, i = 1, 2, …, 50, (c) exceedance probabilities $p_E[D < \bar{D}_{SG}(\tau|\mathbf{e})]$ and quantiles $Q_q[\bar{D}_{SF}(\tau|\mathbf{e})]$, q = 0.05, 0.5 and 0.95, for $\tau = 5 \times 10^5$ yr, and (d) expected (mean) dose $\bar{\bar{D}}_{SF}(\tau)$ and quantiles $Q_q[\bar{D}_{SF}(\tau|\mathbf{e})]$, q = 0.05, 0.5, 0.95. ..... FJ-127

J8.6-17. Summary of results obtained with LHS of size *nLHS* = 300 showing epistemic uncertainty in expected dose $\bar{D}_{SF}(\tau|\mathbf{e})$ to RMEI for $0 \le \tau \le 10^6$ yr that results when only fault displacement events are considered. FJ-128

J8.6-18. Estimate obtained with LHS of size *nLHS* = 300 showing epistemic uncertainty in expected dose $\bar{D}_{SF,r}(\tau|\mathbf{e})$ to RMEI for $0 \le \tau \le 10^6$ yr with r corresponding to ^{242}Pu that results when only fault displacement events are considered: (a) expected dose $\bar{D}_{SF,r}(\tau|\mathbf{e}_i)$, i = 1, 2, …, *nLHS* = 300, (b) expected dose $\bar{D}_{SF,r}(\tau|\mathbf{e}_i)$, i = 1, 2, …, 50, (c) exceedance probabilities $p_E[D < \bar{D}_{SG,r}(\tau|\mathbf{e})]$ and quantiles $Q_q[\bar{D}_{SF,r}(\tau|\mathbf{e})]$, q = 0.05, 0.5 and 0.95, for τ = 500,000 yr, and (d) expected (mean) dose $\bar{\bar{D}}_{SF,r}(\tau)$ and quantiles $Q_q[\bar{D}_{SF,r}(\tau|\mathbf{e})]$, q = 0.05, 0.5, 0.95. ..... FJ-129

FIGURES (Continued)

Page

J8.6-19. Estimates obtained with LHS of size $nLHS = 300$ of expected (mean) dose $\bar{\bar{D}}_{SF,r}(\tau)$ to RMEI for $0 \le \tau \le 10^6$ yr for individual radioactive species that result when only seismic ground motion events are considered. FJ-130

J8.6-20. Results associated with $D_{SF}(\tau|\mathbf{a}_{SF}, \mathbf{e}_{M1})$ for LHS element $\mathbf{e}_1 = [\mathbf{e}_{A1}, \mathbf{e}_{M1}]$ obtained with sampling-based (Monte Carlo) procedures: (a) CCDF for $D_{SF}(5 \times 10^5 \text{ yr}|\mathbf{a}_{SF}, \mathbf{e}_{M1})$ with exceedance probabilities $p_A[D < D_{SF}(5 \times 10^5 \text{ yr}|\mathbf{a}, \mathbf{e}_{M1})|\mathbf{e}_{A1}]$ defined in Equations J4.5-19 and J8.6-36, and (b) expected dose $\bar{D}_{SF}(5 \times 10^5 \text{ yr}|\mathbf{e}_1)$ associated with $D_{SF}(5 \times 10^5 \text{ yr}|\mathbf{a}_{SF}, \mathbf{e}_{M1})$ defined in Equation J4.5-20. ..... FJ-131

J8.6-21. Results associated with $D_{SG}(5 \times 10^5 \text{ yr}|\mathbf{a}_{SF}, \mathbf{e}_{M})$ obtained with sampling-based (Monte Carlo) procedures for an LHS of size $nLHS = 300$: (a) CCDFs for $D_{SF}(5 \times 10^5 \text{ yr}|\mathbf{a}_{SF}, \mathbf{e}_{Mi})$ with exceedance probabilities $p_A[D < D_{SF}(5 \times 10^5 \text{ yr}|\mathbf{a}, \mathbf{e}_{Mi})|\mathbf{e}_{Ai}]$ defined in Equation J4.5-19 for $i = 1, 2, \ldots, nLHS = 300$, (b) CCDFs for $D_{SF}(10^4 \text{ yr}|\mathbf{a}_{SF}, \mathbf{e}_{Mi})$ with exceedance probabilities $p_A[D < D_{SF}(5 \times 10^5 \text{ yr}|\mathbf{a}, \mathbf{e}_{Mi})|\mathbf{e}_{Ai}]$ defined in Equation J4.5-19 for $i = 1, 2, \ldots, 50$, and (c) expected (mean) CCDF and quantile curves, $q = 0.05, 0.5, 00.95$, for CCDFs in (a). FJ-132

J8.6-22. Assessment with replicated sampling of numerical error associated with use of an LHS of size $nLHS = 300$ to determine epistemic uncertainty in expected dose $\bar{D}_{SF}(\tau|\mathbf{e})$ to RMEI for $0 \le \tau \le 10^6$ yr that results when only seismic ground motion events are considered: (a) Replicated estimates of expected (mean) dose $\bar{\bar{D}}_{SF}(\tau)$ and quantiles $Q_q[\bar{D}_{SF}(\tau|\mathbf{e})]$, $q = 0.05, 0.5, 0.95$, and (b) confidence intervals for estimates of expected (mean) dose $\bar{\bar{D}}_{SF}(\tau)$. FJ-133

J9.2-1. Estimate obtained with LHS of size $nLHS = 300$ showing epistemic uncertainty in expected dose $\bar{D}(\tau|\mathbf{e})$ to RMEI for $0 \le \tau \le 20{,}000$ yr that results when all futures are considered: (a) expected dose $\bar{D}(\tau|\mathbf{e}_i)$, $i = 1, 2, \ldots, nLHS = 300$, (b) expected dose $\bar{D}(\tau|\mathbf{e}_i)$, $i = 1, 2, \ldots, 50$, (c) exceedance probabilities $p_E[D < \bar{D}(\tau|\mathbf{e})]$ and quantiles $Q_q[\bar{D}(\tau|\mathbf{e})]$, $q = 0.05, 0.5$ and 0.95, for $\tau = 10^4$ yr, and (d) expected (mean) dose $\bar{\bar{D}}(\tau)$ and quantiles $Q_q[\bar{D}(\tau|\mathbf{e})]$, $q = 0.05, 0.5, 0.95$ FJ-135

J9.2-2. Summary of results obtained with LHS of size $nLHS = 300$ showing epistemic uncertainty in expected dose $\bar{D}(\tau|\mathbf{e})$ to RMEI for $0 \le \tau \le 20{,}000$ yr that results when all futures are considered. FJ-136

J9.2-3. Estimates obtained with LHS of size $nLHS = 300$ of expected (mean) dose $\bar{\bar{D}}_{r}(\tau)$ to RMEI for $0 \le \tau \le 20{,}000$ yr for individual radioactive species that result when all futures are considered. FJ-137

FIGURES (Continued)

Page

J9.2-4. Assessment with replicated sampling of numerical error associated with use of an LHS of size *nLHS* = 300 to determine epistemic uncertainty in expected dose $\bar{D}(\tau|\mathbf{e})$ to RMEI for $0 \le \tau \le 20{,}000$ yr that results when all futures are considered: (a) Replicated estimates of expected (mean) dose $\bar{\bar{D}}(\tau)$ and quantiles $Q_q[\bar{D}(\tau|\mathbf{e})]$, q = 0.05, 0.5, 0.95, and (b) confidence intervals for estimates of expected (mean) dose $\bar{\bar{D}}(\tau)$. FJ-138

J9.3-1. Estimate obtained with LHS of size *nLHS* = 300 showing epistemic uncertainty in expected dose $\bar{D}(\tau|\mathbf{e})$ to RMEI for $0 \le \tau \le 1{,}000{,}000$ yr that results when all futures are considered: (a) expected dose $\bar{D}(\tau|\mathbf{e}_i)$, i = 1, 2, …, *nLHS* = 300, (b) expected dose $\bar{D}(\tau|\mathbf{e}_i)$, i = 1, 2, …, 50, (c) exceedance probabilities $p_E[D < \bar{D}(\tau|\mathbf{e})]$ and quantiles $Q_q[\bar{D}(\tau|\mathbf{e})]$, q = 0.05, 0.5 and 0.95, for $\tau = 10^4$ yr, and (d) expected (mean) dose $\bar{\bar{D}}(\tau)$ and quantiles $Q_q[\bar{D}(\tau|\mathbf{e})]$, q = 0.05, 0.5, 0.95 ..... FJ-139

J9.3-2. Summary of results obtained with LHS of size *nLHS* = 300 showing epistemic uncertainty in expected dose $\bar{D}(\tau|\mathbf{e})$ to RMEI for $0 \le \tau \le 1{,}000{,}000$ yr that results when all futures are considered. FJ-140

J9.3-3. Estimates obtained with LHS of size *nLHS* = 300 of expected (mean) dose $\bar{D}_r(\tau)$ to RMEI for $0 \le \tau \le 1{,}000{,}000$ yr for individual radioactive species that result when all futures are considered. FJ-141

J9.3-4. Assessment with replicated sampling of numerical error associated with use of an LHS of size *nLHS* = 300 to determine epistemic uncertainty in expected dose $\bar{D}(\tau|\mathbf{e})$ to RMEI for $0 \le \tau \le 1{,}000{,}000$ yr that results when all futures are considered: (a) Replicated estimates of expected (mean) dose $\bar{\bar{D}}(\tau)$ and quantiles $Q_q[\bar{D}(\tau|\mathbf{e})]$, q = 0.05, 0.5, 0.95, and (b) confidence intervals for estimates of expected (mean) dose $\bar{D}(\tau|\mathbf{e})$. FJ-142

J11.2-1. Estimate obtained with LHS of size *nLHS* = 300 showing epistemic uncertainty in expected dose $\bar{D}_{HI}(\tau|\mathbf{e})$ to RMEI for $0 \le \tau \le 1{,}000{,}000$ yr that results from a single drilling intrusion at 200,000 years. FJ-143

J11.2-2. Assessment with replicated sampling of numerical error associated with use of an LHS of size *nLHS* = 300 to determine epistemic uncertainty in expected dose $\bar{D}_{HI}(\tau|\mathbf{e})$ to RMEI for $0 \le \tau \le 1{,}000{,}000$ yr that results from a single drilling intrusion at 200,000 years: (a) Replicated estimates of expected (mean) dose $\bar{\bar{D}}_{HI}(\tau)$ and quantiles $Q_q[\bar{D}_{HI}(\tau|\mathbf{e})]$, q = 0.05, 0.5, 0.95, and (b) confidence intervals for estimates of expected (mean) dose $\bar{\bar{D}}_{HI}(\tau)$. FJ-144

K2-1. Illustration of uncertainty and sensitivity analysis results for time-dependent number of failed CSNF WPs in percolation bin 3 under nominal conditions: (a) *NCSFL* for all (i.e., 300) sample elements, (b) PRCCs for *NCSFL*, (c) stepwise rank regressions for *NCSFL* at 600,000, 800,000 and 1,000,000 years, and (d, e) scatterplots for (*WDGA22*, *NCSFL*) at 600,000 and 1,000,000 years. FK-1

FIGURES (Continued)

Page

K4.2-1. Uncertainty and sensitivity analysis results for DS failure time (*DSFLTM*, yr) under nominal conditions: (a) CCDF for *DSFLTM*, (b) Stepwise rank regression for *DSFLTM*, and (c,d,e) Selected scatterplots for *DSFLTM*. FK-2

K4.2-2. Time-dependent numbers of failed CSNF WPs (*NCSFL*) and failed CDSP WPs (*NCDFL*) in percolation bin 3 under nominal conditions: (a, b) *NCSFL* and *NCDFL* for all (i.e., 300) sample elements, (c, d) *NCSFL* and *NCDFL* for first 50 sample elements, and (e, f) PRCCs for *NCSFL* and *NCDFL* FK-3

K4.2-3. Stepwise rank regression analyses and selected scatterplots for number of failed CSNF WPs (*NCSFL*) in percolation bin 3 under nominal conditions: (a) Regressions for *NCSFL* at 6×10^5, 8×10^5 and 1×10^6 years, and (b, c, d) Scatterplots for *NCSFL* at 6×10^5, 8×10^5 and 1×10^6 years FK-4

K4.2-4. Time-dependent numbers of failed CSNF WPs experiencing dripping conditions (*NCSFLAD*) and nondripping conditions (*NCSFLND*) in percolation bin 3 under nominal conditions: (a, b) *NCSFLAD* and *NCSFLND* for all (i.e., 300) sample elements, (c, d) *NCSFLAD* and *NCSFLND* for first 50 sample elements, and (e, f) PRCCs for *NCSFLAD* and *NCSFLND*. FK-5

K4.2-5. Stepwise rank regression analyses and selected scatterplots for numbers of failed CSNF WPs experiencing dripping conditions (*NCSFLAD*) and nondripping conditions (*NCSFLND*) in percolation bin 3 under nominal conditions: (a, b) Regressions for *NCSFLAD* and *NCSFLND* at 6×10^5, 8×10^5 and 1×10^6 years, and (c, d, e, f) Scatterplots for *NCSFLAD* and *NCSFLND* at 8×10^5 years, and (g, h) Scatterplots comparing *NCSFLAD* and *NCSFLND* at 6×10^5 and 8×10^5 years. FK-6

K4.2-6. Time-dependent average breached area on failed CSNF WPs experiencing dripping conditions (*BACSFLAD*) and nondripping conditions (*BACSFLND*) in percolation bin 3 under nominal conditions: (a) *BACSFLAD* for all (i.e., 300) sample elements, (b) *BACSFLAD* for first 50 sample elements, (c) PRCCs for *BACSFLAD*, and (d) Scatterplot comparing *BACSFLAD* and *BACSFLND* at 1×10^6 years. FK-8

K4.2-7. Stepwise rank regression analyses and selected scatterplots for average breached area on failed CSNF WPs experiencing dripping conditions (*BACSFLAD*) in percolation bin 3 under nominal conditions: (a) Regressions for *BACSFLAD* at 6×10^5, 8×10^5 and 1×10^6 years, and (b, c) Scatterplots for *BACSFLAD* and *NCSFLND* at 8×10^5 years. FK-9

K4.3-1. Time-dependent seepage rates (m^3/yr/WP) into the repository above CSNF WPs (*SPRATECS*) and CDSP WPs (*SPRATECD*) in percolation bin 3 under nominal conditions: (a, b) *SPRATECS* and *SPRATECD* for all (i.e., 300) sample elements, (c, d) *SPRATECS* and *SPRATECD* for first 50 sample elements, and (e, f) PRCCs for *SPRATECS* and *SPRATECD*. FK-10

K4.3-2. Stepwise rank regression analyses and selected scatterplots for seepage rate (m^3/yr/WP) into the repository above CSNF WPs (*SPRATECS*) in percolation bin 3 under nominal conditions: (a) Regressions for *SPRATECS*

FIGURES (Continued)

Page

at 1000, 5000 and 100,000 years, and (b, c, d, e) Scatterplots for *SPRATECS* at 1000 years. FK-11

K4.3-3. Time-dependent seepage rates (m^3/yr/WP) into the repository above CSNF WPs (*SPRATECS*) in percolation bins 1, 2, 4 and 5 under nominal conditions: (a, c, e, g) *SPRATECS* for all (i.e., 300) sample elements, and (b, d, f, h) *SPRATECS* for first 50 sample elements FK-12

K4.3-4. Time-dependent seepage rates (m^3/yr/WP) into the repository above CDSP WPs (*SPRATECD*) in percolation bins 1, 2, 4 and 5 under nominal conditions: (a, c, e, g) *SPRATECD* for all (i.e., 300) sample elements, and (b, d, f, h) *SPRATECD* for first 50 sample elements..... FK-13

K4.3-5. Time-dependent temperatures in percolation bin 3 under nominal conditions for CSNF WPs at the drift wall (*TMPCSWL*), on the WP (*TMPCSWP*) and in the invert beneath the WP (*TMPCSINV*) and similarly for CDSP WPs at the drift wall (*TMPCDWL*), on the WP (*TMPCDWP*) and in the invert beneath the WP (*TMPCDINV*): (a, c, e) *TMPCSWL*, *TMPCSWP* and *TMPCSINV*, and (b, d, f) *TMPCDWL*, *TMPCDWP* and *TMPCDINV* FK-14

K4.3-6. Time-dependent relative humidities in percolation bin 3 under nominal conditions for CSNF WPs on the WP (*RHCSWP*) and in the invert beneath the WP (*RHCSINV*) and similarly for CDSP WPs on the WP (*RHCDWP*) and in the invert beneath the WP (*RHCDINV*): (a, c) *RHCSWP* and *RHCSINV*, and (b, d) *RHCDWP* and *RHCDINV* FK-15

K4.3-7. Time-dependent partial pressures for CO_2 (bars) in the invert for dripping conditions for CSNF WPs (*PCO2CSIA*) and CDSP WPs (*PCO2CDIA*) in percolation bin 3 under nominal conditions: (a, b) *PCO2CSIA* and *PCO2CDIA* for all (i.e., 300) sample elements, (c, d) *PCO2CSIA* and *PCO2CDIA* for first 50 sample elements, and (e, f) PRCCs for *PCO2CSIA* and *PCO2CDIA* FK-16

K4.3-8. Stepwise rank regression analyses and selected scatterplots for CO_2 partial pressure (bars) in the invert under dripping conditions for CSNF WPs (*PCO2CSIA*) in percolation bin 3 under nominal conditions: (a) Regressions for *PCO2CSIA* at 1000, 5000 and 10,000 years, and (b, c) Scatterplots for *PCO2CSIA* at 1000 and 10,000 years. FK-17

K4.3-9. Time-dependent ionic strength (mol/kg) in the invert for CSNF WPs experiencing nondripping conditions (*ISCSINND*) and dripping conditions (*ISCSINAD*) in percolation bin 3 under nominal conditions: (a, b) *ISCSINND* and *ISCSINAD* for all (i.e., 300) sample elements, (c, d) *ISCSINND* and *ISCSINAD* for first 50 sample elements, and (e, f) PRCCs for *ISCSINND* and *ISCSINAD*. FK-18

K4.3-10. Time-dependent ionic strength (mol/kg) in the invert for CDSP WPs experiencing nondripping conditions (*ISCDINND*) and dripping conditions (*ISCDINAD*) in percolation bin 3 under nominal conditions: (a, b) *ISCDINND* and *ISCDINAD* for all (i.e., 300) sample elements, (c, d) *ISCDINND* and *ISCDINAD* for first 50 sample elements, and (e, f) PRCCs for *ISCDINND* and *ISCDINAD*. FK-19

FIGURES (Continued)

Page

K4.3-11. Stepwise rank regression analyses and selected scatterplots for ionic strength (mol/kg) in the invert for CSNF WPs experiencing dripping conditions (*ISCSINAD*) in percolation bin 3 under nominal conditions: (a) Regressions for *ISCSINAD* at 1000, 50,000 and 500,000 years, and (b, c, d) Scatterplots for *ISCSINAD* at 1000, 50,000 and 500,000 years. FK-20
K4.3-12. Time-dependent pH in the invert for CSNF WPs experiencing nondripping conditions (*PHCSINND*) and dripping conditions (*PHCSINAD*) in percolation bin 3 under nominal conditions: (a, b) *PHCSINND* and *PHCSINAD* for all (i.e., 300) sample elements, (c, d) *PHCSINND* and *PHCSINAD* for first 50 sample elements, and (e, f) PRCCs for *PHCSINND* and *PHCSINAD*. FK-21
K4.3-13. Stepwise rank regression analyses and selected scatterplots for pH in the invert for CSNF WPs experiencing nondripping conditions (*PHCSINND*) and dripping conditions (*PHCSINAD*) in percolation bin 3 under nominal conditions: (a, b) Regressions for *PHCSINND* and *PHCSINAD* at 1000, 50,000 and 500,000 years, and (c-j) Scatterplots for *PHCSINND* and *PHCSINAD* at 1000, 50,000 and 500,000 years. FK-22
K4.3-14. Time-dependent pH in the invert for CDSP WPs experiencing nondripping conditions (*PHCDINND*) and dripping conditions (*PHCDINAD*) in percolation bin 3 under nominal conditions: (a, b) *PHCDINND* and *PHCDINAD* for all (i.e., 300) sample elements, (c, d) *PHCDINND* and *PHCDINAD* for first 50 sample elements, and (e, f) PRCCS for *PHCDINND* and *PHCDINAD*..... FK-24
K4.4-1. Time-dependent release rates (*ESNP237*, g/yr) and cumulative (i.e., integrated) releases (*ESNP237C*, g) for movement of dissolved ^{237}Np from the EBS to the UZ under nominal conditions: (a, b) *ESNP237* and *ESNP237C* for all (i.e., 300) sample elements, (c, d) *ESNP237* and *ESNP237C* for first 50 sample elements, and (e, f) PRCCs for *ESNP237* and *ESNP237C*. FK-25
K4.4-2. Stepwise rank regression analyses and selected scatterplots for release rates (*ESNP237*, g/yr) and cumulative (i.e., integrated) releases (*ESNP237C*, g) for movement of dissolved ^{237}Np from the EBS to the UZ under nominal conditions: (a, b) Regressions for *ESNP237* and *ESNP237C* at 400,000, 600,000 and 800,000 years, and (c-h) Scatterplots for *ESNP237* and *ESNP237C* at 800,000 years. FK-26
K4.5-1. Dose to RMEI (*DOSTOT*, mrem/yr) for all radioactive species under nominal conditions: (a) *DOSTOT* for all (i.e., 300) sample elements, (b) *DOSTOT* for first 50 sample elements, and (c) PRCCs for *DOSTOT*. FK-28
K4.5-2. Stepwise rank regression analyses and selected scatterplots for dose to RMEI (*DOSTOT*, mrem/yr) for all radioactive species under nominal conditions: (a) Regressions for *DOSTOT* at 400,000, 600,000 and 800,000 years, and (b,c,d) Scatterplots for *DOSTOT* at 400,000, 600,000 and 800,000 years. FK-29
K4.5-3. Selected scatterplots for dose to RMEI (*DOSTOT*, mrem/yr) for all radioactive species under nominal conditions at 800,000 and 1,000,000 years. .. FK-30

FIGURES (Continued)

Page

K5.2-1 Time-dependent ionic strength (mol/kg) in the invert for CSNF WPs (*ISCSINAD*) and CDSP WPs (*ISCDINAD*) experiencing an early drip shield failure under dripping conditions in percolation bin 3: (a, b) *ISCSINAD* and *ISCDINAD* for all (i.e., 300) sample elements, (c, d) *ISCSINAD* and *ISCDINAD* for first 50 sample elements, and (e, f) PRCCs for *ISCSINAD* and *ISCDINAD* FK-31
K5.2-2 Time-dependent pH in the invert for CSNF WPs (*PHCSINAD*) and CDSP WPs (*PHCDINAD*) experiencing an early DS failure under dripping conditions in percolation bin 3: (a, b) *PHCSINAD* and *PHCDINAD* for all (i.e., 300) sample elements, (c, d) *PHCSINAD* and *PHCDINAD* for first 50 sample elements, and (e, f) PRCCs for *PHCSINAD* and *PHCDINAD*..... FK-32
K5.3.1-1. Time-dependent release rates (*ESIC239*, g/yr) and cumulative (i.e., integrated) releases (*ESIC239C*, g) over 20,000 years for the movement of ^{239}Pu irreversibly attached to glass/waste form colloids from the EBS to the UZ resulting from a single early DS failure above a CDSP WP in percolation bin 3 under dripping conditions: (a, b) *ESIC239* and *ESIC239C* for all (i.e., 300) sample elements, (c, d) *ESIC239* and *ESIC239C* for first 50 sample elements, and (e, f) PRCCs for *ESIC239* and *ESIC239C*. FK-33
K5.3.1-2. Stepwise rank regression analyses and selected scatterplots for time-dependent release rates (*ESIC239*, g/yr) and cumulative (i.e., integrated) releases (*ESIC239C*, g) for the movement of ^{239}Pu irreversibly attached to glass/waste form colloids from the EBS to the UZ resulting from a single early DS failure above a CDSP WP in percolation bin 3 under dripping conditions : (a, b) Regressions for *ESIC239* and *ESIC239C* at 3000, 5000 and 10,000 years, and (c-h) Scatterplots for *ESIC239* and *ESIC239C* at 10,000 years. FK-34
K5.3.1-3. Removed. FK-36
K5.3.1-4. Removed FK-37
K5.3.1-5. Time-dependent release rates (*ESNP237*, g/yr) and cumulative (i.e., integrated) releases (*ESNP2379C*, g) over 20,000 years for the movement of dissolved ^{237}Np from the EBS to the UZ resulting from a single early DS failure above a CDSP WP in percolation bin 3 under dripping conditions: (a, b) *ESNP237* and *ESNP237C* for all (i.e., 300) sample elements, (c, d) *ESNP237* and *ESNP237C* for first 50 sample elements, and (e, f) PRCCs for *ESNP237* and *ESNP237C*. FK-38
K5.3.1-6. Stepwise rank regression analyses and selected scatterplots for time-dependent release rates (*ESNP237*, g/yr) and cumulative (i.e., integrated) releases (*ESNP237C*, g) for the movement of dissolved 237Np from the EBS to the UZ resulting from a single early DS failure above a CDSP WP in percolation bin 3 under dripping conditions: (a, b) Regressions for *ESNP237* and *ESNP237C* at 3000, 5000 and 10,000 years, and (c-h) Scatterplots for *ESNP237* and *ESNP237C* at 10,000 years. FK-39
K5.3.1-7. Time-dependent release rates (*ESPU239*, g/yr) and cumulative (i.e., integrated) releases (*ESPU239C*, g) over 20,000 years for the movement of

FIGURES (Continued)

Page

dissolved ^{239}Pu from the EBS to the UZ resulting from a single early DS failure above a CDSP WP in percolation bin 3 under dripping conditions: (a, b) *ESPU239* and *ESPU239C* for all (i.e., 300) sample elements, (c, d) *ESPU239* and *ESPU239C* for first 50 sample elements, and (e, f) PRCCs for *ESPU239* and *ESPU239C*.....FK-41

K5.3.1-8. Stepwise rank regression analyses and selected scatterplots for time-dependent release rates (*ESPU239*, g/yr) and cumulative (i.e., integrated) releases (*ESPU239*, g) for the movement of dissolved ^{239}Pu from the EBS to the UZ resulting from a single early DS failure above a CDSP WP in percolation bin 3 under dripping conditions: (a, b) Regressions for *ESPU239* and *ESPU239C* at 3000, 5000 and 10,000 years, and (c-h) Scatterplots for *ESPU239* and *ESPU239C* at 10,000 years. FK-42

K5.3.1-9. Time-dependent release rates (*ESTC99*, g/yr) and cumulative (i.e., integrated) releases (*ESTC99C*, g) over 20,000 years for the movement of dissolved ^{99}Tc from the EBS to the UZ resulting from a single early DS failure above a CDSP WP in percolation bin 3 under dripping conditions: (a, b) *ESTC99* and *ESTC99C* for all (i.e., 300) sample elements, (c, d) *ESTC99* and *ESTC99C* for first 50 sample elements, and (e, f) PRCCs for *ESTC99* and *ESTC99C*.....FK-44

K5.3.1-10. Stepwise rank regression analyses and selected scatterplots for time-dependent release rates (*ESTC99*, g/yr) and cumulative (i.e., integrated) releases (*ESTC99*, g) for the movement of dissolved ^{99}Tc from the EBS to the UZ resulting from a single early DS failure above a CDSP WP in percolation bin 3 under dripping conditions: (a, b) Regressions for *ESTC99* and *ESTC99C* at 3000, 5000 and 10,000 years, and (c-h) Scatterplots for *ESTC99* and *ESTC99C* at 10,000 years. FK-45

K5.3.2-1. Time-dependent release rates (*ESIC239*, g/yr) and cumulative (i.e., integrated) releases (*ESIC239C*, g) over 20,000 years for the movement of ^{239}Pu irreversibly attached to glass/waste form colloids from the EBS to the UZ resulting from a single early DS failure above a CSNF WP in percolation bin 3 under dripping conditions: (a, b) *ESIC239* and *ESIC239C* for all (i.e., 300) sample elements, (c, d) *ESIC239* and *ESIC239C* for first 50 sample elements, and (e, f) PRCCs for *ESIC239* and *ESIC239C*. FK-47

K5.3.2-2. Removed FK-48

K5.3.2-3. Time-dependent release rates (*ESNP237*, g/yr) and cumulative (i.e., integrated) releases (*ESNP237C*, g) over 20,000 years for the movement of dissolved ^{237}Np from the EBS to the UZ resulting from a single early DS failure above a CNSF WP in percolation bin 3 under dripping conditions: (a, b) *ESNP237* and *ESNP237C* for all (i.e., 300) sample elements, (c, d) *ESNP237* and *ESNP237C* for first 50 sample elements, and (e, f) PRCCs for *ESNP237* and *ESNP237C*. FK-49

K5.3.2-4. Time-dependent release rates (*ESPU239*, g/yr) and cumulative (i.e., integrated) releases (*ESPU239C*, g) over 20,000 years for the movement of dissolved ^{239}Pu from the EBS to the UZ resulting from a single early DS

FIGURES (Continued)

Page

failure above a CNSF WP in percolation bin 3 under dripping conditions: (a, b) *ESPU239* and *ESPU239C* for all (i.e., 300) sample elements, (c, d) *ESPU239* and *ESPU239C* for first 50 sample elements, and (e, f) PRCCs for *ESPU239* and *ESPU239C*.....FK-50
K5.3.2-5. Time-dependent release rates (*ESTC99*, g/yr) and cumulative (i.e., integrated) releases (*ESTC99C*, g) over 20,000 years for the movement of dissolved ^{99}Tc from the EBS to the UZ resulting from a single early DS failure above a CNSF WP in percolation bin 3 under dripping conditions: (a, b) *ESTC99* and *ESTC99C* for all (i.e., 300) sample elements, (c, d) *ESTC99* and *ESTC99C* for first 50 sample elements, and (e, f) PRCCs for *ESTC99* and *ESTC99C*.....FK-51
K5.3.3-1. Removed. FK-52
K5.3.3-2. Removed. FK-53
K5.3.3-3. Time-dependent release rates (*ESNP237*, g/yr) and cumulative (i.e., integrated) releases (*ESNP237C*, g) over 20,000 years for the movement of dissolved ^{237}Np from the EBS to the UZ resulting from the early failure of a CDSP WP in percolation bin 3 under dripping conditions: (a, b) *ESNP237* and *ESNP237C* for all (i.e., 300) sample elements, (c, d) *ESNP237* and *ESNP237C* for first 50 sample elements, and (e, f) PRCCs for *ESNP237* and *ESNP237C*. FK-54
K5.3.3-4. Time-dependent release rates (*ESPU239*, g/yr) and cumulative (i.e., integrated) releases (*ESPU239C*, g) over 20,000 years for the movement of dissolved ^{239}Pu from the EBS to the UZ resulting from the early failure of a CDSP WP in percolation bin 3 under dripping conditions: (a, b) *ESPU239* and *ESPU239C* for all (i.e., 300) sample elements, (c, d) *ESPU239* and *ESPU239C* for first 50 sample elements, and (e, f) PRCCs for *ESPU239* and *ESPU239C*. FK-55
K5.3.3-5. Time-dependent release rates (*ESTC99*, g/yr) and cumulative (i.e., integrated) releases (*ESTC99C*, g) over 20,000 years for the movement of dissolved ^{99}Tc from the EBS to the UZ resulting from the early failure of a CDSP WP in percolation bin 3 under dripping conditions: (a, b) *ESTC99* and *ESTC99C* for all (i.e., 300) sample elements, (c, d) *ESTC99* and *ESTC99C* for first 50 sample elements, and (e, f) PRCCs for *ESTC99* and *ESTC99C*. FK-56
K5.3.5-1. Removed. FK-57
K5.3.5-2. Removed FK-58
K5.3.5-3. Time-dependent release rates (*ESNP237*, g/yr) and cumulative (i.e., integrated) releases (*ESNP237C*, g) over 20,000 years for the movement of dissolved ^{237}Np from the EBS to the UZ resulting from the early failure of a CSNF WP in percolation bin 3 under dripping conditions: (a, b) *ESNP237* and *ESNP237C* for all (i.e., 300) sample elements, (c, d) *ESNP237* and *ESNP237C* for first 50 sample elements, and (e, f) PRCCs for *ESNP237* and *ESNP237C*. FK-59
K5.3.5-4. Time-dependent release rates (*ESPU239*, g/yr) and cumulative (i.e., integrated) releases (*ESPU239C*, g) over 20,000 years for the movement of

FIGURES (Continued)

Page

dissolved ^{239}Pu from the EBS to the UZ resulting from the early failure of a CSNF WP in percolation bin 3 under dripping conditions: (a, b) *ESPU239* and *ESPU239C* for all (i.e., 300) sample elements, (c, d) *ESPU239* and *ESPU239C* for first 50 sample elements, and (e, f) PRCCs for *ESPU239* and *ESPU239C*. FK-60

K5.3.5-5. Time-dependent release rates (*ESTC99*, g/yr) and cumulative (i.e., integrated) releases (*ESTC99C*, g) over 20,000 years for the movement of dissolved ^{99}Tc from the EBS to the UZ resulting from the early failure of a CSNF WP in percolation bin 3 under dripping conditions: (a, b) *ESTC99* and *ESTC99C* for all (i.e., 300) sample elements, (c, d) *ESTC99* and *ESTC99C* for first 50 sample elements, and (e, f) PRCCs for *ESTC99* and *ESTC99C*. FK-61

K5.3.7-1. Time-dependent release rates (*ESNP237*, g/yr) and cumulative (i.e., integrated) releases (*ESNP237C*, g) over 1,000,000 years for the movement of dissolved ^{237}Np from the EBS to the UZ resulting from a single early DS failure above a CDSP WP in percolation bin 3 under dripping conditions: (a, b) *ESNP237* and *ESNP237C* for all (i.e., 300) sample elements, (c, d) *ESNP237* and *ESNP237C* for first 50 sample elements, and (e, f) PRCCs for *ESNP237* and *ESNP237C* FK-63

K5.3.7-2. Time-dependent release rates (*ESPU239*, g/yr) and cumulative (i.e., integrated) releases (*ESPU239C*, g) over 200,000 years for the movement of dissolved ^{239}Pu from the EBS to the UZ resulting from a single early DS failure above a CDSP WP in percolation bin 3 under dripping conditions: (a, b) *ESPU239* and *ESPU239C* for all (i.e., 300) sample elements, (c, d) *ESPU239* and *ESPU239C* for first 50 sample elements, and (e, f) PRCCs for *ESPU239* and *ESPU239C*..... FK-64

K5.3.8-1. Time-dependent release rates (*ESNP237*, g/yr) and cumulative (i.e., integrated) releases (*ESNP237C*, g) over 1,000,000 years for the movement of dissolved ^{237}Np from the EBS to the UZ resulting from a single early DS failure above a CSNF WP in percolation bin 3 under dripping conditions: (a, b) *ESNP237* and *ESNP237C* for all (i.e., 300) sample elements, (c, d) *ESNP237* and *ESNP237C* for first 50 sample elements, and (e, f) PRCCs for *ESNP237* and *ESNP237C*. FK-65

K5.3.8-2. Time-dependent release rates (*ESPU239*, g/yr) and cumulative (i.e., integrated) releases (*ESPU239C*, g) over 200,000 years for the movement of dissolved ^{239}Pu from the EBS to the UZ resulting from a single early DS failure above a CSNF WP in percolation bin 3 under dripping conditions: (a, b) *ESPU239* and *ESPU239C* for all (i.e., 300) sample elements, (c, d) *ESPU239* and *ESPU239C* for first 50 sample elements, and (e, f) PRCCs for *ESPU239* and *ESPU239C*..... FK-66

K5.3.9-1. Time-dependent release rates (*ESNP237*, g/yr) and cumulative (i.e., integrated) releases (*ESNP237C*, g) over 1,000,000 years for the movement of dissolved ^{237}Np from the EBS to the UZ resulting from the early failure of a CDSP WP in percolation bin 3 under dripping conditions: (a, b)

FIGURES (Continued)

Page

ESNP237 and *ESNP237C* for all (i.e., 300) sample elements, (c, d) *ESNP237* and *ESNP237C* for first 50 sample elements, and (e, f) PRCCs for *ESNP237* and *ESNP237C*. FK-67
K5.3.9-2. Time-dependent release rates (*ESPU239*, g/yr) and cumulative (i.e., integrated) releases (*ESPU239C*, g) over 200,000 years for the movement of dissolved ^{239}Pu from the EBS to the UZ resulting from the early failure of a CDSP WP in percolation bin 3 under dripping conditions: (a, b) *ESPU239* and *ESPU239C* for all (i.e., 300) sample elements, (c, d) *ESPU239* and *ESPU239C* for first 50 sample elements, and (e, f) PRCCs for *ESPU239* and *ESPU239C*. FK-68
K5.3.10-1. Time-dependent release rates (*ESNP237*, g/yr) and cumulative (i.e., integrated) releases (*ESNP237C*, g) over 1,000,000 years for the movement of dissolved ^{237}Np from the EBS to the UZ resulting from the early failure of a CDSP WP in percolation bin 3 under nondripping conditions: (a, b) *ESNP237* and *ESNP237C* for all (i.e., 300) sample elements, (c, d) *ESNP237* and *ESNP237C* for first 50 sample elements, and (e, f) PRCCs for *ESNP237* and *ESNP237C*..... FK-69
K5.3.10-2. Time-dependent release rates (*ESPU239*, g/yr) and cumulative (i.e., integrated) releases (*ESPU239C*, g) over 200,000 years for the movement of dissolved ^{239}Pu from the EBS to the UZ resulting from the early failure of a CDSP WP in percolation bin 3 under nondripping conditions: (a, b) *ESPU239* and *ESPU239C* for all (i.e., 300) sample elements, (c, d) *ESPU239* and *ESPU239C* for first 50 sample elements, and (e, f) PRCCs for *ESPU239* and *ESPU239C*. FK-70
K5.3.11-1. Time-dependent release rates (*ESNP237*, g/yr) and cumulative (i.e., integrated) releases (*ESNP237C*, g) over 1,000,000 years for the movement of dissolved ^{237}Np from the EBS to the UZ resulting from the early failure of a CSNF WP in percolation bin 3 under dripping conditions: (a, b) *ESNP237* and *ESNP237C* for all (i.e., 300) sample elements, (c, d) *ESNP237* and *ESNP237C* for first 50 sample elements, and (e, f) PRCCs for *ESNP237* and *ESNP237C*..... FK-71
K5.3.11-2. Time-dependent release rates (*ESPU239*, g/yr) and cumulative (i.e., integrated) releases (*ESPU239C*, g) over 200,000 years for the movement of dissolved ^{239}Pu from the EBS to the UZ resulting from the early failure of a CSNF WP in percolation bin 3 under dripping conditions: (a, b) *ESPU239* and *ESPU239C* for all (i.e., 300) sample elements, (c, d) *ESPU239* and *ESPU239C* for first 50 sample elements, and (e, f) PRCCs for *ESPU239* and *ESPU239C* FK-72
K5.3.12-1. Time-dependent release rates (*ESNP237*, g/yr) and cumulative (i.e., integrated) releases (*ESNP237C*, g) over 1,000,000 years for the movement of dissolved ^{237}Np from the EBS to the UZ resulting from the early failure of a CSNF WP in percolation bin 3 under nondripping conditions: (a, b) *ESNP237* and *ESNP237C* for all (i.e., 300) sample elements, (c, d) *ESNP237*

FIGURES (Continued)

Page

and *ESNP237C* for first 50 sample elements, and (e, f) PRCCs for *ESNP237* and *ESNP237C*.....FK-73
K5.3.12-2. Time-dependent release rates (*ESPU239*, g/yr) and cumulative (i.e., integrated) releases (*ESPU239C*, g) over 200,000 years for the movement of dissolved ^{239}Pu from the EBS to the UZ resulting from the early failure of a CSNF WP in percolation bin 3 under nondripping conditions: (a, b) *ESPU239* and *ESPU239C* for all (i.e., 300) sample elements, (c, d) *ESPU239* and *ESPU239C* for first 50 sample elements, and (e, f) PRCCs for *ESPU239* and *ESPU239C*. FK-74
K5.4.1-1. Time-dependent release rates (*UZIC239*, g/yr) and cumulative (i.e., integrated) releases (*UZIC239C*, g) over 20,000 years for the movement of ^{239}Pu irreversibly attached to slow colloids from the UZ to the SZ resulting from a single early DS failure above a CDSP WP in percolation bin 3 under dripping conditions: (a, b) *UZIC239* and *UZIC239C* for all (i.e., 300) sample elements, (c, d) *UZIC239* and *UZIC239C* for first 50 sample elements, and (e, f) PRCCs for *UZIC239* and *UZIC239C*.....FK-75
K5.4.1-2. Stepwise rank regression analyses and selected scatterplots for time-dependent release rates (*UZIC239*, g/yr) and cumulative (i.e., integrated) releases (*UZIC239C*, g) for the movement of ^{239}Pu irreversibly attached to slow colloids from the UZ to the SZ resulting from a single early DS failure above a CDSP WP in percolation bin 3 under dripping conditions: (a, b) Regressions for *UZIC239* and *UZIC239C* at 3000, 5000 and 10,000 years, and (c-h) Scatterplots for *UZIC239* and *UZIC239C* at 10,000 years. FK-76
K5.4.1-3. Comparison of cumulative releases of ^{239}Pu irreversibly attached to slow colloids into the UZ (*ESSL239C*, g) and out of the UZ (*UZIC239C*, g) at (a) 1000 years, (b) 3000 years, (c) 5000 years and (d) 10,000 years for a single early DS failure above a CDSP WP in percolation bin 3 under dripping conditions.....FK-78
K5.4.1-4. Time-dependent release rates (*UZIF239*, g/yr) and cumulative (i.e., integrated) releases (*UZIF239C*, g) over 20,000 years for the movement of ^{239}Pu irreversibly attached to fast colloids from the UZ to the SZ resulting from a single early DS failure above a CDSP WP in percolation bin 3 under dripping conditions: (a, b) *UZIF239* and *UZIF239C* for all (i.e., 300) sample elements, (c, d) *UZIF239* and *UZIF239C* for first 50 sample elements, and (e, f) PRCCs for *UZIF239* and *UZIF239C*. FK-79
K 5.4.1-5. Stepwise rank regression analyses and selected scatterplots for time-dependent release rates (*UZIF239*, g/yr) and cumulative (i.e., integrated) releases (*UZIF239C*, g) for the movement of ^{239}Pu irreversibly attached to fast colloids from the UZ to the SZ resulting from a single early DS failure above a CDSP WP in percolation bin 3 under dripping conditions : (a, b) Regressions for *UZIF239* and *UZIF239C* at 3000, 5000 and 10,000 years, and (c-h) Scatterplots for *UZIF239* and *UZIF239C* at 10,000 years.....FK-80

FIGURES (Continued)

Page

K5.4.1-6. Comparison of cumulative releases of ^{239}Pu irreversibly attached to fast colloids into the UZ (*ESFA239C*, g) and out of the UZ (*UZIF239C*, g) at (a) 1000 years, (b) 3000 years, (c) 5000 years and (d) 10,000 years for a single early DS failure above a CDSP WP in percolation bin 3 under dripping conditions. FK-82

K5.4.1-7. Time-dependent release rates (*UZNP237*, g/yr) and cumulative (i.e., integrated) releases (*UZNP237C*, g) over 20,000 years for the movement of dissolved ^{237}Np from the UZ to the SZ resulting from a single early DS failure above a CDSP WP in percolation bin 3 under dripping conditions: (a, b) *UZNP237* and *UZNP237C* for all (i.e., 300) sample elements, (c, d) *UZNP237* and *UZNP237C* for first 50 sample elements, and (e, f) PRCCs for *UZNP237* and *UZNP237C*. FK-83

K 5.4.1-8. Stepwise rank regression analyses and selected scatterplots for time-dependent release rates (*UZNP237*, g/yr) and cumulative (i.e., integrated) releases (*UZNP237C*, g) for the movement of dissolved ^{237}Np from the EBS to the UZ resulting from a single early DS failure above a CDSP WP in percolation bin 3 under dripping conditions: (a, b) Regressions for *UZNP237* and *UZNP237C* at 3000, 5000 and 10,000 years, and (c-h) Scatterplots for *UZNP237* and *UZNP237C* at 10,000 years. FK-84

K5.4.1-9. Comparison of cumulative releases of dissolved ^{237}Np into the UZ (*ESNP237C*, g) and out of the UZ (*UZNP237C*, g) at (a) 1000 years, (b) 3000 years, (c) 5000 years and (d) 10,000 years for a single early DS failure above a CDSP WP in percolation bin 3 under dripping conditions. FK-86

K5.4.1-10. Time-dependent release rates (*UZPU239*, g/yr) and cumulative (i.e., integrated) releases (*UZPU239C*, g) over 20,000 years for the movement of dissolved ^{239}Pu from the UZ to the SZ resulting from a single early DS failure above a CDSP WP in percolation bin 3 under dripping conditions: (a, b) *UZPU239* and *UZPU239C* for all (i.e., 300) sample elements, (c, d) *UZPU239* and *UZPU239C* for first 50 sample elements, and (e, f) PRCCs for *UZPU239* and *UZPU239C*. FK-87

K5.4.1-11. Stepwise rank regression analyses and selected scatterplots for time-dependent release rates (*UZPU239*, g/yr) and cumulative (i.e., integrated) releases (*UZPU239*, g) for the movement of dissolved ^{239}Pu from the UZ to the SZ resulting from a single early DS failure above a CDSP WP in percolation bin 3 under dripping conditions: (a, b) Regressions for *UZPU239* and *UZPU239C* at 3000, 5000 and 10,000 years, and (c-h) Scatterplots for *UZPU239* and *UZPU239C* at 10,000 years. FK-88

K5.4.1-12. Comparison of cumulative releases of dissolved ^{239}Pu into the UZ (*ESPU239C*, g) and out of the UZ (*UZPU239C*, g) at (a) 1000 years, (b) 3000 years, (c) 5000 years and (d) 10,000 years for a single early DS failure above a CDSP WP in percolation bin 3 under dripping conditions. FK-90

K5.4.1-13. Time-dependent release rates (*UZTC99*, g/yr) and cumulative (i.e., integrated) releases (*UZTC99C*, g) over 20,000 years for the movement of

FIGURES (Continued)

Page

dissolved ^{99}Tc from the UZ to the SZ resulting from a single early DS failure above a CDSP WP in percolation bin 3 under dripping conditions: (a, b) *UZTC99* and *UZTC99C* for all (i.e., 300) sample elements, (c, d) *UZTC99* and *UZTC99C* for first 50 sample elements, and (e, f) PRCCs for *UZTC99* and *UZTC99C*. FK-91

K5.4.1-14. Stepwise rank regression analyses and selected scatterplots for time-dependent release rates (*UZTC99*, g/yr) and cumulative (i.e., integrated) releases (*UZTC99*, g) for the movement of dissolved ^{99}Tc from the UZ to the SZ resulting from a single early DS failure above a CDSP WP in percolation bin 3 under dripping conditions: (a, b) Regressions for *UZTC99* and *UZTC99C* at 3000, 5000 and 10,000 years, and (c-h) Scatterplots for *UZTC99* and *UZTC99C* at 10,000 years. FK-92

K5.4.1-15. Comparison of cumulative releases of dissolved ^{99}Tc into the UZ (*ESTC99C*, g) and out of the UZ (*UZTC99C*, g) at (a) 1000 years, (b) 3000 years, (c) 5000 years and (d) 10,000 years for a single early DS failure above a CDSP WP in percolation bin 3 under dripping conditions. FK-94

K5.5.1-1. Time-dependent release rates (*SZIC239*, g/yr) and cumulative (i.e., integrated) releases (*SZIC239C*, g) over 20,000 years for the movement of ^{239}Pu irreversibly attached to slow colloids across a subsurface plane at the location of the RMEI resulting from a single early DS failure above a CDSP WP in percolation bin 3 under dripping conditions: (a, b) *SZIC239* and *SZIC239C* for all (i.e., 300) sample elements, (c, d) *SZIC239* and *SZIC239C* for first 50 sample elements, and (e, f) PRCCs for *SZIC239* and *SZIC239C*. FK-95

K5.5.1-2. Time-dependent release rates (*SZIF239*, g/yr) and cumulative (i.e., integrated) releases (*SZIF239C*, g) over 20,000 years for the movement of ^{239}Pu irreversibly attached to fast colloids across a subsurface plane at the location of the RMEI resulting from a single early DS failure above a CDSP WP in percolation bin 3 under dripping conditions: (a, b) *SZIF239* and *SZIF239C* for all (i.e., 300) sample elements, (c, d) *SZIF239* and *SZIF239C* for first 50 sample elements, and (e, f) PRCCs for *SZIF239* and *SZIF239C*. FK-96

K5.5.1-3. Time-dependent release rates (*SZNP237*, g/yr) and cumulative (i.e., integrated) releases (*SZNP237C*, g) over 20,000 years for the movement of dissolved ^{237}Np across a subsurface plane at the location of the RMEI resulting from a single early DS failure above a CDSP WP in percolation bin 3 under dripping conditions: (a, b) *SZNP237* and *SZNP237C* for all (i.e., 300) sample elements, (c, d) *SZNP237* and *SZNP237C* for first 50 sample elements, and (e, f) PRCCs for *SZNP237* and *SZNP237C*. FK-97

K5.5.1-4. Time-dependent release rates (*SZPU239*, g/yr) and cumulative (i.e., integrated) releases (*SZPU239C*, g) over 20,000 years for the movement of dissolved ^{239}Pu across a subsurface plane at the location of the RMEI resulting from a single early DS failure above a CDSP WP in percolation bin 3 under dripping conditions: (a, b) *SZPU239* and *SZPU239C* for all (i.e., 300)

FIGURES (Continued)

Page

sample elements, (c, d) *SZPU239* and *SZPU239C* for first 50 sample elements, and (e, f) PRCCs for *SZPU239* and *SZPU239C*. FK-98
K5.5.1-5. Time-dependent release rates (*SZTC99*, g/yr) and cumulative (i.e., integrated) releases (*SZTC99C*, g) over 20,000 years for the movement of dissolved ^{99}Tc across a subsurface plane at the location of the RMEI resulting from a single early DS failure above a CDSP WP in percolation bin 3 under dripping conditions: (a, b) *SZTC99* and *SZTC99C* for all (i.e., 300) sample elements, (c, d) *SZTC99* and *SZTC99C* for first 50 sample elements, and (e, f) PRCCs for *SZTC99* and *SZTC99C*. FK-99
K5.6.1-1. Time-dependent dose to the RMEI (*DOIC239*, mrem/yr) over 20,000 years for the movement of ^{239}Pu irreversibly attached to slow colloids across a subsurface plane at the location of the RMEI resulting from a single early DS failure above a CDSP WP in percolation bin 3 under dripping conditions: (a) *DOIC239* for all (i.e., 300) sample elements, (b) *DOIC239* for first 50 sample elements, and (c) PRCCs for *DOIC239*. FK-100
K5.6.1-2. Time-dependent dose to the RMEI (*DOIF239*, mrem/yr) over 20,000 years for the movement of ^{239}Pu irreversibly attached to fast colloids across a subsurface plane at the location of the RMEI resulting from a single early DS failure above a CDSP WP in percolation bin 3 under dripping conditions: (a) *DOIF239* for all (i.e., 300) sample elements, (b) *DOIF239* for first 50 sample elements, and (c) PRCCs for *DOIF239*. FK-101
K5.6.1-3. Time-dependent dose to the RMEI (*DONP237*, mrem/yr) over 20,000 years for the movement of dissolved ^{237}Np across a subsurface plane at the location of the RMEI resulting from a single early DS failure above a CDSP WP in percolation bin 3 under dripping conditions: (a) *DONP237*for all (i.e., 300) sample elements, (b) *DONP237*for first 50 sample elements, and (c) PRCCs for *DONP237*. FK-102
K5.6.1-4. Time-dependent dose to the RMEI (*DOPU239*, mrem/yr) over 20,000 years for the movement of dissolved ^{239}Pu across a subsurface plane at the location of the RMEI resulting from a single early DS failure above a CDSP WP in percolation bin 3 under dripping conditions: (a) *DOPU239* for all (i.e., 300) sample elements, (b) *DOPU239* for first 50 sample elements, and (c) PRCCs for *DOPU239*. FK-103
K5.6.1-5. Time-dependent dose to the RMEI (*DOTC99*, mrem/yr) over 20,000 years for the movement of dissolved ^{99}Tc across a subsurface plane at the location of the RMEI resulting from a single early DS failure above a CDSP WP in percolation bin 3 under dripping conditions: (a) *DOTC99* for all (i.e., 300) sample elements, (b) *DOTC99* for first 50 sample elements, and (c) PRCCs for *DOTC99*. FK-104
K5.7.1-1. Expected dose to RMEI (*EXPDOSE*, mrem/yr) over [0, 20,000 yr] for all radioactive species resulting from early DS failure: (a) *EXPDOSE* for all (i.e., 300) sample elements, (b) *EXPDOSE* for first 50 sample elements, and (c) PRCCs for *EXPDOSE*..... FK-105

FIGURES (Continued)

Page

K5.7.1-2. Stepwise rank regression analyses and selected scatterplots for expected dose to RMEI (*EXPDOSE*, mrem/yr) over [0, 20,000 yr] for all radioactive species resulting from early DS failure: (a) Regressions for *EXPDOSE* at 3000, 5000 and 10,000 years, and (b,c,d) Scatterplots for *EXPDOSE* at 10,000 years..... FK-106
K5.7.1-3. Expected dose to RMEI (*EXPDOSE*, mrem/yr) over [0, 1,000,000 yr] for all radioactive species resulting from early DS failure: (a) *EXPDOSE* for all (i.e., 300) sample elements, (b) *EXPDOSE* for first 50 sample elements, and (c) PRCCs for *EXPDOSE*..... FK-107
K5.7.1-4. Stepwise rank regression analyses and selected scatterplots for expected dose to RMEI (*EXPDOSE*, mrem/yr) over [0, 1,000,000 yr] for all radioactive species resulting from early DS failure: (a) Regressions for *EXPDOSE* at 50,000, 200,000 and 500,000 years, and (b,c,d) Scatterplots for *EXPDOSE* at 500,000 years. FK-108
K5.7.2-1. Expected dose to RMEI (*EXPDOSE*, mrem/yr) over [0, 20,000 yr] for all radioactive species resulting from early WP failure: (a) *EXPDOSE* for all (i.e., 300) sample elements, (b) *EXPDOSE* for first 50 sample elements, and (c) PRCCs for *EXPDOSE*. FK-110
K5.7.2-2. Stepwise rank regression analyses and selected scatterplots for expected dose to RMEI (*EXPDOSE*, mrem/yr) over [0, 20,000 yr] for all radioactive species resulting from early WP failure: (a) Regressions for *EXPDOSE* at 3000, 5000 and 10,000 years, and (b,c,d) Scatterplots for *EXPDOSE* at 10,000 years..... FK-111
K5.7.2-3. Expected dose to RMEI (*EXPDOSE*, mrem/yr) over [0, 1,000,000 yr] for all radioactive species resulting from early WP failure: (a) *EXPDOSE* for all (i.e., 300) sample elements, (b) *EXPDOSE* for first 50 sample elements, and (c) PRCCs for *EXPDOSE*. FK-112
K5.7.2-4. Stepwise rank regression analyses and selected scatterplots for expected dose to RMEI (*EXPDOSE*, mrem/yr) over [0, 1,000,000 yr] for all radioactive species resulting from early WP failure: (a) Regressions for *EXPDOSE* at 50,000, 200,000 and 500,000 years, and (b,c,d) Scatterplots for *EXPDOSE* at 500,000 years. FK-113
K5.7.3-1. Expected dose to RMEI (*EXPDOSE*, mrem/yr) over [0, 20,000 yr] for all radioactive species resulting from both early DS failure and early WP failure: (a) *EXPDOSE* for all (i.e., 300) sample elements, (b) *EXPDOSE* for first 50 sample elements, and (c) PRCCs for *EXPDOSE*. FK-115
K5.7.3-2. Stepwise rank regression analyses and selected scatterplots for expected dose to RMEI (*EXPDOSE*, mrem/yr) over [0, 20,000 yr] for all radioactive species resulting from both early DS failure and early WP failure: (a) Regressions for *EXPDOSE* at 3000, 5000 and 10,000 years, and (b,c,d) Scatterplots for *EXPDOSE* at 10,000 years..... FK-116
K5.7.3-3. Expected dose to RMEI (*EXPDOSE*, mrem/yr) over [0, 1,000,000 yr] for all radioactive species resulting from both early DS failure and early WP failure: (a) *EXPDOSE* for all (i.e., 300) sample elements, (b) *EXPDOSE* for first 50 sample elements, and (c) PRCCs for *EXPDOSE*. FK-118

FIGURES (Continued)

Page

K5.7.3-4. Stepwise rank regression analyses and selected scatterplots for expected dose to RMEI (*EXPDOSE*, mrem/yr) over [0, 1,000,000 yr] for all radioactive species resulting from both early DS failure and early WP failure: (a) Regressions for *EXPDOSE* at 50,000, 200,000 and 500,000 years, and (b,c,d) Scatterplots for *EXPDOSE* at 500,000 years. FK-119

K5.7.4-1. Expected dose to RMEI (*EXPDOSE*, mrem/yr) over [0, 1,000,000 yr] for all radioactive species resulting from early DS failure, early WP failure and nominal process WP failure: (a) *EXPDOSE* for all (i.e., 300) sample elements, (b) *EXPDOSE* for first 50 sample elements, and (c) PRCCs for *EXPDOSE* FK-121

K5.7.4-2. Stepwise rank regression analyses and selected scatterplots for expected dose to RMEI (*EXPDOSE*, mrem/yr) over [0, 1,000,000 yr] for all radioactive species resulting from early DS failure, early WP failure and nominal process WP failure: (a) Regressions for *EXPDOSE* at 50,000, 200,000 and 500,000 years, and (b,c,d) Scatterplots for *EXPDOSE* at 500,000 years. FK-122

K6.2-1. Time-dependent temperatures in percolation bin 3 for CSNF WPs at the drift wall (*TMPCSWL*), on the WP (*TMPCSWP*) and in the invert beneath the WP (*TMPCSINV*) and similarly for CDSP WPs at the drift wall (*TMPCDWL*), on the WP (*TMPCDWP*) and in the invert beneath the WP (*TMPCDINV*) resulting from an igneous intrusive event at 250 years that destroys all WPs in the repository: (a, c, e) *TMPCSWL*, *TMPCSWP* and *TMPCSINV*, and (b, d, f) *TMPCDWL*, *TMPCDWP* and *TMPCDINV* FK-125

K6.2-2. Time-dependent seepage rates (m^3/yr/WP) into the repository above CSNF WPs (*SPRATECS*) resulting from an igneous intrusive event at 250 years that destroys all WPs in the repository: (a) Bin 1, (b) Bin 2, (c) Bin 3, (d) Bin 4, and (e) Bin 5 ..... FK-126

K6.2-3. Time-dependent ionic strength (mol/kg) under dripping conditions in the invert for CSNF WPs (*ISCSINAD*) and CDSP WPs (*ISCDINAD*) in percolation bin 3 resulting from an igneous intrusive event at 250 years that destroys all WPs in the repository: (a, b) *ISCSINAD* and *ISCDINAD* for all (i.e., 300) sample elements, (c, d) *ISCSINAD* and *ISCDINAD* for first 50 sample elements, and (e, f) PRCCs for *ISCSINAD* and *ISCDINAD* FK-127

K6.2-4. Time-dependent pH under dripping conditions in the invert for CSNF WPs (*PHCSINAD*) and CDSP WPs (*PHCDINAD*) in percolation bin 3 resulting from an igneous intrusive event at 250 years that destroys all WPs in the repository: (a, b) *PHCSINAD* and *PHCDINAD* for all (i.e., 300) sample elements, (c, d) *PHCSINAD* and *PHCDINAD* for first 50 sample elements, and (e, f) PRCCs for *PHCSINAD* and *PHCDINAD* FK-128

K6.3.1-1. Time-dependent release rates (*ESIC239*, g/yr) and cumulative (i.e., integrated) releases (*ESIC239C*, g) over 20,000 years for the movement of ^{239}Pu irreversibly attached to glass/ waste form colloids from the EBS to the UZ resulting from an igneous intrusive event at 10 years that destroys all WPs in the repository: (a, b) *ESIC239* and *ESIC239C* for all (i.e., 300)

FIGURES (Continued)

Page

sample elements, (c, d) *ESIC239* and *ESIC239C* for first 50 sample elements, and (e, f) PRCCs for *ESIC239* and *ESIC239C* FK-129
K6.3.1-2. Stepwise rank regression analyses and selected scatterplots for time-dependent release rates (*ESIC239*, g/yr) and cumulative (i.e., integrated) releases (*ESIC239C*, g) for the movement of ^{239}Pu irreversibly attached to glass/ waste form colloids from the EBS to the UZ resulting from an igneous intrusive event at 10 years that destroys all WPs in the repository: (a, b) Regressions for *ESIC239* and *ESIC239C* at 3000, 5000 and 10,000 years, and (c-h) Scatterplots for *ESIC239* and *ESIC239C* at 10,000 years..... FK-130
K6.3.1-3. Removed FK-132
K6.3.1-4. Removed FK-133
K6.3.1-5. Time-dependent release rates (*ESNP237*, g/yr) and cumulative (i.e., integrated) releases (*ESNP237C*, g) over 20,000 years for the movement of dissolved ^{237}Np from the EBS to the UZ resulting from an igneous intrusive event at 10 years that destroys all WPs in the repository: (a, b) *ESNP237* and *ESNP237C* for all (i.e., 300) sample elements, (c, d) *ESNP237* and *ESNP237C* for first 50 sample elements, and (e, f) PRCCs for *ESNP237* and *ESNP237C* FK-135
K6.3.1-6. Stepwise rank regression analyses and selected scatterplots for time-dependent release rates (*ESNP237*, g/yr) and cumulative (i.e., integrated) releases (*ES NP237C*, g) for the movement of dissolved ^{237}Np from the EBS to the UZ resulting from an igneous intrusive event at 10 years that destroys all WPs in the repository: (a, b) Regressions for *ESNP237* and *ESNP237C* at 3000, 5000 and 10,000 years, and (c-h) Scatterplots for *ESNP237* and *ESNP237C* at 10,000 years FK-136
K6.3.1-7. Time-dependent release rates (*ESPU239*, g/yr) and cumulative (i.e., integrated) releases (*ESPU239C*, g) over 20,000 years for the movement of dissolved ^{239}Pu from the EBS to the UZ resulting from an igneous intrusive event at 10 years that destroys all WPs in the repository: (a, b) *ESPU239* and *ESPU239C* for all (i.e., 300) sample elements, (c, d) *ESPU239* and *ESPU239C* for first 50 sample elements, and (e, f) PRCCs for *ESPU239* and *ESPU239C* FK-138
K6.3.1-8. Stepwise rank regression analyses and selected scatterplots for time-dependent release rates (*ESPU239*, g/yr) and cumulative (i.e., integrated) releases (*ESPU239*, g) for the movement of dissolved ^{239}Pu from the EBS to the UZ resulting from an igneous intrusive event at 10 years that destroys all WPs in the repository: (a, b) Regressions for *ESPU239* and *ESPU239C* at 3000, 5000 and 10,000 years, and (c-h) Scatterplots for *ESPU239* and *ESPU239C* at 10,000 years..... FK-139
K6.3.1-9. Time-dependent release rates (*ESTC99*, g/yr) and cumulative (i.e., integrated) releases (*ESTC99C*, g) over 20,000 years for the movement of dissolved ^{99}Tc from the EBS to the UZ resulting from an igneous intrusive event at 10 years that destroys all WPs in the repository: (a, b) *ESTC99* and *ESTC99C* for all

FIGURES (Continued)

Page

(i.e., 300) sample elements, (c, d) *ESTC99* and *ESTC99C* for first 50 sample elements, and (e, f) PRCCs for *ESTC99* and *ESTC99C*. FK-141
K6.3.1-10. Stepwise rank regression analyses and selected scatterplots for time-dependent release rates (*ESTC99*, g/yr) and cumulative (i.e., integrated) releases (*ESTC99C*, g) for the movement of dissolved ^{99}Tc from the EBS to the UZ resulting from an igneous intrusive event at 10 years that destroys all WPs in the repository: (a, b) Regressions for *ESTC99* and *ESTC99C* at 3000, 5000 and 10,000 years, and (c-h) Scatterplots for *ESTC99* and *ESTC99C* at 10,000 years. FK-142
K6.3.2-1. Time-dependent release rates (*ESIC239*, g/yr) and cumulative (i.e., integrated) releases (*ESIC239C*, g) over 200,000 years for the movement of ^{239}Pu irreversibly attached to glass/ waste form colloids from the EBS to the UZ resulting from an igneous intrusive event at 250 years that destroys all WPs in the repository: (a, b) *ESIC239* and *ESIC239C* for all (i.e., 300) sample elements, (c, d) *ESIC239* and *ESIC239C* for first 50 sample elements, and (e, f) PRCCs for *ESIC239* and *ESIC239C*. FK-144
K6.3.2-2. Removed. FK-145
K6.3.2-3. Time-dependent release rates (*ESNP237*, g/yr) and cumulative (i.e., integrated) releases (*ESNP237C*, g) over 1,000,000 years for the movement of dissolved ^{237}Np from the EBS to the UZ resulting from an igneous intrusive event at 250 years that destroys all WPs in the repository: (a, b) *ESNP237* and *ESNP237C* for all (i.e., 300) sample elements, (c, d) *ESNP237* and *ESNP237C* for first 50 sample elements, and (e, f) PRCCs for *ESNP237* and *ESNP237C*..... FK-146
K6.3.2-4. Time-dependent release rates (*ESPU239*, g/yr) and cumulative (i.e., integrated) releases (*ESPU239C*, g) over 200,000 years for the movement of dissolved ^{239}Pu from the EBS to the UZ resulting from an igneous intrusive event at 250 years that destroys all WPs in the repository: (a, b) *ESPU239* and *ESPU239C* for all (i.e., 300) sample elements, (c, d) *ESPU239* and *ESPU239C* for first 50 sample elements, and (e, f) PRCCs for *ESPU239* and *ESPU239C*. FK-147
K6.4.1-1. Time-dependent release rates (*UZIC239*, g/yr) and cumulative (i.e., integrated) releases (*UZIC239C*, g) over 20,000 years for the movement of ^{239}Pu irreversibly attached to slow colloids from the UZ to the SZ resulting from an igneous intrusive event at 10 years that destroys all WPs in the repository: (a, b) *UZIC239* and *UZIC239C* for all (i.e., 300) sample elements, (c, d) *UZIC239* and *UZIC239C* for first 50 sample elements, and (e, f) PRCCs for *UZIC239* and *UZIC239C* FK-149
K6.4.1-2. Stepwise rank regression analyses and selected scatterplots for time-dependent release rates (*UZIC239*, g/yr) and cumulative (i.e., integrated) releases (*UZIC239C*, g) for the movement of ^{239}Pu irreversibly attached to slow colloids from the UZ to the SZ resulting from an igneous intrusive event at 10 years that destroys all WPs in the repository: (a, b) Regressions for

FIGURES (Continued)

Page

UZIC239 and *UZIC239C* at 3000, 5000 and 10,000 years, and (c-h) Scatterplots for *UZIC239* and *UZIC239C* at 10,000 years FK-150
K6.4.1-3. Comparison of cumulative releases of ^{239}Pu irreversibly attached to slow colloids into the UZ (*ESSL239C*, g) and out of the UZ (*UZIC239C*, g) at (a) 1000 years, (b) 3000 years, (c) 5000 years and (d) 10,000 years for an igneous intrusive event at 10 years that destroys all WPs in the repository FK-152
K6.4.1-4. Time-dependent release rates (*UZIF239*, g/yr) and cumulative (i.e., integrated) releases (*UZIF239C*, g) over 20,000 years for the movement of ^{239}Pu irreversibly attached to fast colloids from the UZ to the SZ resulting from an igneous intrusive event at 10 years that destroys all WPs in the repository: (a, b) *UZIF239* and *UZIF239C* for all (i.e., 300) sample elements, (c, d) *UZIF239* and *UZIF239C* for first 50 sample elements, and (e, f) PRCCs for *UZIF239* and *UZIF239C* FK-153
K6.4.1-5. Stepwise rank regression analyses and selected scatterplots for time-dependent release rates (*UZIF239*, g/yr) and cumulative (i.e., integrated) releases (*UZIF239C*, g) for the movement of ^{239}Pu irreversibly attached to fast colloids from the UZ to the SZ resulting from an igneous intrusive event at 10 years that destroys all WPs in the repository: (a, b) Regressions for *UZIF239* and *UZIF239C* at 3000, 5000 and 10,000 years, and (c-h) Scatterplots for *UZIF239* and *UZIF239C* at 10,000 years FK-154
K6.4.1-6. Comparison of cumulative releases of ^{239}Pu irreversibly attached to fast colloids into the UZ (*ESFA239C*, g) and out of the UZ (*UZIF239C*, g) at (a) 1000 years, (b) 3000 years, (c) 5000 years and (d) 10,000 years for an igneous intrusive event at 10 years that destroys all WPs in the repository FK-156
K6.4.1-7. Time-dependent release rates (*UZNP237*, g/yr) and cumulative (i.e., integrated) releases (*UZNP237C*, g) over 20,000 years for the movement of dissolved ^{237}Np from the UZ to the SZ resulting from an igneous intrusive event at 10 years that destroys all WPs in the repository: (a, b) *UZNP237* and *UZNP237C* for all (i.e., 300) sample elements, (c, d) *UZNP237* and *UZNP237C* for first 50 sample elements, and (e, f) PRCCs for *UZNP237* and *UZNP237C* FK-157
K6.4.1-8. Stepwise rank regression analyses and selected scatterplots for time-dependent release rates (*UZNP237*, g/yr) and cumulative (i.e., integrated) releases (*UZNP237C*, g) for the movement of dissolved ^{237}Np from the EBS to the UZ resulting from an igneous intrusive event at 10 years that destroys all WPs in the repository: (a, b) Regressions for *UZNP237* and *UZNP237C* at 3000, 5000 and 10,000 years, and (c-h) Scatterplots for *UZNP237* and *UZNP237C* at 10,000 years FK-158
K6.4.1-9. Comparison of cumulative releases of dissolved ^{237}Np into the UZ (*ESNP237C*, g) and out of the UZ (*UZNP237C*, g) at (a) 1000 years, (b) 3000 years, (c) 5000 years and (d) 10,000 years for an igneous intrusive event at 10 years that destroys all WPs in the repository FK-160
K6.4.1-10. Time-dependent release rates (*UZPU239*, g/yr) and cumulative (i.e., integrated) releases (*UZPU239C*, g) over 20,000 years for the movement of

FIGURES (Continued)

Page

dissolved ^{239}Pu from the UZ to the SZ resulting from an igneous intrusive event at 10 years that destroys all WPs in the repository: (a, b) *UZPU239* and *UZPU239C* for all (i.e., 300) sample elements, (c, d) *UZPU239* and *UZPU239C* for first 50 sample elements, and (e, f) PRCCs for *UZPU239* and *UZPU239C* FK-161

K6.4.1-11. Stepwise rank regression analyses and selected scatterplots for time-dependent release rates (*UZPU239*, g/yr) and cumulative (i.e., integrated) releases (*UZPU239*, g) for the movement of dissolved ^{239}Pu from the UZ to the SZ resulting from an igneous intrusive event at 10 years that destroys all WPs in the repository: (a, b) Regressions for *UZPU239* and *UZPU239C* at 3000, 5000 and 10,000 years, and (c-h) Scatterplots for *UZPU239* and *UZPU239C* at 10,000 years FK-162

K6.4.1-12. Comparison of cumulative releases of dissolved ^{239}Pu into the UZ (*ESPU239C*, g) and out of the UZ (*UZPU239C*, g) at (a) 1000 years, (b) 3000 years, (c) 5000 years and (d) 10,000 years for an igneous intrusive event at 10 years that destroys all WPs in the repository FK-164

K6.4.1-13. Time-dependent release rates (*UZTC99*, g/yr) and cumulative (i.e., integrated) releases (*UZTC99C*, g) over 20,000 years for the movement of dissolved ^{99}Tc from the UZ to the SZ resulting from an igneous intrusive event at 10 years that destroys all WPs in the repository: (a, b) *UZTC99* and *UZTC99C* for all (i.e., 300) sample elements, (c, d) *UZTC99* and *UZTC99C* for first 50 sample elements, and (e, f) PRCCs for *UZTC99* and *UZTC99C* FK-165

K6.4.1-14. Stepwise rank regression analyses and selected scatterplots for time-dependent release rates (*UZTC99*, g/yr) and cumulative (i.e., integrated) releases (*UZTC99*, g) for the movement of dissolved ^{99}Tc from the UZ to the SZ resulting from an igneous intrusive event at 10 years that destroys all WPs in the repository: (a, b) Regressions for *UZTC99* and *UZTC99C* at 3000, 5000 and 10,000 years, and (c-h) Scatterplots for *UZTC99* and *UZTC99C* at 10,000 years FK-166

K6.4.1-15. Comparison of cumulative releases of dissolved ^{99}Tc into the UZ (*ESTC99C*, g) and out of the UZ (*UZTC99C*, g) at (a) 1000 years, (b) 3000 years, (c) 5000 years and (d) 10,000 years for an igneous intrusive event at 10 years that destroys all WPs in the repository FK-168

K6.5.1-1. Time-dependent release rates (*SZIC239*, g/yr) and cumulative (i.e., integrated) releases (*SZIC239C*, g) over 20,000 years for the movement of ^{239}Pu irreversibly attached to slow colloids across a subsurface plane at the location of the RMEI resulting from an igneous intrusive event at 10 years that destroys all WPs in the repository: (a, b) *SZIC239* and *SZIC239C* for all (i.e., 300) sample elements, (c, d) *SZIC239* and *SZIC239C* for first 50 sample elements, and (e, f) PRCCs for *SZIC239* and *SZIC239C* FK-169

K6.5.1-2. Stepwise rank regression analyses and selected scatterplots for time-dependent release rates (*SZIC239*, g/yr) and cumulative (i.e., integrated) releases (*SZIC239C*, g) for the movement of ^{239}Pu irreversibly attached to slow colloids across a subsurface plane at the location of the RMEI resulting

FIGURES (Continued)

Page

from an igneous intrusive event at 10 years that destroys all WPs in the repository: (a, b) Regressions for *SZIC239* and *SZIC239C* at 3000, 5000 and 10,000 years, and (c-h) Scatterplots for *SZIC239* and *SZIC239C* at 10,000 years FK-170

K6.5.1-3. Comparison of cumulative releases of ^{239}Pu irreversibly attached to slow colloids into the SZ (*UZIC239C*, g) and across a subsurface plane at the location of the RMEI (*SZIC239C*, g) at (a) 1000 years, (b) 3000 years, (c) 5000 years and (d) 10,000 years for an igneous intrusive event at 10 years that destroys all WPs in the repository FK-172

K6.5.1-4. Time-dependent release rates (*SZIF239*, g/yr) and cumulative (i.e., integrated) releases (*SZIF239C*, g) over 20,000 years for the movement of ^{239}Pu irreversibly attached to fast colloids across a subsurface plane at the location of the RMEI resulting from an igneous intrusive event at 10 years that destroys all WPs in the repository: (a, b) *SZIF239* and *SZIF239C* for all (i.e., 300) sample elements, (c, d) *SZIF239* and *SZIF239C* for first 50 sample elements, and (e, f) PRCCs for *SZIF239* and *SZIF239C* FK-173

K6.5.1-5. Stepwise rank regression analyses and selected scatterplots for time-dependent release rates (*SZIF239*, g/yr) and cumulative (i.e., integrated) releases (*SZIF239C*, g) for the movement of ^{239}Pu irreversibly attached to fast colloids across a subsurface plane at the location of the RMEI resulting from an igneous intrusive event at 10 years that destroys all WPs in the repository: (a, b) Regressions for *SZIF239* and *SZIF239C* at 3000, 5000 and 10,000 years, and (c-h) Scatterplots for *SZIF239* and *SZIF239C* at 10,000 years FK-174

K6.5.1-6. Comparison of cumulative releases of ^{239}Pu irreversibly attached to fast colloids into the SZ (*UZIF239C*, g) and across a subsurface plane at the location of the RMEI (*SZIF239C*, g) at (a) 1000 years, (b) 3000 years, (c) 5000 years and (d) 10,000 years for an igneous intrusive event at 10 years that destroys all WPs in the repository FK-176

K6.5.1-7. Time-dependent release rates (*SZNP237*, g/yr) and cumulative (i.e., integrated) releases (*SZNP237C*, g) over 20,000 years for the movement of dissolved ^{237}Np across a subsurface plane at the location of the RMEI resulting from an igneous intrusive event at 10 years that destroys all WPs in the repository: (a, b) *SZNP237* and *SZNP237C* for all (i.e., 300) sample elements, (c, d) *SZNP237* and *SZNP237C* for first 50 sample elements, and (e, f) PRCCs for *SZNP237* and *SZNP237C* FK-177

K6.5.1-8. Stepwise rank regression analyses and selected scatterplots for time-dependent release rates (*SZNP237*, g/yr) and cumulative (i.e., integrated) releases (*SZNP237C*, g) for the movement of dissolved ^{237}Np across a subsurface plane at the location of the RMEI resulting from an igneous intrusive event at 10 years that destroys all WPs in the repository: (a, b) Regressions for *SZNP237* and *SZNP237C* at 3000, 5000 and 10,000 years, and (c-h) Scatterplots for *SZNP237* and *SZNP237C* at 10,000 years FK-178

K6.5.1-9. Comparison of cumulative releases of dissolved ^{237}Np into the SZ (*UZNP237C*, g) and across a subsurface plane at the location of the RMEI

FIGURES (Continued)

Page

(*SZNP237C*, g) at (a) 1000 years, (b) 3000 years, (c) 5000 years and (d) 10,000 years for an igneous intrusive event at 10 years that destroys all WPs in the repository FK-180
K6.5.1-10. Time-dependent release rates (*SZPU239*, g/yr) and cumulative (i.e., integrated) releases (*SZPU239C*, g) over 20,000 years for the movement of dissolved ^{239}Pu across a subsurface plane at the location of the RMEI resulting from an igneous intrusive event at 10 years that destroys all WPs in the repository: (a, b) *SZPU239* and *SZPU239C* for all (i.e., 300) sample elements, (c, d) *SZPU239* and *SZPU239C* for first 50 sample elements, and (e, f) PRCCs for *SZPU239* and *SZPU239C* FK-181
K6.5.1-11. Stepwise rank regression analyses and selected scatterplots for time-dependent release rates (*SZPU239*, g/yr) and cumulative (i.e., integrated) releases (*SZPU239C*, g) for the movement of dissolved ^{239}Pu across a subsurface plane at the location of the RMEI resulting from an igneous intrusive event at 10 years that destroys all WPs in the repository: (a, b) Regressions for *SZPU239* and *SZPU239C* at 3000, 5000 and 10,000 years, and (c-h) Scatterplots for *SZPU239* and *SZPU239C* at 10,000 years FK-182
K6.5.1-12. Comparison of cumulative releases of dissolved ^{239}Pu into the SZ (*UZPU239C*, g) and across a subsurface plane at the location of the RMEI (*SZPU239C*, g) at (a) 1000 years, (b) 3000 years, (c) 5000 years and (d) 10,000 years for an igneous intrusive event at 10 years that destroys all WPs in the repository FK-184
K6.5.1-13. Time-dependent release rates (*SZTC99*, g/yr) and cumulative (i.e., integrated) releases (*SZTC99C*, g) over 20,000 years for the movement of dissolved ^{99}Tc across a subsurface plane at the location of the RMEI resulting from an igneous intrusive event at 10 years that destroys all WPs in the repository: (a, b) *SZTC99* and *SZTC99C* for all (i.e., 300) sample elements, (c, d) *SZTC99* and *SZTC99C* for first 50 sample elements, and (e, f) PRCCs for *SZTC99* and *SZTC99C* FK-185
K6.5.1-14. Stepwise rank regression analyses and selected scatterplots for time-dependent release rates (*SZTC99*, g/yr) and cumulative (i.e., integrated) releases (*SZTC99C*, g) for the movement of dissolved ^{99}Tc across a subsurface plane at the location of the RMEI resulting from an igneous intrusive event at 10 years that destroys all WPs in the repository: (a, b) Regressions for *SZTC99* and *SZTC99C* at 3000, 5000 and 10,000 years, and (c-h) Scatterplots for *SZTC99* and *SZTC99C* at 10,000 years FK-186
K6.5.1-15. Comparison of cumulative releases of dissolved ^{99}Tc into the SZ (*UZTC99C*, g) and across a subsurface plane at the location of the RMEI (*SZTC99C*, g) at (a) 1000 years, (b) 3000 years, (c) 5000 years and (d) 10,000 years for an igneous intrusive event at 10 years that destroys all WPs in the repository FK-188
K6.5.2-1. Time-dependent release rates (*SZIC239*, g/yr) and cumulative (i.e., integrated) releases (*SZIC239C*, g) over 200,000 years for the movement of ^{239}Pu irreversibly attached to slow colloids across a subsurface plane at the location of the RMEI resulting from an igneous intrusive event at 250 years

FIGURES (Continued)

Page

that destroys all WPs in the repository: (a, b) *SZIC239* and *SZIC239C* for all (i.e., 300) sample elements, (c, d) *SZIC239* and *SZIC239C* for first 50 sample elements, and (e, f) PRCCs for *SZIC239* and *SZIC239C* FK-189

K6.5.2-2. Time-dependent release rates (*SZIF239*, g/yr) and cumulative (i.e., integrated) releases (*SZIF239C*, g) over 200,000 years for the movement of ^{239}Pu irreversibly attached to fast colloids across a subsurface plane at the location of the RMEI resulting from an igneous intrusive event at 250 years that destroys all WPs in the repository: (a, b) *SZIF239* and *SZIF239C* for all (i.e., 300) sample elements, (c, d) *SZIF239* and *SZIF239C* for first 50 sample elements, and (e, f) PRCCs for *SZIF239* and *SZIF239C* FK-190

K6.5.2-3. Time-dependent release rates (*SZNP237*, g/yr) and cumulative (i.e., integrated) releases (*SZNP237C*, g) over 1,000,000 years for the movement of dissolved ^{237}Np across a subsurface plane at the location of the RMEI resulting from an igneous intrusive event at 250 years that destroys all WPs in the repository: (a, b) *SZNP237* and *SZNP237C* for all (i.e., 300) sample elements, (c, d) *SZNP237* and *SZNP237C* for first 50 sample elements, and (e, f) PRCCs for *SZNP237* and *SZNP237C* FK-191

K6.5.2-4. Time-dependent release rates (*SZPU239*, g/yr) and cumulative (i.e., integrated) releases (*SZPU239C*, g) over 200,000 years for the movement of dissolved ^{239}Pu across a subsurface plane at the location of the RMEI resulting from an igneous intrusive event at 250 years that destroys all WPs in the repository: (a, b) *SZPU239* and *SZPU239C* for all (i.e., 300) sample elements, (c, d) *SZPU239* and *SZPU239C* for first 50 sample elements, and (e, f) PRCCs for *SZPU239* and *SZPU239C* FK-192

K6.6.1-1. Time-dependent dose to the RMEI (*DOIC239*, mrem/yr) over 20,000 years for the movement of ^{239}Pu irreversibly attached to slow colloids across a subsurface plane at the location of the RMEI resulting from an igneous intrusive event at 10 years that destroys all WPs in the repository: (a) *DOIC239* for all (i.e., 300) sample elements, (b) *DOIC239* for first 50 sample elements, and (c) PRCCs for *DOIC239* FK-193

K6.6.1-2. Stepwise rank regression analyses and selected scatterplots for time-dependent dose to the RMEI (*DOIC239*, mrem/yr) for the movement of ^{239}Pu irreversibly attached to slow colloids across a subsurface plane at the location of the RMEI (*SZIC239*, g/yr) resulting from an igneous intrusive event at 10 years that destroys all WPs in the repository: (a) Regressions for *DOIC239* at 3000, 5000 and 10,000 years, (b,c,d) Scatterplots for *DOIC239* at 10,000 years, and (e) Scatterplot comparing *SZIC239* and *DOIC239* at 10,000 years .. FK-194

K6.6.1-3. Time-dependent dose to the RMEI (*DOIF239*, mrem/yr) over 20,000 years for the movement of ^{239}Pu irreversibly attached to fast colloids across a subsurface plane at the location of the RMEI resulting from an igneous intrusive event at 10 years that destroys all WPs in the repository: (a) *DOIF239* for all (i.e., 300) sample elements, (b) *DOIF239* for first 50 sample elements, and (c) PRCCs for *DOIF239* FK-196

FIGURES (Continued)

Page

K6.6.1-4. Stepwise rank regression analyses and selected scatterplots for time-dependent dose to the RMEI (*DOIF239*, mrem/yr) for the movement of ^{239}Pu irreversibly attached to fast colloids across a subsurface plane at the location of the RMEI (*SZIF239*, g/yr) resulting from an igneous intrusive event at 10 years that destroys all WPs in the repository: (a) Regressions for *DOIF239* at 3000, 5000 and 10,000 years, (b,c,d) Scatterplots for *DOIF239* at 10,000 years, and (e) Scatterplot comparing *SZIF239* and *DOIF239* at 10,000 years... FK-197

K6.6.1-5. Time-dependent dose to the RMEI (*DONP237*, mrem/yr) over 20,000 years for the movement of dissolved ^{237}Np across a subsurface plane at the location of the RMEI resulting from an igneous intrusive event at 10 years that destroys all WPs in the repository: (a) *DONP237* for all (i.e., 300) sample elements, (b) *DONP237*for first 50 sample elements, and (c) PRCCs for *DONP237*..... FK-198

K6.6.1-6. Stepwise rank regression analyses and selected scatterplots for time-dependent dose to the RMEI (*DONP237*, mrem/yr) for the movement of dissolved ^{237}Np across a subsurface plane at the location of the RMEI (*SZNP237*, g/yr) resulting from an igneous intrusive event at 10 years that destroys all WPs in the repository: (a) Regressions for *DONP237* at 3000, 5000 and 10,000 years, (b,c,d) Scatterplots for *DONP237* at 10,000 years, and (e) Scatterplot comparing *SZNP237* and *DONP237* at 10,000 years..... FK-199

K6.6.1-7. Time-dependent dose to the RMEI (*DOPU239*, mrem/yr) over 20,000 years for the movement of dissolved ^{239}Pu across a subsurface plane at the location of the RMEI resulting from an igneous intrusive event at 10 years that destroys all WPs in the repository: (a) *DOPU239* for all (i.e., 300) sample elements, (b) *DOPU239* for first 50 sample elements, and (c) PRCCs for *DOPU239* FK-201

K6.6.1-8. Stepwise rank regression analyses and selected scatterplots for time-dependent dose to the RMEI (*DOPU239*, mrem/yr) for the movement of dissolved ^{239}Pu across a subsurface plane at the location of the RMEI (*SZPU239*, g/yr) resulting from an igneous intrusive event at 10 years that destroys all WPs in the repository: (a) Regressions for *DOPU239*at 3000, 5000 and 10,000 years, (b,c,d) Scatterplots for *DOPU239* at 10,000 years, and (e) Scatterplot comparing *SZPU239* and *DOPU239* at 10,000 years FK-202

K6.6.1-9. Time-dependent dose to the RMEI (*DOTC99*, mrem/yr) over 20,000 years for the movement of dissolved ^{99}Tc across a subsurface plane at the location of the RMEI resulting from an igneous intrusive event at 10 years that destroys all WPs in the repository: (a) *DOTC99* for all (i.e., 300) sample elements, (b) *DOTC99* for first 50 sample elements, and (c) PRCCs for *DOTC99*..... FK-204

K6.6.1-10. Stepwise rank regression analyses and selected scatterplots for time-dependent dose to the RMEI (*DOTC99*, mrem/yr) for the movement of dissolved ^{99}Tc across a subsurface plane at the location of the RMEI (*SZTC99*, g/yr) resulting from an igneous intrusive event at 10 years that destroys all WPs in the repository: (a) Regressions for *DOTC99* at 3000,

FIGURES (Continued)

Page

5000 and 10,000 years, (b,c,d) Scatterplots for *DOTC99* at 10,000 years, and (e) Scatterplot comparing *SZTC99* and *DOTC99* at 10,000 years FK-205
K6.6.2-1. Time-dependent dose to the RMEI (*DOIC239*, mrem/yr) over 200,000 years for the movement of ^{239}Pu irreversibly attached to slow colloids across a subsurface plane at the location of the RMEI resulting from an igneous intrusive event at 250 years that destroys all WPs in the repository: (a) *DOIC239* for all (i.e., 300) sample elements, (b) *DOIC239* for first 50 sample elements, and (c) PRCCs for *DOIC239* FK-207
K6.6.2-2. Time-dependent dose to the RMEI (*DOIF239*, mrem/yr) over 200,000 years for the movement of ^{239}Pu irreversibly attached to fast colloids across a subsurface plane at the location of the RMEI resulting from an igneous intrusive event at 250 years that destroys all WPs in the repository: (a) *DOIF239* for all (i.e., 300) sample elements, (b) *DOIF239* for first 50 sample elements, and (c) PRCCs for *DOIF239* FK-208
K6.6.2-3. Time-dependent dose to the RMEI (*DONP237*, mrem/yr) over 1,000,000 years for the movement of dissolved ^{237}Np across a subsurface plane at the location of the RMEI resulting from an igneous intrusive event at 250 years that destroys all WPs in the repository: (a) *DONP237*for all (i.e., 300) sample elements, (b) *DONP237*for first 50 sample elements, and (c) PRCCs for *DONP237* FK-209
K6.6.2-4. Time-dependent dose to the RMEI (*DOPU239*, mrem/yr) over 200,000 years for the movement of dissolved ^{239}Pu across a subsurface plane at the location of the RMEI resulting from an igneous intrusive event at 250 years that destroys all WPs in the repository: (a) *DOPU239* for all (i.e., 300) sample elements, (b) *DOPU239* for first 50 sample elements, and (c) PRCCs for *DOPU239* FK-210
K6.7.1-1. Expected dose to RMEI (*EXPDOSE*, mrem/yr) over [0, 20,000 yr] for all radioactive species resulting from igneous intrusion: (a) *EXPDOSE* for all (i.e., 300) sample elements, (b) *EXPDOSE* for first 50 sample elements, and (c) PRCCs for *EXPDOSE* FK-211
K6.7.1-2. Stepwise rank regression analyses and selected scatterplots for expected dose to RMEI (*EXPDOSE*, mrem/yr) over [0, 20,000 yr] for all radioactive species resulting from igneous intrusion: (a) Regressions for *EXPDOSE* at 3000, 5000 and 10,000 years, and (b,c,d) Scatterplots for *EXPDOSE* at 10,000 years FK-212
K6.7.2-1. Expected dose to RMEI (*EXPDOSE*, mrem/yr) over [0, 1,000,000 yr] for all radioactive species resulting from igneous intrusion: (a) *EXPDOSE* for all (i.e., 300) sample elements, (b) *EXPDOSE* for first 50 sample elements, and (c) PRCCs for *EXPDOSE* FK-214
K6.7.2-2. Stepwise rank regression analyses and selected scatterplots for expected dose to RMEI (*EXPDOSE*, mrem/yr) over [0, 1,000,000 yr] for all radioactive species resulting from igneous intrusion: (a) Regressions for *EXPDOSE* at 50,000, 200,000 and 500,000 years, and (b,c,d) Scatterplots for *EXPDOSE* at 500,000 years FK-215

FIGURES (Continued)

Page

K6.8.1-1. Expected dose to RMEI (*EXPDOSE*, mrem/yr) over [0, 20,000 yr] for all radioactive species resulting from igneous eruption: (a) *EXPDOSE* for all (i.e., 300) sample elements, (b) *EXPDOSE* for first 50 sample elements, and (c) PRCCs for *EXPDOSE* FK-217
K6.8.1-2. Stepwise rank regression analyses and selected scatterplots for expected dose to RMEI (*EXPDOSE*, mrem/yr) over [0, 20,000 yr] for all radioactive species resulting from igneous eruption: (a) Regressions for *EXPDOSE* at 3000, 5000 and 10,000 years, and (b,c,d) Scatterplots for *EXPDOSE* at 10,000 years..... FK-218
K6.8.2-1. Expected dose to RMEI (*EXPDOSE*, mrem/yr) over [0, 1,000,000 yr] for all radioactive species resulting from igneous eruption: (a) *EXPDOSE* for all (i.e., 300) sample elements, (b) *EXPDOSE* for first 50 sample elements, and (c) PRCCs for *EXPDOSE* FK-219
K6.8.2-2. Stepwise rank regression analyses and selected scatterplots for expected dose to RMEI (*EXPDOSE*, mrem/yr) over [0, 1,000,000 yr] for all radioactive species resulting from igneous eruption: (a) Regressions for *EXPDOSE* and (b,c,d) Scatterplots for *EXPDOSE* at 500,000 years..... FK-220
K7.3-1. Removed FK-221
K7.3-2. Removed FK-222
K7.3-3. Removed FK-223
K7.3-4. Removed FK-224
K7.3-5. Time-dependent release rates (*ESNP237*, g/yr) and cumulative (i.e., integrated) releases (*ESNP237C*, g) over 20,000 years for the movement of dissolved ^{237}Np from the EBS to the UZ resulting from a seismically induced fractional damaged area of 10^{-6}(32.6 m^2) at 200 years to all CDSP WPs in the repository: (a, b) *ESNP237* and *ESNP237C* for all (i.e., 300) sample elements, (c, d) *ESNP237* and *ESNP237C* for first 50 sample elements, and (e, f) PRCCs for *ESNP237* and *ESNP237C*..... FK-225
K7.3-6. Stepwise rank regression analyses and selected scatterplots for time-dependent release rates (*ESNP237*, g/yr) and cumulative (i.e., integrated) releases (*ES NP237C*, g) for the movement of dissolved ^{237}Np from the EBS to the UZ resulting froma seismically induced fractional damaged area of 10^{-6}(32.6 m^2) at 200 years to all CDSP WPs in the repository: (a, b) Regressions for *ESNP237* and *ESNP237C* at 3000, 5000 and 10,000 years, and (c-h) Scatterplots for *ESNP237* and *ESNP237C* at 10,000 years FK-226
K7.3-7. Time-dependent release rates (*ESPU239*, g/yr) and cumulative (i.e., integrated) releases (*ESPU239C*, g) over 20,000 years for the movement of dissolved ^{239}Pu from the EBS to the UZ resulting from a seismically induced fractional damaged area of 10^{-6}(32.6 m^2) at 200 years to all CDSP WPs in the repository: (a, b) *ESPU239* and *ESPU239C* for all (i.e., 300) sample elements, (c, d) *ESPU239* and *ESPU239C* for first 50 sample elements, and (e, f) PRCCs for *ESPU239* and *ESPU239C* FK-228
K7.3-8. Stepwise rank regression analyses and selected scatterplots for time-dependent release rates (*ESPU239*, g/yr) and cumulative (i.e., integrated) releases (*ESPU239*, g) for the movement of dissolved ^{239}Pu from the EBS to

FIGURES (Continued)

Page

the UZ resulting from a seismically induced fractional damaged area of 10^{-6}(32.6 m^2) at 200 years to all CDSP WPs in the repository: (a, b) Regressions for *ESPU239* and *ESPU239C* at 3000, 5000 and 10,000 years, and (c-h) Scatterplots for *ESPU239* and *ESPU239C* at 10,000 years FK-229

K7.3-9. Time-dependent release rates (*ESTC99*, g/yr) and cumulative (i.e., integrated) releases (*ESTC99C*, g) over 20,000 years for the movement of dissolved ^{99}Tc from the EBS to the UZ resulting from a seismically induced fractional damaged area of 10^{-6}(32.6 m^2) at 200 years to all CDSP WPs in the repository: (a, b) *ESTC99* and *ESTC99C* for all (i.e., 300) sample elements, (c, d) *ESTC99* and *ESTC99C* for first 50 sample elements, and (e, f) PRCCs for *ESTC99* and *ESTC99C* FK-231

K7.3-10. Stepwise rank regression analyses and selected scatterplots for time-dependent release rates (*ESTC99*, g/yr) and cumulative (i.e., integrated) releases (*ESTC99*, g) for the movement of dissolved ^{99}Tc from the EBS to the UZ resulting from a seismically induced fractional damaged area of 10^{-6}(32.6 m^2) at 200 years to all CDSP WPs in the repository: (a, b) Regressions for *ESTC99* and *ESTC99C* at 3000, 5000 and 10,000 years, and (c-h) Scatterplots for *ESTC99* and *ESTC99C* at 10,000 years FK-232

K7.4-1. Time-dependent release rates (*UZIC239*, g/yr) and cumulative (i.e., integrated) releases (*UZIC239C*, g) over 20,000 years for the movement of ^{239}Pu irreversibly attached to glass colloids from the UZ to the SZ resulting from a seismically induced fractional damaged area of 10^{-6}(32.6 m^2) at 200 years to all CDSP WPs in the repository: (a, b) *UZIC239* and *UZIC239C* for all (i.e., 300) sample elements, (c, d) *UZIC239* and *UZIC239C* for first 50 sample elements, and (e, f) PRCCs for *UZIC239* and *UZIC239C* FK-234

K7.4-2. Time-dependent release rates (*UZIF239*, g/yr) and cumulative (i.e., integrated) releases (*UZIF239C*, g) over 20,000 years for the movement of ^{239}Pu irreversibly attached to glass colloids from the UZ to the SZ resulting from a seismically induced fractional damaged area of 10^{-6}(32.6 m^2) at 200 years to all CDSP WPs in the repository: (a, b) *UZIF239* and *UZIF239C* for all (i.e., 300) sample elements, (c, d) *UZIC239* and *UZIC239C* for first 50 sample elements, and (e, f) PRCCs for *UZIF239* and *UZIF239C* FK-235

K7.4-3. Time-dependent release rates (*UZNP237*, g/yr) and cumulative (i.e., integrated) releases (*UZNP2379C*, g) over 20,000 years for the movement of dissolved ^{237}Np from the UZ to the SZ resulting from a seismically induced fractional damaged area of 10^{-6}(32.6 m^2) at 200 years to all CDSP WPs in the repository: (a, b) *UZNP237* and *UZNP237C* for all (i.e., 300) sample elements, (c, d) *UZNP237* and *UZNP237C* for first 50 sample elements, and (e, f) PRCCs for *UZNP237* and *UZNP237C* FK-236

K7.4-4. Time-dependent release rates (*UZPU239*, g/yr) and cumulative (i.e., integrated) releases (*UZPU239C*, g) over 20,000 years for the movement of dissolved ^{239}Pu from the UZ to the SZ resulting from a seismically induced fractional damaged area of 10^{-6}(32.6 m^2) at 200 years to all CDSP WPs in the repository: (a, b) *UZPU239* and *UZPU239C* for all (i.e., 300) sample

FIGURES (Continued)

Page

elements, (c, d) *UZPU239* and *UZPU239C* for first 50 sample elements, and (e, f) PRCCs for *UZPU239* and *UZPU239C* FK-237

K7.4-5. Time-dependent release rates (*UZTC99*, g/yr) and cumulative (i.e., integrated) releases (*UZTC99C*, g) over 20,000 years for the movement of dissolved ^{99}Tc from the UZ to the SZ resulting from a seismically induced fractional damaged area of 10^{-6}(32.6 m^2) at 200 years to all CDSP WPs in the repository: (a, b) *UZTC99* and *UZTC99C* for all (i.e., 300) sample elements, (c, d) *UZTC99* and *UZTC99C* for first 50 sample elements, and (e, f) PRCCs for *UZTC99* and *UZTC99C* FK-238

K7.5-1. Time-dependent release rates (*SZIC239*, g/yr) and cumulative (i.e., integrated) releases (*SZIC239C*, g) over 20,000 years for the movement of ^{239}Pu irreversibly attached to glass colloids across a subsurface plane at the location of the RMEI resulting from a seismically induced fractional damaged area of 10^{-6}(32.6 m^2) at 200 years to all CDSP WPs in the repository: (a, b) *SZIC239* and *SZIC239C* for all (i.e., 300) sample elements, (c, d) *SZIC239* and *SZIC239C* for first 50 sample elements, and (e, f) PRCCs for *SZIC239* and *SZIC239C* FK-239

K7.5-2. Time-dependent release rates (*SZIF239*, g/yr) and cumulative (i.e., integrated) releases (*SZIF239C*, g) over 20,000 years for the movement of ^{239}Pu irreversibly attached to glass colloids across a subsurface plane at the location of the RMEI resulting from a seismically induced fractional damaged area of 10^{-6}(32.6 m^2) at 200 years to all CDSP WPs in the repository: (a, b) *SZIF239* and *SZIF239C* for all (i.e., 300) sample elements, (c, d) *SZIC239* and *SZIC239C* for first 50 sample elements, and (e, f) PRCCs for *SZIF239* and *SZIF239C* FK-240

K7.5-3. Time-dependent release rates (*SZNP237*, g/yr) and cumulative (i.e., integrated) releases (*SZNP2379C*, g) over 20,000 years for the movement of dissolved ^{237}Np across a subsurface plane at the location of the RMEI resulting from a seismically induced fractional damaged area of 10^{-6}(32.6 m^2) at 200 years to all CDSP WPs in the repository: (a, b) *SZNP237* and *SZNP237C* for all (i.e., 300) sample elements, (c, d) *SZNP237* and *SZNP237C* for first 50 sample elements, and (e, f) PRCCs for *SZNP237* and *SZNP237C* FK-241

K7.5-4. Time-dependent release rates (*SZPU239*, g/yr) and cumulative (i.e., integrated) releases (*SZPU239C*, g) over 20,000 years for the movement of dissolved ^{239}Pu across a subsurface plane at the location of the RMEI resulting from a seismically induced fractional damaged area of 10^{-6}(32.6 m^2) at 200 years to all CDSP WPs in the repository: (a, b) *SZPU239* and *SZPU239C* for all (i.e., 300) sample elements, (c, d) *SZPU239* and *SZPU239C* for first 50 sample elements, and (e, f) PRCCs for *SZPU239* and *SZPU239C* FK-242

K7.5-5. Time-dependent release rates (*SZTC99*, g/yr) and cumulative (i.e., integrated) releases (*SZTC99C*, g) over 20,000 years for the movement of dissolved ^{99}Tc from across a subsurface plane at the location of the RMEI resulting from a

FIGURES (Continued)

Page

seismically induced fractional damaged area of 10^{-6}(32.6 m^2) at 200 years to all CDSP WPs in the repository: (a, b) *SZTC99* and *SZTC99C* for all (i.e., 300) sample elements, (c, d) *SZTC99* and *SZTC99C* for first 50 sample elements, and (e, f) PRCCs for *SZTC99* and *SZTC99C* FK-243

K.7.6-1. Time-dependent dose to the RMEI (*DOIC239*, mrem/yr) over 20,000 years for the movement of ^{239}Pu irreversibly attached to slow colloids across a subsurface plane at the location of the RMEI resulting from a seismically induced fractional damaged area of 10^{-6}(32.6 m^2) at 200 years to all CDSP WPs in the repository: (a) *DOIC239* for all (i.e., 300) sample elements, (b) *DOIC239* for first 50 sample elements, and (c) PRCCs for *DOIC239* FK-245

K.7.6-2. Time-dependent dose to the RMEI (*DOIF239*, mrem/yr) over 20,000 years for the movement of ^{239}Pu irreversibly attached to fast colloids across a subsurface plane at the location of the RMEI resulting from a seismically induced fractional damaged area of 10^{-6}(32.6 m^2) at 200 years to all CDSP WPs in the repository: (a) *DOIF239* for all (i.e., 300) sample elements, (b) *DOIF239* for first 50 sample elements, and (c) PRCCs for *DOIF239* FK-246

K.7.6-3. Time-dependent dose to the RMEI (*DONP237*, mrem/yr) over 20,000 years for the movement of dissolved ^{237}Np across a subsurface plane at the location of the RMEI resulting from a seismically induced fractional damaged area of 10^{-6}(32.6 m^2) at 200 years to all CDSP WPs in the repository: (a) *DONP237*for all (i.e., 300) sample elements, (b) *DONP237*for first 50 sample elements, and (c) PRCCs for *DONP237* FK-247

K.7.6-4. Time-dependent dose to the RMEI (*DOPU239*, mrem/yr) over 20,000 years for the movement of dissolved ^{239}Pu across a subsurface plane at the location of the RMEI resulting from a seismically induced fractional damaged area of 10^{-6}(32.6 m^2) at 200 years to all CDSP WPs in the repository: (a) *DOPU239* for all (i.e., 300) sample elements, (b) *DOPU239* for first 50 sample elements, and (c) PRCCs for *DOPU239* FK-248

K.7.6-5. Time-dependent dose to the RMEI (*DOTC99*, mrem/yr) over 20,000 years for the movement of dissolved ^{99}Tc across a subsurface plane at the location of the RMEI resulting from a seismically induced fractional damaged area of 10^{-6}(32.6 m^2) at 200 years to all CDSP WPs in the repository: (a) *DOTC99*for all (i.e., 300) sample elements, (b) *DOTC99* for first 50 sample elements, and (c) PRCCs for *DOTC99* FK-249

K.7.7.1-1. Expected dose to RMEI (*EXPDOSE*, mrem/yr) over [0, 20,000 yr] for all radioactive species resulting from seismic ground motion: (a) *EXPDOSE* for all (i.e., 300) sample elements, (b) *EXPDOSE* for first 50 sample elements, and (c) PRCCs for *EXPDOSE* FK-250

K.7.7.1-2. Stepwise rank regression analyses and selected scatterplots for expected dose to RMEI (*EXPDOSE*, mrem/yr) over [0, 20,000 yr] for all radioactive species resulting from seismic ground motion: (a) Regressions for *EXPDOSE* at 3000, 5000 and 10,000 years, and (b,c,d) Scatterplots for *EXPDOSE* at 10,000 years FK-251

FIGURES (Continued)

Page

K.7.7.2-1. Expected dose to RMEI (*EXPDOSE*, mrem/yr) over [0, 1,000,000 yr] for all radioactive species resulting from seismic ground motion: (a) *EXPDOSE* for all (i.e., 300) sample elements, (b) *EXPDOSE* for first 50 sample elements, and (c) PRCCs for *EXPDOSE* FK-253
K.7.7.2-2. Stepwise rank regression analyses and selected scatterplots for expected dose to RMEI (*EXPDOSE*, mrem/yr) over [0, 1,000,000 yr] for all radioactive species resulting from seismic ground motion: (a) Regressions for *EXPDOSE* at 50,000, 200,000 and 500,000 years, and (b,c,d) Scatterplots for *EXPDOSE* at 500,000 years FK-254
K.7.8.1-1. Expected dose to RMEI (*EXPDOSE*, mrem/yr) over [0, 20,000 yr] for all radioactive species resulting from seismic fault displacement: (a) *EXPDOSE* for all (i.e., 300) sample elements, (b) *EXPDOSE* for first 50 sample elements, and (c) PRCCs for *EXPDOSE* FK-256
K.7.8.1-2. Stepwise rank regression analyses and selected scatterplots for expected dose to RMEI (*EXPDOSE*, mrem/yr) over [0, 20,000 yr] for all radioactive species resulting from seismic fault displacement: (a) Regressions for *EXPDOSE* at 3000, 5000 and 10,000 years, and (b,c,d) Scatterplots for *EXPDOSE* at 10,000 years FK-257
K.7.8.2-1. Expected dose to RMEI (*EXPDOSE*, mrem/yr) over [0, 1,000,000 yr] for all radioactive species resulting from seismic fault displacement: (a) *EXPDOSE* for all (i.e., 300) sample elements, (b) *EXPDOSE* for first 50 sample elements, and (c) PRCCs for *EXPDOSE* FK-259
K.7.8.2-2. Stepwise rank regression analyses and selected scatterplots for expected dose to RMEI (*EXPDOSE*, mrem/yr) over [0, 1,000,000 yr] for all radioactive species resulting from seismic fault displacement: (a) Regressions for *EXPDOSE* at 50,000, 200,000 and 500,000 years, and (b,c,d) Scatterplots for *EXPDOSE* at 500,000 years FK-260
K.8.1-1 Expected dose to RMEI (*EXPDOSE*, mrem/yr) over [0, 20,000 yr] for all scenario classes: (a) *EXPDOSE* for all (i.e., 300) sample elements, (b) *EXPDOSE* for first 50 sample elements, and (c) PRCCs for *EXPDOSE* FK-262
K.8.1.-2 Stepwise rank regression analyses and selected scatterplots for expected dose to RMEI (*EXPDOSE*, mrem/yr) over [0, 20,000 yr] for all scenario classes: (a) Regressions for *EXPDOSE* at 3000, 5000 and 10,000 years, and (b,c,d) Scatterplots for *EXPDOSE* at 10,000 years FK-263
K.8.2-1 Expected dose to RMEI (*EXPDOSE*, mrem/yr) over [0, 1,000,000 yr] for all scenario classes: (a) *EXPDOSE* for all (i.e., 300) sample elements, (b) *EXPDOSE* for first 50 sample elements, and (c) PRCCs for *EXPDOSE* FK-265
K.8.2-2 Stepwise rank regression analyses and selected scatterplots for expected dose to RMEI (*EXPDOSE*, mrem/yr) over [0, 1,000,000 yr] for all scenario classes: (a) Regressions for *EXPDOSE* at 50,000, 200,000 and 500,000 years, and (b,c,d) Scatterplots for *EXPDOSE* at 500,000 years FK-266

FIGURES (Continued)

Page

L-1. Percolation Flux over the Repository Area....L-101
L-2. CSNF and Defense HLW Waste Package Surface Temperatures, 10th Percentile Infiltration Scenario, Medium Thermal Conductivity....L-102
L-3. CSNF and Defense HLW Peak Waste Package Surface Temperature Distribution, 10th Percentile Infiltration Scenario, Medium Thermal Conductivity....L-103
L-4. CSNF and Defense HLW Waste Package Surface Temperature Range, 10th Percentile Infiltration Scenario....L-104
L-5. Average CSNF and Defense HLW Peak Waste Package Surface Temperature, 10th Percentile Infiltration Scenario....L-105
L-6. Maximum CO_2 Partial Pressure: (a) Group 1 Starting Water, (b) Group 2 Starting Water, (c) Group 3 Starting Water, and (d) Group 4 Starting Water....L-106
L-7. Depth Where Stress Corrosion Cracks Can Initiate and Propagate Along the Circumference of the Waste Package Outer Lid Closure Weld Region....L-108
L-8. CSNF Waste Form Degradation for Expected Value Coefficients with Varying pH....L-109
L-9. Defense HLW Waste Form Degradation for Expected Value Coefficients at Different Temperatures....L-110
L-10. Fraction of Seepage that Can Enter a Waste Package with General Corrosion Breaches....L-111
L-11. Dissolved Concentration Limits....L-112
L-12. General Schematic Diagram of a Single EBS Radionuclide Transport Network in Simplified TSPA....L-113
L-13. General Schematic Diagram of a Single EBS Radionuclide Transport Network Used in the Simplified TSPA....L-114

N-1. Venn diagram of overlapping damage modes....N-15

O-1. Fraction of Locations with the Potential for Localized Corrosion Initiation: (a) Bin1, CDSP; (b) Bin1, CSNF; (c) Bin2, CDSP; (d) Bin2, CSNF; (e) Bin3, CDSP; (f) Bin3, CSNF; (g) Bin4, CDSP; (h) Bin4, CSNF; (i) Bin5, CDSP; and (j) Bin5, CSNF....O-7
O-2. Fraction of Locations in Each Percolation Subregion with the Potential for Localized Corrosion Initiation....O-12
O-3. Average Delta E for Percolation Subregion 3, CSNF, for 300 Epistemic Realizations....O-13

P-1. (a) Comparison of the Mean Annual Dose for the Impact Evaluation Case with the Base Case for the Waste Package EF Modeling Case and (b) Major Radionuclide Dose Contributors for the Corrected Case....P-39
P-2. (a) Comparison of the Mean Annual Dose for the Impact Evaluation Case with the Base Case for the Drip Shield EF Modeling Case and (b) Major Radionuclide Dose Contributors for the Corrected Case....P-40

FIGURES (Continued)

Page

P-3. (a) Comparison of the Mean Annual Dose for the Impact Evaluation Case with the Base Case for the Seismic FD Modeling Case and (b) Major Radionuclide Dose Contributors for the Corrected Case....P-41

P-4. (a) Comparison of the Mean Annual Dose for the Impact Evaluation Case with the Base Case for the Seismic GM Modeling Case and (b) Major Radionuclide Dose Contributors for the Corrected Case....P-42

P-5. (a) Comparison of the Mean Annual Dose for the Impact Evaluation Case with the Base Case for the Igneous Intrusion Modeling Case and (b) Major Radionuclide Dose Contributors for the Corrected Case....P-43

P-6. Mean Annual Dose for the Igneous Intrusion Modeling Case: Base Case and Probability of the Igneous Event set to 10^{-7} per year for (a) 20,000 Years and (b) 1,000,000 Years....P-44

P-7. Mean Annual Dose for the Volcanic Eruption Modeling Case: Base Case and Probability of the Igneous Event set to 10^{-7} per year for (a) 20,000 Years and (b) 1,000,000 Years....P-45

P-8. Mean Annual Dose Comparison for the Base Case and the Impact Evaluation Case with Updated Longitudinal Dispersivity for the Igneous Intrusion Modeling Case....P-46

P-9. Comparison of Mean Annual Dose Contribution from ^{226}Ra and ^{230}Th for the Base Case and the Impact Evaluation Case with Updated Longitudinal Dispersivity for the Igneous Intrusion Modeling Case....P-47

P-10. Major Radionuclide Dose Contributors for the Impact Evaluation Case with Updated Longitudinal Dispersivity for the Igneous Intrusion Modeling Case....P-48

P-11. Mean Seepage Flux Comparison for Percolation Subregion 3 for the Base Case and the Impact Evaluation Case for the Seismic FD Modeling Case....P-49

P-12. Mean Annual Dose Comparisons for the Base Case and the Impact Evaluation Case for the Seismic FD Modeling Case....P-50

P-13. Mean Annual Dose Comparisons for the Base Case and the Impact Evaluation Case for the Igneous Intrusion Modeling Case....P-51

P-14. Mean Annual Dose Comparisons for the Base Case and the Impact Evaluation Case for the Seismic Ground Motion Modeling Case to Evaluate the Impact of the GoldSim Solver Error....P-52

P-15. Mean Annual Dose Comparisons for the Base Case and the Impact Evaluation Case for the Igneous Intrusion Modeling Case to Evaluate the Impact of the GoldSim Solver Error....P-53

P-16. Mean Annual Dose Comparisons for the Base Case and the Impact Evaluation Case for the Seismic GM Modeling Case to Evaluate the Impact of UZ Transport Delay of some Radionuclides through the Fault Zones....P-54

P-17. Mean Annual Dose Comparisons of Major Radionuclides for the Base Case and the Impact Evaluation Case for the Seismic Ground Motion Modeling Case to Evaluate the Impact of Unsaturated Zone Transport Error through the Fault Zones....P-55

FIGURES (Continued)

Page

P-18. Mean Annual Dose Comparisons for the Base Case and the Impact Evaluation Case for the Igneous Intrusion Modeling Case to Evaluate the Impact of Unsaturated Zone Transport Error through the Fault Zones P-56
P-19. Mean Annual Dose Comparisons of Major Radionuclides for the Base Case and the Impact Evaluation Case for the Igneous Intrusion Modeling Case to Evaluate the Impact of Unsaturated Zone Transport Error through the Fault Zones..... P-57

TABLES

Page

8.1-1. Performance Demonstration Results for Individual Protection Standard T8.1-1
8.1-2. Performance Demonstration Results for Groundwater Protection Standard T8.1-1
8.1-3. Performance Demonstration Results for Human Intrusion Standard with Drilling Event at 200,000 years After Closure T8.1-1
8.1-4. Uncertainty in Projections of Peak Mean Annual Dose (mrem) for Individual Protection Standard T8.1-1
8.1-5. Uncertainty Importance Ranking as a function of time for Key TSPA-LA Model Parameters T8.1-2

8.3-1. Decay of Total Curie Inventory as a Function of Time and Dominant Contributors to Total Curie Inventory T8.3-1

C3-1. Software Codes Specific to the PMA TC-1
C3-2. TSPA-LA Model Software Codes used in the PMA TC-1
C3-3. Unqualified Software TC-2
C3-4. FEHM Software Documents TC-2
C3-5. TSPA_Input_DBv2.2 Software Documents TC-3
C3-6. iTough V5.0 Software Documents TC-3
C4-1. TSPA-LA Model Parameters Changed or Deleted for the PMA TC-4
C4-2. Input Parameters Added for the PMA TC-13
C4-3. Sources and Parameter Entry Form Numbers for the PMA-Specific Direct Inputs TC-53
C5-1. Assumptions Identified as Potentially Conservative and Significant to Annual Dose Rate TC-58
C6-1. Relative Humidity Threshold for 0.5mM Fluoride Concentration TC-67
C6-2. Stoichiometries of Waste Degradation Reactions TC-69
C6-3. Parameter Values Used in Diffusion-Dominated Simulations TC-69
C6-4. Parameter Values Used in Liquid Influx Simulations TC-70
C6-5. Controlling Factors for CSNF Dissolution TC-70
C6-6. Controlling Parameter Distributions for CSNF Degradation TC-71
C6-7. Distribution of T_{RC} Used in the Glass Degradation Model for PMA TC-71
C6-8. Recommended Uncertainties for Radionuclide Solubilities TC-72
C6-9. Uncertain Parameters for the Impacts of Reducing Zones in the PMA TC-73
C6-10. Cumulative Distribution for FPVO for Use in the PMA (log_{10}-transformed) TC-73
C9-1. Impact Assessment Summary Table TC-74

E-1. Summary of Responses to International Review Team Summary Review Comments E-3

F-1. Summary of the Dynamically Linked Libraries used in the TSPA-LA Model F-19
F-2. *fehmn_v2_24-01.dll* Input Files F-20
F-3. *MFCP_LA.dll* Input Files F-26
F-4. *SEEPAGEDLL_LA.dll* Input Files F-27

TABLES (Continued)

Page

F-5. sz_conv_3.10.dll Input Files F-28
F-6. *wapdeg.dll* Input Files F-30
F-7. *MkTable_LA.dll* Input Files F-30
F-8. *SCCD.dll* Input Files F-31
F-9. PREWAP_LA.exe Output Files F-31
F-10. PassTable1D_LAv2.dll Input Files F-32
F-11. PassTable3D LAv2.dll Input Files F-32
F-12. GetThk.dll Input Files F-32
F-13. FAR_1-2.dll Input Files F-33

H-1. Applicable Regulatory Requirements of 10 CFR Part 63 and NUREG-1804 Acceptance Criteria Addressed in this Document H-7

I-1. Explanation of the Column Headings in Table I-2 ..... I-5
I-2. Model Implementation for Included Features, Events, and Processes I-6

K3-1. High-Level Summary of Epistemically Uncertain Variables (i.e., elements of **e**) Considered in the TSPA-LA (Sensitivity Analysis Name) TK-1
K3-2. High-Level Summary of Epistemically Uncertain Variables (i.e., elements of **e**) Considered in the TSPA-LA (TSPA Parameter Name) TK-27
K3-3. Detailed Summary of Epistemically Uncertain Variables (i.e., elements of **e**) Considered in the TSPA-LA (TSPA Parameter Name) TK-53
K3-4. Alphabetic Listing of the Various TSPA-LA Model Results Considered in Uncertainty and Sensitivity Analyses for Nominal (N), Drip Shield Early Failure (ED), Waste Package Early Failure (EW), Igneous Intrusive (II), Igneous Eruptive (IE), Seismic Ground Motion (SG), and Seismic Fault Displacement (SF) Modeling Cases in Appendix K4, K5, K6, and K7 ..... TK-115
K4.1-1. Summary of TSPA-LA Model Results Considered in Uncertainty and Sensitivity Analyses for the Nominal Scenario Class TK-119

K5.1-1. Summary of TSPA-LA Model Results Considered in Uncertainty and Sensitivity Analyses for the Early Failure Scenario Classes TK-121
K5.1-2 Summary of Uncertainty and Sensitivity Analysis Results for the Early Failure Scenario Class for Release from the Engineered Barrier System TK-124
K5.1-3 Summary of Uncertainty and Sensitivity Analysis Results for Radionuclide Movement from the UZ to the SZ Resulting from Early DS Failure Above a CDSP WP Under Dripping Conditions TK-130
K5.1-4 Summary of Uncertainty and Sensitivity Analysis Results for Radionuclide Movement in the SZ Across a Subsurface Plane at the Location of the RMEI Resulting from Early DS Failure Above a CDSP WP Under Dripping Conditions TK-132
K5.1-5 Summary of Uncertainty and Sensitivity Analysis Results for Dose to the RMEI from Selected Radionuclides Resulting from Early DS Failure Above a CDSP WP Under Dripping Conditions TK-134

TABLES (Continued)

Page

K5.1-6 Summary of Uncertainty and Sensitivity Analysis Results for Expected Dose to the RMEI (*EXPDOSE*, mrem/yr) Resulting from Early Failures TK-135

K6.1-1. Summary of TSPA-LA Model Results Considered in Uncertainty and Sensitivity Analyses for the Igneous Scenario Classes TK-137

K6.1-2 Summary of Uncertainty and Sensitivity Analysis Results for Radionuclide Movement from the EBS to the UZ Resulting from an Igneous Intrusive Event that Destroys All WPs in the Repository TK-139

K6.1-3 Summary of Uncertainty and Sensitivity Analysis Results for Radionuclide Movement from the UZ to the SZ Resulting from an Igneous Intrusive Event that Destroys all WPs in the Repository. TK-141

K6.1-4 Summary of Uncertainty and Sensitivity Analysis Results for Radionuclide Movement in the SZ Across a Subsurface Plane at the Location of the RMEI Resulting from an Igneous Intrusive Event That Destroys all WPs in the Repository. TK-143

K6.1-5 Summary of Uncertainty and Sensitivity Analysis Results for Dose to the RMEI from Selected Radionuclides Resulting from an Igneous Intrusive Event that Destroys All WPs in the Repository. TK-145

K6.1-6 Summary of Uncertainty and Sensitivity Analysis Results for Effected Dose to the RMEI (*EXPDOSE*, mrem/yr) Resulting from Igneous Events TK-146

K7.1-1. Summary of TSPA-LA Model Results Considered in Uncertainty and Sensitivity Analyses for the Seismic Scenario Classes TK-147

K7.1-2 Summary of Uncertainty and Sensitivity Analysis Results for Radionuclide Movement from the EBS to the UZ Resulting from a Seismically Induced Damaged Area of 10^{-6} (32.6 m^2) at 10 yrs to All CDSP WPs in the Repository TK-149

K7.1-3 Summary of Uncertainty and Sensitivity Analysis Results for Radionuclide Movement from the UZ to the SZ Resulting from a Seismically Induced Damaged Area of 10^{-6} (32.6 m^2) at 10 yrs to All CDSP WPs in the Repository TK-150

K7.1-4 Summary of Uncertainty and Sensitivity Analysis Results for Radionuclide Movement in the SZ Across a Subsurface Plane at the Location of the RMEI Resulting from a Seismically Induced Damaged Area of 10^{-6} (32.6 m^2) at 10 yrs to All CDSP WPs in the Repository TK-153

K7.1-5 Summary of Uncertainty and Sensitivity Analysis Results for Dose to the RMEI from Selected Radionuclides Resulting from a Seismically Induced Damaged Area of 10^{-6} (32.6 m^2) at 10 yrs to All CDSP WPs in the Repository. TK-155

K7.1-6 Summary of Uncertainty and Sensitivity Analysis Results for Expected Dose to the RMEI (*EXPD05*, mrem/yr) Resulting from Seismic Events TK-156

K9-1. Summary of Selected Sensitivity Analysis Results TK-157

TABLES (Continued)

Page

L-1. Bounded Hazard Curve for Horizontal Peak Ground Velocity at the Emplacement Drifts L-57
L-2. Average Percolation Rate over the Repository Area L-57
L-3. Spatial Variability and Uncertainty Distributions for 1/α for Methods A, B, C, and D L-58
L-4. Spatial Variability and Uncertainty Distributions Fracture Permeability (log (k [m2])) L-58
L-5. Flow Focusing Factor L-59
L-6. Drip Shield General Corrosion Rate Ratio for Titanium Grade 29 Frame Material L-59
L-7. Probability of Failure for the Drip Shield Plates L-60
L-8. Probability of Failure for the Drip Shield Framework L-61
L-9. Weibull Parameters for Alloy 22 Waste Package Outer Barrier General Corrosion L-62
L-10. Time that Relative Humidity Exceeds 75 percent Threshold L-62
L-11. Stress and Stress Intensity Factor Coefficients L-62
L-12. Average Depth Where SCC Cracks Can Initiate and Propagate L-63
L-13. Probability of Nonzero Damage for the Waste Package Surrounded by Rubble L-64
L-14. Conditional Damaged Areas on the Waste Package Surrounded by Rubble L-64
L-15. Probability of TAD-Bearing and CDSP Waste Package Rupture (17-mm-Thick Waste Package Outer Barrier, Degraded Internals) L-65
L-16. Probability of Nonzero Damage for the TAD-bearing Waste Package, Free Movement Underneath the Drip Shield L-66
L-17. Probability of Nonzero Damage for the CDSP Waste Package, Free Movement Underneath the Drip Shield L-67
L-18. Conditional Damage Area on TAD-bearing and CDSP Waste Packages When Damaged Due to Free Motion Underneath the Drip Shield L-68
L-19. Initial Radionuclide Inventory and Treatment L-69
L-20. Uncertainty Multipliers for Grams per Waste Package for Each Waste Type L-71
L-21. Gap and Grain Boundary Fractions for CSNF Waste Forms L-71
L-22. Coefficients in CSNF Degradation Rate Model L-71
L-23. CSNF Waste Form Degradation Covariance Matrix for Alkaline Conditions L-71
L-24. CSNF Waste Form Degradation Covariance Matrix for Acidic Conditions L-72
L-25. DHLW Glass Degradation Parameters L-72
L-26. Dissolved Concentration Limits (without Uncertainty) L-73
L-27. Dissolved Concentration Limit Uncertainty Terms L-73
L-28. Mixing Cell Steel Parameters Used in Calculation of Corrosion Product Mass and Volume of Water L-74
L-29. Metal Mass Fractions and Atomic Weights Used in Calculation of Corrosion Product Mass and Volume of Water L-74
L-30. Properties of Corrosion Product Used in Calculation of Corrosion Product Mass and Volume of Water L-74
L-31. Free Water Diffusion Coefficients L-75

TABLES (Continued)

Page

L-32. Calculation of Average Unsaturated Zone Layer Thickness L-76
L-33. Layer Contact and Thickness from the GFM2000 Contact Information L-77
L-34. Layer Average Residual Saturation L-79
L-35. Unsaturated Zone Layer Average Properties for Determination of Matrix Hydraulic Conductivity L-80
L-36. Unsaturated Zone Layer Average Matrix and Fracture Porosity L-88
L-37. Unsaturated Zone Layer Fracture and Matrix Percolation Flux (mm/yr) L-89
L-38. Unsaturated Zone Fracture and Matrix Groundwater Velocity L-90
L-39. Unsaturated Zone Layer Groundwater Travel Times (yr) L-92
L-40. Unsaturated Zone Layer Average Rock Density L-93
L-41. Unsaturated Zone Layer Distribution Coefficients L-94
L-42. Average Specific Discharge in Flow Path Segments L-95
L-43. Saturated Zone Horizontal Anisotropy L-95
L-44. Saturated Zone Specific Discharge Multiplier L-96
L-45. Saturated Zone Flowing Interval Porosity L-96
L-46. Saturated Zone Distribution Coefficients in mL/g L-97
L-47. Groundwater Biosphere Dose Conversion Factors for the Present-Day Climate L-99

M-1. Net Infiltration Rates (mm/yr) used in the Integrated Multiple Assumptions and Release Code Event Tree Branches for Infiltration M-16
M-2. Infiltration Rates (mm/yr) used in TSPA-LA (Modified from Table L-2) M-17
M-3a. Seepage Fraction and Flow Rate as a Function of Infiltration Rate M-18
M-3b. Summary Statistics for Probabilistic Seepage Evaluation (Intact Drifts) M-19
M-4. Comparison of Solubility Limits used in TSPA-LA and EPRI M-20
M-5. Inventory used in EPRI Model (Based on SNL 2007) and in TSPA-LA Model M-21
M-6. Unsaturated Zone Layer Distribution Coefficients M-22
M-7. Saturated Zone Layer Distribution Coefficients M-22
M-8. BDCFs used in EPRI Model M-23

P-1. Comparison of Mean Seepage Fraction for Various Percolation Subregions for Nominal Conditions P-27
P-2. Comparison of Mean Seepage Fraction for Various Percolation Subregions for Seismic Fault Displacement Modeling Case P-27
P-3. Comparison of Mean Seepage Fraction for Various Percolation Subregions for the Seismic Ground Motion Modeling Case P-27
P-4. Comparison of Mean Seepage Flux (m^3/yr) at 1,000,000 years for Various Percolation Subregions for the Seismic Ground Motion Modeling Case P-28
P-5. Quantitative Evaluation of the Impact of GoldSim Software Error on Various Modeling Cases Based on Dose P-28
P-6. Discussion of Other Minor Implementation Errors P-29
P-7. Impact Assessment Summary Table P-37

TABLES (Continued)

Page

INTENTIONALLY LEFT BLANK

8. POSTCLOSURE PERFORMANCE DEMONSTRATION

As stated in the introduction (Section 1.0), this Total System Performance Assessment for the License Application (TSPA-LA) report provides the technical basis to support the License Application (LA) for a nuclear waste repository at Yucca Mountain. This particular section of the report presents the postclosure performance assessment results and, in doing so, addresses the fundamental risk triplet (Kaplan and Garrick 1982 [DIRS 100557]), namely: (1) what can happen, (2) how likely is it to happen, and (3) what are the consequences if it does happen. The first two elements of the risk triplet are addressed via consideration of scenario classes, which represent a broad spectrum of potential future system states, and by accounting for the major sources of aleatory uncertainty. The third component is addressed by utilizing Total System Performance Assessment (TSPA) submodels of key processes (e.g., water flow, radionuclide mobilization and release, dissolved and colloidal phase transport through the natural barriers, and radiologic dose) and by accounting for the epistemic uncertainty in the current knowledge of those processes. Risk insights are developed based on:

- Projections of annual doses to the reasonably maximally exposed individual (RMEI) for a set of release scenarios, which are grouped into four classes
- Identifying the scenario classes and modeling cases that produce the most significant releases and dominate the projected doses
- Determining the sources of uncertainty that are most influential in producing the spread of the distribution of projected doses
- Identifying the key radionuclides that contribute the most to the projected annual doses.

The four scenario classes include Nominal, Early Failure, Seismic, and Igneous. Detailed descriptions of the technical basis of these scenario classes and their associated modeling cases are presented in Sections 6.3 through 6.6. These scenario classes collectively encompass all the included features, events, and processes (FEPs) that affect postclosure performance. The procedure used to screen the FEPs is discussed in Section 6.1.1; all the identified FEPs and the screening arguments are documented in Appendix I.

The TSPA presented herein focused on quantifying the postclosure performance of the repository system, which is composed of three major barriers, namely: (1) upper natural barrier, (2) engineered barrier system (EBS), and (3) lower natural barrier. The upper natural barrier consists of the topography and surface soils of the mountain, the unsaturated tuff units above the repository, and rock strata in which the repository is constructed. The EBS includes the waste packages (WPs), drip shields (DSs), waste forms, cladding (associated with the commercial spent nuclear fuel [CSNF], DOE spent nuclear fuel [DSNF], and naval spent nuclear fuel [NSNF]), and the drift invert; no credit is taken, however, for cladding performance. The lower natural barrier below the repository includes the unsaturated rock layers beneath the repository as well as the volcanic rock units and the alluvial material in the saturated zone (SZ) that extends from the repository site to the designated accessible environment boundary. A depiction of these three major barriers and the fundamental processes contributing to postclosure performance is presented on Figure 8-1.

The postclosure performance of this system of multiple barriers was analyzed for scenarios representing a broad range of likely and unlikely conditions. At a fundamental level, the postclosure performance of the repository is quantified through a detailed computer analysis of:

- How the system of multiple barriers would function in response to changes in the hydrologic, geologic, and geochemical conditions expected to be induced by the decay heat, as well as by projected future climate changes
- How the multiple barriers could be affected by likely and unlikely disruptive events potentially induced by seismic and igneous activity at or near the site area
- How radionuclides could be released from the EBS, migrate through the multiple barriers, and potentially enter the biosphere pathways at the designated RMEI location.

As required by the disposal standards, the postclosure performance is quantified for time periods of 10,000 years and 1,000,000 years after closure.

Because of the inherent uncertainties in making such long-term projections, this TSPA is largely based on a probabilistic modeling approach that accounts for uncertainties in parameters and in future conditions. Other sources of uncertainty, such as potential early failure of the EBS components arising from undetected defects, are included in the early failure scenario class. In addition, a TSPA projection was developed for a human intrusion scenario. This separate TSPA addresses the regulatory requirement to demonstrate performance for a hypothetical inadvertent drilling event, which is assumed to release radionuclides directly to the groundwater.

It is important to note that this TSPA utilizes the knowledge base, site characterization data, and EBS design compiled over the past two plus decades. Since the inception of the Yucca Mountain Project, scientists and engineers at the U.S. Department of Energy (DOE) national laboratories and other organizations have been refining the technical basis in preparation for this performance demonstration. The technical basis has been critically reviewed by both internal and external peer review groups to ensure that it is scientifically defensible. In addition, it has been documented in a manner that is traceable and auditable. The technical basis that directly supports the TSPA-LA Model is documented in Volumes I and II, as well as in the numerous analysis and modeling reports that are explicitly cited throughout this document.

In this section, the postclosure performance demonstration results for the proposed Yucca Mountain repository are presented and explained. Probabilistic projections of annual doses and activity concentrations (i.e., radionuclide activity per unit volume) in groundwater, at the designated location of the RMEI, were developed for comparison to the applicable radiation protection standards. The demonstration of conformance with the radiation protection standards is presented using the following regulatory and statistical metrics:

1. Projected annual dose and activity concentration histories at the RMEI location (based on the propagation of epistemic and aleatory uncertainties through the TSPA-LA Model)
2. Statistical metrics for the projected distributions, including the mean, median, and 5th and 95th percentiles of the annual dose and activity concentration

3. Largest or peak mean annual doses computed for comparison with the dose limits specified for 10,000 years after closure and the largest median annual doses for post 10,000 years but within the period of geologic stability (i.e., 1,000,000 years)

4. Peak of the mean activity concentrations computed for comparison with the groundwater protection limits specified for 10,000 years after closure.

With regard to the probabilistic projections of the dose metrics, the following mathematical terminology is used in the subsequent sections: (1) annual dose is the projected annual dose to the RMEI conditional on one specific sampled value of aleatory (irreducible or stochastic) and epistemic (reducible or lack of knowledge) uncertainty; (2) expected annual dose is the expected value of annual dose to the RMEI over aleatory uncertainty, conditional on epistemic uncertainty; (3) mean annual dose is the expected value of annual dose computed over both the aleatory and epistemic uncertainty; and (4) median annual dose is the median of the distribution of expected annual dose.

As demonstrated in Section 7.3.1, the probabilistic projections are statistically stable. Stability is determined by comparing TSPA-LA Model results computed using three independent samples of uncertain parameters, termed replicates. Because the comparison showed that the TSPA-LA Model results are statistically stable, any of the three replicates could be chosen for presentation and comparison with the radiation protection standards. Results from the first replicate are presented in this section and are the subject of analyses reported in the appendices.

Comparisons of the TSPA projections with the applicable U.S. Nuclear Regulatory Commission (NRC) radiation protection standards are presented first and in a summary manner (Section 8.1). Explanation of the performance demonstration results is developed based on the probabilistic projections for the individual scenario classes and modeling cases (Section 8.2). Additional insights to the factors affecting the isolation characteristics of the repository system are developed by examining the performance capabilities of the natural and engineered barriers (Section 8.3). The final part of this section highlights the technical basis for confidence, credibility, and defensibility of the performance demonstration (Section 8.4).

INTENTIONALLY LEFT BLANK

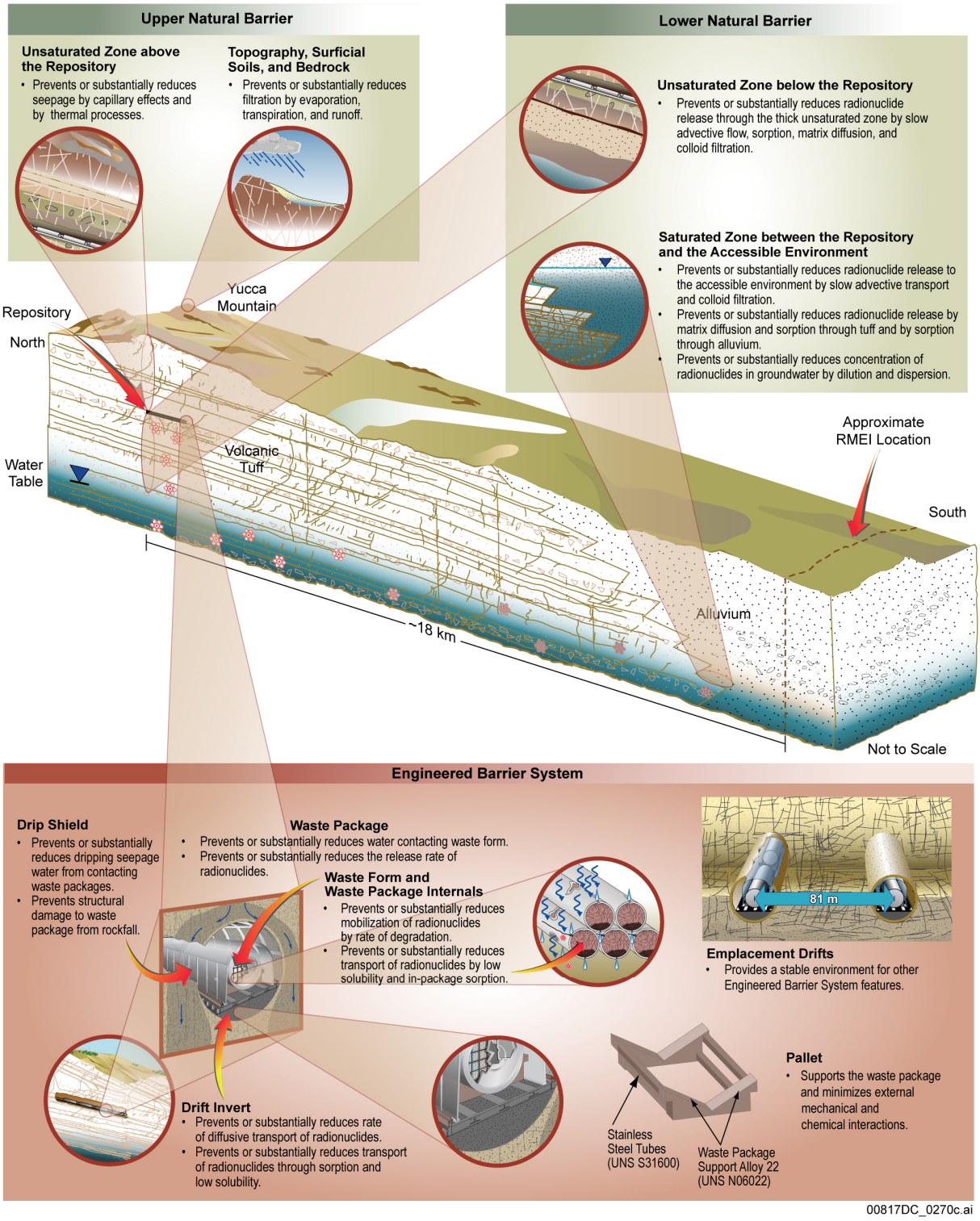

Figure 8-1. Illustration of the Multiple Barriers of Yucca Mountain Repository System

INTENTIONALLY LEFT BLANK

8.1 CONFORMANCE WITH RADIATION PROTECTION STANDARDS

The U.S. Environmental Protection Agency (EPA) and NRC regulations for a high-level radioactive waste (HLW) repository at Yucca Mountain require that DOE demonstrate a reasonable expectation of compliance with the applicable radiation protection standards. The proposed EPA regulation 40 CFR Part 197 (2005 [DIRS 175755]) establishes three separate and distinct radiation protection standards for the Yucca Mountain Repository. As the licensing agency, the NRC adopted these three radiation protection standards as follows:

- Individual Protection Standard After Permanent Closure (10 CFR 63.311 [DIRS 178394]), which considers the required characteristics of the RMEI as described in 10 CFR 63.312 [DIRS 180319].
- Individual Protection Standard for Human Intrusion (10 CFR 63.321 [DIRS 178394]) according to the Human Intrusion Scenario described in 10 CFR 63.322 [DIRS 180319].
- Separate Standards for Protection of Ground Water (10 CFR 63.331 [DIRS 180319]) using the representative volume specified in 10 CFR 63.332 [DIRS 180319].

The EPA and NRC proposed regulations for Individual Protection and Human Intrusion establish two sets standards for annual doses to the RMEI corresponding to: (1) the time period of 10,000 years after closure, and (2) the time period after 10,000 years but within the period of geologic stability, defined as 1,000,000 years in 10 CFR 63.302 [DIRS 178394]. In contrast, the Separate Standards for Protection of Ground Water set limits for annual dose and activity concentrations (i.e., radionuclide activity per unit volume) for only the 10,000-year period following repository closure. For the purpose of making performance projections for these time periods, the characteristics of the RMEI are defined in 10 CFR 63.312 [DIRS 180319] and the RMEI is taken to reside approximately 18 km (11 mi) downgradient of the repository.

Detailed probabilistic projections developed for this postclosure performance demonstration will be presented and explained in the subsequent sections. At this point, however, it is beneficial to preview the high-level results in a tabulation of peak mean and largest median values for annual doses and activity concentrations for direct comparisons with the numerical limits set in three radiation protection standards. Comparisons of the projected performance metrics and regulatory limits are summarized in Tables 8.1-1 through 8.1-3. To highlight the spread in the computed distribution of expected annual doses, additional statistical parameters are presented in Table 8.1-4 to better clarify the comparison with the limits of the Individual Protection Standard.

As shown in the tabular comparisons, the numerical limits prescribed in all three standards are met, with the peak annual doses and activity concentrations falling well below the limits. These numerical comparisons, however, represent only a part of the postclosure performance demonstration and many detailed calculations and graphical outputs are presented in Sections 8.2 to elucidate the comparisons with the regulatory requirements. For the purposes of explaining the basis for a reasonable expectation of compliance, this section and the subsequent sections address the following fundamental questions regarding the TSPA of the repository and the probabilistic projections of the regulatory metrics:

1. What scenario classes and modeling cases were considered and how were they analyzed to make probabilistic performance projections?

2. What processes or site characteristics modeled in the scenario class were most important to postclosure performance?

3. What multiple-barrier attributes and/or characteristics were most influential in reducing the radionuclide release rates, rate of water or radionuclide movement?

4. What radionuclides in the nuclear waste inventory contribute the most to the annual doses and why?

5. What model parameters are most dominant in determining the uncertainty or spread in the projected performance metrics?

In addition, it is important to identify the plausible and potentially important conservatisms incorporated into the TSPA-LA Model, as well as to explain how the performance projections have been cross-checked to ensure that they are technically sound and defensible.

The next sections describe and explain the projections that constitute the postclosure performance demonstration for the three radiation protection standards. The exposure models and conversion factors used to calculate annual dose and activity concentrations in groundwater are summarized in the Biosphere Component Model section (Section 6.3.11) and described in detail in *Biosphere Model Report* (SNL 2007 [DIRS 177399], Sections 6.11 and 6.12). The annual doses to the RMEI are calculated for two separate exposure scenarios, namely, groundwater and volcanic (SNL 2007 [DIRS 177399], Section 6.1.3).

8.1.1 Individual Protection Standard

To provide a postclosure performance demonstration for the Individual Protection Standard (10 CFR 63.311 [DIRS 178394]), a comprehensive TSPA-LA Model (Sections 1 through 6) of the repository system was developed and applied to:

- Analyze potential releases of radionuclides from the EBS
- Evaluate all potential pathways of radionuclide transport through the multiple barriers and to the accessible environment
- Project (i.e., analyze and calculate as a function of time) the annual doses to the RMEI.

The NRC Proposed Rule 10 CFR 63.311(a) [DIRS 178394] states "(a) DOE must demonstrate, using performance assessment, that there is a reasonable expectation that the reasonably maximally exposed individual receives no more than the following annual dose from releases from the undisturbed Yucca Mountain disposal system: (1) 0.15 mSv (15 mrem) for 10,000 years following disposal; and (2) 3.5 mSv (350 mrem) after 10,000 years, but within the period of geologic stability."

NRC Proposed Rule 10 CFR 63.311(b) [DIRS 178394] specifies that the "performance assessment must include all potential environmental pathways of radionuclide transport and exposure." It is important to clarify that, in NRC Proposed Rule 10 CFR 63.311(a) [DIRS 178394], "undisturbed Yucca Mountain disposal system" means that the repository is not affected by human intrusion (10 CFR 63.322 [DIRS 180319]), which is addressed separately in Section 8.1.3. This term is distinct from the regulatory definition of undisturbed performance (10 CFR 63.302 [DIRS 180319]).

To demonstrate compliance with this standard, the peak or largest *mean value* of the projected annual doses to the RMEI is used as the primary performance metric for comparisons with the above numerical limits for 10,000 years and the largest *median value* is used for comparison with the post-10,000-year limit; these metrics are in accordance with 10 CFR 63.303 [DIRS 178394]. The projections of postclosure performance take into account both likely and unlikely FEPs (10 CFR 63.342 [DIRS 178394]) (Appendix I). These FEPs and their affects on waste isolation are quantified in four scenario classes: Nominal, Early Failure, Seismic, and Igneous. Detailed descriptions of the technical basis of these scenario classes and their associated modeling cases are presented in Sections 6.3 through 6.6.

8.1.1.1 Scenario Classes Considered and Calculation of Total Annual Doses

As described in Section 6.1.2, probabilistic projections of the total expected annual dose to the RMEI are computed as a combination of the calculated expected annual doses for each of the four scenario classes; the expectation is taken over all aleatory (i.e., randomly occurring in time) uncertainties. Mathematically, the total expected annual dose to the RMEI, denoted by $\bar{D}_T(\tau \mid \mathbf{e})$ for time τ in years, is defined as the sum of the expected annual doses for each scenario class (Section 6.1.2.2 and Appendix J4.6):

$$\bar{D}_T(\tau \mid \mathbf{e}) = \bar{D}_N(\tau \mid \mathbf{e}) + \bar{D}_E(\tau \mid \mathbf{e}) + \bar{D}_I(\tau \mid \mathbf{e}) + \bar{D}_S(\tau \mid \mathbf{e}) \qquad \text{(Eq. 8.1.1-1)}$$

In the above equation, the terms $\bar{D}_N(\tau \mid \mathbf{e})$, $\bar{D}_E(\tau \mid \mathbf{e})$, $\bar{D}_I(\tau \mid \mathbf{e})$, and $\bar{D}_S(\tau \mid \mathbf{e})$ represent the expected annual dose estimates for the four Scenario Classes, namely, Nominal, Early Failure, Igneous, and Seismic, respectively. The term $\mathbf{e}$ represents the set of the epistemically uncertain model parameters, sampled in the probabilistic simulation of postclosure performance.

While the term for the Nominal Scenario Class, $\bar{D}_N(\tau \mid \mathbf{e})$, consists of only one modeling case, the other expected annual dose terms in Equation 8.1.1-1 are the sum of expected values for the various modeling cases. Specifically, the doses for the Early Failure, Igneous, and Seismic Scenario Classes are computed as following:

$$\bar{D}_E(\tau \mid \mathbf{e}) = \bar{D}_{WP}(\tau \mid \mathbf{e}) + \bar{D}_{DS}(\tau \mid \mathbf{e}) \qquad \text{(Eq. 8.1.1-2)}$$

$$\bar{D}_I(\tau \mid \mathbf{e}) = \bar{D}_{II}(\tau \mid \mathbf{e}) + \bar{D}_{VE}(\tau \mid \mathbf{e}) \qquad \text{(Eq. 8.1.1-3)}$$

$$\bar{D}_S(\tau \mid \mathbf{e}) = \bar{D}_{GM}(\tau \mid \mathbf{e}) + \bar{D}_{FD}(\tau \mid \mathbf{e}) \qquad \text{(Eq. 8.1.1-4)}$$

where the terms $\bar{D}_{WP}(\tau|\mathbf{e})$ and $\bar{D}_{DS}(\tau|\mathbf{e})$ are the expected annual dose estimates for the Waste Package and Drip Shield Early Failure (EF) Modeling Cases, respectively; $\bar{D}_{II}(\tau|\mathbf{e})$ and $\bar{D}_{VE}(\tau|\mathbf{e})$ are the expected annual dose estimates for the Igneous Intrusion and Volcanic Eruption Modeling Cases; and $\bar{D}_{GM}(\tau|\mathbf{e})$ and $\bar{D}_{FD}(\tau|\mathbf{e})$ are the expected annual dose estimates for the Seismic Ground Motion (GM) and Seismic Fault Displacement (FD) Modeling Cases, respectively.

A very important point regarding the TSPA-LA Model implementation of Equation 8.1.1-1 is that, although the expected annual dose for the Nominal Modeling Case, $\bar{D}_N(\tau|\mathbf{e})$, is calculated for the post-10,000-year compliance period, $\bar{D}_N(\tau|\mathbf{e})$ is not added into the total dose calculation for $\bar{D}_T(\tau|\mathbf{e})$. Rather, for the post-10,000-year period, the TSPA-LA Model implicitly produces the sum $\bar{D}_N(\tau|\mathbf{e})+\bar{D}_S(\tau|\mathbf{e})$ instead of calculating the individual quantities $\bar{D}_N(\tau|\mathbf{e})$ and $\bar{D}_S(\tau|\mathbf{e})$ separately. This combination of modeling cases was performed to ensure proper coupling between the WP and DS damage abstractions in the Seismic GM Modeling Case and the corrosion processes in the Nominal Modeling Case. The damage abstraction takes into account the increased susceptibility to seismic damage as a result of corrosion induced thinning of the WP outer barrier, DS plate, and frame (Section 6.6.1.2.2).

8.1.1.2 Projections of Annual Doses and Major Observations

Projections of postclosure performance for comparison with the Individual Protection Standard were developed using the Monte Carlo simulation methodology, which is described in Appendix J. This methodology incorporates aleatory and epistemic uncertainties into the projections in two separate computational loops: (1) an outer calculational loop that samples probability distributions for model parameters with epistemic uncertainty using the Latin hypercube sampling technique (Helton and Davis 2002 [DIRS 163475]), and (2) an inner loop that evaluates expected annual dose accounting for distributions representing quantities with aleatory uncertainties. The methodology produced an ensemble of expected annual dose outcomes for each scenario class, which were then combined using Equation 8.1.1-1, using the separate terms $\bar{D}_N(\tau|\mathbf{e})$ and $\bar{D}_S(\tau|\mathbf{e})$ for 10,000-year results and including the combined term $\bar{D}_N(\tau|\mathbf{e})+\bar{D}_S(\tau|\mathbf{e})$ for post-10,000-year results.

The main result of the Monte Carlo simulation process is a set of realizations for the expected annual dose histories for the RMEI, which are generally plotted in the form of a multi-realization plot. The multi-realization plots developed for demonstrating compliance with the Individual Protection Standard are shown on Figure 8.1-1 for 10,000 years after closure and Figure 8.1-2 for the post-10,000-year period (i.e., after 10,000 years but within the period of geologic stability [defined by the proposed NRC rule [DIRS 178394] to end at one million years]). Curves for the mean, median, and 5th and 95th percentiles dose histories are superimposed on each multi-realization plot. The total mean annual dose history, which is plotted as the red curve, was computed by taking the arithmetic average of the 300 expected annual dose values, for individual time planes along the curves. Similarly, the median dose history, plotted as the blue curve, was constructed from points obtained by sorting the 300 expected values from lowest to highest, and

then averaging the two middle values. Curves for the 5th and 95th percentiles are also plotted to illustrate the spread in the expected annual dose histories; 90 percent (or 270 of the 300 epistemic realizations) of the projected dose histories fall between these two percentile curves. For a detailed description of the calculation of total annual dose see Section 6.1.2.2.

For the 10,000-year disposal period, the largest mean and median annual doses to the RMEI are estimated to be about 0.2 mrem and 0.15 mrem, respectively; these projected doses are below the individual protection limit of 15 mrem. Similarly, the largest mean and median annual doses for the post-10,000-year period but within the period of geologic stability are estimated to be about 2 mrem and 1 mrem, respectively; these projected peak values are also below the individual protection limit of 350 mrem. To provide a perspective of the epistemic uncertainty of the performance projections, the annual dose history curves corresponding to the 5th and 95th percentiles are included in the multi-realization plots.

Important risk insights can be gained by disaggregating the total annual doses into the mean annual dose histories for the individual modeling cases; these individual projections are shown on Figure 8.1-3. From those dose curves, the following general observations can be drawn about the projected postclosure performance demonstration:

- Total mean annual doses calculated for both the 10,000-year and post-10,000-year time periods are dominated by releases for the Seismic GM and Igneous Intrusion Modeling Cases.
- Mean annual doses for the Waste Package EF and Seismic FD Modeling Cases are relatively small and are estimated to be on the order of 10^{-2} mrem or less for both the 10,000-year and post-10,000-year time periods.
- Mean annual doses projected for Drip Shield EF and Igneous Volcanic Eruption Modeling Cases are on the order of 10^{-3} mrem or less for both the 10,000-year and post-10,000-year time periods.

With regards to the first observation, the Seismic GM Modeling Case dominates the total mean annual dose for 10,000 years after closure, whereas for the post-10,000-year period, the Igneous Intrusion Modeling Case dominates the total mean annual dose to the RMEI for most of the time period.

An important clarification regarding the projections for the Seismic GM Modeling Case is that the expected annual doses for the 10,000-year time period are only from releases from the damaged co-disposed (CDSP) WPs (Table 6.3.7-1). The contribution to expected annual doses from the commercial spent nuclear fuel (CSNF) WPs were evaluated and found to be insignificant, due to the very low frequency of seismic induced failures of the transportation, aging, and disposal (TAD) packages. The basis for the low frequency is addressed in the following sections and explained in greater detail in Section 7.3.2.6.1.3.7, which examines probability of damage to CSNF WPs by seismic events during the 10,000-year period and the contribution to expected annual dose of these events.

Additional discussion and explanation of the projections for the seven modeling cases is presented in Section 8.2.

8.1.1.3 Disruptive Events Important to Postclosure Performance

From a cause-and-effect view point, clearly the most important disruptive events potentially impacting postclosure performance are the vibratory ground motion and igneous intrusion (i.e., magmatic dike rising through the earth's crust and intersecting the repository). Based on the FEPs screening process, the seismic and igneous disruptions only affect the EBS. In the case of vibratory ground motion, the important aspect is the cumulative damage and failure of the WPs and DSs. It is important to clarify, however, that while WP and DS failures could be caused by a single extreme ground motion event, failure would more typically occur as a result of a sequence of many small to moderate vibratory ground motions over a period of time with stress corrosion cracking (SCC) accumulating from these events. In the case of the igneous intrusion into the repository area, however, the damage and failure of the EBS is a single discrete event that causes complete failure of both WPs and DSs.

For the purposes of risk insights, it is valuable to examine the estimated annual frequencies for these disruptive events and processes. The occurrence of seismic events is described as a Poisson process with the smallest peak ground velocity (PGV) having an annual exceedance frequency of 4.287×10^{-4}/yr and largest PGV with an exceedance frequency of 10^{-8}/yr (Figure 6.6-6; and SNL 2007 [DIRS 176828], Figure 6-7). During the first 10,000 years after closure, only four potentially damaging seismic ground motion events are expected to occur; whereas for the 1,000,000-year period, approximately 430 potentially damaging seismic events are expected to occur. In contrast, the mean annual frequency of a dike intersecting the repository is estimated to be 1.7×10^{-8}/yr (BSC 2004 [DIRS 169989]). This frequency is just slightly greater than the NRC frequency of 10^{-8}/yr for very unlikely events and processes, which are excluded from the performance assessment for the LA by regulation (10 CFR 63.342(b) [DIRS 178394]). While both disruptive events are possible, the potential impacts of seismic ground motion events are much more probable and, therefore, these events are the focus of the subsequent discussion.

Seismically Induced Damage and Failure Mechanisms—Vibratory ground motions can lead to drift degradation and rockfall accumulation on the DS. Subsequent failure of the DS can occur as a result of dynamic loading and deformation and/or by static loading by accumulated rockfall. The ability of the DS to withstand the static and dynamic loading diminishes with time because general corrosion reduces the thickness of the titanium DS plate and framework. Ultimately, the DSs will fail as a result of load-induced buckling or rupture. A histogram of DS failures for the Seismic GM Modeling Case is shown on Figure 8.1-4; the histogram for the Nominal Modeling Case is also shown for the purposes of comparison. As shown, DS failures occur earlier due to the combined effects of nominal and seismic ground motion as compared to nominal process alone. These probabilistic projections of DS and WP failures are described and explained in more detail in Section 8.2.

Seismically induced damage of the WPs is most likely to occur from deformation or denting of the outer wall. These localized areas of deformation or denting develop residual stresses that are susceptible to SCC. Rupture of a WP could potentially occur as a result of kinematic loading caused by package-to-pallet and/or package-to-package impacts. It is important to understand that in the case of the WP, seismic crack damage is more likely to occur than rupture. Projections of CDSP and CSNF WP failures by seismic crack damage as a function of time are

shown on Figure 8.1-5. As can be noted by comparing Figure 8.1-5(a) and Figure 8.1-5(b), the CSNF WP is much less likely to be damaged than is the CDSP WP. A detailed discussion of seismic related damage and failure mechanisms is presented in Section 6.6.1.1.2 and in *Seismic Consequence Abstraction* (SNL 2007 [DIRS 176828]).

All of these potential degradation, damage, and failure mechanisms have been evaluated for this performance demonstration (Section 6.6). The technical basis for the performance analysis of seismic and igneous intrusion consequences are documented in *Seismic Consequence Abstraction* (SNL 2007 [DIRS 176828]) and *Number of Waste Packages Hit by Igneous Intrusion* (SNL 2007 [DIRS 177432]), respectively.

8.1.1.4 Multiple Barrier Processes that Contribute to Postclosure Performance

The multiple barrier processes that are important to postclosure performance have largely been identified in previous TSPAs (Williams 2001[DIRS 157307]) of the Yucca Mountain repository. The modeling studies conducted in support of this TSPA-LA have provided additional insights and understanding, particularly with regard to individual features of natural and engineered barriers. From a high-level perspective, some of the fundamental barrier processes and characteristics that are typically influential in determining how well the system of multiple barriers isolates (i.e., contains and confines) the nuclear waste are:

- Net infiltration into the unsaturated zone (UZ) and seepage into the drifts
- Mechanical strength and corrosion rate properties of the WPs and DSs
- Solubilities for key radioelements such as neptunium, uranium, and plutonium
- Radionuclide sorption onto corrosion products inside the WPs
- Diffusion limited radionuclide releases from failed WPs
- Sorption and matrix diffusion properties of the UZ and SZ underlying the repository.

With regard to infiltration and seepage, these attributes are important because they determine: (1) dripping and non-dripping environments on WP and DS surfaces, and (2) water flow into a failed WP and the ensuant mobilization and release of radionuclides. The strength properties of the WP outer barrier (i.e., Alloy 22 [UNS N06022]) and DS plate (i.e., Titanium Grade 7) and frame (i.e., Titanium Grade 29) determine their capability to withstand dynamic and static loads induced by vibratory ground motion (Section 6.6.1.2). General corrosion and SCC are important processes affecting WP structural integrity because they progressively reduce metal barrier thickness over a period of time. The general corrosion rate of the WP outer barrier is temperature-dependent, which makes the WP surface temperature an important factor. The importance of radioelement solubilities is derived from the fact that they limit the release rates from the waste form. Solubilities of such radioelements as neptunium, uranium, and plutonium are particularly important because they have relatively large initial inventories and produce radionuclide species that have very long half-lives. Corrosion of the WP internals produces metal oxides that provide sorption sites for a variety of fission products and actinide elements (Section 6.3.8). Diffusional release of radionuclides from a failed WP is a function of the breach geometry (e.g., cracks and patches) and effectively limits the rate of release to the natural barrier. The sorption properties of the volcanic tuff and alluvium layers in the UZ and SZ influence the rate of subsurface migration to the RMEI location.

8.1.1.5 Radionuclides Important to Postclosure Performance

In general, the radionuclides in the nuclear waste that dominate the calculation of annual doses typically have a combination of unique characteristics such as: (1) large initial inventories in the nuclear waste, (2) moderately to highly soluble, (3) very long half-lives (e.g., $\geq 10^5$ years), and (4) low to non-sorbing properties. The radionuclides that become important to dose also depend on the time frame considered (i.e., 10,000 years or 1,000,000 years after closure), because of the effect of radionuclide decay on the activity concentrations. In-growth of radionuclides via chain decay, over a very long period of time, can also be an important process that determines the role and importance of actinide elements in the actinium, uranium, neptunium, and thorium series (Figure 6.3.7-4). For the three modeling cases involving groundwater releases, the basic transport processes of advection, dispersion, matrix diffusion, and sorption can play an important role. Moreover, the specific modes (e.g., dissolved and colloidal phases) of transport can also be important; the modes analyzed for each radionuclide are listed in Table 6.3.7-6.

The contributions of the individual radionuclides to the total mean annual dose is shown on Figure 8.1-6 and 8.1-7 for 10,000 years and post-10,000 years, respectively. It is important to acknowledge that some questionable, potentially unrealistic, values of mass dispersivity were found to have been sampled in the probabilistic calculation of the decay chain transport through the SZ; in addition, three radionuclides, namely ^{36}Cl, ^{79}Se, and ^{126}Sn, were inadvertently omitted from the initial TSPA-LA Model runs for the 10,000-year time period. The issues of the dispersivity value and three omitted radionuclides were addressed in a Condition Report (CR 11152). The impact of these issues on the overall analysis is discussed in Appendix P.

Important Radionuclides for the 10,000-Year Performance Projection—From the dose curves shown on Figure 8.1-6, it is clear that the principal contributors to the total mean annual dose, ranked from highest to lowest, are: ^{99}Tc (half-life 2.13×10^5 years), ^{14}C (half-life 5,715 years), ^{239}Pu (half-life 2.41×10^4 years), ^{129}I (half-life 1.57×10^7 years), and ^{240}Pu (half-life 6.56×10^3 years). Collectively, these five radionuclides account for about 98 percent of the peak of the total mean annual dose, which occurs at the end of 10,000 years. The single largest contributor is ^{99}Tc, which accounts for about 56 percent of the peak of the total mean annual dose to the RMEI.

The fission products, ^{99}Tc and ^{129}I, and the activation product, ^{14}C, collectively represent about 83 percent of the total mean annual dose. Their large contribution to total mean annual dose is largely explained by the fact that they are very soluble in water, do not sorb in earth materials, and have long half-lives relative to the 10,000-year time frame. The significance of the technetium, iodine, and carbon radioelements being very soluble is because their release rates are limited only by: (1) the waste form degradation rate, (2) rate and extent of water ingress into the WP, and (3) mass transport mechanism (i.e., diffusion and/or advection) out of the WP. The non-sorbing property is important because these radionuclides are transported from the EBS, through the natural barrier, and to the RMEI at the rate at which the groundwater naturally travels (i.e., no delay by chemical retardation). Their relatively long half-lives, compared to 10,000 years, means that decay would not appreciably reduce their activity level. In contrast to its mobility characteristics, ^{99}Tc has the smallest mean biosphere dose conversion factor (BDCF) (SNL 2007 [DIRS 177399], Figure 6.13-2) of all the major radionuclides; the mean BDCF for ^{14}C is the second lowest. On a mass per package basis, ^{99}Tc has a larger initial inventory than

the ^{129}I and ^{14}C inventory (Table 6.3.7-5), which in part explains the ranking of these three radionuclides.

The two actinides, ^{239}Pu and ^{240}Pu, together contribute about 14 percent to the total mean annual dose with ^{239}Pu by itself contributing about 11 percent. The contribution of these two plutonium species to total mean annual dose is explained by their large initial inventory (Table 6.3.7-5), mode (i.e., dissolved and colloidal) of transport in groundwater, and broad range of transport times in the SZ. With regard to mode of transport, plutonium species are transported through groundwater in dissolved phase and reversible colloids, as well as fast (i.e., not retarded by matrix diffusion or attachment/detachment process) and slow irreversible colloids (Table 6.3.7-6). Detailed probabilistic simulations of plutonium transport through the SZ as reversible colloids, which neglect effects of decay, indicate median transport times ranging from 3,000 years to greater than 1,000,000 years, with a median among all realizations of about 95,000 years (SNL 2007 [DIRS 183750], Table 6-10[a]). In the case of plutonium species in the form of slow irreversible colloids, probabilistic simulations of transport through the SZ that neglect effects of decay indicate transport times ranging from 100 years to about 500,000 years, with a median among all realizations of about 4,500 years (SNL 2007 [DIRS 183750], Table 6-10[a]). In contrast, the simulations for the fast irreversible plutonium colloids range from 10 years to about 1,800 years, with a median among all realizations of about 60 years (SNL 2007 [DIRS 183750], Table 6-10[a]). The TSPA-LA Model projections indicate that the dissolved phase and reversible colloids account for the larger fraction of the contribution to total mean annual dose.

Important Radionuclides for the Post-10,000-Year Performance Projection—Figure 8.1-7 shows the contributors to the total mean annual dose. Ranked from highest to lowest, the four main contributors at 1,000,000 years are: ^{226}Ra (half-life 1,600 years), ^{242}Pu (half-life 3.75×10^5 years), ^{237}Np (half-life 2.14×10^6 years), and ^{129}I (half-life 1.57×10^7 years). These four radionuclides collectively account for nearly 80 percent of the peak mean dose. In marked contrast to ^{242}Pu, ^{237}Np, and ^{129}I, ^{226}Ra has a very small initial inventory in the nuclear waste, relatively short half-life, and sorbs strongly on the geologic media, yet it accounts for about 31 percent of the mean annual dose at 1,000,000 years. This seemingly contrary outcome is explained by: (1) its unique nuclear and chemical properties, and (2) its relatively large BDCF. The nuclear properties of ^{226}Ra explain its persistence in the nuclear waste for potentially millions of years, while its chemical properties explain its rate of migration in the UZ and SZ.

A key nuclear property of ^{226}Ra is that it exhibits in-growth from other radionuclides in the uranium series decay chain (Figure 6.3.7-4). The relevant part of that decay chain consists of the following:

$$^{234}U \text{ (half-life 240,000 yrs)} \rightarrow {}^{230}Th \text{ (half-life 77,000 yrs)} \rightarrow {}^{226}Ra \text{ (half-life 1,600 yrs).}$$

This decay chain is significant because it means that even after ^{226}Ra depletes its initial inventory, it will be continuously replenished so long as there is a source of ^{230}Th and ^{234}U. While both ^{226}Ra and ^{230}Th have relatively small initial inventories in the nuclear waste, the precursor ^{234}U has a significant initial inventory. Also, the large contrast in half-lives between ^{226}Ra and ^{230}Th means that ^{226}Ra will ultimately reach a state of secular equilibrium with ^{230}Th. Similarly, after ^{230}Th depletes its initial inventory, its activity will be in secular equilibrium with

its precursor ^{234}U. The net effect is that ^{226}Ra will persist in the waste form for potentially millions of years.

One of the important chemical properties of ^{226}Ra is that it exhibits high sorption in the unsaturated tuff layers, particularly in the Zeolitic and devitrified tuff (Table 6.3.9-2). This high sorption is also exhibited in the volcanic units and alluvium of the SZ (Table 6.3.10-2). These sorption properties have the effect of greatly slowing the ^{226}Ra rate of migration through the lower natural barrier, to the extent that the activity concentrations of ^{226}Ra would diminish by simple decay before reaching the RMEI location. This transport delay effect is demonstrated in the probabilistic analysis of breakthrough curves (SNL 2007 [DIRS 183750], Figure 6-14[a]) for ^{226}Ra migration through the SZ and to the RMEI location.

The breakthrough curves for ^{226}Ra are reproduced on Figure 8.1-8. It is important to note that the breakthrough curves shown on Figure 8.1-8 do not account for decay during transport; rather, the decay is accounted for when the time-dependent releases of ^{226}Ra from the UZ are computed (SNL 2007 [DIRS 183750], Section 6.5). A statistical analysis of these projections shows that the majority of the ^{226}Ra transport times at the RMEI location are much greater than 10,000 years; more specifically for individual realizations, the median transport times (i.e., the times when relative mass equals 0.5 on Figure 8.1-8a) in the SZ range from 18,000 years to more than 1,000,000 years (SNL 2007 [DIRS 183750], Table 6-10[a]). The 50th percentile of the median ^{226}Ra transport times among all realizations is estimated to be about 731,000 years (SNL 2007 [DIRS 183750], Table 6-10[a]). For these magnitudes of transport times, ^{226}Ra would experience from about 11 to more than 600 half-lives of decay before reaching the RMEI, thus reducing the activity concentration by factors $(1/2)^{11}$ to $(1/2)^{600}$. These decay factors suggest that ^{226}Ra activity concentrations, and dose to the RMEI results from decay during transport of the parents.

To understand how ^{226}Ra actually becomes important to dose, one needs to examine the transport characteristics of its two precursors—^{230}Th and ^{234}U. The radionuclide ^{230}Th is transported in water as a reversible colloidal phase and a solute (Table 6.3.7-6); whereas ^{234}U is transported only as a solute. Because ^{234}U is weakly sorbed in the geologic media, it is transported through the UZ and SZ at rates many times faster than ^{230}Th or ^{226}Ra. A statistical analysis of the probabilistic breakthrough curves (SNL 2007 [DIRS 183750], Table 6-10[a]) for the SZ that neglect effects of decay shows that the median transport times (through the SZ) for ^{230}Th range from about 1,000 years to over 1,000,000 years, with the 50th percentile of the median transport times among all realizations being greater than 1,000,000 years. In contrast, the median transport times for ^{234}U ranges from 200 to more than 900,000 years; the 50th percentile of the median transport times for all realizations is about 8,900 years. Thus, it follows that the doses from ^{226}Ra are primarily the direct result of the mobilization and groundwater transport of ^{234}U (and to a lesser extent ^{230}Th) with subsequent chain decay to ^{226}Ra. This pattern of radionuclide in-growth occurs along the groundwater flow path.

As noted earlier, ^{226}Ra has a relatively large BDCF value. This is in part due to the fact that its BDCF accounts for several decay products (SNL 2007 [DIRS 177399], Table 6.12-1). In fact, the ^{226}Ra and one of its nuclear progeny, ^{210}Pb, have the highest BDCF values (SNL 2007 [DIRS 177399], Figure 6.13-2) of all the radionuclides considered in the groundwater exposure calculation; moreover, as implemented in the TSPA-LA Model, the ^{226}Ra BDCF includes the

contribution of ^{210}Pb, which on average accounts for about 42 percent of the composite BDCF value.

The results discussed herein contain additional issues identified during analysis. The issues and potential impacts are discussed in Appendix P, in particular in Section P15. Incorporation of any changes related to these issues may modify the interpretation of these results.

8.1.1.6 Model Parameters Influencing Uncertainty in Expected Annual Doses

Uncertainty and sensitivity analyses were conducted to identify the TSPA-LA Model parameters that were most influential in determining the spread in the total expected annual dose projections (Appendix K). Based on those analyses, three model parameters were identified as having the largest influence on the overall uncertainty in the total expected annual doses to the RMEI. These three parameters are (1) occurrence rate of igneous events, IGRATE; (2) residual stress threshold for Alloy 22, SCCTHRP; and (3) temperature dependence parameter for Alloy 22 general corrosion rate, WDGCA22. The importance ranking of these three model parameters varies with time, which is illustrated in Table 8.1-5. Appendix K, Figure K8.1-2, provides information for times prior to 20,000 years, and Figure K8.2-2 provides information for times after 20,000 years. These model parameters are described below; Table K3-4 provides additional details.

IGRATE Parameter—This parameter is the estimated annual frequency of an igneous dike intersecting the repository, which is characterized as an epistemic uncertain quantity. The annual frequency of an igneous event intersecting the repository ranges from approximately 7.4×10^{-10}/yr to 5.5×10^{-8}/yr for the 5th and 95th percentiles, respectively, with a mean annual frequency of 1.7×10^{-8}/yr. In a given epistemic realization, the annual frequency of an igneous event is sampled from the cumulative distribution function (CDF) for IGRATE, and is used to determine the probability that an igneous event occurs. As discussed in Section 6.5.1, the Igneous Intrusion Modeling Case assumes that any intrusion penetrating the repository footprint would destroy all DSs and WPs and, therefore, the raw waste form would be exposed to seepage with ensuant radionuclide transport.

SCCTHRP Parameter—This parameter is the residual stress threshold for the Alloy-22 WP outer barrier, which is represented as an epistemically uncertain value. This parameter represents the initiation threshold for the onset of SCC. Thus, when the residual stress in the outer barrier of a WP exceeds this threshold, then SCC is presumed to occur. As explained in Section 6.3.5, the primary causes of residual stresses in the WP outer barrier would be low-frequency, high-peak ground velocity seismic ground motions, which could cause impacts from WP-to-WP, from WP-to-emplacement pallet, and from WP-to-DS; these impacts could potentially cause dynamic loads that dent the outer barrier, which could result in creation of residual stresses. The uncertainty in this model parameter is represented using a uniform distribution.

WDGCA22 Parameter—This parameter relates to the temperature dependence for the general corrosion rate of the Alloy 22 WP outer barrier, which is characterized as an epistemically uncertain quantity. As explained in Section 6.3.5, this parameter determines the magnitude of this temperature dependence and directly influences the short-term and long-term general

corrosion rates of the Alloy 22. Larger values of this parameter correspond to higher general corrosion rates while WP temperatures are above 60 ºC, and to lower general corrosion rates when WP temperatures are below 60 ºC. This parameter is sampled from a truncated normal distribution

It is important to clarify that the parameter names IGRATE, SCCTHRP, and WDGCA22 are those used in the uncertainty and sensitivity analyses. The corresponding parameter names used in the TSPA-LA Model and the TSPA Input database are Igneous_Event_Prob_a, Stress_Thresh_A22_a, and C1_GenCorr_A22_a, respectively. More detailed discussion of the importance of these and other model parameters is given in Appendix K.

8.1.2 Groundwater Protection

The performance demonstration for the Groundwater Protection Standard was conducted in a manner consistent with the NRC requirements of 10 CFR 63.331 [DIRS 180319]. The radiation protection limits, set in the Groundwater Protection Standard, are restricted to the first 10,000 years after closure; thus, a performance demonstration for this standard beyond this time period was not conducted. The NRC implementation of this standard requires that the DOE TSPA: (1) evaluate potential releases for undisturbed performance, and (2) show a reasonable expectation that the level of radioactivity in a representative volume of groundwater does not exceed the numerical limits in 10 CFR 63.331 ([DIRS 180319], Table 1).

NRC Table 1 establishes limits for selected radionuclides and specific types of radiation emitted. More specifically, Table 1 limits radionuclides in the representative volume in terms of three performance metrics:

1. Combined ^{226}Ra and ^{228}Ra activity concentrations (pCi/L) in groundwater is ≤ 5 pCi/L (natural background included)

2. Gross alpha activity (including ^{226}Ra but excluding radon and uranium isotopes) concentration is ≤ 15 pCi/L (natural background included)

3. Combined beta- and photon-emitting radionuclides doses to the whole body or any organ (based on drinking 2 liters of water per day from the representative volume) is ≤ 4 mrem.

Performance calculations for all three regulatory metrics are for the point of highest concentration in the plume of contamination in the accessible environment. The calculations of whole body and organ doses are based on using the representative volume of groundwater of 3,000 acre-ft/yr, as specified in 10 CFR 63.332 [DIRS 180319].

It is important to clarify that the term undisturbed performance, as defined in the NRC regulations (10 CFR 63.302 [DIRS 180319]), means that "human intrusion or the occurrence of unlikely natural features, events, and processes do not disturb the disposal system." The NRC defines unlikely as "features, events, and processes, or sequences of events and processes, i.e., those that are estimated to have less than one chance in 10 and at least one chance in 10,000 of occurring within 10,000 years" (10 CFR 63.342(b) [DIRS 178394]). Simply stated, the performance demonstration for the groundwater protection standard requires that the TSPA

assess radionuclide releases caused by "likely" FEPs (i.e., having an annual frequency of 10^{-5}/yr or greater).

Scenario Classes and Modeling Cases Considered—The regulatory definitions for undisturbed performance and unlikely FEPs were used to select specific modeling cases for inclusion in the performance demonstration for this standard. The results of that screening are summarized below:

- Nominal Modeling Case included
- Waste Package EF Modeling Case included
- Drip Shield EF Modeling Case included
- Igneous Intrusion Modeling Cases excluded
- Volcanic Eruption Modeling Cases excluded
- Seismic GM Modeling Case included (for PGVs with annual frequency greater than 10^{-5}/yr only)
- Seismic FD Modeling Case excluded.

The Nominal Modeling Case by definition represents all the expected or likely FEPs. However, because of the inherent characteristics of the natural barrier and performance of the EBS, the effects of corrosion on the WPs (and DSs) are expected to be very small and thus the WPs and DSs are not expected to fail within the 10,000 years for this modeling case.

The Waste Package and Drip Shield EF Modeling Cases were selected for inclusion in the performance demonstration because the probability of an early failure of a WP or DS is greater than 10^{-5} (Section 6.4).

Both the Igneous Intrusion and the Volcanic Eruption Modeling Cases have mean annual frequencies of occurrence that are much less than 10^{-5} per year (Section 6.5). In fact, these two modeling cases are characterized by unlikely FEPs with estimated mean annual frequencies of slightly greater than 10^{-8} per year (Section 6.5). On this basis, the two igneous modeling cases were excluded from consideration in the performance demonstration for groundwater protection.

The Seismic GM Modeling Case represents events and processes with mean exceedance frequencies in the range from 10^{-8} to 4.287×10^{-4} per year (SNL 2007 [DIRS 176828], Section 6.4.3). In contrast, the Seismic FD Modeling Case represents events that do not occur with mean exceedance frequencies greater than 10^{-7} per year (Section 6.6.1.2.3). Therefore, the Seismic GM Modeling Case events with mean exceedance frequencies in the range from 10^{-5} to 4.3×10^{-4} per year are considered to be likely and are included in the TSPA for the groundwater protection standard. The Seismic FD Modeling Case is excluded because of its low annual exceedance frequency near 10^{-7} per year (SNL 2007 [DIRS 176828], Table 6-67).

In summary, the performance demonstration for the Groundwater Protection Standard considered radionuclide releases for FEPs that were represented in the Waste Package and Drip Shield EF

Modeling Cases, and the Seismic GM Modeling Case. The early failure and ground motion modeling cases are implemented in a probabilistic manner to determine the number of WPs failed as a function of time in a given realization (Sections 6.4 and 6.6). As indicated previously, the projections for this standard are based on considering releases only from the damaged CDSP WPs; the potential releases from the CSNF WPs were omitted because the contribution to expected annual dose from seismic damage to CSNF WPs has been shown to be insignificant (Section 7.3.2.6.1.3).

Probabilistic projections for the three groundwater protection metrics were developed for the time period of 10,000 years and compared to the specified numerical limits. Those comparisons are presented and explained below.

8.1.2.1 Projections for Combined ^{226}Ra and ^{228}Ra

The performance demonstration for this first metric of the Groundwater Protection Standard is based on the combined activity concentration for ^{226}Ra and ^{228}Ra. The probabilistic projections of the time history of the activity concentrations are presented on Figure 8.1-9. The curves shown are background, mean, and 95th percentile activity concentrations of combined radium species (excluding background). As shown on Figure 8.1-9, the 95th percentile value for the combined radium concentration is less than the mean value. This result was a consequence of a few realizations that projected relatively high, but still small, radium concentrations that skewed the distribution of radium concentrations and caused the mean value to be higher than the 95th percentile value.

The curves on Figure 8.1-9 show that the peak mean groundwater concentration of combined ^{226}Ra and ^{228}Ra at the RMEI location is less than 10^{-5} pCi/L, which is well below the 5 pCi/L limit found in 10 CFR 331 ([DIRS 180319], Table 1). The naturally occurring background activity concentration of combined radium at the site is estimated to be ~0.5 pCi/L (SNL 2008 [DIRS 183750], Section 6.8.5, Table 6-18). At this background level, the projected peak radium activity concentrations of less than 10^{-5} pCi/L for the postulated repository releases would not make any measurable change to the background level in groundwater at the RMEI location. The fundamental reasons for the very low combined radium concentrations at the RMEI location are as follows:

^{228}Ra Activity Concentration—The chemical and nuclear properties of ^{228}Ra, together with its very small inventory, largely explain its small contribution to the total radium activity concentrations. As previously stated, the radioelement radium sorbs very strongly in the geologic media (Tables 6.3.9-2 and 6.3.10-2). This chemical property translates into ^{228}Ra taking very long transport times to migrate through the lower natural barrier. As previously stated, the projected mass breakthrough curves for radium through the SZ alone are predominantly greater than 10,000 years. However, if one postulates a hypothetical fast pathway with a very unlikely transport time, for example, of 500 years, then ^{228}Ra, with a half-life of 5.8 years, would experience about 86 half-lives of decay before reaching the RMEI location. This would reduce its activity by a factor of $(1/2)^{86} \sim 10^{-26}$. The initial total inventory ^{228}Ra in the CDSP WPs can be estimated by multiplying its specific activity (Table 6.3.7-5) times the number of grams of ^{228}Ra per package (Table 6.3.7-5) times the total number of CDSPs (Table 6.3.7-1) or $(2.72 \times 10^{2}$ Ci/g $\times \sim 2 \times 10^{-5}$ g/pkg $\times$ 3416 pkg) = 18.6 Ci or less than 20 Ci. This means that,

after 86 half-lives of decay, the original quantity of ^{228}Ra would be reduced to 2×10^{-13} pCi. Mixing this activity in the representative volume of 3,000 acre-ft would suggest that the ^{228}Ra activity concentration in the groundwater would likely be undetectable.

Considering that ^{228}Ra is a member of the thorium series, it could potentially reach the RMEI location via transport of its precursor ^{232}Th and subsequent in-growth. The relevant part of the decay chain is:

$$^{232}\text{Th (half-life } 1.4 \times 10^{10} \text{ years)} \rightarrow {}^{228}\text{Ra}$$

Because of its extraordinarily long half-life, the ^{232}Th is for all practical purposes a stable element for time periods of 10,000 years. For this reason, it is conservatively assumed that ^{228}Ra and ^{232}Th are in secular equilibrium and the activity of ^{228}Ra is the same as the ^{232}Th.

In the absence of ^{228}Ra inventory regeneration by in-growth and considering characteristically long radium transport times (through the SZ alone), it is reasonable to expect the activity concentrations for ^{228}Ra to show effectively undetectable levels for 10,000 years after disposal.

^{226}Ra Activity Concentration—The explanation for the projected low ^{226}Ra activity concentrations is similar to that for ^{228}Ra. The primary difference is that ^{226}Ra is a member of the uranium series with its two primary precursors being ^{234}U (half-life 240,000 years) and ^{230}Th (half-life 7.54×10^4 years). Over a time period of 10,000 years, the ^{234}U activity would experience a decay change of about 3 percent, which is a relatively small amount of in-growth to ^{230}Th. Similarly, about 9 percent of ^{230}Th activity would decay to ^{226}Ra in 10,000 years. In contrast, ^{226}Ra activity would diminish by almost 99 percent over the 10,000 years.

As noted previously, the median ^{226}Ra transport times through SZ for individual Monte Carlo realizations range from 18,000 years to more than 1,000,000 years, with the median over all realizations exceeding 700,000 years. The median ^{230}Th transport times through SZ for individual realizations range from about 1,000 years to more than 1,000,000 years, with a median for all realizations of greater than 1,000,000 years. Because the ^{226}Ra will be inventory limited, and its projected long transport times in the SZ, it is reasonable to expect that ^{226}Ra activity concentration would be low. Moreover, ^{226}Ra is limited by the small in-growth from ^{230}Th, occurring along the groundwater flow path.

Thus, the probabilistic projections for the combined radium groundwater standard demonstrate a reasonable expectation that the level of radioactivity in a representative volume of groundwater (i.e., 3,000 acre-ft) would not exceed the numerical limit of 5 pCi/L for groundwater protection.

8.1.2.2 Projections for Gross Alpha Activity

The performance demonstration for this metric of the Groundwater Protection Standard is based on a calculation of the gross alpha activity, including ^{226}Ra but excluding ^{222}Rn and Uranium species (10 CFR 63.331). The TSPA Biosphere Component Model, documented in DTN: MO0702PAGWPROS001_R0 [DIRS 179328], identifies 15 primary radionuclides that have one or more alpha emitters in their decay chain to the next tracked radionuclide. The specific alpha emitting radionuclides to consider in estimating the gross alpha are:

- ^{210}Pb (half-life 22.3 years)
- ^{226}Ra (half-life 1,600 years)
- ^{227}Ac (half-life 21.8 years)
- ^{228}Th (half-life 1.913 years)
- ^{229}Th (half-life 7,300 years)
- ^{230}Th (half-life 75,400 years)
- ^{232}Th (half-life 1.4×10^{10} years)
- ^{231}Pa (half-life 32,800 years)
- ^{237}Np (half-life 2.14×10^{6} years)
- ^{238}Pu (half-life 87.7 years)
- ^{239}Pu (half-life 24,100 years)
- ^{240}Pu (half-life 6,560 years)
- ^{242}Pu (half-life 3.75×10^{5} years)
- ^{241}Am (half-life 433 years)
- ^{243}Am (half-life 7,370 years).

The probabilistic projections for gross alpha activity concentrations over the 10,000-year time period are shown on Figure 8.1-10. The activity concentration for gross alpha was calculated based on the annual mass flux of the alpha emitting radionuclides across the boundary of the accessible environment and collected in the representative groundwater volume of 3,000 acre-ft/yr. The plot on this figure shows curves for the mean and 95th percentile for gross alpha activity concentration. The peak mean activity concentration is projected to be less than 1×10^{-4} pCi/L (excluding background). This activity concentration is below the ground-water protection standard of 15 pCi/L (found in 10 CFR 331 [DIRS 180319], Table 1) for gross alpha and well below the natural background level of ~0.5 pCi/L in the site groundwater. As a result, the postulated releases of the alpha emitting radionuclides are effectively limited by the EBS and sufficiently confined to the lower natural barrier.

The radionuclides making the largest contributions to mean gross alpha activity are ^{237}Np, ^{239}Pu, ^{240}Pu, and ^{242}Pu. These four radionuclides have relatively large initial inventories (in the CSNF waste form) and long to very long half-lives. Moreover, the three plutonium species are transported through the groundwater pathway in both dissolved and colloidal phases. The low contributions of the other alpha emitters can be plausibly explained by examining their initial inventories (Table 6.3.7-5), decay chain properties (Figure 6.3.7-4), half-lives (Figure 6.3.7-4), and sorption properties (Tables 6.3.9-2 and 6.3.10-2) (i.e., distribution coefficient or K_d). A qualitative examination leads to the following observations and inferences explained below.

Low Inventory, Short Half-Lives, and Strong Sorption—The alpha emitting radionuclide ^{228}Th is easily eliminated as a potentially significant contributor to gross alpha because its very short half-life of 1.913 years and low initial inventory (provided by the decay of ^{245}Cm) will most likely deplete before loss of containment. Similarly, the radionuclides ^{238}Pu and ^{241}Am have relatively short half-lives; equally important is the fact that they are strongly sorbed in the UZ rock layers and in the volcanic units and alluvium of the SZ. Thus, it is reasonable to expect that these two alpha emitters are not likely to reach the accessible environment in most TSPA-LA realizations. Thus, based on these qualitative arguments, ^{228}Th, ^{238}Pu, and ^{241}Am will likely not make a significant contribution to the gross alpha activity concentrations.

Secular Equilibrium and Sorption—The alpha emitting radionuclides ^{210}Pb, ^{226}Ra, and ^{227}Ac are not likely to be significant contributors to gross alpha because their activity is controlled via secular equilibrium with their precursor radionuclides, namely:

$$^{232}\text{Th (half-life } 1.4 \times 10^{10} \text{ years)} \rightarrow {}^{228}\text{Ra (half-life 5.8 years)} \rightarrow {}^{210}\text{Pb}$$

$$^{230}\text{Th (half-life 77,000 years)} \rightarrow {}^{226}\text{Ra}$$

$$^{231}\text{Pa (half-life 32,800 years)} \rightarrow {}^{227}\text{Ac.}$$

As was explained earlier for the combined radium groundwater standard, these radionuclide species are unlikely to produce significant activity concentrations at the accessible environment boundary because of the sorption properties of both radium and its precursor thorium. In the case of the radioelement protactinium, its initial inventory in the WPs is low and its sorption properties in the unsaturated rock layers is relatively high (e.g., mean K_ds of ~5,000 mL/g), which suggests that the precursors (^{232}Th, ^{230}Th, and ^{231}Pa) or the daughters (^{210}Pb, ^{226}Ra, and ^{227}Ac) are not likely to contribute appreciably to the gross alpha activity levels.

Very High Sorption—The radioelement americium has the property of being very strongly sorbed in the unsaturated rock layers (e.g., mean K_ds of 400 to about 5,000 mL/g), as well as in the volcanic units (e.g., mean K_ds of 400 to about 5,000 mL/g) and alluvium (e.g., mean K_ds of ~5,000 mL/g) of the SZ. On the other hand, this radioelement has a significant initial inventory in the CSNF and can also be transported in colloidal phase (i.e., reversible and irreversible).

Thus, the probabilistic projections for this regulatory performance metric show a reasonable expectation that the level of radioactivity in a representative volume of groundwater would not exceed the numerical limit of 15 pCi/L for groundwater protection.

8.1.2.3 Projections for Combined Beta- and Photon-Emitting Radionuclides

The performance demonstration for this metric of the Groundwater Protection Standard is based on combined beta- and photon-emitting radionuclides; both the primary beta emitters and any daughter products that decay by beta-emission are considered. The annual doses from exposure to beta-photon emitters are quantified in terms of both whole body and organ dose. The TSPA Biosphere Component Model documented in the *Biosphere Model Report* (SNL 2007 [DIRS 177399], Table 6.15-4), identifies a total of 19 primary radionuclides that are used to compute this groundwater protection metric.

Some of the more prominent beta emitters are: ^{14}C, ^{36}Cl, ^{79}Se, ^{90}Sr, ^{99}Tc, ^{129}I, ^{135}Cs, and ^{137}Cs. Of this set, only ^{90}Sr and ^{137}Cs have short half-lives (~ 30 years) relative to the 10,000 year time period. Some of the beta-photon emitters are daughter products of alpha and beta emitters (SNL 2007 [DIRS 177399], Table 6.15-4) such as ^{137m}Ba, ^{228}Ac, ^{212}Pb, and ^{208}Tl. Because this group of radioisotopes has half-lives ranging from minutes to several hours, they are not included in radionuclide transport calculations; however, the associated conversion factors are included in calculating the beta-photon dose. The projections of annual doses for these radionuclides are evaluated as a function of the release rates from the repository, in-growth, and groundwater transport to the accessible environment.

Probabilistic projections for the mean whole body and thyroid annual doses for the 10,000-year time period are shown on Figure 8.1-11; a curve for the 95th percentile is also shown. These annual doses were calculated by summing all the annual doses from the beta- and photon-emitting radionuclides included in the TSPA-LA Model. The peak mean annual drinking water dose to the thyroid is estimated to be about 0.2 mrem. The whole body dose shown on the same figure takes into account the effect on all organs and includes the organ-dose weighting factors. The peak mean annual drinking water dose to the whole body in this case is estimated to be about 4×10^{-2} mrem. The radionuclide that dominates the mean thyroid dose is ^{129}I, whereas ^{99}Tc dominates the mean whole body dose.

Thus, the probabilistic projections for combined beta-photon dose demonstrate a reasonable expectation that the annual doses to the whole body or any organ would not exceed the numerical limit of 4 mrem.

8.1.3 Human Intrusion Protection

As required by the proposed NRC regulation, a performance demonstration was developed for the Human Intrusion Standard (10 CFR 63.321 [DIRS 178394]). The probabilistic projections provide an estimate of the annual dose to the RMEI resulting from a stylized human intrusion drilling scenario and compare the result to the dose limits that the geologic repository at the Yucca Mountain site must meet. The EPA regulation 40 CFR Part 197 (2005 [DIRS 175755]) clarifies that the performance assessment for the Human Intrusion Scenario is to be presented separately and not integrated into the TSPA for the Individual Protection Standard.

The Human Intrusion Standard parallels the Individual Protection Standard in that the same numerical limits for annual dose must be met. More specifically, the Human Intrusion Standard (10 CFR 63.321 (a) and (b) in the proposed NRC regulation [DIRS 178394]) specifies that the DOE must:

1. Determine the earliest time after disposal that a WP would degrade sufficiently that a drilling intrusion could occur without recognition by the drillers

2. Demonstrate a reasonable expectation that the RMEI, as a result of the human intrusion, will not receive an annual dose of:

    a. 0.15 mSv (15 mrem) for 10,000 years following disposal

    b. 3.5 mSv (350 mrem) after 10,000 years, but within the period of geologic stability

3. Include all potential environmental pathways of radionuclide transport and exposure subject to the requirements of 10 CFR 63.322 [DIRS 180319].

The characteristics and assumptions of the stylized Human Intrusion Scenario are specified in the NRC regulation 10 CFR 63.322 [DIRS 180319]. That section of the regulation prescribes the following scenario characteristics for the drilling event:

- There is a single human intrusion as a result of exploratory drilling for ground water, per 10 CFR 63.322(a).
- The intruders drill a borehole directly through a degraded WP into the uppermost aquifer underlying the Yucca Mountain Repository, per 10 CFR 63.322 (b).
- The drillers use the common techniques and practices that are currently employed in exploratory drilling for ground water in the region surrounding Yucca Mountain, per 10 CFR 63.322 (c).
- Careful sealing of the borehole does not occur, instead natural degradation processes gradually modify the borehole, per 10 CFR 63.322 (d).
- No particulate waste material falls into the borehole, per 10 CFR 63.322 (e).
- The exposure scenario includes only those radionuclides transported to the SZ by water (e.g., water enters the WP, releases radionuclides, and transports radionuclides by way of the borehole to the SZ), per 10 CFR 63.322 (f).
- No releases are included which are caused by unlikely natural processes and events, per 10 CFR 63.322 (g).

With regard to the last specification, the NRC regulation defines unlikely natural processes and events as those having a probability of less than one chance in 10 and at least one chance in 10,000 of occurring within 10,000 years of disposal, as defined in 10 CFR 63.342(b) [DIRS 178394]. This probability statement is equivalent to a cut-off annual frequency criterion of $\leq 10^{-5}$/yr for exclusion of unlikely processes and events.

For the purposes of the TSPA, it is assumed that inadvertent drilling into the repository results in a penetration of the DS and WP, as well as creating a direct pathway to the groundwater. The conceptualization of the scenario includes radionuclides transported vertically through the UZ, horizontally along the SZ, and then withdrawn with the groundwater at the location of the RMEI. The exposure characteristics for the RMEI are as defined in 10 CFR 63.312(a) through (e) [DIRS 180319].

8.1.3.1 Determination of Earliest Time for Drilling Intrusion

A detailed technical study was conducted to establish a technical basis to address the first requirement of the Human Intrusion Standard (i.e., 10 CFR 63.321(a) [DIRS 178394]). That study, which is presented in Section 6.7.2, examined three general aspects of the hypothetical drilling intrusion, namely:

1. Capability of intact DSs and WPs to resist penetration by drilling technology typically used in groundwater exploration
2. Drilling operating characteristics (i.e., change-in-conditions) that would or would not indicate drill-bit impingement on a metallic anthropogenic structure

3. Degradation of DSs and WPs by nominal processes and likely disruptive events that could provide a physical pathway for a drill-bit to penetrate the WP without recognition by the drillers.

With regard to the scenario conditions, likely processes and events refers to those events with a frequency of occurrence greater than or equal to 10^{-5}/yr, as specified by the NRC regulation.

The technical basis, which is summarized herein, was used to develop a bounding estimate of 200,000 years for the earliest time of WP penetration (without recognition by drillers). That bounding estimate was used in the probabilistic projections of annual dose to the RMEI, which are presented in Section 8.1.3.2

Capability of Intact DSs and WPs to Resist Drilling Penetration

The 15-mm (0.59 in.) thick Titanium Grade 7 DS plate and 25-mm (0.98 in.) thick Alloy 22 WP outer barrier constitutes a significant double barrier to potential groundwater drilling intrusion. In the case of the CSNF package, which is a canister within a canister, there would be an additional 50.8-mm (2 in.) thick stainless steel barrier to resisting potential drilling intrusion. The capability of the DS and WP barriers to resist a drilling penetration was examined from two perspectives: (1) drill-bits typically used in groundwater exploration in rock formations, and (2) scenario of drill string free-fall through an open drift and potentially penetrating a DS and WP.

Drilling Technology—Drilling technology that would be used in drilling water wells through welded tuff at Yucca Mountain would typically utilize roller bits (IADC 1992 [DIRS 155232]) to drill through the rock formations. Roller bits are very effective in drilling through welded tuff formations and basically cause brittle failure of the rock matrix and break and crush the rock to facilitate removal. This type of drill-bit, however, would be ineffective in attempting to bore through the metal barriers because of the high compressive strength and ductility of titanium and stainless steel. Penetration of these intact metal barriers would require a drill-bit designed to induce metal failure; such types of drill-bits are not typically used in exploratory drilling for water in the Southwestern United States. Moreover, attempts to drill through intact DSs and/or WPs would result in significant changes to the drilling operation characteristics, which would be clear indicators of the drill-string encountering a metallic anthropogenic structure.

Drill-String Free-Fall and Impingement on WP—A drill-string entering an open emplacement drift could experience a free-fall and, in turn, directly impacting the intact DS and WP. The potential for WP penetration was evaluated for the case of a 300 m, 14-metric ton drill-string assembly (i.e., drill pipe, drill collar, and drill-bit) assuming no DS present with drop heights of 1.8 m (i.e., approximate distance to CSNF) and 1.6 m (i.e., approximate distance to CDSP). A bound for the maximum impact velocity of such a drill-string free-fall was estimated to be about 5.9 m/s for both the CSNF and CDSP packages.

The potential for rupture of the WP outer barrier for the above conditions was evaluated by utilizing calculational results from detailed structural analyses for WP-to-pallet impacts (SNL 2007 [DIRS 178851], Section 6.3.2), which provide strain-based rupture conditions as a function of impact velocities. This comparative analysis indicates that the drill-string impact would not penetrate an intact WP. A more likely outcome of a drill-string free-fall would be impingement on and deformation of the DS. In the unlikely event that the DS was actually penetrated by the drill-string, it would absorb the impact energy, which would reduce the impact velocity, and further reduce the potential for penetration of the WP.

Drilling Operating Characteristics

Drilling operations generally involve monitoring of the bit operating conditions as the drill-string penetrates the rock formations. Typical characteristics that are monitored by drillers include circulating fluid properties and rates, drilling stability, bit weight, and rotary speed. Significant changes in any of these types of operating characteristics generally prompt the driller to examine and resolve the change in operating characteristics. In the case of a drill-string entering an open emplacement drift and impinging the DS and/or WP, the following changes in the operating characteristics would likely occur:

- Loss of circulation fluid
- Sudden changes in rotary speed
- Rapid increase in drill-string vibration.

Moreover, driller attempts to correct volumetric problems with the circulating fluid (i.e., by spot cementing and setting cases) would be largely thwarted by the large drift volume and physical presence of the DS and WP. These problems would likely prompt the driller to remove the drill-string from the borehole and examine the drill-bit. Such diagnostic actions by the driller would lead to recognition that a metallic anthropogenic structure had been encountered.

Under conditions of a drift collapse, however, changes in some operational characteristics could be muted and, therefore, less recognizable. For example, the loss of circulating fluid in a collapsed drift (i.e., filled with rubble) would still occur but could be mitigated by the driller. Changes in drill-bit rotation speed would be unaffected until the drill-bit encountered the DS, at which time the drill-string would exhibit vibration. Drift collapse would primarily occur as a result of cumulative effects of seismic events (i.e., vibratory ground motion) in the lithophysal regions of the repository. Such drift collapse events are currently projected to occur in the post-10,000-year time period.

Degradation of Drip Shields and Waste Packages by Nominal and Disruptive Scenario Conditions

The study considered four scenarios for WP and DS degradation: (1) nominal degradation of the DSs and WPs, (2) DS early failures (i.e., having an undetected defect that could cause an early failure), (3) DS and WP failures as a result of igneous intrusion disruptive events, and (4) DS and

WP failures as a result of seismic events (i.e., seismic ground motion and seismic fault displacement). Of these scenario conditions, three were screened-out because their frequency of occurrence was less than the NRC cut-off of 1 chance in 10 in 10,000 years or 10^{-5}/yr, namely:

- Early Failure: The probability that a drilling intrusion encounters a DS early failure occurring at the same location is estimated to be 7×10^{-6}
- Igneous Intrusion: Exceedance frequency of igneous events in the repository footprint estimated to be less than 10^{-5}/yr but greater than 10^{-8}/yr
- Seismic Fault displacement: Exceedance frequency of seismic fault displacement in the repository footprint is estimated to be less than 2.5×10^{-7}/yr.
- Seismic Ground Motion: (1) peak ground velocities, with exceedance frequencies greater than or equal to 10^{-5}/yr, are relatively low and unlikely to induce dynamic loads sufficient to cause DS plate failure, and (2) exceedance frequency of seismic-induced large block movements, which could rupture DSs and damage WPs, are less than 1.17×10^{-6}/yr (DTN MO0712PBANLNWP.000_R0 [DIRS 184664], file *Nonlith LC Calculation Rev03.xmcd*).

Thus, nominal degradation processes are the most probable way that a penetration (i.e., opening) could develop in the DSs and WPs that could potentially a serve as a physical pathway to groundwater drilling—facilitating a penetration without recognition by the drillers.

In the case of the DSs, thinning of the titanium DS plate would occur over geologic time periods. Over a period of 10,000 years, for example, the extent of thinning of the 15-mm-thick DS plate by general corrosion is projected to be approximately 0.66 mm or a thinning of about 4 percent of the total thickness. This projection is based on a high corrosion rate corresponding to a 0.9999 quantile (Section 6.3.5.1.3). Assuming this same corrosion rate, the DS plate failure time is projected to occur at about 230,000 years; this estimate is corroborated by more detailed probabilistic projections for nominal conditions that calculate the first DS plate failure occurring at about 270,000 years (Figure 8.1-4). Those detailed probabilistic projections, also for nominal conditions, indicate that the mean failure time of the first penetration of WP outer barrier by general corrosion patches occurs at about 440,000 years (DTN: MO0709TSPAWPDS.000 [DIRS 183170]).

Based on the above considerations and evaluations, the estimate of the earliest time a driller could penetrate a WP, without recognition by the driller, was taken to be 200,000 years. This time is a conservative bound to DS fail time and neglects the lifetime of the WPs.

8.1.3.2 Projections of Annual Doses for Human Intrusion

To address the second requirement of the Human Intrusion Standard (10 CFR 63.321(b) [DIRS 178394]), a probabilistic TSPA methodology, analogous to that used to demonstrate

performance with the Individual Protection and Groundwater Protection Standards, was used to make projections of the annual dose. The calculations of annual dose to the RMEI were performed for all environmental pathways, as specified in 10 CFR 63.321(c) [DIRS 178394]. Based on the analysis described above, the earliest time after disposal for the drilling intrusion was taken to be 200,000 years.

As described in Section 6.1.2.5, the type of WP (i.e., CSNF or CDSP) assumed to be penetrated is sampled in the analysis so that probabilistic projections of annual dose reflect the radionuclide releases from the various waste forms (Section 6.3.5). Based on the proportion of WP types, the probability of sampling a CSNF WP is ~0.7, whereas the probability of selecting a CDSP WP is ~0.3. The location of the penetration in the repository footprint was also sampled so as to reflect the range of percolation fluxes that would induce waste dissolution and releases.

The probabilistic projections of expected annual dose for the Human Intrusion Scenario are presented on Figure 8.1-12. The plots show the curves for the mean, median, and 5th and 95th percentiles of the distribution of expected annual doses for the period of geologic stability. The peak of the mean annual dose to the RMEI occurs within a few thousand years after inclusion. The peak mean and median annual individual doses are projected to be less than 0.008 mrem and 0.006 mrem, respectively, well below the regulatory limit of 350 mrem. The annual doses at the 5th and 95th percentiles are calculated to be approximately 0.001 mrem and 0.017 mrem, respectively.

The contributions of individual radionuclides to the total mean annual dose for the Human Intrusion Scenario for 1,000,000 years after repository closure, is shown on Figure 8.1-13. ^{99}Tc (half-life 2.13×10^5 yrs), ^{129}I (half-life 1.57×10^7 yrs), ^{36}Cl (half-life 3.01×10^5 yrs), and ^{237}Np (half-life 2.14×10^6 yrs) dominate the mean annual dose from 200,000 years to about 300,000 years; thereafter, dominance then transitions to ^{79}Se (half-life 2.95×10^5 yrs), ^{135}Cs (half-life 2.30×10^6 yrs), ^{242}Pu (half-life 3.75×10^5 yrs), and ^{237}Np (half-life 2.14×10^6 yrs). The ^{242}Pu, which is transported through the SZ in both dissolved and colloidal form, dominates the peak mean annual dose at 1,000,000 years.

Thus, these projections demonstrate that there is a reasonable expectation that the mean annual doses to the RMEI would be well below the limits for the Human Intrusion Standard. Moreover, the projections indicate that the system of multiple barriers would be sufficiently robust and resilient to limit annual doses for the prescribed Human Intrusion Scenario.

INTENTIONALLY LEFT BLANK

Table 8.1-1. Performance Demonstration Results for Individual Protection Standard

Time After Closure (yrs)	Projected Peak Mean Annual Dose (mrem)	Time of Peak Mean Annual Dose (yr)	Projected Peak Median Annual Dose (mrem)	Time of Peak Median Annual Dose (yr)	Limit for Annual Dose (mrem)
10,000	0.24	10,000	0.12	10,000	15 (mean)
1,000,000	2.30	1,000,000	0.99	~760,000	350 (median)

Source: Output DTN: MO0709TSPAREGS.000 [DIRS 182976]; Regulatory Limits from 10 CFR 63.311(a) ([DIRS 178394])

Table 8.1-2. Performance Demonstration Results for Groundwater Protection Standard

Type of Limit	Projected Peak Mean Activity Concentration or Annual Dose	Natural Background Level	Limit for Activity Concentration or Annual Dose
Combined Ra-226 & Ra-228	$<10^{-5}$ pCi/L	0.5 pCi/L	5 pCi/L
Gross Alpha Activity	$<10^{-4}$ pCi/L	0.5 pCi/L	15 pCi/L
Dose from Combined Beta & Photon Emitting Radionuclides	Whole Body ~ 0.04 mrem Thyroid ~ 0.17 mrem	Background level excluded in regulatory requirement	4 mrem

Source: Output DTN: MO0709TSPAREGS.000 [DIRS 182976]; Regulatory Limits from 10 CFR 63.331 ([DIRS 180319])

Table 8.1-3. Performance Demonstration Results for Human Intrusion Standard with Drilling Event at 200,000 years After Closure

Time After Closure (yrs)	Projected Peak Mean Annual Dose (mrem)	Limit for Annual Dose (mrem)
10,000	0	15 (mean)
1,000,000	$< 10^{-2}$	350 (median)

Source: Output DTN: MO0709TSPAREGS.000 [DIRS 182976]; Regulatory Limits from 10 CFR 63.321(b) ([DIRS 178394])

Table 8.1-4. Uncertainty in Projections of Peak Mean Annual Dose (mrem) for Individual Protection Standard

Time After Closure (yrs)	Mean	Median	5th Percentile	95th Percentile
10,000	0.24	0.12	6.43×10^{-3}	0.71
1,000,000	2.30	0.88	0.18	9.55

Source: Output DTN: MO0709TSPAREGS.000 [DIRS 182976]

Table 8.1-5. Uncertainty Importance Ranking as a function of time for Key TSPA-LA Model Parameters

Time After Closure (yrs)	Two Most Important Parameters at the Selected Time	
3,000	SCCTHRP	IGRATE
5,000	SCCTHRP	IGRATE
10,000	SCCTHRP	IGRATE
125,000	IGRATE	SCCTHRP
250,000	WDGCA22	IGRATE
500,000	IGRATE	WDGCA22
1,000,000	IGRATE	WDGCA22

Source: Output DTN: MO0709TSPASENS.000 [DIRS 182982]

NOTE: IGRATE = occurrence rate of igneous events

SCCTHRP = SCC stress threshold

WDGCA22 = temperature dependence parameter for alloy 22 general corrosion rate

Importance related to expected dose to RMEI for all scenario classes.

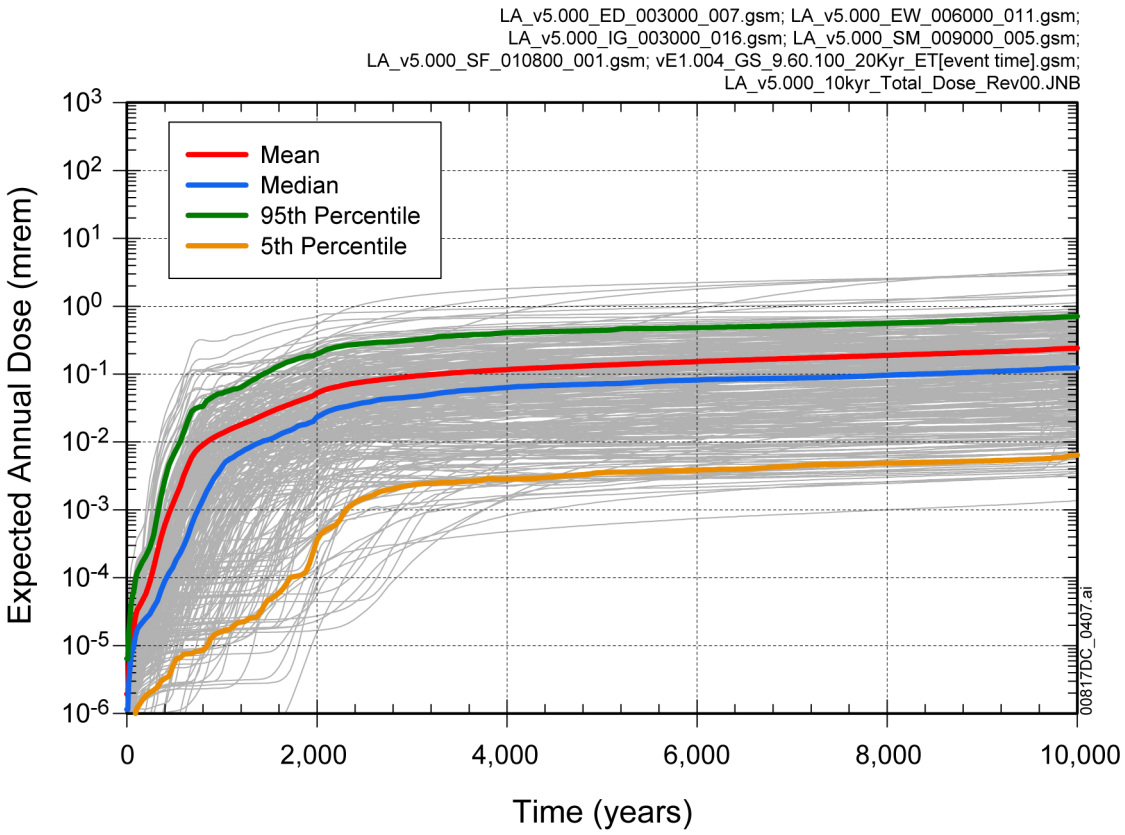

Source: Output DTN: MO0709TSPAREGS.000 [DIRS 182976].

Figure 8.1-1. Probabilistic Projections of Total Expected Annual Dose for 10,000 Years after Closure

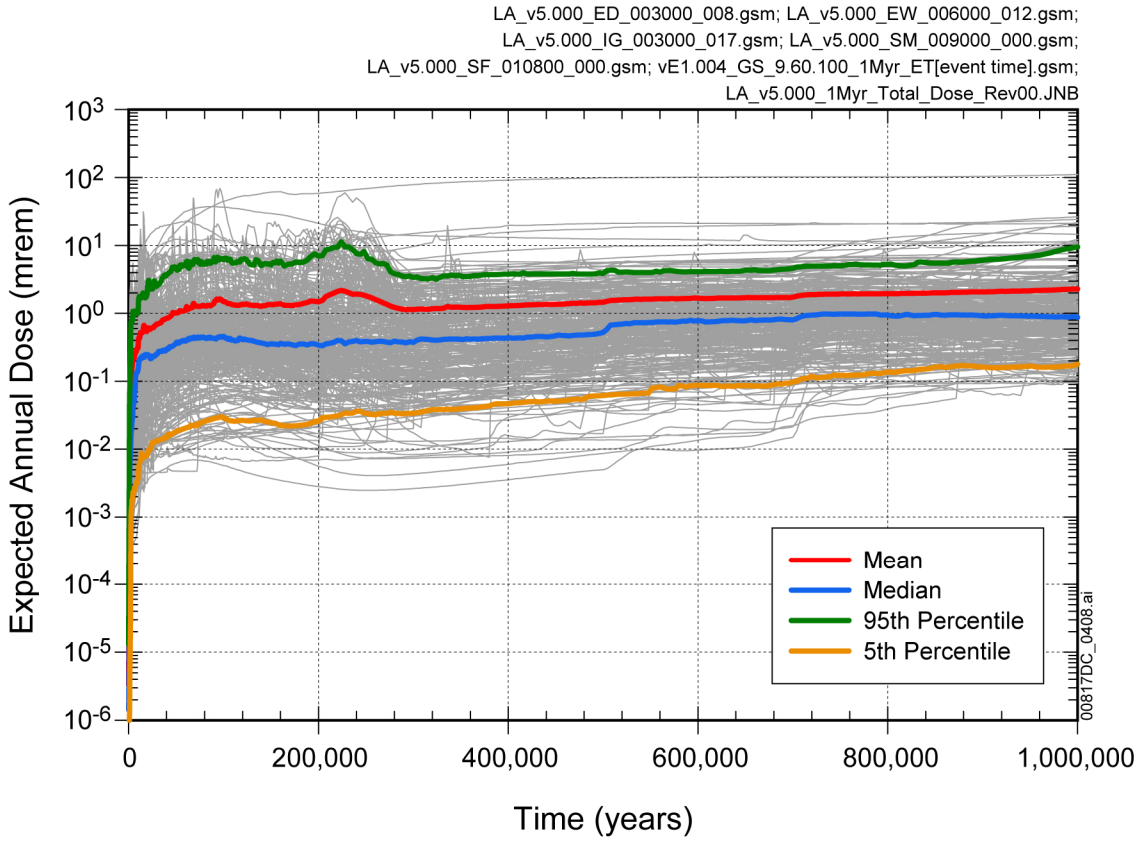

Source: Output DTN: MO0709TSPAREGS.000 [DIRS 182976].

Figure 8.1-2. Probabilistic Projections of Total Expected Annual Dose for 1,000,000 Years after Closure

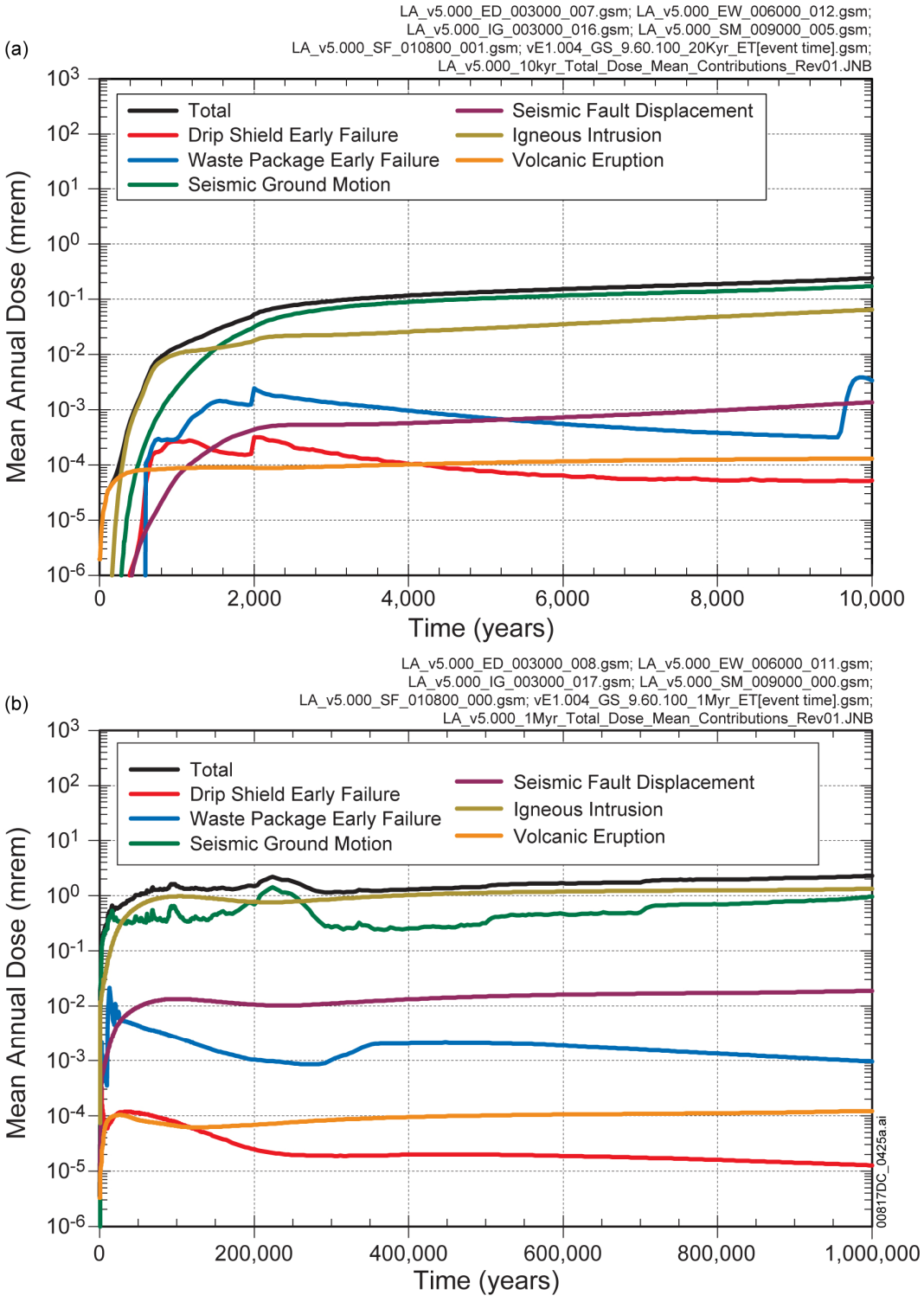

Source: Output DTN: MO0709TSPAREGS.000 [DIRS 182976].

Figure 8.1-3. Relative Contributions of Scenario Modeling Cases to Total Mean Annual Dose for (a) 10,000 Years and (b) 1,000,000 Years after Repository Closure

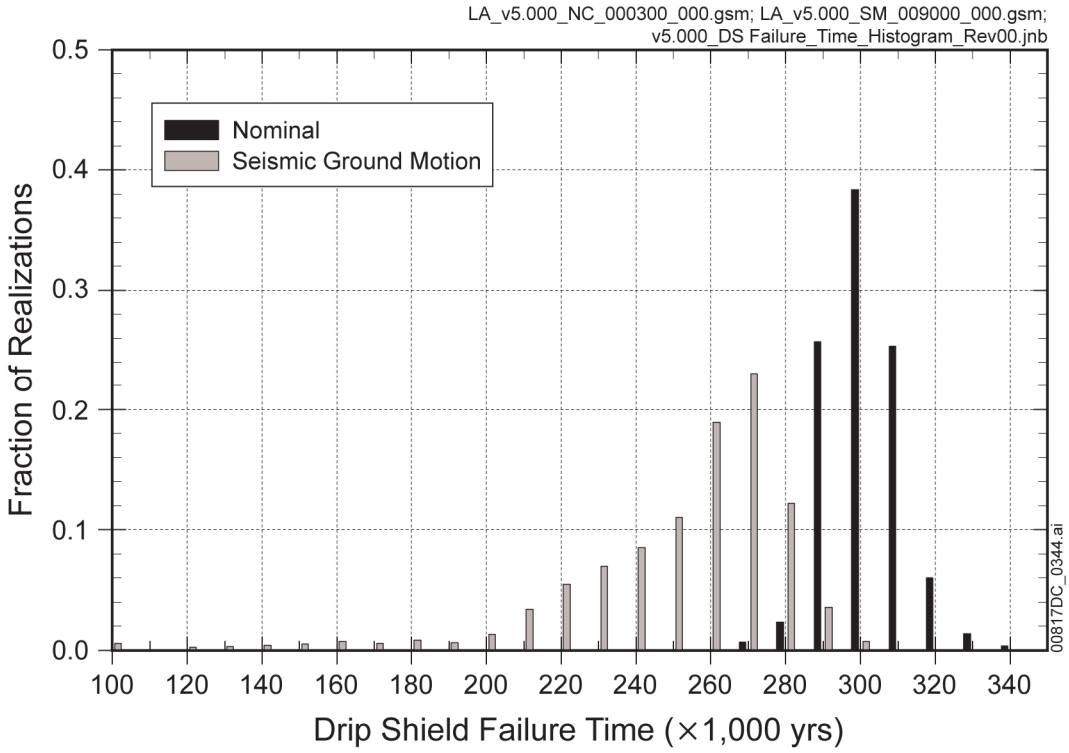

Source: Output DTN: MO0709TSPAREGS.000 [DIRS 182976].

NOTE: Nominal failures are due to general corrosion. Seismic ground motion failures are caused by the combined effects of general corrosion, vibratory ground motion, and rockfall.

Figure 8.1-4. Histogram of Drip Shield Failure for the Nominal and Seismic Ground Motion Modeling Cases

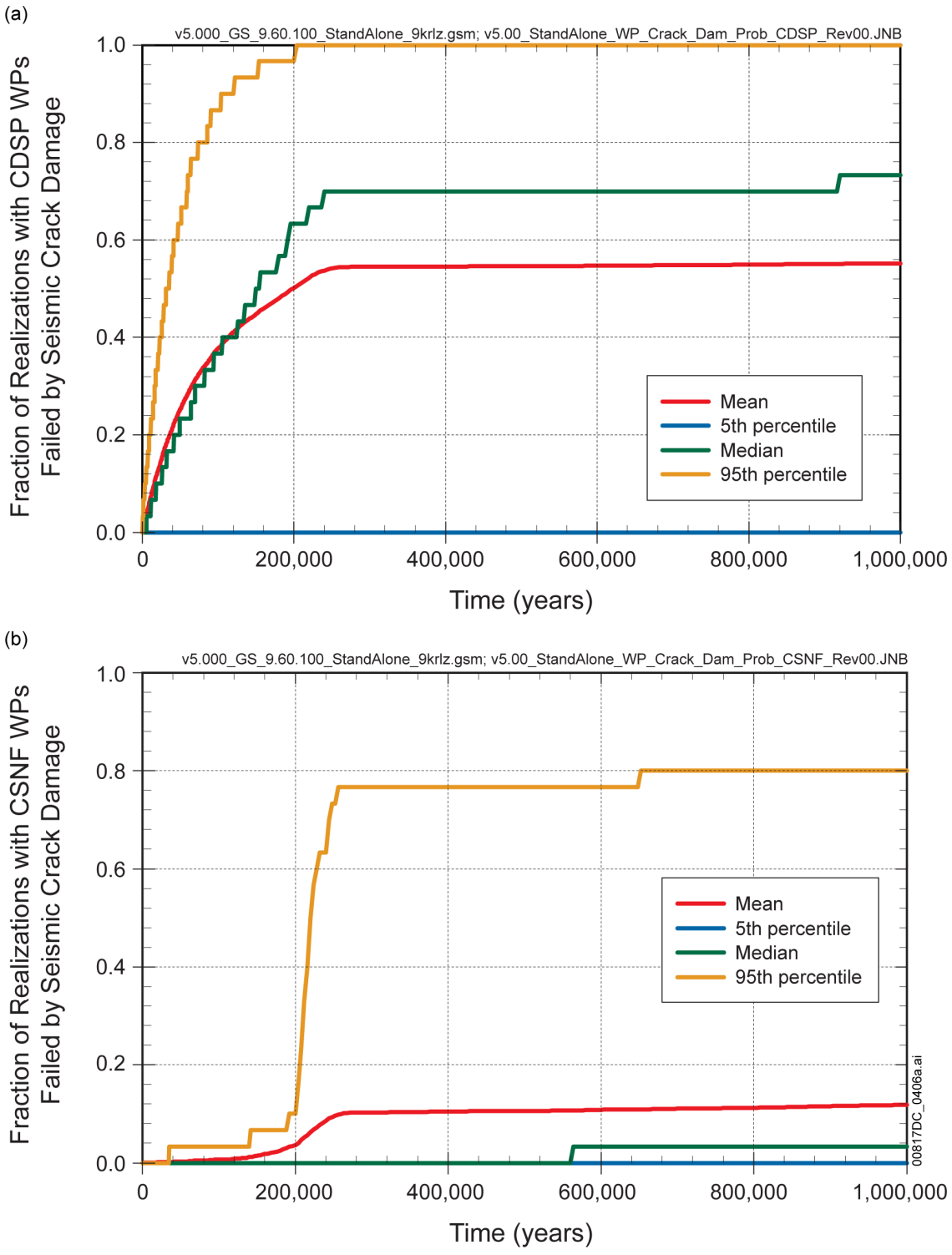

Source: Output DTNs: MO0709TSPAREGS.000 [DIRS 182976]; and MO0709TSPAWPDS.000 [DIRS 183170].

Figure 8.1-5. Fraction of (a) CDSP WPs and (b) CSNF WPs Failed for by Seismic Crack Damage as a Function of Time for Percolation Subregion 3

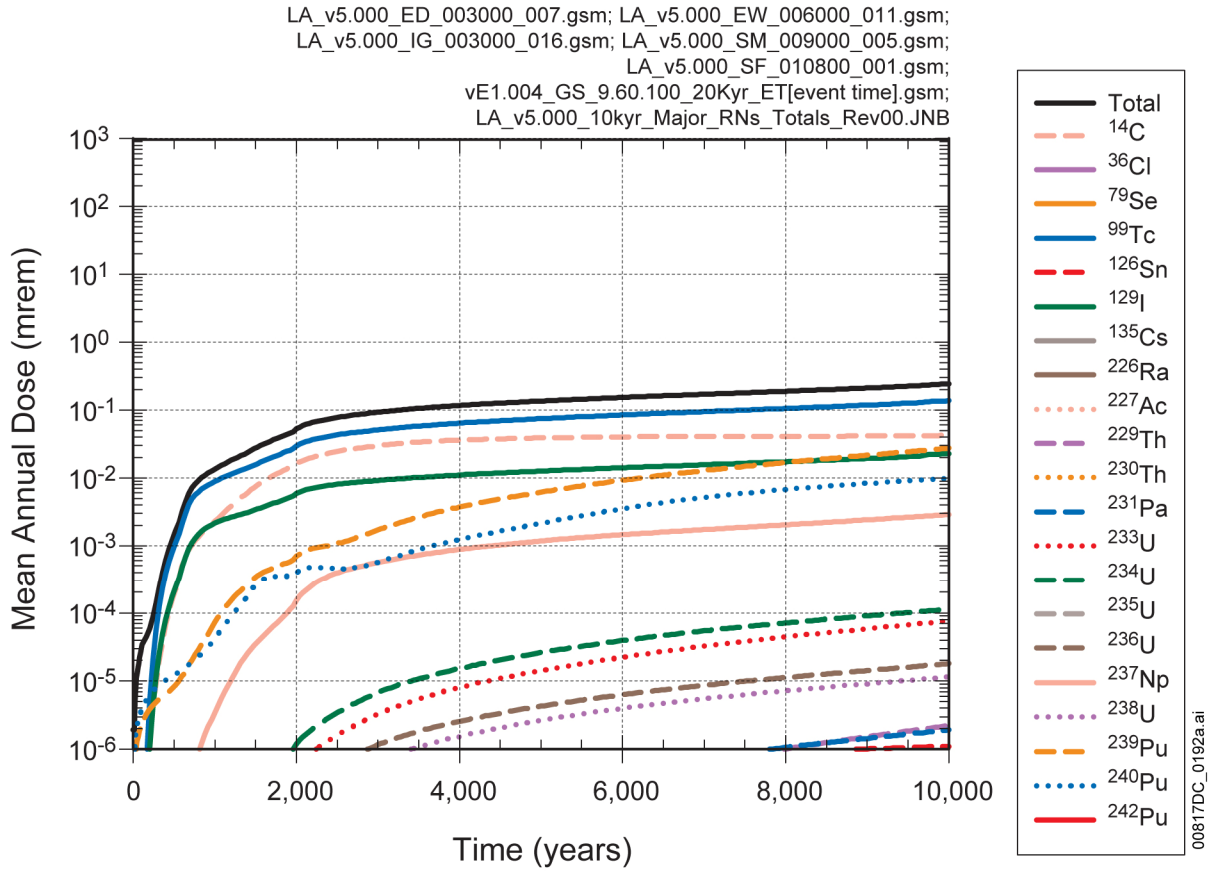

Source: Output DTN: MO0709TSPAREGS.000 [DIRS 182976].

Figure 8.1-6. Contribution of Individual Radionuclides to Total Mean Annual Dose for 10,000 Years after Repository Closure

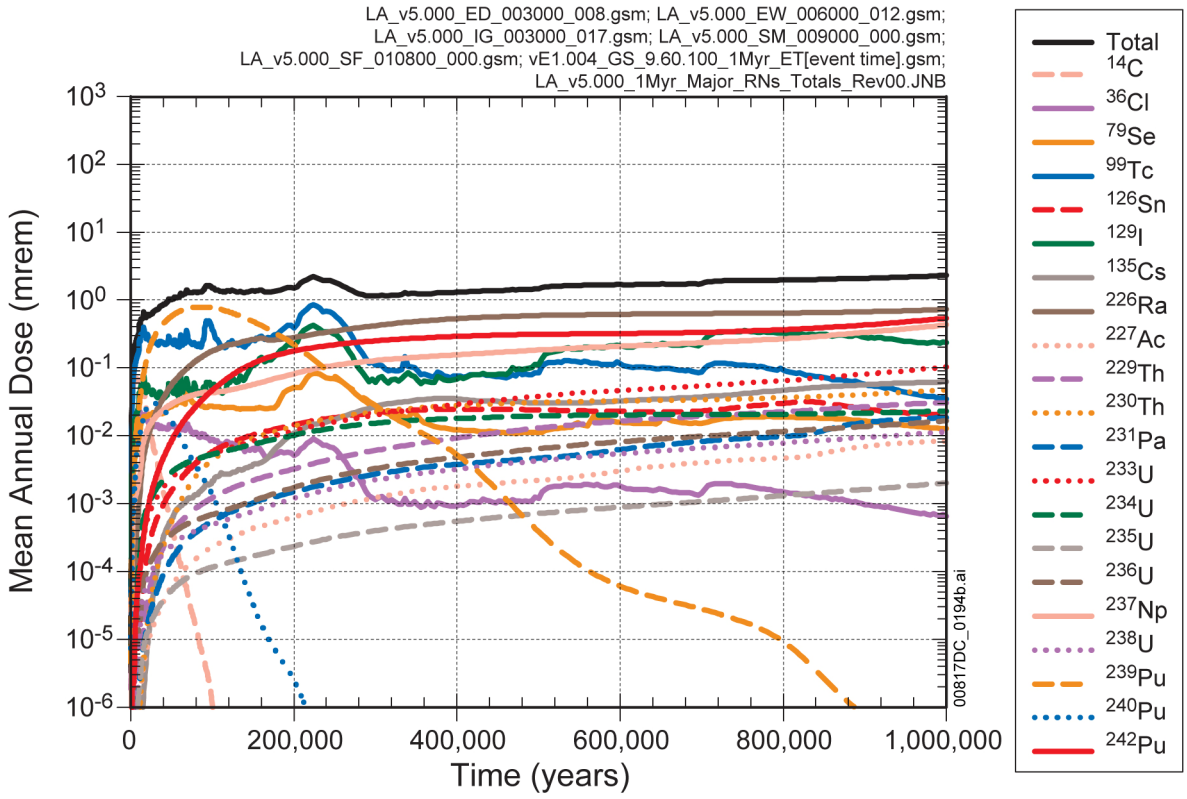

Source: Output DTN: MO0709TSPAREGS.000 [DIRS 182976].

Figure 8.1-7. Contribution of Individual Radionuclides to Total Mean Annual Dose for 1,000,000 Years after Repository Closure

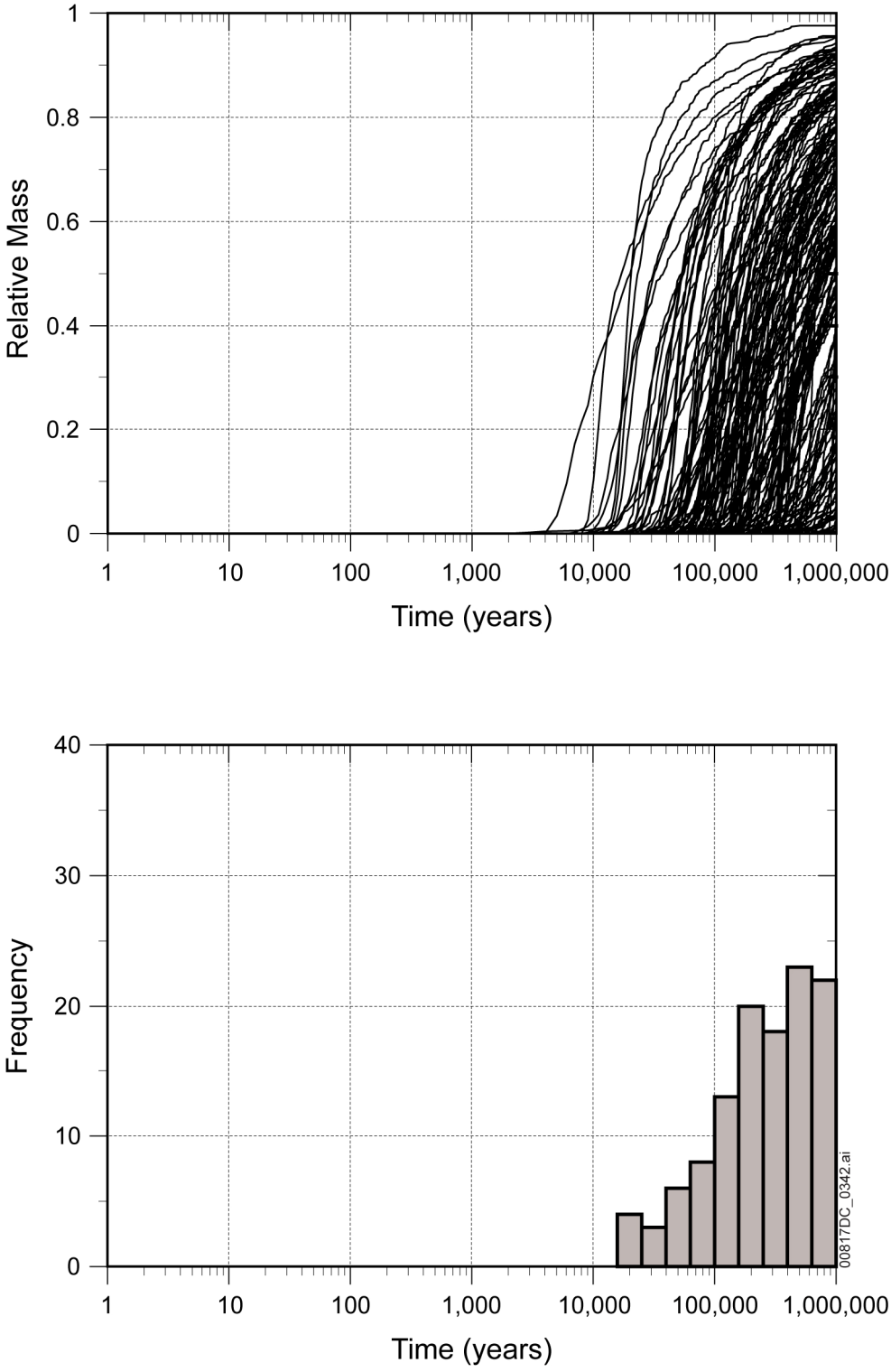

Sources: SNL 2007 [DIRS 183750], Figure 6-14[a].

Figure 8.1-8. Radium Mass Breakthrough Curves (upper) and Median Transport Times (lower) at the RMEI Location

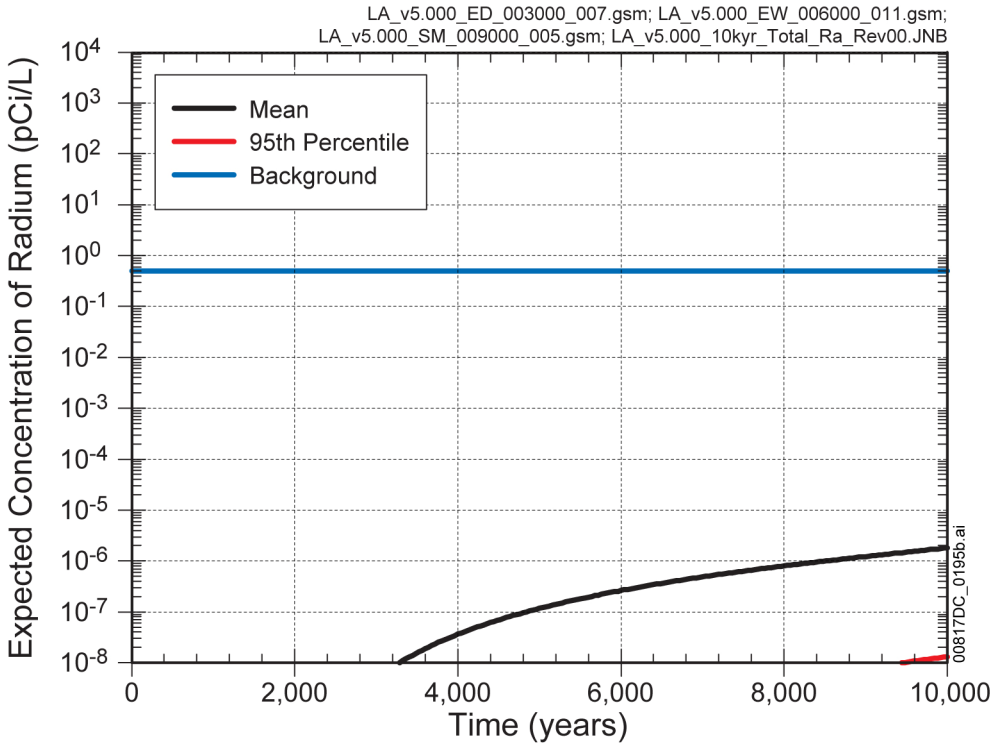

Source: Output DTN: MO0709TSPAREGS.000 [DIRS 182976].

Figure 8.1-9. Probabilistic Projections of Activity Concentrations Total Radium (^{226}Ra and ^{228}Ra) in Groundwater, Excluding Natural Background, for 10,000 Years after Closure

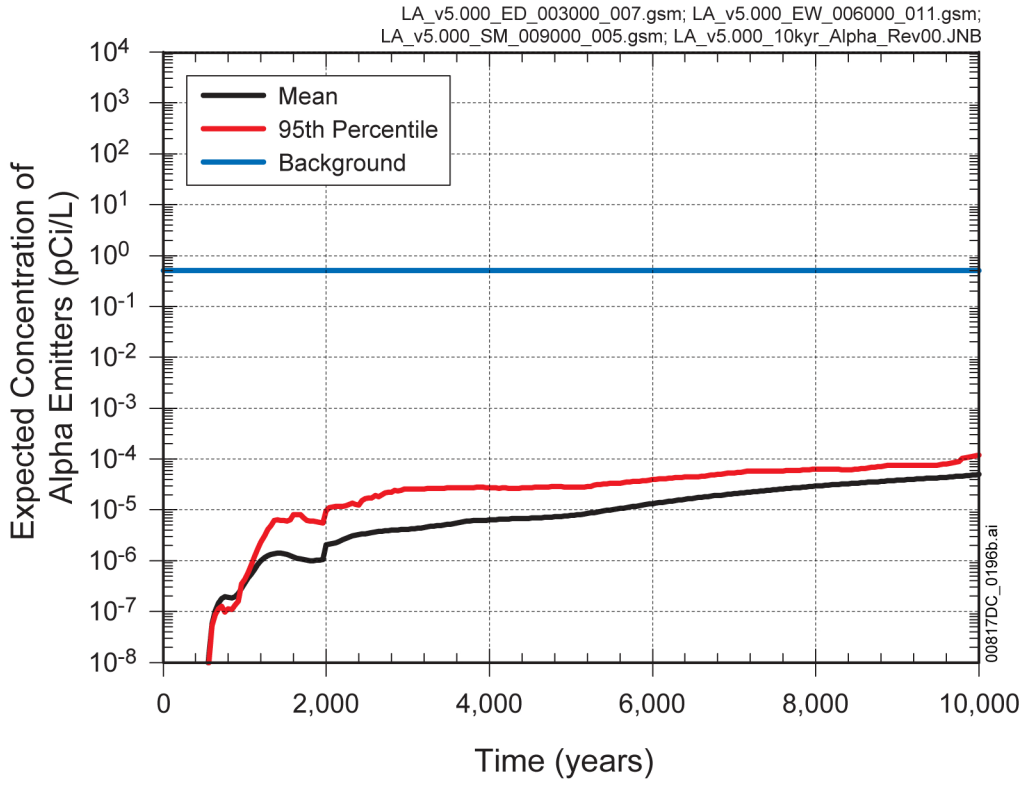

Source: Output DTN: MO0709TSPAREGS.000 [DIRS 182976].

Figure 8.1-10. Probabilistic Projections of Activity Concentration of Gross Alpha and ^{226}Ra (Excluding Radon and Uranium) in Groundwater for 10,000 Years after Closure

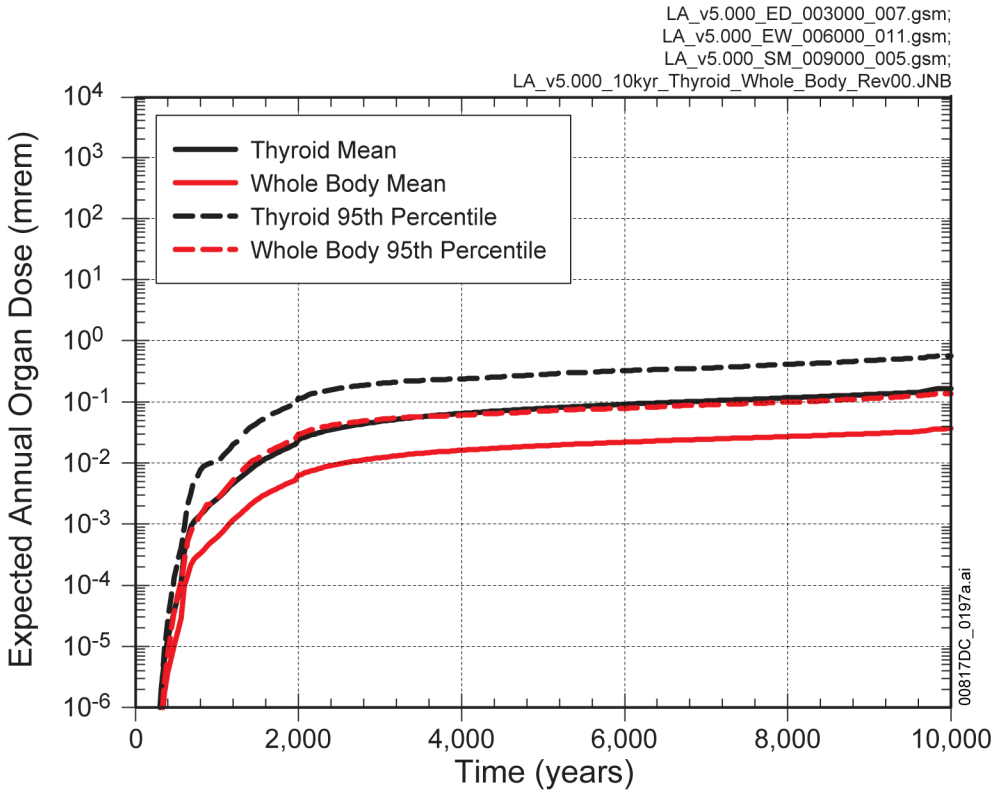

Source: Output DTN: MO0709TSPAREGS.000 [DIRS 182976].

Figure 8.1-11. Probabilistic Projections of Annual Drinking Water Doses for Combined Beta and Photon Emitting Radionuclides for 10,000 Years after Closure

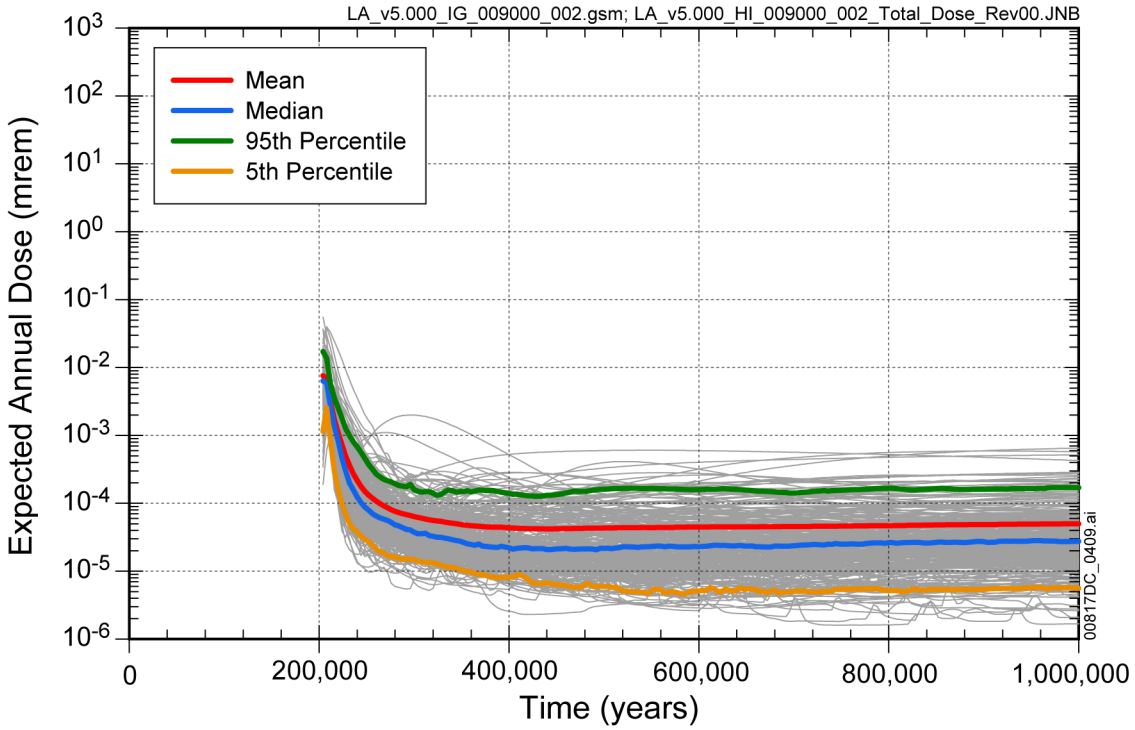

Source: Output DTN: MO0709TSPAREGS.000 [DIRS 182976].

Figure 8.1-12. Probabilistic Projections for Expected Annual Doses for the Human Intrusion Scenario for 1,000,000 Years after Closure with Drilling Event at 200,000 Years

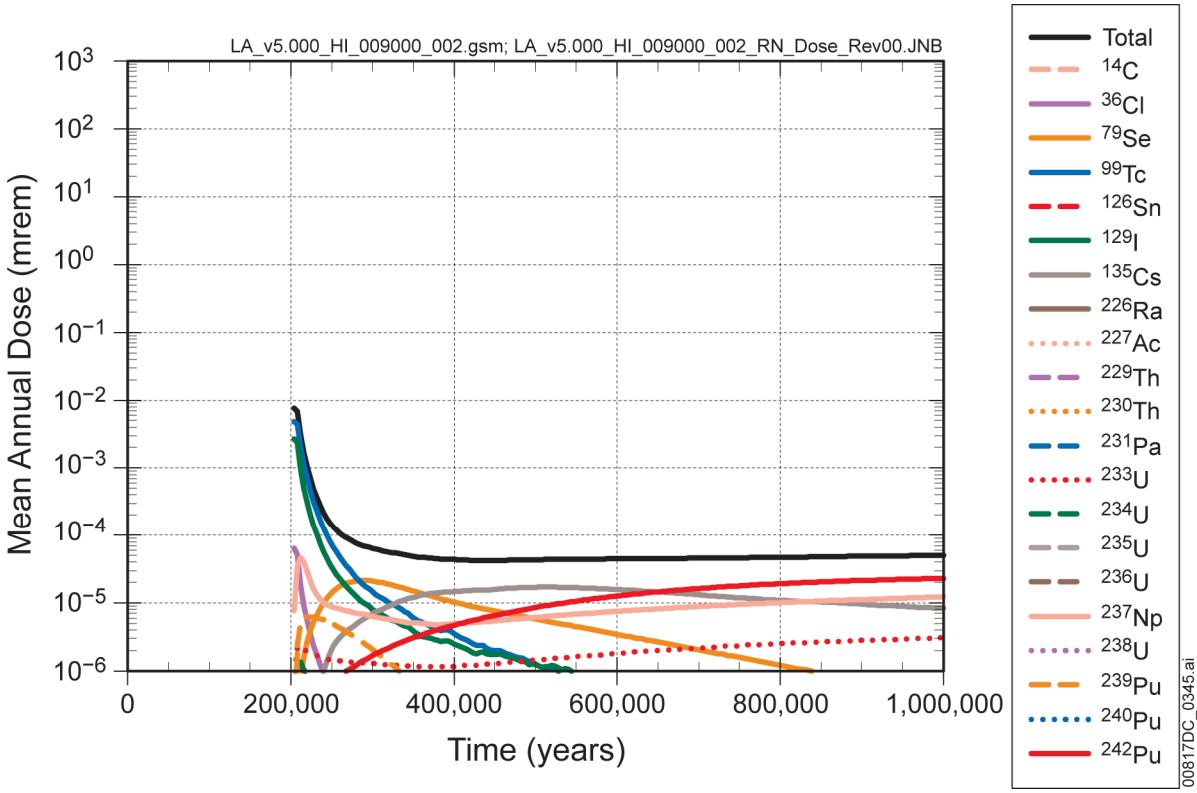

Source: Output DTN: MO0709TSPAREGS.000 [DIRS 182976].

Figure 8.1-13. Contribution of Individual Radionuclides to Mean Annual Dose for the Human Intrusion Scenario for 1,000,000 Years after Repository Closure

INTENTIONALLY LEFT BLANK

8.2 PROJECTIONS FOR INDIVIDUAL MODELING CASES

To clarify and help explain the performance demonstration for the EPA Individual Protection Standard, this section presents the probabilistic projections for the individual modeling cases. As indicated previously, the projections of total expected annual dose to the RMEI are based on a summation (Equation 8.1.1-1) of the expected annual doses over scenario modeling cases. The individual scenario class modeling cases include: (1) Nominal, (2) Waste Package EF, (3) Drip Shield EF, (4) Igneous Intrusion, (5) Volcanic Eruption, (6) Seismic GM, and (7) Seismic FD. As stated earlier, the Nominal Modeling Case is not explicitly included in the sum of total expected annual doses because it is embedded in the Seismic GM Modeling Case.

The performance projections presented herein for these modeling cases are organized in a manner so as to address the five fundamental performance questions identified earlier in Section 8.1. The supporting technical basis for the inferences and observations made regarding characteristics important to postclosure performance are also presented or cited. As will be explained in subsections that follow, the examination of the expected annual doses for the individual modeling cases leads to the following fundamental observations about relative importance of these modeling cases:

- Total mean annual doses to the RMEI for time periods after a few hundred years are largely dominated by Seismic GM and Igneous Intrusion Modeling Cases
- Mean annual doses for Waste Package EF and Seismic FD Modeling Cases are similar and estimated to contribute about 10^{-2} mrem or less to the total mean annual dose
- Mean annual doses for the Drip Shield EF and Volcanic Eruption Modeling Cases are estimated to contribute less than 10^{-3} mrem to the total mean annual dose.

For the 10,000-year period, the Seismic GM Modeling Case contributed about 71 percent and the Igneous Intrusion Modeling Case contributed about 27 percent of the peak total mean annual dose (i.e., 0.2 mrem). In contrast, for the post-10,000-year period, the Seismic GM and Igneous Intrusion Modeling Cases contributed almost equally to the peak total mean annual dose of 1 to 2 mrem.

For the Seismic GM Modeling Case, the important phenomenon is the accumulated WP damage induced by the vibratory ground motion. As indicated on Figure 8.1-5, the CDSP WPs, which contain the defense high-level waste (DHLW) glass and DOE spent nuclear fuel (DSNF), have a higher probability of failure from vibratory ground motion than the more robust CSNF WPs. The probabilistic projections for this modeling case are presented later in Section 8.2.4.

With regard to the Igneous Intrusion Modeling Case, it is important to understand that this particular modeling case represents the consequences of unlikely disruptive events with a mean annual frequency estimated to be 1.7×10^{-8} per year (Section 6.5.1.1). Moreover, the TSPA submodel for these phenomena assumes that all the 3,416 CDSP WPs and 8,213 CSNF WPs (Table 6.3.7-1) are completely failed by the hypothetical magmatic intrusion.

8.2.1 Nominal Modeling Case

The Nominal Scenario Class consists of a single modeling case that is a representation of a set of possible repository futures in which: (1) disruptive events and conditions and (2) DS and WP early failures are excluded. Moreover, the Nominal Modeling Case serves as a 'reference system state' from which all other modeling cases are developed. The system attributes for the Nominal Modeling Case are defined in terms of likely and unlikely FEPs that describe natural evolution of the natural and engineered barriers over geologic time frames, in the absence of disruptive events. That evolution includes changes in climate, infiltration and seepage into the drifts, exposure of the EBS components to water, progressive chemical degradation, and failure of the DSs and WPs, with eventual mobilization, release, and migration of radionuclides; this evolution of the reference state is included in the other modeling cases. The technical description for the representation of this nominal evolution is summarized in Section 6.3.

From a high-level point of view, this modeling case basically describes the evolution of the nuclear waste and repository system in the absence of disruptive events and processes. The system response for the Nominal Modeling Case is a function of a spectrum of processes:

1. Climate changes and attendant changes in net infiltration into the Upper Natural Barrier
2. Seepage of percolating water into the repository drifts
3. Changes to the water chemistry induced by repository heating
4. Progressive degradation of the engineered barriers by corrosion processes (i.e., general corrosion, localized corrosion, and stress corrosion cracking [SCC]) and failure
5. Accumulation of moisture inside the WPs, degradation and dissolution of the waste forms, and mobilization of the radionuclides
6. Migration of dissolved and colloidal-phase radionuclides from the EBS
7. Water flow and radionuclide transport through the Lower Natural Barrier and to the accessible environment
8. Water withdrawal and exposure to the RMEI.

The detailed technical basis (i.e., conceptual models, model abstractions, supporting data, and TSPA model parameter values and their uncertainty characterizations) for the Nominal Modeling Case is documented in numerous analysis and/or modeling reports.

The probabilistic projections of expected annual dose for this modeling case are shown on Figure 8.2-1. As can be seen from this plot, there are no doses to the RMEI in the 10,000-year regulatory time period. This is consistent with calculations for the EBS performance that indicate no realizations of DS failures in the 10,000-year time period (Section 8.1, Figure 8.1-4 and DTN: MO0709TSPAWPDS.000 [DIRS 183170]). With the DSs intact, the WPs would experience very little degradation by general corrosion in a humid-air environment.

The first realization with a failed (i.e., creation of a breach) CDSP or CSNF WP by nominal corrosion processes is projected to occur between 100,000 years to 150,000 years. The WP failure mechanism is typically SCC of the closure-lid welds. The extent of cracking gradually increases with time, leading to the ingress of moisture inside the WP and attendant diffusive radionuclide releases. Realizations with WP failures by corrosion penetrations through the Alloy 22 outer barrier are observed at about 450,000 years. By 1,000,000 years, approximately 60 percent of the WPs are projected to be failed by SCC and about 10 percent by general corrosion breaches. The projections indicate that the DSs are intact until about 270,000 years (Figure 8.1-4), with failure occurring by thinning of the 15-mm thick titanium DS (Section 6.3.5.1). All the DSs are projected to be completely failed by about 340,000 years.

The probabilistic projections for the post-10,000-year period indicate that there is no radiologic exposure until after about 140,000 years after closure. The peak mean and median annual doses for this reference modeling case are 0.5 mrem and 0.3 mrem, respectively. The peak mean annual dose at the RMEI location occurs at about 730,000 years, with two radionuclides dominating the peak annual dose. These radionuclides are the highly soluble, long-lived, and mobile radionuclide species ^{129}I and ^{99}Tc. The second order contributors to this peak dose value are ^{135}Cs and ^{79}Se (Figure 8.2-2). This peak is a modeling artifact driven by the time stepping and WP failure methodology but is similar to the overall peak at 1,000,000 years.

It is very important to differentiate the Nominal Modeling Case results from those for other modeling cases. The Nominal Modeling Case projection of mean annual dose should not be taken as a representation of compliance with radiation protection limits. The mean annual dose for the Nominal Modeling Case is not included in the calculation of the total mean annual doses for the 10,000-year period because there are no projected WP failures by nominal degradation processes in this time period. Rather, the effect of nominal DS and WP corrosion processes for the post-10,000-year period are accounted for in the Seismic GM Modeling Case. The Nominal Modeling Case only provides a reference system state for comparison with the other six modeling cases.

8.2.2 Early Failure Scenario Class Modeling Cases

The projections for early failure modeling cases demonstrate postclosure performance for conditions of DS and WP early failures. As described in Section 6.4, DS and WP early failures are generally attributed to the presence of undetected flaws (e.g., weld flaws and improper weld filler material) and manufacturing defects. Such undetected flaws and defects could possibly be introduced during manufacturing or construction of the barriers, or possibly during handling and emplacement (e.g., damaged welds). In the case of a DS, this type of defect would diminish the DS's ability to withstand the dynamic and static loadings; however, such defects are treated in the TSPA-LA Model as having failed immediately. Similarly, a WP with a defective closure-lid weld, for example, would lead to a shorter period of containment than for nominal performance, but also is treated as an immediate failure at the time of closure.

The DS and WP early failures were simulated in the TSPA-LA Model as a random process described by a Poisson distribution; thus, the number of failed DSs and WPs is a random variable and is sampled from applicable probability distributions (Sections 6.4.1 and 6.4.2). The

following information and calculations (Sections 6.4.1 and 6.4.2, Tables 6.4-1 and 6.4-2) are useful in developing risk insights to DS and WP early failures:

Drip Shield Early Failure

- Probability of 1 or more DS early failures: 0.0166
- Expected number of DS early failures: 0.0181
- Expected number of DS early failures conditional on one or more occurring: 1.09
- Mean probability of DS early failure: 1.56×10^{-6}

Waste Package Early Failure

- Probability of 1 or more WP early failures: 0.442
- Expected number of WP early failures: 1.09
- Expected number of WP early failures conditional on one or more occurring: 2.46
- Mean probability of WP early failure: 9.36×10^{-5}.

The results listed above are documented in output DTN: MO0707WPDRIPSD.000 [DIRS 183005].

For these two early failure modeling cases, the repository system response is developed by applying the process models described for the Nominal Modeling Case to the DSs and WPs that are affected by early failure. Generally speaking, the two early failure modeling cases describe the repository system response as a function of:

1. Changes of climate states, net infiltration, seepage into the drift, and water chemistry as represented in the Nominal Modeling Case (except no degradation of WPs by corrosion)

2. Total number of DS early failures in each realization

3. Total number of CDSP WP and CSNF WP early failures in each realization

4. Ingress of water to the failed WPs, mobilization, and the eventual release of radionuclides from the EBS

5. Water flow and transport of dissolved and colloidal phase radionuclides through the Lower Natural Barrier and to the accessible environment

6. Water withdrawal and radiologic exposure at the RMEI location.

It is important to emphasize that WPs associated with early failed DSs are also assumed to be failed in the TSPA-LA Model. The associated radionuclide releases from these early failed DSs and WPs are assumed to occur at the time of repository closure.

The models and TSPA methodology used to simulate the occurrence of early failures and their impacts on the performance of the affected WPs and DSs are presented in Section 6.4. Section 6.4 also summarizes the supporting technical basis for the abstraction of early failures.

Model parameter values and their uncertainty characterizations are documented in *Analysis of Mechanisms for Early Waste Package/Drip Shield Failure* (SNL 2007 [DIRS 178765]).

8.2.2.1 Drip Shield Early Failure Modeling Case

As indicated by probabilistic analysis of early failures, the total number of DS early failures is estimated to be very small. For example, the probability of three or more DS early failures is about 2×10^{-4} (Table 6.4-1). As implemented in the TSPA-LA Model, the DS early failures are accounted for by simply removing the DS as a barrier to seepage for a given realization. In its implementation, the number of 'n' failed DSs means that the associated 'n' WPs are also assumed to have failed; thus, 'n' failed DSs define the inventory at risk for this modeling case.

The expected annual dose histories for the Drip Shield EF Modeling Case are shown in Figure 8.2-3; this plot shows multi-realization projections for both the (a) 10,000-year period after closure, and (b) post-10,000 years to 1,000,000 years. The mean, median, and 5th and 95th percentile curves are superimposed on the plot to illustrate the central tendency and uncertainty. The uncertainty or spread reflects the epistemic uncertainty in the TSPA-LA Model parameters and representation of the evolution of the future conditions. The projections for the first 10,000 years show an early peak around 1,000 years (not the peak annual dose for the time period, however), which is primarily due to contribution from early failed CDSP WPs (see Section 7.7.1.1). Because the CDSP WPs produce less decay heat than the CSNF WPs, the relative humidity in the CDSP WP emplacement locations goes above 95 percent and diffusive transport of radionuclide starts before 10,000 years. The peak mean and median annual doses of about 3×10^{-4} mrem and 4×10^{-5} mrem, respectively, occur at approximately 2,000 years; the mean and median annual doses decline thereafter and drop to about 4×10^{-5} mrem and 7×10^{-6} mrem, respectively, at 10,000 years. The abrupt increase in the dose histories at 2,000 years is due to the change in the climate (monsoonal to glacial transition). In the post-10,000-year period, the figure shows a second peak occurring at about 40,000 years with a mean of $\sim 10^{-4}$ mrem and median of $\sim 10^{-5}$ mrem.

The primary radionuclides that contribute to the mean annual dose for the Drip Shield EF Modeling Case are shown on Figure 8.2-4. In the first 2,000 years after repository closure, three soluble and mobile radionuclides dominate dose: ^{99}Tc, ^{129}I, and ^{14}C. From 2,000 years to 10,000 years, the ^{14}C drops in importance and is replaced by ^{239}Pu. At the outset of the post-10,000-year period, the mean annual dose is dominated by ^{239}Pu and ^{99}Tc. The radionuclide ^{239}Pu creates the secondary peak mean annual dose at about 40,000 years, but diminishes in importance by about 200,000 years due to radionuclide decay. From that point forward, ^{242}Pu, ^{237}Np, and ^{226}Ra dominate the mean annual doses.

8.2.2.2 Waste Package Early Failure Modeling Case

From the probabilistic analysis of early failures, the number of WP early failures is estimated to be relatively small. For example, the probability of three or more WP early failures is about 0.12 (Table 6.4-1). As implemented in the TSPA-LA Model, the WP early failure is conceptualized as complete failure with respect to radionuclide containment (Section 6.4.2.2), at the time of repository closure. The overlying DS is not affected by the early failure of the WP. The number of early failed WPs defines the radionuclide source term for this modeling case. The

radionuclide releases from these WP early failures occur by diffusive transport from the waste form with sorbing radionuclides delayed by sorption on corrosion products (Section 6.3.8).

The expected annual dose histories for this modeling case are shown in the multi-realization projections in Figure 8.2-5 for both the (a) 10,000-year period after closure, and (b) post-10,000 years. The expected annual doses account for aleatory uncertainties associated with characteristics of the early failed WPs, such as the number of early failed WPs, type of early failed WPs (CDSP or CSNF), and their locations in the repository. The mean, median, and 5th and 95th percentile curves are shown on Figure 8.2-5 to highlight the uncertainty in the expected annual doses.

For the first 10,000 years after repository closure, there is an initial peak between 1,000 and 2,000 years which is primarily due to contribution from early failed CDSP WPs. Because the CDSP WPs produce less decay heat than the CSNF WPs, the relative humidity in the CDSP WP emplacement locations goes above 95 percent and diffusive transport of radionuclides starts. The abrupt jump in the dose histories at 2,000 years is due to the change in the climate state (monsoonal to glacial transition). Between 9,000 and 10,000 years, the dose histories increase with the peak mean and median annual doses estimated to be about 4×10^{-3} mrem and 2×10^{-4} mrem. This peak is due to the early failed CSNF WPs, which have cooled and have relative humidity environments that promote diffusive transport. For post-10,000 years, the peak mean and median annual doses reach levels of approximately 2×10^{-2} mrem and 4×10^{-3} mrem, respectively, at about 12,000 years and then gradually decline. At about 260,000 years the mean annual dose curve again ascends forming one last broad peak at about 450,000 years; the onset of this increase coincides with the onset of DS failures by general corrosion at about 270,000 years (Figure 8.1-4) and, in turn, seepage directly onto the early failed WPs. The mean and median doses at one million years are about 1×10^{-3} mrem and 2×10^{-4} mrem, respectively.

The major radionuclides that contribute to the mean annual dose for the Waste Package EF Modeling Case are shown on Figure 8.2-6. In the first 10,000 years postclosure, soluble and mobile radionuclides, in particular, ^{99}Tc, ^{14}C, and ^{129}I, dominate the estimate of mean annual dose. In the post-10,000-year period, after ^{99}Tc and ^{129}I decline, the peak mean annual dose is dominated by ^{239}Pu up to about 200,000 years; thereafter, ^{242}Pu, ^{226}Ra, and ^{237}Np are the primary contributors to the peak mean annual dose.

8.2.3 Igneous Scenario Class Modeling Cases

The projections for the Igneous Scenario Class demonstrate postclosure performance for unlikely igneous events and processes that could disrupt the repository system. As noted earlier, the estimated annual frequency of igneous activity at the repository site is 1.7×10^{-8} /yr (Section 6.5.1.1). This frequency is just slightly greater than the NRC frequency of 10^{-8} /yr for very unlikely events and processes, which are excluded from the performance demonstration for the LA by regulation (10 CFR 63.342 [DIRS 178394]). As described in Section 6.5, the Igneous Scenario Class consists of two modeling cases: (1) the Igneous Intrusion Modeling Case that represents the interaction of a hypothetical intrusive magma with the repository and attendant release of radionuclides to the groundwater pathway, and (2) the Volcanic Eruption Modeling Case that represents a hypothetical volcanic eruption at the land surface and the release of radionuclides to the atmospheric pathway.

8.2.3.1 Igneous Intrusion Modeling Case

In this modeling case, a simulated magmatic dike intersects the footprint of the repository causing failure of the EBS. Radionuclide releases that are attributed to the intrusion, and are transported away from the repository, are analyzed in a manner analogous to that for the Nominal Modeling Case, but differ in the conceptualization of the EBS failure. There are two main components to the model: (1) the behavior of the WPs and other EBS elements damaged by an igneous intrusion, and (2) groundwater flow and radionuclide transport away from the WPs. For the purposes of ensuring conservatism in the annual doses to the RMEI, the modeling case assumes that all the WPs in the repository are completely destroyed, exposing the waste forms to percolating groundwater with subsequent degradation, radionuclide mobilization, and transport.

Radionuclide transport occurs through the invert and into the UZ, depending on solubility limits and the rate of water flux through the intruded drifts. It is assumed that the drifts do not act as a capillary barrier, and the seepage water flux into a magma-intruded drift is equal to the percolation flux in the overlying host rock. No barrier performance credit is taken for water diversion by the remnants of the DS or WP, and cladding is assumed to be fully degraded. Because the thermal, chemical, hydrological, and mechanical conditions in the drift following igneous intrusion are uncertain, the EBS is assumed to be completely failed.

The expected annual dose histories for the Igneous Intrusion Modeling Case are shown in Figure 8.2-7 for both the (a) 10,000-year period and (b) post-10,000-year period. The mean, median, and 5th and 95th percentile curves are displayed on a multi-realization plot. The expected annual dose to the RMEI takes into account aleatory uncertainty associated with characteristics of the igneous intrusion, such as the number of future events and the time at which they may occur. These figures indicate that the peak mean annual dose to the RMEI for the 10,000-year time period is less than 0.1 mrem and for the post-10,000-year time period is about 1.3 mrem. The median annual dose at 1,000,000 years is about 0.4 mrem.

The radionuclides that contribute most to the mean annual dose are shown on Figure 8.2-8. Figure 8.2-8a shows that radionuclides ^{99}Tc and ^{129}I dominate the estimate of the mean for the first 4,000 years and ^{239}Pu, ^{99}Tc, and ^{240}Pu dominate the estimate of the mean for the remainder of the 10,000-year postclosure period. Figure 8.2-8b shows that ^{239}Pu, which is transported both in dissolved and colloidal form, dominates the peak mean annual dose for the first 200,000 years and radionuclides ^{242}Pu, ^{237}Np, and ^{226}Ra dominate the estimate of the mean for the remainder of the post-10,000-year time period.

8.2.3.2 Volcanic Eruption Modeling Case

In this modeling case, the disruption is conceptualized as a volcanic eruptive conduit intersecting the repository footprint resulting in the dispersal of waste-contaminated tephra in the atmosphere, with attendant deposition of contaminated ash on the land surface. The performance projections evaluate the post-eruption consequences due to waste redistributed from upstream in the Fortymile Wash watershed and deposited at the RMEI location. WPs in the direct path of the conduit are assumed to be destroyed and entrained into the hypothetical eruption. As described in Section 6.3.11, the radiologic exposure scenario is that the RMEI exposure arises from

contaminated volcanic ash deposited on surface soil and the subsequent radionuclide transport from surface soil to other environmental media (e.g., air and plants).

As noted in Section 6.5.2.1.1, the probabilistic calculations of igneous disruptions indicate that there is about a 70 percent probability that no WPs would be hit by a volcanic conduit intersecting the repository. The small conduit diameters relative to drift spacing implies that 70 percent of the conduits potentially intersecting the repository footprint would intersect between drifts and therefore not impact any WPs. In the 30 percent of the realizations in which one or more packages are intersected, the most likely number hit is four and the maximum number hit is seven.

The expected annual dose histories for this modeling case are shown on Figure 8.2-9 for both the (a) 10,000-year period and (b) post-10,000-year period. The expected annual dose takes into account aleatory uncertainty associated with characteristics of the eruption such as number of WPs intersected by the eruption, the fraction of waste-containing magma ejected in the atmosphere, eruption power, wind direction, and wind speed. The mean, median, and 5th and 95th percentile curves on Figure 8.2-9 show uncertainty in the value of the expected annual dose, taking into account epistemic uncertainty associated with incomplete knowledge of the behavior of the physical system during and after the disruptive event. These figures show that the mean annual dose for 10,000 years postclosure is about 1×10^{-4} mrem and is largely uniform for the post-10,000-year time period with the peak mean less than 2×10^{-4} mrem. The median annual dose is less than 6×10^{-5} mrem at 1,000,000 year.

The radionuclides contributions to the mean annual dose are shown on Figure 8.2-10. Because transport of radionuclides to the location of the RMEI is more rapid in the Volcanic Eruption Modeling Case than in the Igneous Intrusion Modeling Case, radionuclides with short half-lives are able to contribute to the estimate of the mean annual dose estimate. Examples of two short-lived radionuclides are ^{137}Cs and ^{238}Pu, which make significant contributions to the dose at early times, but their contributions drop off rapidly because of radioactive decay. At 300 years, ^{241}Am dominates the total, but its contribution rapidly diminishes after about 1,000 years, also due to radioactive decay. These short-lived radionuclides are able to reach the location of the RMEI before they decay because atmospheric transport to this location is relatively rapid. After 1,000 years, ^{239}Pu and ^{240}Pu are the dominant contributors until approximately 100,000 years; thereafter ^{226}Ra, ^{229}Th, and ^{237}Np become the dominant contributors out to 1,000,000 years.

8.2.4 Seismic Scenario Class Modeling Cases

The probabilistic projections for the Seismic Scenario Class demonstrate postclosure performance for likely and unlikely seismic events. As described in Section 6.6, the Seismic Scenario Class consists of two modeling cases: (1) Seismic GM Modeling Case, and (2) Seismic FD Modeling Case. These modeling cases take into account the aleatory uncertainty of the timing of these events, effects of the seismic events on DSs and WPs, and attendant radionuclide releases. This scenario class also takes into account changes in seepage, WP degradation, and flow in the EBS, as well as the conditions associated with the nominal evolution of the repository system. The likelihood and intensity/magnitude of these seismic events are defined by hazard curves, which were developed as part of the probabilistic seismic hazard analysis (CRWMS M&O 1998 [DIRS 103731]).

8.2.4.1 Seismic Ground Motion Modeling Case

The Seismic GM Modeling Case focuses on postclosure performance as a function of disruptions caused by vibratory ground motion. As described in Section 6.6.1, the likelihood and intensity of ground motion is defined by the mean seismic hazard curve (i.e., relation of peak ground velocities to exceedance frequencies (Figure 6.6-6)). Depending on the timing, sequence, and intensity of the ground motion events, the DSs and WPs can accumulate damage and/or fail. In the case of the DSs, seismic ground motion could cause damage or failure by dynamic loading and/or static loading by rockfall resulting in bucking or rupture (Section 6.6.1.1.2). Similarly, the WPs could be damaged or fail by: (1) local strain that exceeds ultimate tensile strength, (2) deformations creating residual stresses that induce SCC, and (3) lithostatic loading from rubble that causes a puncture of the outer barrier by the WP internals (Section 6.6.1.1.2). Both the DSs and WPs are also degraded by the general corrosion (Section 6.6.2.3). The number of failed CDSP and CSNF WPs determine the source term for the radionuclide transport calculations and projections of expected annual dose to the RMEI.

The expected annual dose histories for the Seismic GM Modeling Case are shown on Figure 8.2-11; multi-realization projections are presented for both the (a) 10,000-year period, and (b) post-10,000-year period. The expected annual dose histories take into account aleatory uncertainty associated with characteristics of future events such as number of events, times of events, and the peak ground velocity of the event. The mean, median, and 5th and 95th percentile curves on Figure 8.2-11 show uncertainty in the value of the expected annual dose, taking into account epistemic uncertainty associated with the incomplete knowledge of the behavior of the physical system during and after the disruptive event. These figures show that the mean annual dose for 10,000 years postclosure is less than 0.2 mrem, while for the post-10,000-year period it is less than 2 mrem. The median annual dose at one million years is less than 0.5 mrem.

The radionuclides that contribute most to the estimate of mean annual dose for this modeling case are presented on Figure 8.2-12. The mean dose curves on Figure 8.2-12a illustrate that three radionuclides, ^{99}Tc, ^{14}C, and ^{129}I, contribute the most to the peak mean annual dose for the 10,000-year time period; during this time period CDSP WPs are the primary containers damaged because the CSNF WPs are much more resistant to seismic damage. The predominant mechanism causing damage to the CDSP WPs and CSNF WPs consisted of small cracks that result in releases from the WPs by diffusion. As can be seen on Figure 8.2-12b, the dominant radionuclides contributing to the peak at approximately 230,000 years are ^{99}Tc, ^{129}I, and ^{79}Se. From 200,000 years to about 800,000 years, the dominant radionuclides are ^{99}Tc, ^{129}I, ^{226}Ra, ^{135}Cs, and ^{242}Pu. After 800,000 years, ^{242}Pu, ^{129}I, and ^{237}Np are the three major contributors to the mean annual dose for this modeling case.

8.2.4.2 Seismic Fault Displacement Modeling Case

The Seismic FD Modeling Case demonstrates postclosure performance as a function of disruptions caused by fault displacement. As described in Section 6.6.1, the characterization of the fault is based on data from known faults in the vicinity of the site area. The disruption in this modeling case is conceptualized as a sudden discontinuity in the profile of the repository. The location and magnitude of the fault displacement determines the number of DSs and WPs that

are disrupted. A mean displacement hazard curve provides the basis for calculating the magnitude of the simulated fault displacement. The WPs are presumed to be sheared if the displacement exceeds a threshold value. As noted in Section 6.6.1.2.3, damage of the DSs and WPs by fault displacement is not expected to occur if the mean annual frequency is greater than 2.5×10^{-7}/yr.

The expected annual dose histories for the Seismic FD Modeling Case are shown on Figure 8.2-13; the figure shows expected annual dose to the RMEI for both the (a) 10,000-year period, and (b) post-10,000-year period. The expected annual dose takes into account aleatory uncertainty associated with characteristics associated with the number of DSs and WPs disrupted. The mean, median, and 5th and 95th percentile curves on Figure 8.2-13 show uncertainty in the value of the expected annual dose, taking into account epistemic uncertainty associated with incomplete knowledge of the behavior of the physical system during and after the disruptive event. These figures show that the mean annual dose for 10,000 years postclosure is less than 2×10^{-3} mrem and for 1,000,000 years postclosure less than 2×10^{-2} mrem. The peak median annual dose for the 1,000,000-year time period is approximately 10^{-2} mrem.

The contribution of individual radionuclides to mean annual dose are shown in the results presented on Figure 8.2-14 for both the 10,000-year and post-10,000-year period after closure. The plot for the 10,000-year period (Figure 8.2-14(a)) shows that ^{99}Tc and ^{129}I dominate the dose for the first 4,000 years after closure, and ^{99}Tc, ^{239}Pu, ^{129}I, and ^{240}Pu are the dominant radionuclides contributing to dose at 10,000 years. As can be noted from Figure 8.2-14b, ^{239}Pu dominates the mean annual doses up to about 200,000 years; thereafter, the radionuclides ^{242}Pu, ^{226}Ra, and ^{237}Np remain dominant contributors for the remainder of the 1,000,000 years.

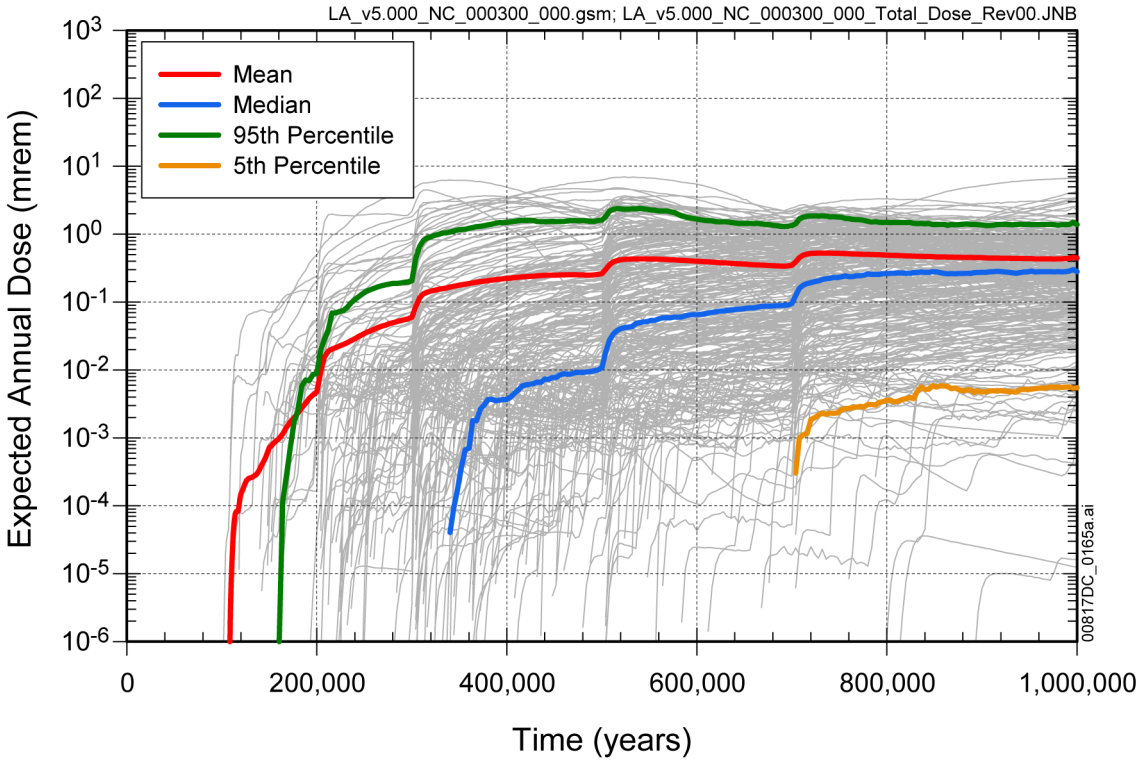

Source: Output DTN: MO0709TSPAREGS.000 [DIRS 182976]

Figure 8.2-1. Probabilistic Projections of Expected Annual Dose for the Nominal Modeling Case for 1,000,000 Years after Repository Closure

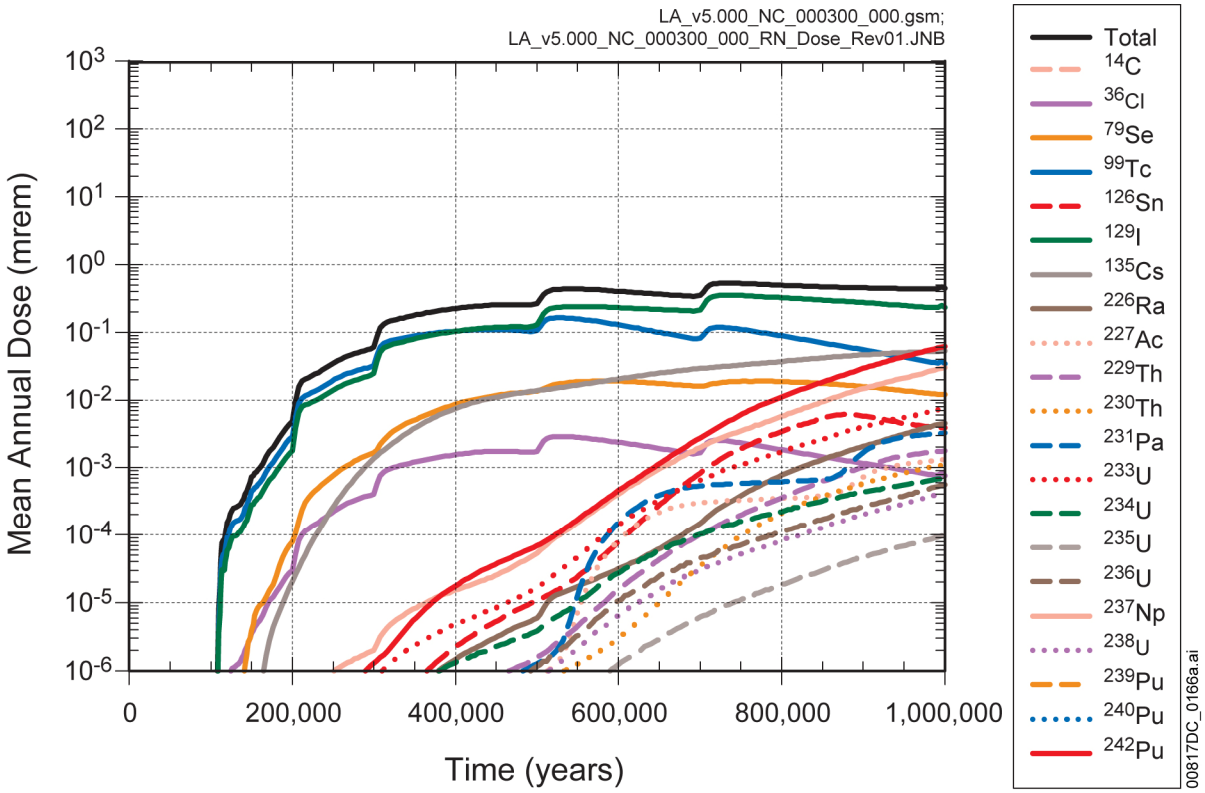

Source: Output DTN: MO0709TSPAREGS.000 [DIRS 182976]

Figure 8.2-2. Contribution of Individual Radionuclides to Mean Annual Dose for the Nominal Modeling Case for 1,000,000 Years after Repository Closure

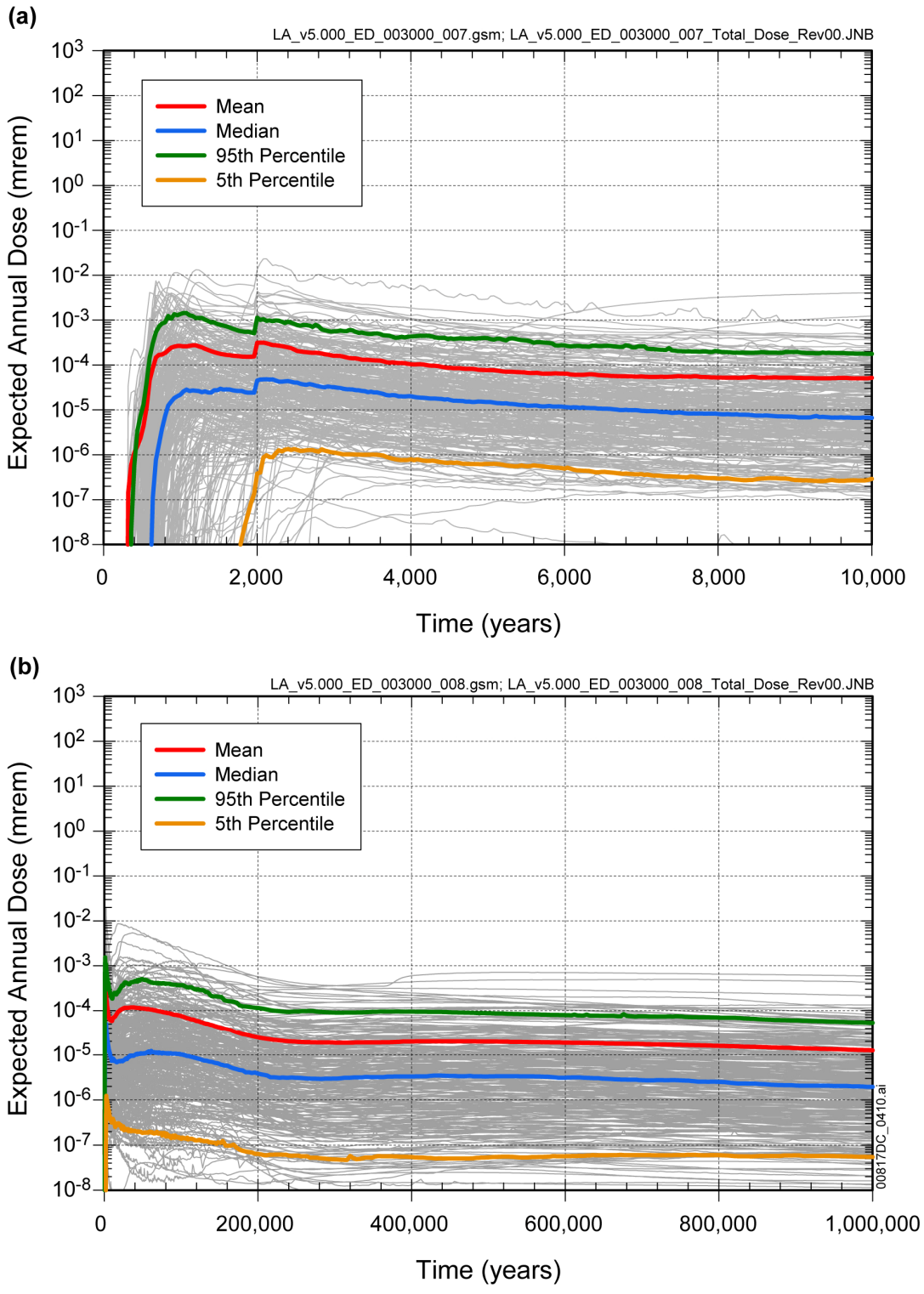

Source: Output DTN: MO0709TSPAREGS.000 [DIRS 182976]

Figure 8.2-3. Probabilistic Projections of Expected Annual Dose for the Drip Shield Early Failure Modeling Case for (a) 10,000 Years and (b) 1,000,000 Years after Repository Closure

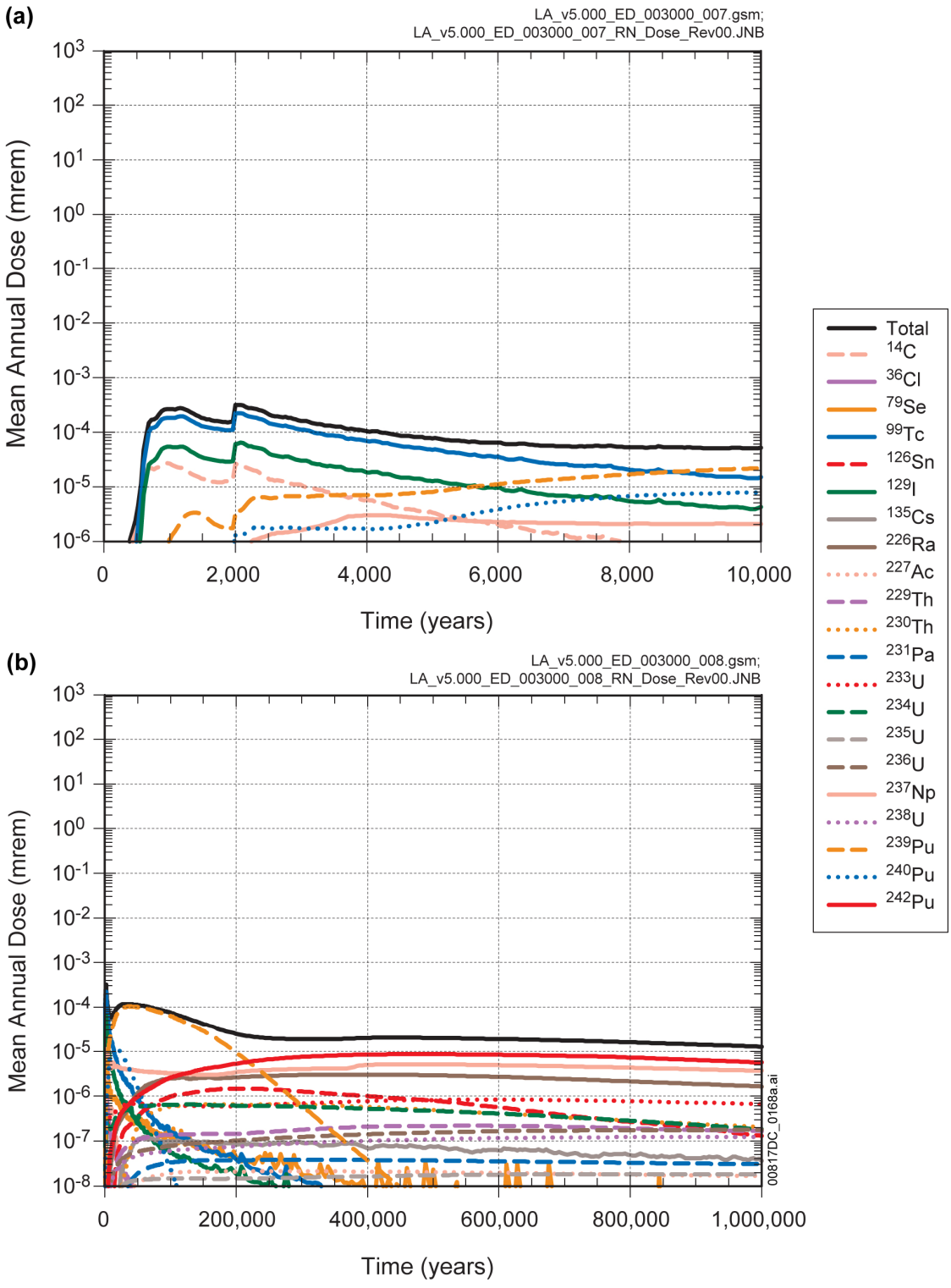

Source: Output DTN: MO0709TSPAREGS.000 [DIRS 182976]

Figure 8.2-4. Contribution of Individual Radionuclides to Mean Annual Dose for Drip Shield Early Failure Modeling Case for (a) 10,000 Years and (b) 1,000,000 Years After Repository Closure

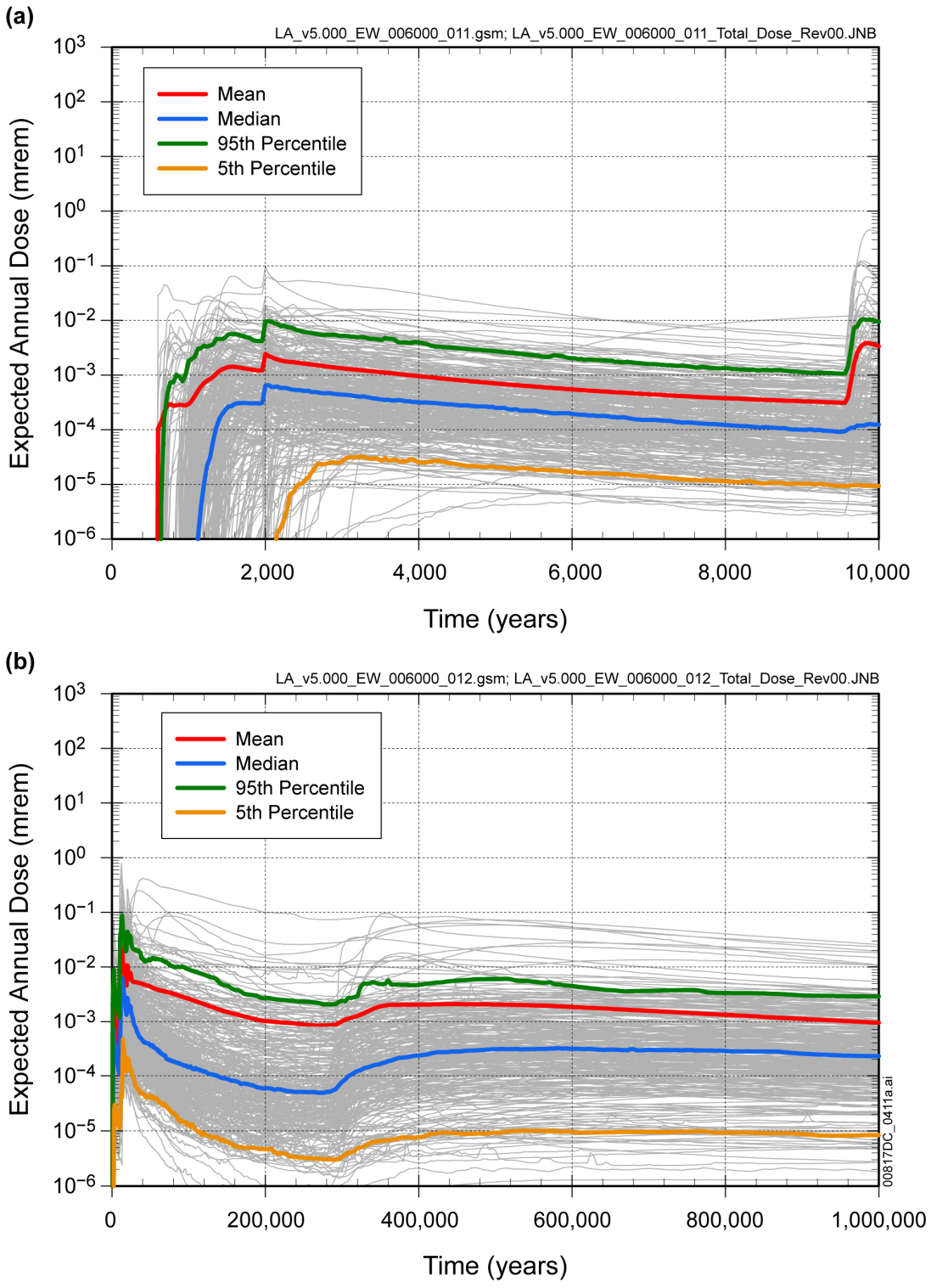

Source: Output DTN: MO0709TSPAREGS.000 [DIRS 182976]

Figure 8.2-5. Probabilistic Projections of Expected Annual Dose for Waste Package Early Failure Modeling Case for (a) 10,000 Years and (b) 1,000,000 Years after Repository Closure

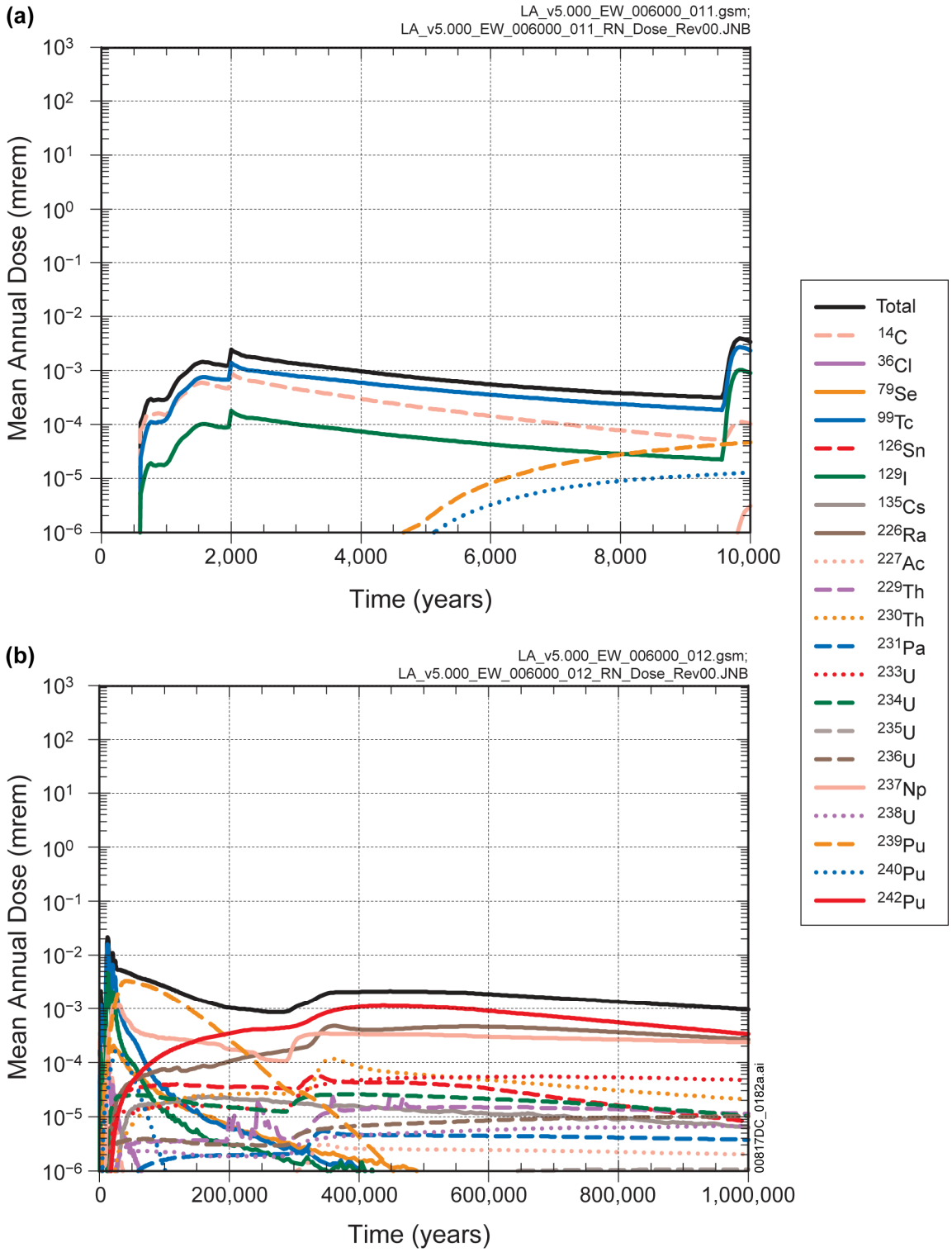

Source: Output DTN: MO0709TSPAREGS.000 [DIRS 182976]

Figure 8.2-6. Contribution of Individual Radionuclides to Mean Annual Dose for Waste Package Early Failure Modeling Case for (a) 10,000 Years and (b) 1,000,000 Years after Repository Closure

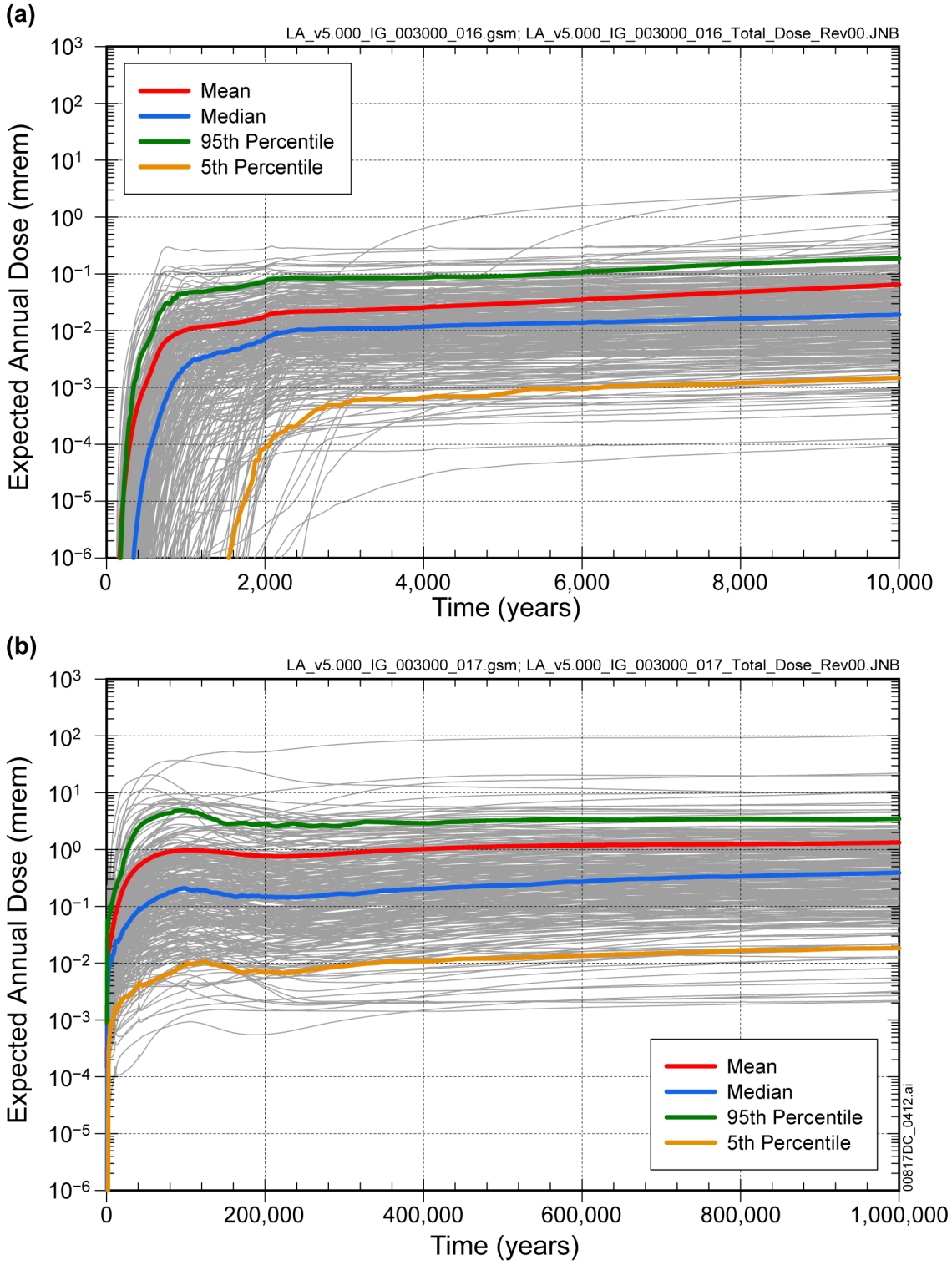

Source: Output DTN: MO0709TSPAREGS.000 [DIRS 182976]

Figure 8.2-7. Probabilistic Projections of Expected Annual Dose for the Igneous Intrusion Modeling Case for (a) 10,000 Years and (b) 1,000,000 Years after Repository Closure

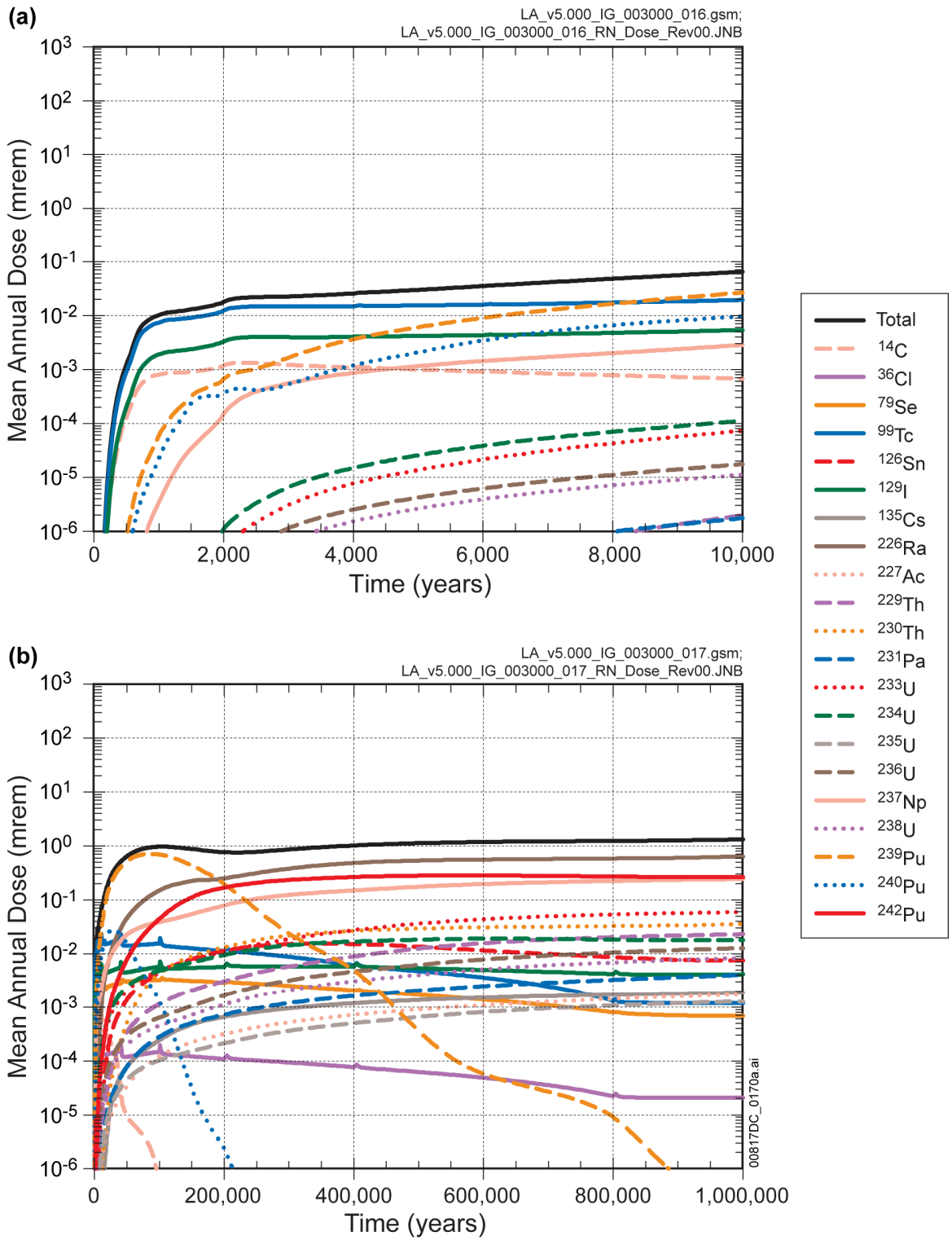

Source: Output DTN: MO0709TSPAREGS.000 [DIRS 182976]

Figure 8.2-8. Contribution of Individual Radionuclides to Mean Annual Dose for the Igneous Intrusion Modeling Case for (a) 10,000 Years and (b) 1,000,000 Years After Repository Closure

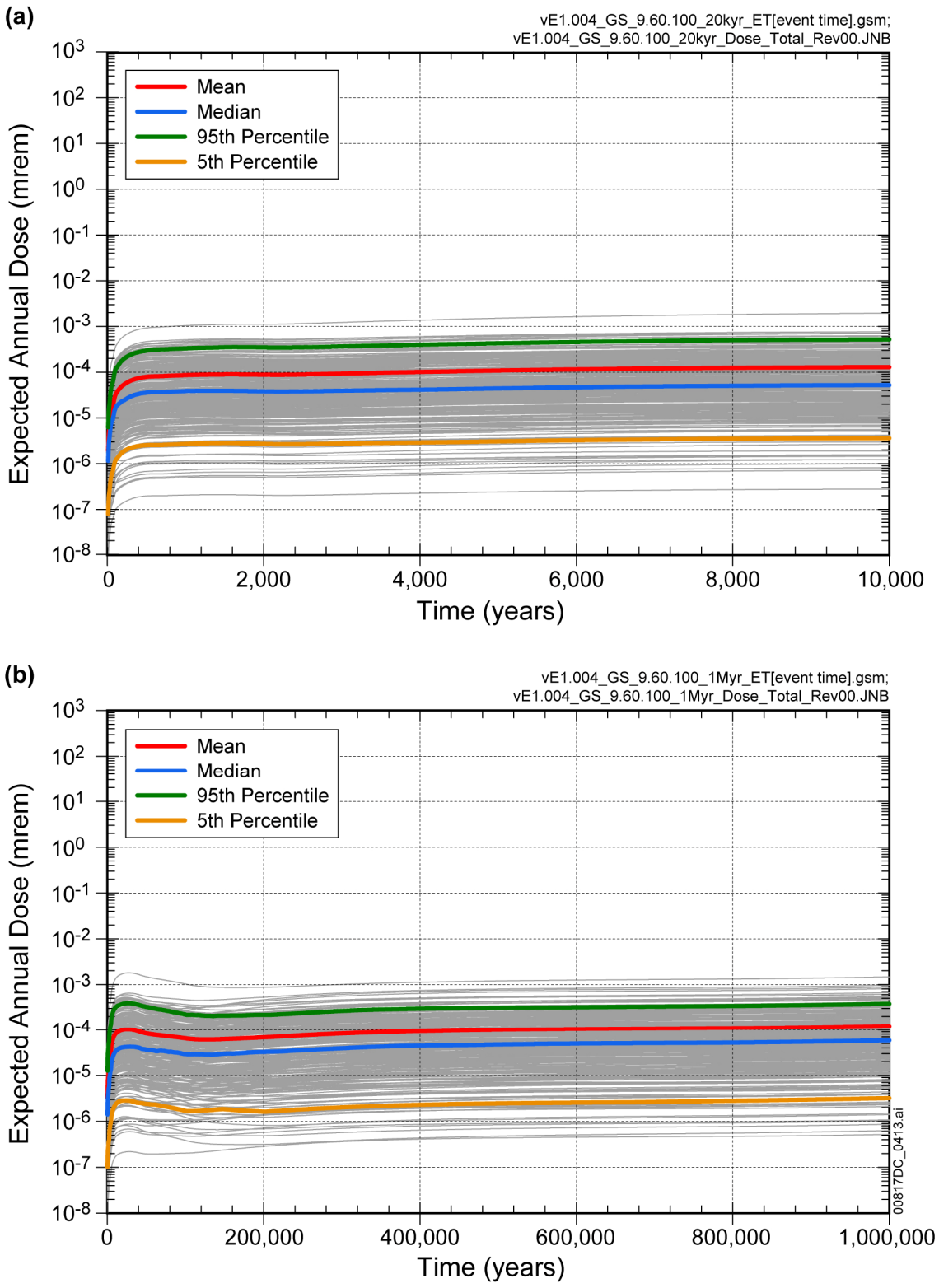

Source: Output DTN: MO0709TSPAREGS.000 [DIRS 182976]

Figure 8.2-9. Probabilistic Projections of Expected Annual Dose for the Volcanic Eruption Modeling Case for (a) 10,000 Years and (b) 1,000,000 Years after Repository Closure

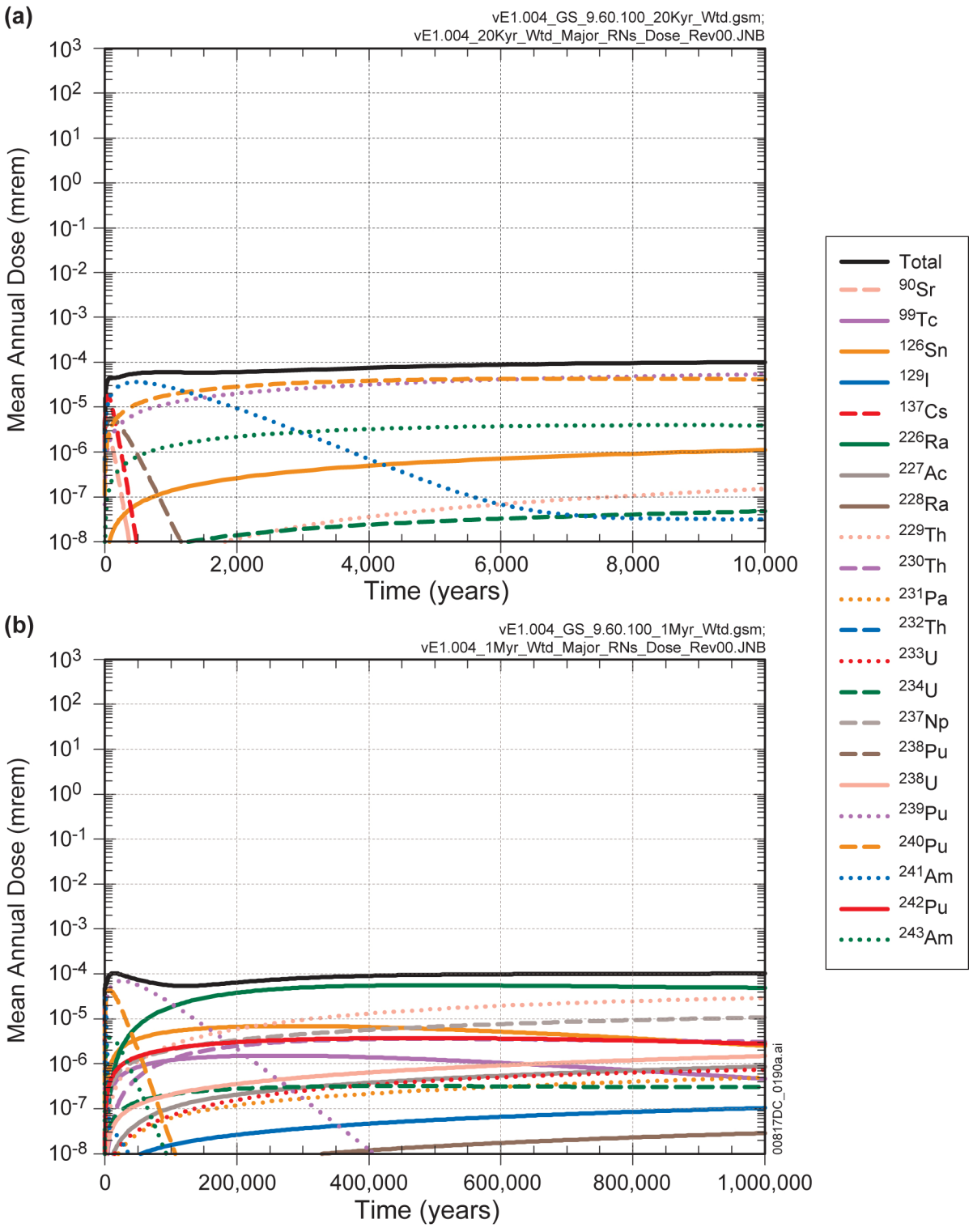

Source: Output DTN: MO0709TSPAREGS.000 [DIRS 182976]

Figure 8.2-10. Contribution of Individual Radionuclides to Mean Annual Dose for the Volcanic Eruption Modeling Case for (a) 10,000 Years and (b) 1,000,000 Years after Repository Closure

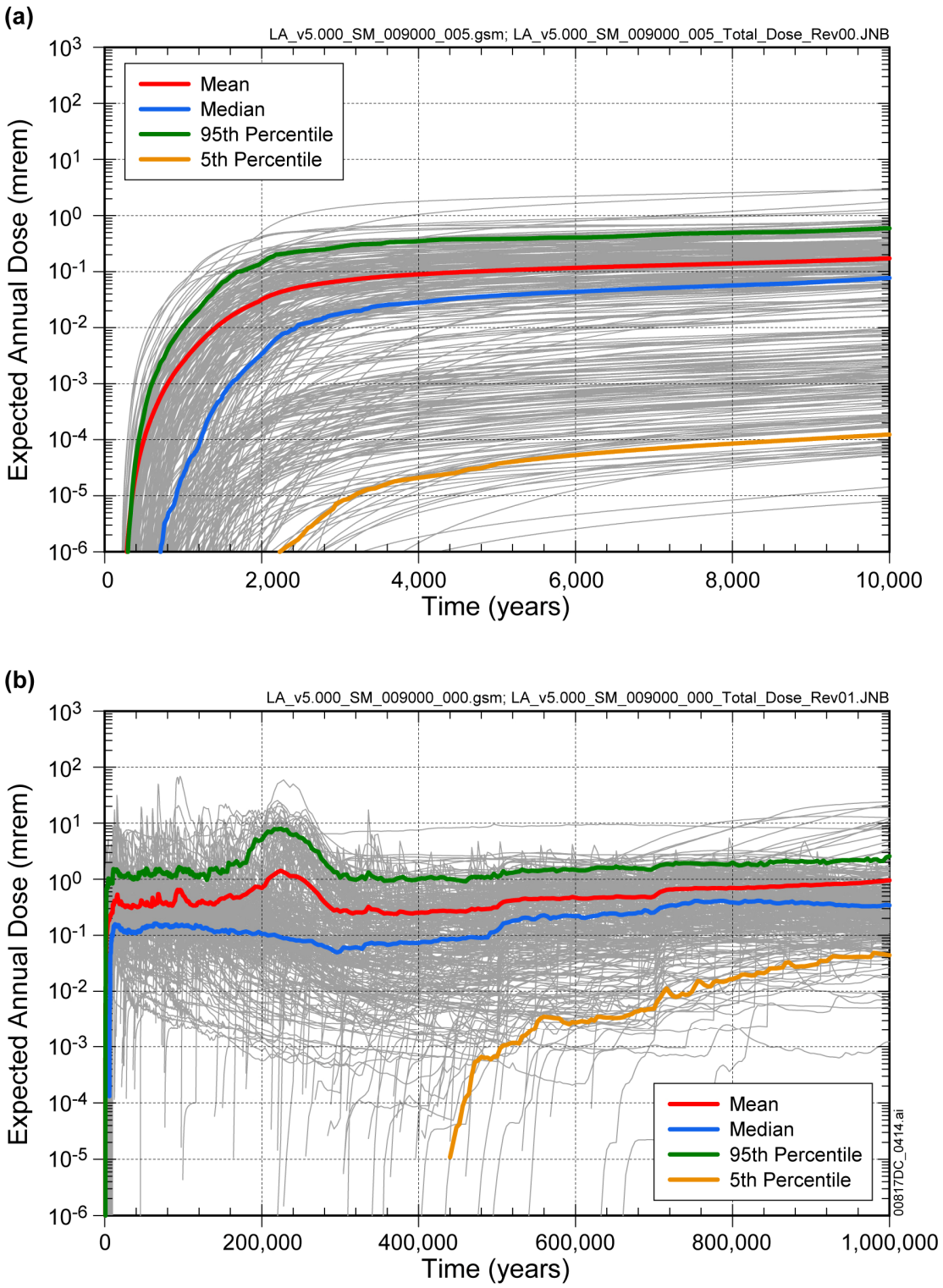

Source: Output DTN: MO0709TSPAREGS.000 [DIRS 182976]

Figure 8.2-11. Probabilistic Projections of Expected Annual Dose for the Seismic Ground Motion Modeling Case for (a) 10,000 Years and (b) 1,000,000 Years after Repository Closure

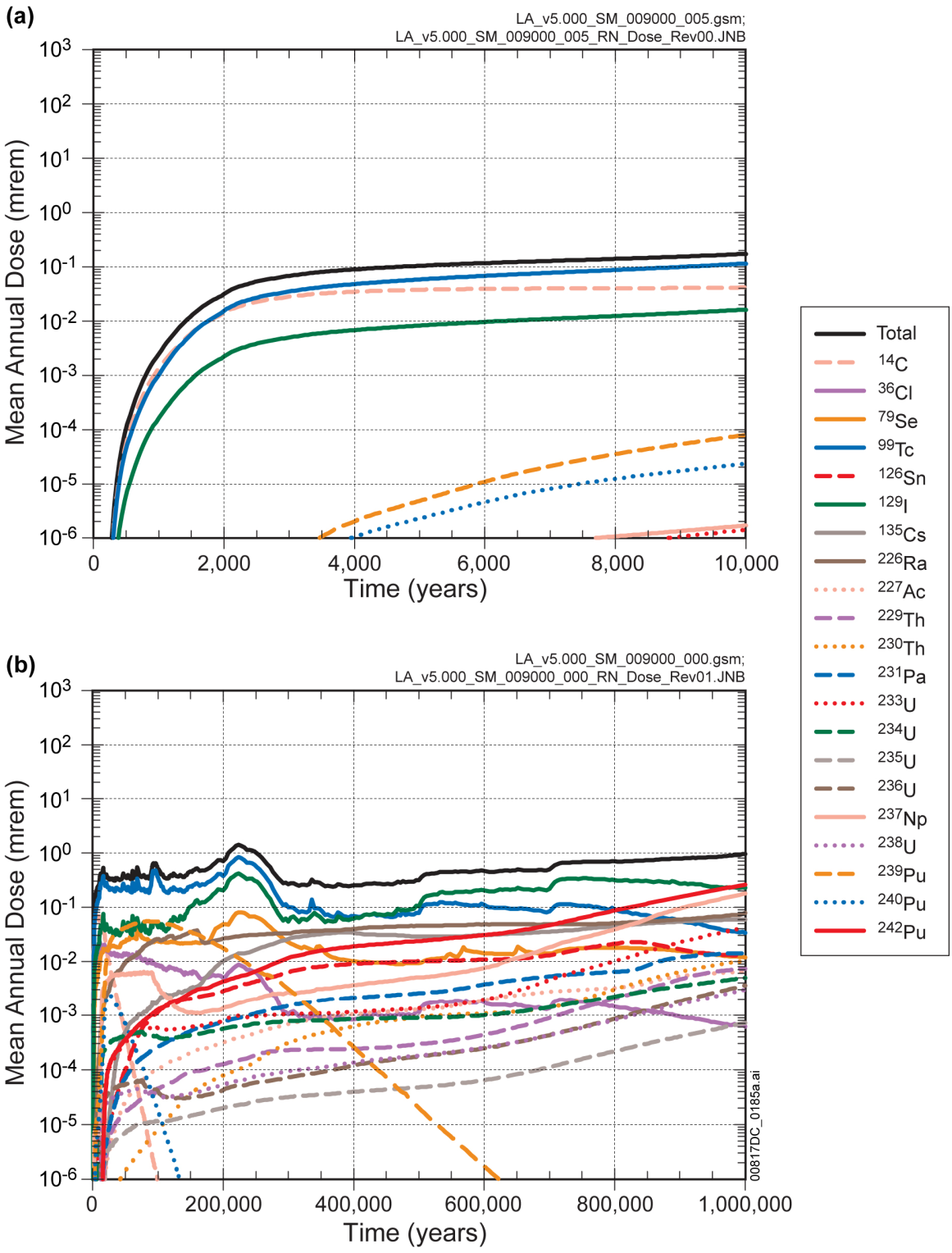

Source: Output DTN: MO0709TSPAREGS.000 [DIRS 182976]

Figure 8.2-12. Contribution of Individual Radionuclides to Mean Annual Dose for the Seismic Ground Motion Modeling Case for (a) 10,000 Years and (b) 1,000,000 Years after Repository Closure

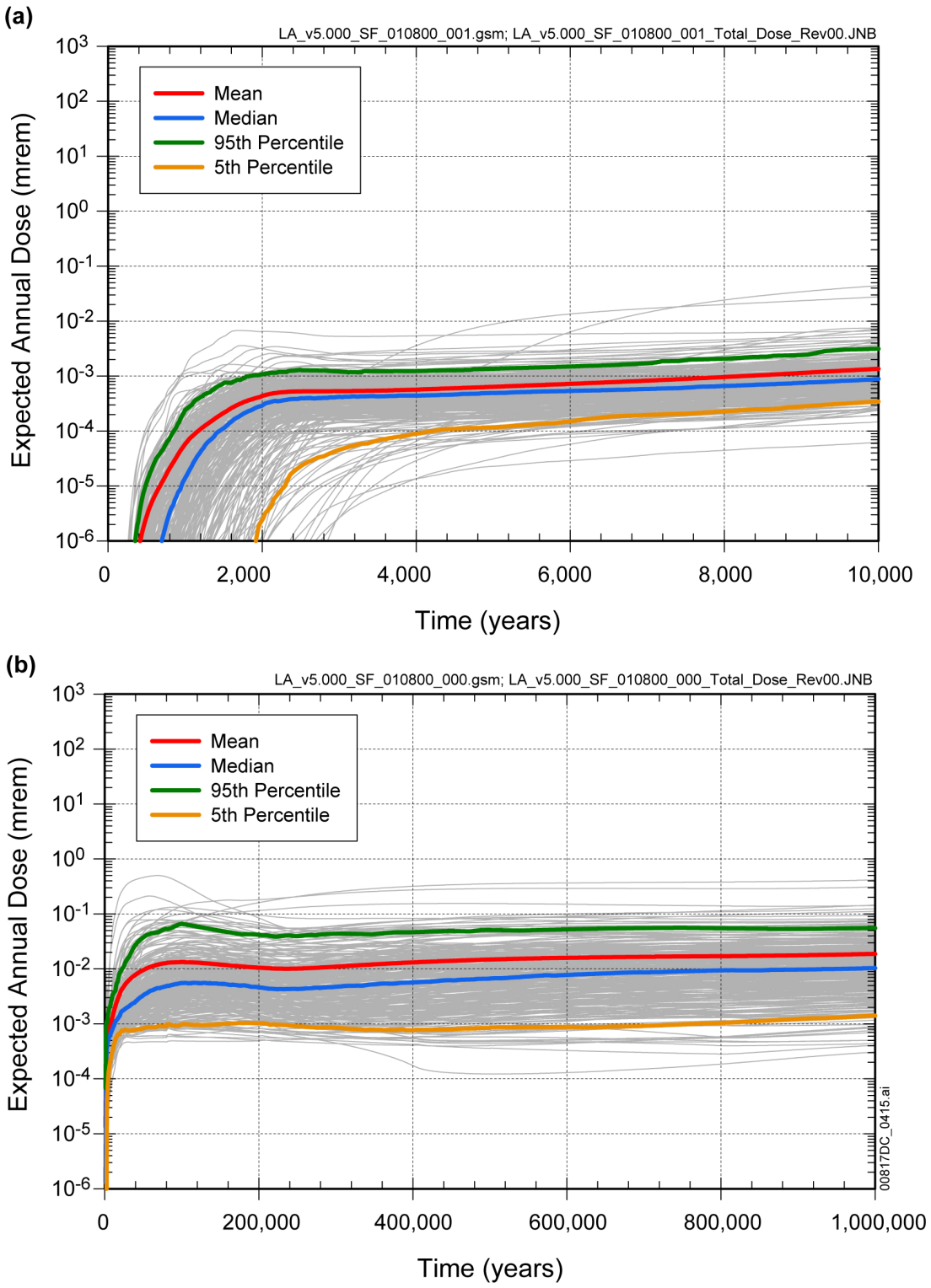

Source: Output DTN: MO0709TSPAREGS.000 [DIRS 182976]

Figure 8.2-13. Probabilistic Projections of Expected Annual Dose for the Seismic Fault Displacement Modeling Case for (a) 10,000 Years and (b) 1,000,000 Years after Repository Closure

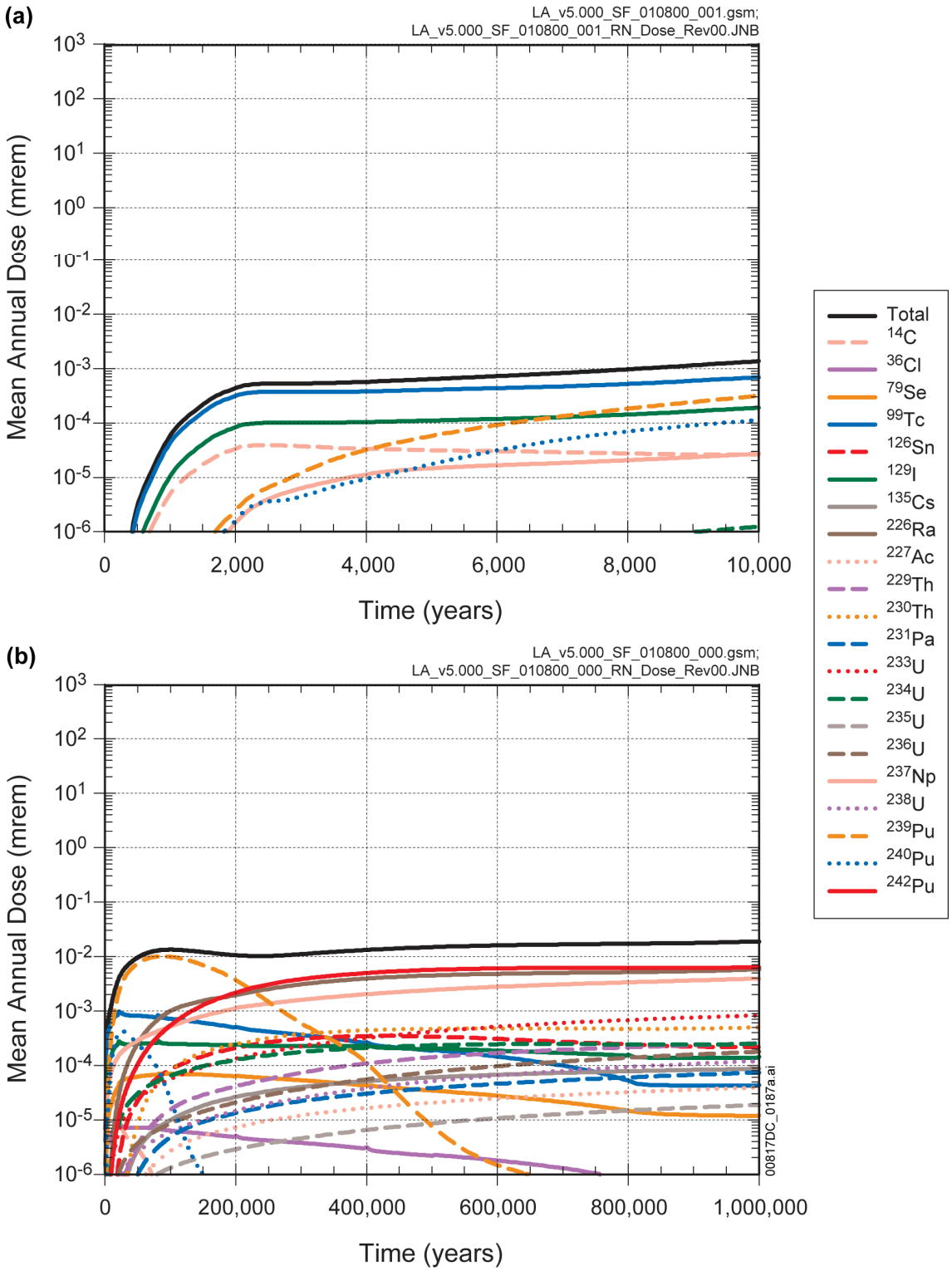

Source: Output DTN: MO0709TSPAREGS.000 [DIRS 182976]

Figure 8.2-14. Contribution of Individual Radionuclides to Mean Annual Dose for the Seismic Fault Displacement Modeling Case for (a) 10,000 Years and (b) 1,000,000 Years After Repository Closure

8.3 DESCRIPTION OF MULTIPLE BARRIER CAPABILITY

In the previous sections of this report, the DOE performance demonstrations for the three NRC radiation protections standards: (1) Individual-Protection (10 CFR 63.311) [DIRS 178394], (2) Human-Intrusion (10 CFR 63.321) [DIRS 178394], and (3) Groundwater Protection (10 CFR 63.331) [DIRS 180319], were presented and explained. The performance projections for these three standards demonstrated the isolation capability of the multiple barriers acting as an integrated system. In this section, both qualitative and quantitative descriptions are presented to explain the performance characteristics and capabilities of the individual barriers. In addition to providing valuable insights to barrier capability, this information also addresses the NRC requirements of 10 CFR 63.115 [DIRS 180319] for multiple barriers, which specifies that the DOE demonstration of compliance must:

- "(a) Identify those design features of the engineered barrier system, and natural features of the geologic setting, that are considered barriers important to waste isolation.

- (b) Describe the capability of barriers, identified as important to waste isolation, to isolate waste, taking into account uncertainties in characterizing and modeling the behavior of the barriers.

- (c) Provide the technical basis for the description of the capability of barriers, identified as important to waste isolation, to isolate waste. The technical basis for each barrier's capability shall be based on and consistent with the technical basis for the performance assessments used to demonstrate compliance with 10 CFR 63.113 (b) and (c)."

Identifying the multiple barriers is a relatively straightforward task, and a brief discussion of the Upper Natural Barrier, EBS, and Lower Natural Barrier, as well as their key features, is given in a subsequent section. With regard to providing the technical bases for barrier capability, that information is extensive and consists of site characterization data and numerous modeling studies that have been conducted over the past two decades. The technical bases for the multiple barriers are documented in numerous Yucca Mountain Project (YMP) reports, many of which are cited in Sections 1 through 6 of this report.

The main purpose of this section is to describe and explain the performance capability of the individual barriers and their barrier features. For this reason, this section is organized into four general parts:

1. Description of the major radionuclides selected to illustrate barriers capability

2. Identification of multiple barriers and their primary barrier features

3. Description of barrier capability in the absence of disruptive events, as defined by a composite modeling case of the Nominal Modeling Case plus Early Failure Modeling Cases

4. Description of barrier capability in the presence of disruptive events, as defined by Seismic GM Modeling Case.

With regard to item 4, the Seismic GM Modeling case was selected to illustrate barrier capability because: (1) frequencies of occurrence of seismic events are much greater than those for other disruptive events and (2) seismic ground motion has been shown to be important to postclosure performance (Section 8.1.1.2).

Selected performance projections of barrier capability will be presented, which highlight each barrier's inherent capability to isolate (i.e., contain and/or confine) the radionuclides that may pose the most risk over the range of plausible future system states. These projections also provide an additional technical basis for the performance demonstration results presented in Sections 8.1 and 8.2. Because of current programmatic and computational constraints, however, the TSPA-LA results for parts (3) and (4) will be documented in a separate addendum to this report.

8.3.1 Radionuclides Selected to Demonstrate Multiple Barrier Capability

One of the basic and important functions of the multiple barriers is to prevent or substantially reduce the rate of radionuclide movement from the repository to the accessible environment. To demonstrate the range of barrier capability but yet limit the number of calculations, a small subset of radionuclides was selected for the barrier performance demonstrations. That subset was selected from two lists: (1) radionuclides identified as dominating the mean annual doses to the RMEI for the 10,000-year and post-10,000-year time periods, and (2) radionuclides identified as dominating the curie inventory for the 10,000-year and post-10,000-year time periods. The first list of important radionuclides was developed directly from the probabilistic projections of mean annual dose (Section 8.1, Figure 8.1-7). The second list was compiled by examining the inventory decay histories, which is discussed herein.

Calculations of inventory decay histories for the major radionuclides are shown on Figure 8.3-1 for the two compliance periods of 10,000 years and post-10,000 years (i.e., after 10,000 years but within 1,000,000 years). The time dependent behavior of individual radionuclides is the result of simple radioactive decay and, in some cases, decay chain in-growth. From the curves on these plots, one can note that in the first 100 years, two fission products, ^{90}Sr (half-life of 28.8 years) and ^{137}Cs (half-life of 30 years), dominate the inventory; thereafter, the actinide radionuclide ^{241}Am (half-life of 432.7 years) dominates to about 1,000 years, ^{240}Pu (half-life of 6,560 years) dominates to about 7,000 years, and then ^{239}Pu (half-life of 2.41×10^4 years) dominates to about 115,000 years. Dominance then shifts to the fission product ^{99}Tc (half-life of 2.13×10^5 years) for the majority of time in the 1,000,000-year time period.

More refined insights to inventory dominance can be gained by examining plots of the fraction of total activity, at time 't', for each radionuclide; two plots are shown on Figure 8.3-2 for 10,000 years and 1,000,000 years. From these plots, it is evident that the dominant radionuclides in the curie inventory, grouped by compliance period, are:

1. For 10,000 years: ^{137}Cs and ^{90}Sr, ^{241}Am, ^{240}Pu and ^{239}Pu
2. For post-10,000 years: ^{239}Pu, ^{99}Tc, ^{237}Np, ^{233}U, and ^{229}Th.

At closure, the three radionuclides, ^{137}Cs, ^{90}Sr, and ^{241}Am, collectively represent about 85 percent of the total curie inventory with ^{137}Cs representing about 46 percent, ^{90}Sr about 29

percent, and ^{241}Am about 10 percent. From Figure 8.3-2(a), it can be clearly seen that ^{241}Am dominates the curie inventory in the interval from 100 to 1,000 years. Dominance shifts to ^{240}Pu and ^{239}Pu from 1,000 years to 10,000 years with these two actinides alone representing more than 90 percent of the inventory at the end of 10,000 years. As shown on Figure 8.3-2 (b), ^{239}Pu dominance peaks at about 50,000 years. From roughly 100,000 years to 1,000,000 years, the inventory dominance shifts to ^{99}Tc (half-life of 2.13×10^5 years) until roughly 850,000 years then transitions to dominance by three actinides: ^{237}Np (half-life of 2.14×10^6 years), ^{233}U (half-life of 1.59×10^5 years), and ^{229}Th (half-life of 7.3×10^3 years); the curves for ^{233}U and ^{229}Th overlay due to secular equilibrium. The latter three actinides are members of a decay chain in the neptunium series (Figure 6.3.7-4). A summary of the decay history of the total curie inventory and the major contributors is presented in Table 8.3-1; the percentages shown in the table were calculated directly from the data files used to create Figure 8.3-1.

Comparing the above radionuclides that dominate the inventory with the radionuclides identified as important to mean annual doses to the RMEI, namely, for the 10,000-year compliance period: ^{99}Tc, ^{14}C, ^{129}I, ^{239}Pu, ^{36}Cl, ^{79}Se, and ^{240}Pu, and for the post-10,000-year compliance period: ^{226}Ra, ^{242}Pu, ^{237}Np, ^{129}I, ^{233}U, ^{135}Cs, ^{230}Th, ^{99}Tc, ^{229}Th, and ^{231}Pa; it can be noted that the radionuclides that dominate the inventory also appear in the list of radionuclides important to dose, with the exception of the short-lived ^{137}Cs, ^{90}Sr, and ^{241}Am.

Based on the above considerations, the following subset of radionuclides was selected for use in describing barrier capabilities with regards to reducing or substantially reducing the rate of radionuclide movement:

These radionuclides represent a broad range of nuclear properties, geochemical behavior, and transport characteristics including:

- Large initial inventory and short half-life: ^{137}Cs, ^{90}Sr, ^{241}Am, ^{240}Pu
- Highly soluble, non-sorbing, long half-life and major contributor to dose: ^{99}Tc
- Solubility limited, strongly sorbed, long half-life, transported in dissolved and colloidal phases, and important contributor to dose: ^{239}Pu and ^{242}Pu
- Moderately soluble, low sorbing, very long half-life, and transported in dissolved phase: ^{237}Np and ^{234}U
- Low initial inventory, strongly sorbed, and important contributor to colloids or decay chain in-growth: ^{243}Am, ^{230}Th, and ^{226}Ra.

The primary barrier performance metrics that will be used are: seepage flux, DS and WP lifetimes and radionuclide release rates. The release rates are computed at the following barrier interfaces: (1) EBS outer boundary, (2) UZ and SZ interface, and (3) SZ and accessible environment interface.

8.3.2 Identification of Barriers for Yucca Mountain Repository System

As noted earlier, the Yucca Mountain Repository system is comprised of three barriers, namely, the Upper Natural Barrier, the EBS, and the Lower Natural Barrier (Figure 8-1). Collectively, these three barriers function to: (1) prevent or substantially reduce the rate of movement of water or radionuclides from the repository to the accessible environment, or (2) prevent or substantially reduce the release rate of radionuclides from the repository. A brief description of these barriers and their features is given below:

1. Upper Natural Barrier—Barrier features include the topography and surface soils of the mountain, the unsaturated tuff units above the repository, and the rock in which the repository is constructed.

2. EBS—Barrier features include the emplacement drifts, DSs, WPs, waste forms, cladding (associated with CSNF, DSNF, and NSNF), WP pallets, and ballast in the emplacement drift inverts.

3. Lower Natural Barrier—Barrier features include the volcanic rock in the UZ beneath the repository and the volcanic rock and alluvial material in the SZ between the repository and the accessible environment.

It is important to clarify that the Upper Natural Barrier is the portion of the geologic strata that extends from land surface to the bottom of the repository emplacement horizon. The Lower Natural Barrier extends from the base of the repository horizon to the water table and includes the SZ below the water table that extends from the repository footprint to the accessible environment boundary at approximately 18 km.

For the Upper Natural Barrier, the capability of the barrier features is described with respect to how they prevent or substantially reduce the rate and amount of water that may seep into the repository drifts and, ultimately, to the accessible environment. In contrast, the capability of the EBS features is described with respect to how they prevent or substantially reduce the release rate of radionuclides from the WPs. In the case of the Lower Natural Barrier, the capability of the barrier features is described in terms of how they prevent or substantially reduce the rate of movement of radionuclides from the repository to the accessible environment.

8.3.2.1 Upper Natural Barrier

The Upper Natural Barrier serves to prevent or substantially reduce the rate of water percolating downward through the UZ. More specifically, this barrier is important to postclosure performance because percolating water and the ensuant drift seepage are the only means by which radionuclides could be mobilized from the nuclear waste and transported by groundwater to the accessible environment. This barrier is the thick UZ formation of Yucca Mountain, which is composed of surficial soils and the unsaturated tuffs; namely, the Tiva Canyon welded (TCw), Paintbrush nonwelded (PTn), and Topopah Springs welded (TSw) units.

The location and elevation of the repository provide further advantage to the favorable and unique barrier characteristics of the geologic and hydrogeologic setting of the Yucca Mountain site. These favorable barrier characteristics include:

- A semiarid climate with limited precipitation and significant evapotranspiration
- A thickness of rock and soil above the repository of at least 200 m and up to more than 400 m
- Geologic, geochemical, and geomechanical characteristics that are compatible with the design and construction of an effective EBS
- Geomechanical and thermal characteristics that provide a stable facility with adequate capacity for waste disposal.

The semiarid climate in the Yucca Mountain is characterized by mean annual precipitation rates of 100 to 300 mm/yr (BSC 2004 [DIRS 169734], Figure 7-6).

Topography and Surficial Soils—The topography and surficial soils play a significant role as barriers to water because they limit the net infiltration into the UZ. The surficial soils function as a barrier by diverting (as runoff) some of the water that arrives as precipitation and run-on, and by storage in the soil, some of which is returned to the atmosphere as evapotranspiration. Thus, the volume of water that is diverted or evaporated would not percolate into the UZ rock layers as net infiltration. Recent studies of infiltration (SNL 2007 [DIRS 182145]) for the Yucca Mountain site indicate that the surficial soils are a very effective natural barrier to surface infiltration. For example, detailed water balance calculations for present-day climate shows that the mean net infiltration rate is less than 10 percent of the mean precipitation rate (SNL 2007 [DIRS 182145], Table 6.5.7.4-1); these water balance calculations also indicate that the processes of evapotranspiration and runoff reduce the net infiltration rate by as much as 88 percent.

Unsaturated Tuff Units—Water flow in the fractured welded tuffs that host the repository (i.e., TSw hydrogeologic unit) occurs primarily in widely distributed fractures (e.g., fracture density, spacing, and apertures). In contrast, the PTn hydrogeologic unit (located above the TSw hydrogeologic unit) is characterized by matrix-dominated flow. The matrix-dominated flow in the PTn unit attenuates, or dampens, the amplitude of pulses of percolation caused by variable infiltration and lateral heterogeneity.

As part of the UZ Flow Model development over the past decade, the steady-state nature of the flow fields and the damping of transient pulses were evaluated in different studies. The work of Wang and Narasimhan (1985 [DIRS 108835]; 1993 [DIRS 106793], Figure 7.4.7), for example, indicates that effects of infiltration pulses at the surface are damped by the underlying tuff units, especially the PTn. The welded tuff of the repository horizon exhibited only small changes in saturations, pressures, and potentials from steady-state values in response to the transient pulses. Pan et al. (1997 [DIRS 164181]) investigated transient flow behavior for downward water flow through sloping layers in the UZ.

Wu et al. (2002 [DIRS 161058], pp. 35-1 to 35-12) analyzed the capillary barrier capacities in unsaturated units and indicated that, on average, it took several thousand years for water to travel through the PTn. Wu et al. (2000 [DIRS 154918]; 2002 [DIRS 161058]) analyzed the implications of capillary barrier development in subunits of the PTn for lateral diversion of flow in the PTn. Along sloping layers, strong capillary barriers, if formed, will promote lateral diversions. A more recent study, conducted by Zhang et al. (2006 [DIRS 180273]) using three-dimensional and one-dimensional model results, shows that the PTn can attenuate episodic infiltration pulses significantly, most percolating water is damped by the subunits at the top of the PTn, and a small percentage of that water flux is diverted into faults.

Within the repository horizon, ambient unsaturated flow and thermo-hydrologic processes are favorable to the natural barrier function of preventing or substantially reducing the movement of water into emplacement drifts. Thermo-hydrologic (TH) analyses (SNL 2007 [DIRS 181383]) of the postclosure thermal period, for example, show that the decay heat will raise host rock temperatures and create dry-out zones around the emplacement drifts (Figure 6.3.3-3). These dry-out zones would vaporize locally percolating water and induce water (liquid and vapor) flow away from the drift. Current analyses of TH processes indicate that dry-out zones or vaporization barriers may effectively extend upwards of about 11 meters (Section 6.3.2.1) into the host rock and would persist for several centuries (SNL 2007 [DIRS 181383], Table 6.3-50[a]). As the host rock cools to temperature below boiling, the locally percolating water would create a zone of increased saturation at the drift crown and around the drift opening, resulting in the formation of a capillary-barrier (SNL 2007 [DIRS 181244], Section 6.1.4). The extent of the capillary-barrier effect would be limited to a relatively thin layer around the opening but would be sufficiently effective to divert flow around the drift (Figure 6.3.3-4); this diversion of ambient water flow, in turn, would reduce the seepage flux to drift.

8.3.2.2 Engineered Barrier System

The primary features of the EBS include the emplacement drifts, DSs, WPs, cladding, waste forms, WP pallets, and the drift invert. While the WPs remain without a major breach (e.g., an opening or tear/puncture created by general corrosion or seismic loading), none of the waste can be exposed to water, and no release of radionuclides can occur. The WP outer barrier will be made of Alloy 22, a corrosion-resistant nickel alloy. Even if some WPs were to be breached, the intact DSs would prevent seepage from contacting the waste. Similarly, the Titanium Grade 7 DS is sufficiently resistant to both general corrosion and localized corrosion and should not be breached by either of these nominal processes for more than 10,000 years. The barrier capability of the EBS features, however, can be diminished by potential disruptive events and processes, such as seismic ground motion, fault displacement, and igneous intrusion.

The favorable barrier characteristics of the EBS include:

- A stable thermal, mechanical hydrologic, and chemical environment affected principally by the thermal effects of radioactive decay
- Corrosion resistant metals that are designed to perform and function in the thermal, mechanical, hydrologic, and chemical environments expected in the emplacement drifts

- DS, WP, and cladding materials with designs and fabrication methods that reduce the potential effects of SCC, and other physical-chemical degradation processes

- Generally low radionuclide solubility and high sorption characteristics of radionuclides (on corrosion products) delaying or preventing their release even in rare early breach of WPs

- Delayed transport of radionuclides through the EBS due to low rates of water advection through the EBS features, and the slow diffusion of radionuclides through any continuous water film that is expected to be highly tortuous.

Evidence from natural and man-made openings in unsaturated underground environments indicates that such openings effectively limit the movement of water and often create stable conditions in which fragile materials may be preserved for tens of thousands of years. Analogue data from Pena Blanca indicate that underground openings provide a significant reduction in seepage compared to the amount of water infiltration that enters the UZ (SNL 2007 [DIRS 181244], Section 7.3[a] and 8.1[a]). Emplacement drifts provide the thermal, mechanical, hydrologic, and chemical environment in which the rest of the EBS features function. These environments are affected by the heat caused by the decay of radioactive materials in the waste, in particular, in the CSNF waste form. Although these environments are expected to change with time, in the absence of unlikely disruptive events such as low probability seismic or igneous events, the rate of change is very slow.

Drip Shields—The corrosion resistant Titanium Grade 7 DSs are installed over the WPs prior to repository closure. The DSs divert any potential seepage from the Upper Natural Barrier and water condensate (that may form from the water vapor in the air) around the WPs to the emplacement drift invert. In addition, the DS protects the WP from the potential effects of rockfall.

Waste Packages—As long as they remain without a major breach, WPs prevent contact between water and the waste form and prevent the release of radionuclides. Should water contact the WPs, any resultant corrosion of the Alloy 22 WP is expected to proceed slowly under the nominal corrosion degradation conditions and result in initial breaches in the form of hairline cracks that still limit the movement of water that could potentially contact the waste form, and thus, reduce the release rate of radionuclides from the WPs. Note that localized corrosion of WPs is not expected to occur under the repository condition (Section 6.3.5.2.3). The 50-mm thick stainless steel WP inner vessel and the 25-mm thick transport, aging, and disposal (TAD) canister are expected to provide some performance benefit for waste containment, and could potentially contribute to the reduction of the rate of radionuclide release after WPs are breached. The performance benefit of these specific WP components, much like CSNF cladding, are not considered in the TSPA-LA Model.

Cladding—Zircaloy cladding is a highly corrosion-resistant component of the CSNF that prevents or substantially reduces the contact of water with the waste form and reduces the release rate of radionuclides. For the purposes of conservatism, no performance credit is taken in the TSPA-LA Model for CSNF cladding effects on release rate.

Waste Forms—The waste forms that will be disposed of, include spent nuclear fuel (SNF) and HLW glass (vitrified). These waste forms are solid materials that generally degrade slowly in the unsaturated environment of the repository, thus reducing the release rate of radionuclides, although the DSNF is assumed to degrade instantaneously in the TSPA-LA Model.

Pallets—The WP pallet provides stability of the WP in the case of a seismic event and keeps the WP elevated above the floor of the emplacement drift as well. Thus, direct contact between the WP and the invert is not possible until the pallet degrades. This behavior is not considered in the TSPA-LA Model.

Inverts—The emplacement drift invert is composed of two parts: a steel invert structure and ballast (or fill). In the unsaturated repository environment, the granular materials in the invert slow the diffusive movement of radionuclides into the Lower Natural Barrier.

The features described above give the EBS the ability to prevent or significantly reduce the seepage water from contacting the waste forms, thereby substantially reducing the potential radionuclide release and rate of release from the waste into the Lower Natural Barrier.

8.3.2.3 Lower Natural Barrier

The features of the Lower Natural Barrier include the UZ tuff layers immediately below the repository and the SZ that extends downgradient from the repository to the accessible environment. The UZ includes a portion of the Topopah Springs welded (TSw) and Calico Hills nonwelded (CHn), and Crater Flat undifferentiated (CFu) units (Ortiz et al. 1985 [DIRS 101280]). These unsaturated rock layers represent a total vertical transport path of 250 to 380 m across the repository footprint with an average of about 300 m to the water table for present-day climate conditions. Under the wetter climates, however, the travel distance through the UZ may be as much as 120 m less due to a higher water table under the glacial transition climate. The SZ is composed of volcanic units and alluvial sediments (Section 6.3.10) with the flow path extending a distance of about 18 km to the accessible environment boundary. The first 12 to 14 km of the SZ flow path is in fractured volcanic rocks, while the remainder of the flow path is through alluvial sediments. The projected direction of the groundwater transport pathway is southeast from the repository site, transitioning to a southerly direction towards the designated accessible environment boundary in the Amargosa Desert.

The role of the Lower Natural Barrier is to prevent or substantially reduce the rate of movement of radionuclides from the repository to the accessible environment. The Lower Natural Barrier performs this role through the intrinsic site characteristics that are directly reflected by such factors as: (1) slow advective water transport, (2) matrix diffusion and sorption of dissolved phase radionuclides, (3) dispersion/dilution of dissolved and colloidal phase radionuclides, (4) reversible filtration of irreversible colloidal phase radionuclides, and (5) radioactive decay and ingrowth. Section 6.3.9.1 discusses the flow and transport processes involved in determining the capability of the UZ, while the relevant SZ processes are discussed in Section 6.3.10.1.

Some of the fundamental and important performance characteristics of the Yucca Mountain Lower Natural Barrier include:

- Low deep percolation rates through the UZ as a result of hydrologic efficiency of the Upper Natural Barrier (i.e., surficial soils with characteristically high evapotranspiration, matrix flow through the PTn, and lateral flow focusing into faults in the northern part of the repository footprint)

- High porosity vitric rock layers (i.e., CHn in southern half of repository) and low permeability zeolitic rock layers (i.e., CHn and CFu), both types of rock layers that have capability to strongly sorb a variety of radionuclides and delay transport

- Long transport path through the SZ volcanic units with capability to delay radionuclides as dissolved radionuclides diffuse into and out of the pores in the rock, increasing the likelihood of sorption onto mineral surfaces, as well as promoting retardation of irreversible colloids (via reversible filtration)

- Lower advective transport through the higher porosity SZ alluvium, with capability to delay radionuclides via sorption of selected radionuclides on mineral particle surfaces and dilution as a result of longitudinal and transverse dispersion.

The performance characteristics of the UZ units below the repository have been analyzed using detailed three-dimensional flow and transport modeling studies. The rates of radionuclide movement through the UZ portion have bee studied using a particle tracking technique which is documented in *Particle Transport Model and Abstraction of Transport Processes* (SNL 2008 [DIRS 184748]). That report presents sensitivity analysis for breakthrough times for various radionuclide species. Analogous studies have been performed for the SZ to develop an understanding radionuclide transport to the accessible environment. Those studies are documented in *Saturated Zone Flow and Transport Model Abstraction* (SNL 2008 [DIRS 183750]).

INTENIONALLY LEFT BLANK

Table 8.3-1. Decay of Total Curie Inventory as a Function of Time and Dominant Contributors to Total Curie Inventory

Time After Closure (yrs)	Percent of Total Initial Curie Inventory	Major Contributors to Total Inventory at Time after Closure
0	100.00	Cs -137 (46%), Sr-90 (29%), Am-241 (10%)
10	81.2	Cs -137 (45%), Sr-90 (28%), Am241 (12%)
100	20.75	Am-241 (41%), Cs -137 (22 %), Sr-90 (13%), Pu-238 (11%))
1,000	4.20	Am-241 (48%), Pu-240 (29%), Pu-239 (19%)
10,000	1.18	Pu-239 (52%), Pu-240 (40%)
100,000	0.10	Pu-239 (46%), Tc-99 (27%)
500,000	0.03	Tc-99 (26%), Th-229 (9%), Th-230 (9%), Ra-226 (9%), U-233 (9%), Np-237 (9%), Pu-242 (8%), U-234 (7%)
1,000,000	0.02	U-233 (15%), Th-229 (15%), Np-237 (14%), Tc-99 (9%), Th-230 (7%), Ra-226 (7%), Cs-135 (7%), U-236 (6%), Pu-242 (6%)

Source: Output DTN: MO0709TSPAREGS.000 [DIRS 182976]

INTENTIONALLY LEFT BLANK

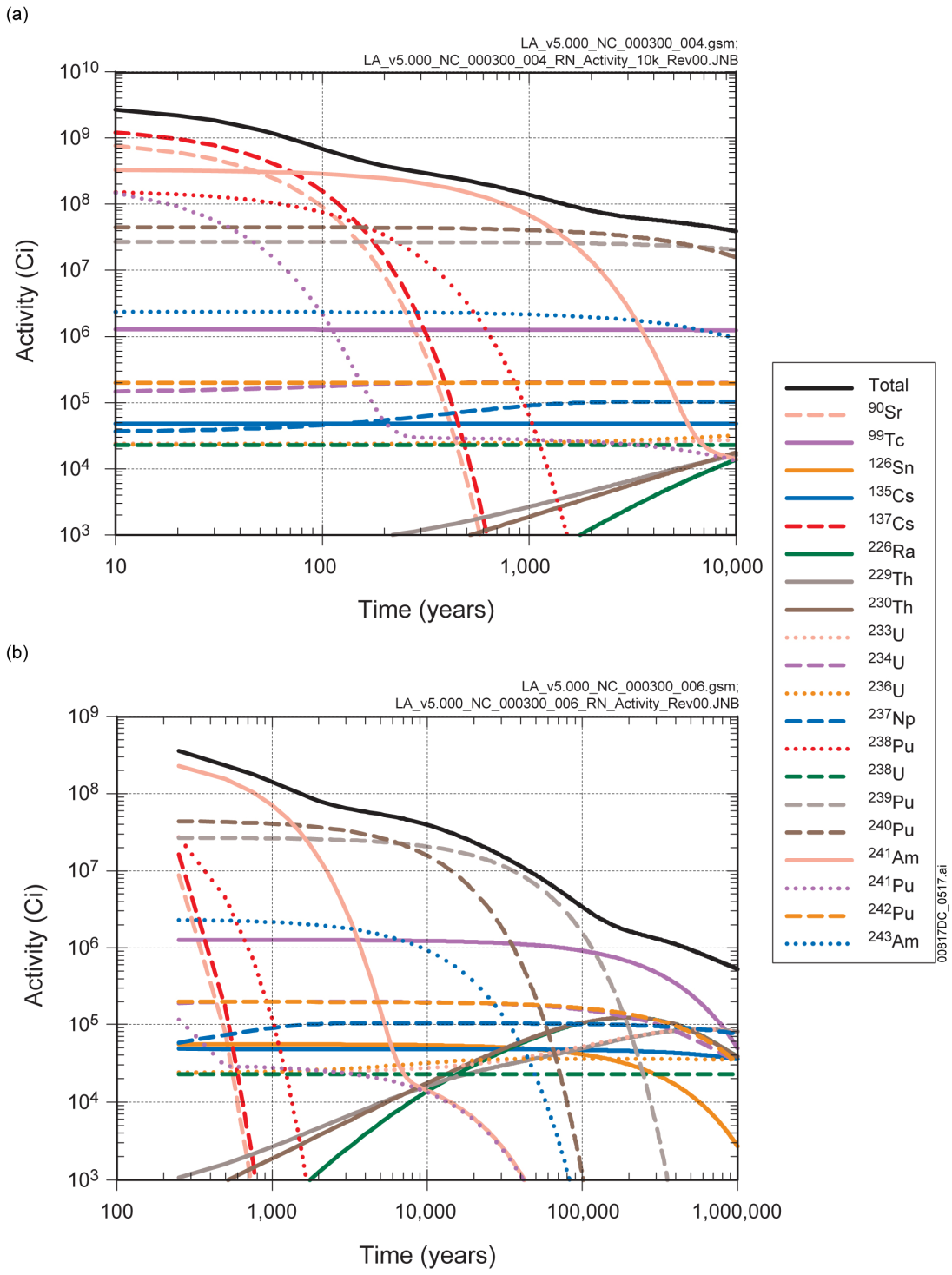

Source: Output DTN: (a) MO0708TSPAVALI.000 [DIRS 182985]; and (b) MO0709TSPALAMO.000 [DIRS 182981].

Figure 8.3-1. Mean Radionuclide Activities in the Nuclear Waste as a Function of Time for (a) 10,000 Years and (b) 1,000,000 Years after Repository Closure

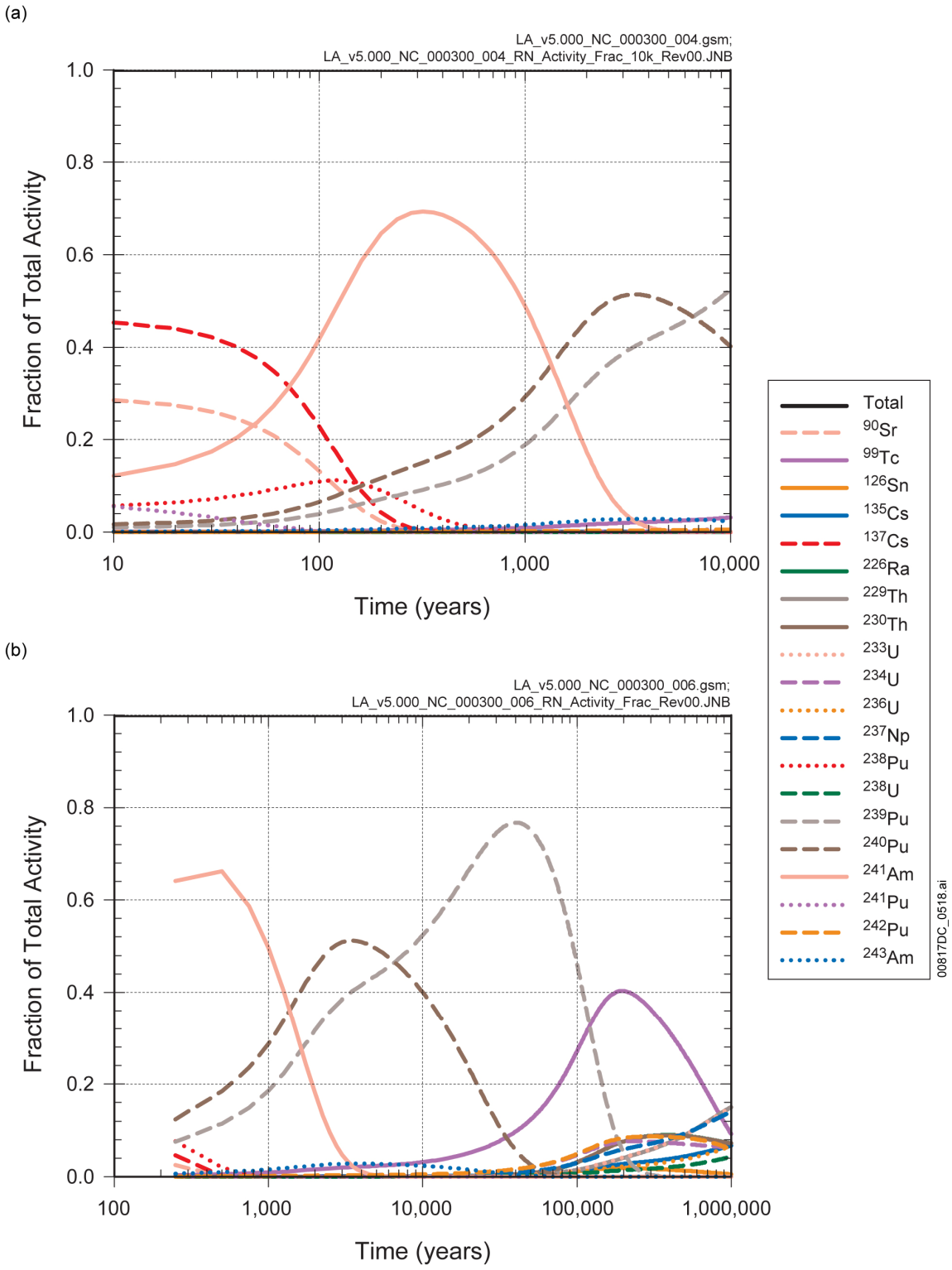

Source: Output DTN: MO0709TSPAREGS.000 [DIRS 182976]

Figure 8.3-2. Mean Radionuclide Contributions to Total Inventory as a Function of Time for (a) 10,000 Years and (b) 1,000,000 Years after Repository Closure

8.4 VALIDITY AND DEFENSIBILITY OF PERFORMANCE DEMONSTRATION

This section outlines the YMP activities that were conducted to ensure that the postclosure performance demonstration for the Yucca Mountain repository would be technically sound and defensible and, therefore, suitable to support the LA. In preparation for the LA, the YMP planned and successfully completed several programmatic activities to ensure that the:

1. TSPA-LA Model and its component models were validated for their intended use, controlled, and documented.

2. Software that implements the TSPA-LA Model was verified and validated through computational testing.

3. Models and input parameters account for the major sources of aleatory and epistemic uncertainties, are supported by appropriate evidence, and are maintained in a controlled database.

4. Performance projections are corroborated, to the extent possible, by other independent means, including auxiliary analyses and comparison with other separate TSPAs.

5. Technical basis for the TSPA-LA methodology was peer reviewed to ensure it is based on well established scientific principles, captures the important phenomena and couplings, and was supported by site characterization data.

The above programmatic activities are presented in Section 7, Volume II, of this report. The description of the TSPA-LA Model is presented in Section 6 of this report; the technical basis for the component models and TSPA input database is documented in several supporting analysis and/or model reports and TSPA Data Input Packages. Moreover, the supporting documentation was prepared in a manner that would ensure the technical basis is auditable and traceable so as to facilitate the licensing review.

Since the issuance of the *Total System Performance Assessment for the Site Recommendation* (CRWMS M&O 2000 [DIRS 143665]), the YMP's TSPA methodology (i.e., models, uncertainty treatment and propagation, code/software, and input parameters) has been significantly improved and refined as a result of:

- Continued scrutiny of the conceptual and mathematical models through internal and external peer reviews

- Further development and testing of TSPA-LA component models and submodels

- Statistical analysis of data and development of improved characterizations of uncertainty.

In addition, plausible and potentially significant model conservatisms have been identified, the rationale for their use explained, and their impact on postclosure performance metrics evaluated.

This section provides a summary of the specific YMP technical and programmatic activities conducted to ensure that the DOE postclosure performance demonstration is suitable to support the LA for the nuclear waste repository at Yucca Mountain.

8.4.1 Validation of TSPA Model and Component Models

At present, the applicable NRC regulation, NRC Proposed Rule 10 CFR Part 63 ([DIRS 178394] and [DIRS 180319]), does not contain requirements for model validation. However, the joint NRC/SKI white paper (Eisenberg et al. 1999 [DIRS 155354], p. 31) notes two essential elements for model validation: (1) procedures for the development of confidence in models, and (2) documentation of results from confidence building activities. These validation elements are incorporated in *Technical Work Plan for: Total System Performance Assessment FY 07-08 Activities* (SNL 2008 [DIRS 184920], Section 2.3.5) and are in accordance with:

- SCI-PRO-002, *Planning for Science Activities*
- SCI-PRO-006, *Models*.

Development and validation of the TSPA-LA Model and its components were planned and controlled in accordance with SCI-PRO-002 and documented in accordance with SCI-PRO-006. It is important to clarify and emphasize that model validation should be viewed as a progressive confidence building process and not an end-state.

The full range of model validation activities conducted for the TSPA-LA is illustrated on Figure 7.1-2. Some of the primary model validation requirements from the two procedures are highlighted here.

During-Development Model Validation—Activities in this first phase of model validation encompassed planning, reviewing, checking, and documenting, which focused on:

- Ensuring the model formulation, assumptions, and simplifications are defensible.
- Ensuring the model theory is consistent with fundamental scientific principles, such as conservation of mass, energy, and momentum.
- Documenting the selection of input parameters and/or input data and explaining how the selection process builds confidence in the model.
- Documenting plans for model calibration activities, and/or initial boundary condition runs, and/or run convergences, and a discussion of how the activity or activities build confidence in the model. Activities also included a discussion of impacts of any run non-convergences.
- Identifying and documenting the potential impacts of uncertainties on model results.

A detailed description of the during-development model validation activities is presented in Section 7.1.2 (Volume II).

Post-Development Model Validation—In this stage of model validation, technical activities involve conducting various computational analyses and evaluations to ensure that the processes modeled are understood and appropriately described. Moreover, the analyses and evaluations demonstrate that the required level of model validation has been fully achieved. The major activities performed for the post-development model validation include:

- Corroborating the abstraction model results to the results of the validated mathematical model or process model from which the abstraction model was derived (Section 7.6)
- Performing auxiliary analyses to corroborate the results with the TSPA-LA Model and/or submodels (Section 7.7)
- Comparing the relevant TSPA-LA component models or submodels with available analogue information (Section 7.8)
- Utilizing internal and external peer reviews to evaluate defensibility of models and identifying potential areas of component model or submodel development improvement (Section 7.9).

More information on the post-development model validation activities is presented in Section 7.1.3.

The TSPA-LA Model and the 11 component models (Section 6) have been validated in accordance with the appropriate procedures. Documentation of the model validation is presented in each of the supporting analysis and/or model reports and includes a description of the validation procedure, validation criteria, and validation results.

8.4.2 Verification and Validation of TSPA Software and Input Data

The TSPA-LA Model and its component models are integrated into the GoldSim software (GoldSim 2007 [DIRS 181903]). The version of the GoldSim software used for the TSPA-LA was verified by the vendor, GoldSim Technology Group, by conducting a broad spectrum of computational tests. The software verification consisted of over 250 tests that covered the program's capabilities, including the user interface, user-defined expressions, internal functions, and distributed processing capabilities. These tests included:

- 93 basic functional tests
- 23 time and Monte Carlo tests
- 130 contaminant transport tests
- 17 reliability module tests.

As part of the verification testing, the software was run through tests that exercise the graphical user interface, internal functions, stochastic processes, contaminant transport code, and result displays for the purpose of demonstrating that the software performed its numerical, logical, and input/output operation correctly. All verification tests were performed in accordance with a verification plan (DOE 2007 [DIRS 181107]).

The YMP staff reran all the verification test cases to provide an independent check; the software testing was performed in accordance with IM-PRO-004, *Qualification of Software*. For added confidence, key functions and capabilities of the simulation software were combined into four TSPA-developed tests, and the results were compared to independently generated results. The independent tests are described in the *Design Document for: GoldSim v9.60* (DOE 2007 [DIRS 181107], Section 7.2.1), and the results are shown in *Software Validation Report for: GoldSim v9.60 on Windows 2000* (DOE 2007 [DIRS 181109], Sections 4.2.34 through 4.2.37). The integrated system software (GoldSim) was qualified in accordance with IM-PRO-004. In addition to verification of the software, testing was performed to verify the computational stability and convergence. This included testing the:

1. Stability of the statistical sampling used in the Monte Carlo simulations (Section 7.3.1)

2. Numerical accuracy of the expected dose calculation (Section 7.3.2)

3. Convergence of the time stepping used in the numerical integration of the model equations (Section 7.3.3)

4. Spatial discretization of the repository system (Section 7.3.4).

5. Stability of transport models using the FEHM particle-tracking methodology (Section 7.3.5).

All of this computational testing was performed for the various modeling cases to ensure that the GoldSim model was ready for use in the performance demonstration for the LA.

The input database for the GoldSim software stores all the TSPA-LA input parameter values and distributions. This input database is used to categorize, store, and retrieve fixed and distributed values of the TSPA-LA Model parameters. The database is programmed with user controls featuring read and write access and audit trails. These controls were designed to ensure the security, integrity, and traceability of the information used in the TSPA-LA Model analyses. A controlled, standalone TSPA Input Database was developed using a commercially available desktop database manager, Microsoft Access 2000. It is a Microsoft Windows based, multi-user relational database solution that allows data entry, viewing, and querying, as well as report preparation. The TSPA Input Database was qualified in accordance with IM-PRO-004.

The parameter values are obtained from controlled sources maintained by the project data and information systems, such as project documents, the Technical Data Management System (TDMS), and the Technical Information Center. The TDMS database is a project-wide database, whereas the TSPA Input Database is used only for the TSPA-LA Model. Each of the parameter sets used in the TSPA Input Database has a data tracking number (DTN) to provide the link to the TDMS database or a reference to the controlled source of the information, such as an analysis and/or model report. The TDMS maintains the qualification status all of its contents. The TSPA Model inputs are controlled and well documented by using the TSPA Input Database. An important configuration management feature of the TSPA Input Database is that it supports the independent verification of every parameter value used in the TSPA-LA Model.

GoldSim software and the TSPA input database have been verified. Additional information on the validation and verification is presented in Section 7.

8.4.3 Uncertainty Characterization Reviews

In preparation for the LA, the Lead Laboratory undertook a substantive effort to systematically review the TSPA uncertainty and variability characterizations for consistency, defensibility, and traceability. A special review team was formed to carefully examine parameter uncertainty and variability representations, correct or modify them as necessary, and ensure that the supporting documentation would facilitate the regulatory review.

The central objective of the uncertainty characterization reviews was to ensure that the treatment of parameter uncertainty and variability was of suitable quality for the LA. To accomplish this objective, the review team focused on:

- Confirming that the stochastic parameter representations appropriately reflect the major sources of uncertainty and/or variability
- Verifying that the probability distributions were supported by appropriate evidence and derived using sound statistical methods and interpretations
- Ensuring that model parameter representations (i.e., probability distributions) were reasonable and defensible, as opposed to depicting extreme variations that could potentially introduce risk dilution (i.e., wider distribution and lower peak mean annual dose).

Uncertainty characterizations were also reviewed with respect to appropriate up-scaling, data modeling, and use of professional judgment in assigning subjective distributions.

A core team of five senior staff members was formed with special expertise in probability and statistics, uncertainty analysis, TSPA modeling, and knowledge of the regulatory guidance regarding consistent treatment of uncertainty and variability. In addition, a small group of SMEs were used to support the core team and to facilitate the reviews of data, parameters, and model abstractions. The review team conducted fifteen formal reviews that were performed to scrutinize the uncertainty characterizations of some forty TSPA input parameters and their associated abstractions.

Because of the relatively large number (~400) of probabilistic parameters used in the TSPA-LA Model, it was necessary to prioritize the parameters for review. The prioritization was developed based on the importance ranking of the scenario modeling cases and parameters within those modeling cases. The ranking of the scenario modeling cases was as follows (from highest to lowest):

1. Seismic Scenario Class, Seismic GM Modeling Case
2. Igneous Scenario Class, Igneous Intrusion Modeling Case
3. Igneous Scenario Class, Volcanic Eruption Modeling Case
4. Early Failure Scenario Class, Waste Package EF Modeling Case

5. Early Failure Scenario Class, Drip Shield EF Modeling Case
6. Seismic Scenario Class, Seismic FD Modeling Case
7. Nominal Scenario Class, Nominal Modeling Case.

A list of 40 plus TSPA-LA parameters (Section 7.4, Tables 7.4-1 through 7.4-3) was compiled. The review focused on parameters whose uncertainty or variability (when propagated through the TSPA-LA Model) would have the greatest influence on the magnitude of the dose results, and the uncertainty in the dose results.

The 15 reviews produced several findings, recommendations, and corrective actions that resulted in improvement in the technical basis and documentation of the parameter uncertainty characterizations. A few of the key improvements to parameter uncertainty characterizations included:

- Unsaturated zone (UZ)—effective soil depth for surface infiltration and weighting factors for UZ flow fields
- Engineered Barrier System (EBS)—general corrosion of the drip shield and waste package internals
- Saturated zone (SZ)—groundwater specific discharge multiplier and flowing interval thickness.

A more detailed discussion of the uncertainty characterization reviews conducted for the TSPA-LA is presented in Section 7.4.

8.4.4 Corroboration of TSPA-LA Model Results

A number of methods (Section 7.0) have been utilized to build confidence in the TSPA-LA Model. One of those approaches is based on corroborating the TSPA-LA performance projections using a simplified and independent computer model (Section 7.7). Performance projections presented in Sections 8.1 and 8.2 were corroborated through: (1) use of a simplified TSPA-LA analysis, and (2) comparison with the Electric Power Research Institute (EPRI) independent assessment of postclosure performance for the proposed repository. The simplified TSPA-LA analysis and the EPRI results have been used to check for consistency of results for the important modeling cases.

The confidence building achieved through these corroborations of the TSPA-LA Model results is emphasized in the following paragraphs.

8.4.4.1 Comparison with Simplified TSPA Analysis Results

A separate and simpler implementation of the performance assessment of postclosure performance (Appendix L) was developed for the specific purpose of corroborating the performance projection results produced with the TSPA-LA Model. That implementation is in a standalone and separate computer code designated as the Simplified TSPA. The Simplified TSPA code uses a Monte Carlo approach to incorporate epistemic and aleatory uncertainties to the probabilistic calculation of mean annual doses. While the formulation of its component

models generally parallels those of the TSPA-LA Model, the Simplified TSPA code employs several simplifications. A detailed enumeration of the differences between the TSPA-LA Model and Simplified TSPA is presented in Section 7.7.2, Table 7.7.2-1. Three important simplifications are: (1) the repository is represented as a single homogeneous region, (2) flow and transport through UZ and SZ are one-dimensional, and (3) approximation for decay chain transport is more conservative.

Thus far, the Simplified TSPA has only been applied to four of the seven TSPA-LA modeling cases (Section 6.1.2) to calculate the mean annual doses to the RMEI. More specifically, the Simplified TSPA has been applied to: Nominal, Waste Package EF, Seismic GM, and Igneous Intrusion. These specific modeling cases were selected because previous TSPAs indicated they would have the greatest influence on the total mean annual doses to the RMEI. This observation is also confirmed in the TSPA-LA results presented in Section 8.1.

Nominal Modeling Case Results—The TSPA-LA Model projections for this case are shown on Figure 8.2-1 and for Simplified TSPA on Figure 7.7.2-5. The TSPA-LA Model projects a dose history where the exposure begins at about 130,000 years and increases, reaching a peak at 1,000,000 years. The Simplified TSPA results show a similar trend, but the WP failures occur later, so exposures are delayed until roughly 300,000 years. TSPA-LA Model results show that a peak mean annual dose for this modeling case is about 0.4 mrem, which compares reasonably well with the Simplified TSPA projection of about 0.2 mrem. A time-slice comparison between the two mean annual dose projections is discussed Section 7.7.2.2 and shown on Figure 7.7.2-6. With regard to radionuclides important to dose, the TSPA-LA Model results show ^{129}I as the main contributor, with small contributions from ^{99}Tc, ^{135}Cs, and ^{242}Pu. The Simplified TSPA results also show the mean annual dose to be dominated by ^{129}I, with lesser contributions from ^{242}Pu. The main difference between the two model results for the Nominal Modeling Case is the timing of WP failures and radionuclide releases. This is explained by the fact that the Simplified TSPA represents the repository as a single block with average properties, and as such does not account for spatial variability.

Waste Package Early Failure Modeling Case Results—For this modeling case, the TSPA-LA Model results are shown on Figure 8.2-5 and the Simplified TSPA results on Figure 7.7.2-2. The TSPA-LA Model results show a relatively flat mean annual dose history over the 1,000,000-year time period, with doses varying from about 10^{-3} to 10^{-1} mrem. The Simplified TSPA shows a similar trend, but the doses vary from about 10^{-2} to 10^{-1} mrem. A time-slice comparison between the two mean annual dose projections is discussed Section 7.7.2.1 and shown on Figure 7.7.2-3. The TSPA-LA Model results indicate that ^{242}Pu, ^{226}Ra (daughter product of ^{230}Th), and ^{237}Np dominate the mean annual dose. In the Simplified TSPA projections, the mean annual dose at 1,000,000 years is dominated by ^{229}Th (daughter product of ^{233}U) and ^{242}Pu and with lesser contributions from ^{237}Np. The differences in radionuclides contributing to the dose are attributed to how the decay chain transport is approximated in the Simplified TSPA code.

Seismic Ground Motion Modeling Case Results—Graphical results for this modeling case are shown on Figure 8.2-11 for the TSPA-LA Model and on Figure 7.7.2-8 for the Simplified TSPA. Both the TSPA-LA Model and Simplified TSPA results show the mean annual doses histories to rise to a peak mean value and then remain relatively flat. However, the TSPA-LA Model shows a peak mean annual dose of about 0.1 mrem, whereas the Simplified TSPA shows a higher value

of about 1 mrem. A time-slice comparison between the two mean annual dose projections is discussed Section 7.7.2.3 and shown on Figure 7.7.2-9. The TSPA-LA Model results show ^{99}Tc and ^{129}I as the main contributors to dose for the majority of the 1,000,000-year time period, whereas the Simplified TSPA dose history is largely dominated by ^{242}Pu, ^{237}Np, and ^{229}Th.

Igneous Intrusion Modeling Case Results—For this modeling case, the TSPA-LA Model results are shown on Figure 8.2-7 and the Simplified TSPA results on Figure 7.7.2-11. The TSPA-LA Model results show a mean annual dose history that rises until reaching a peak of 1 mrem at about 80,000 years and then remaining relatively flat thereafter. The Simplified TSPA results indicate a similar trend but reach a peak mean annual dose of 10 mrem. A time-slice comparison between the two mean annual dose projections is discussed Section 7.7.2.4 and shown on Figure 7.7.2-12. In both the TSPA-LA Model and Simplified TSPA projections, the initial peak dose is attributed to ^{239}Pu. From about 200,000 years to 1,000,000 years, the TSPA-LA Model results show that dose is largely attributed to ^{226}Ra, ^{242}Pu, and ^{237}Np. For this same time interval, the Simplified TSPA results show ^{242}Pu, ^{237}Np, and ^{229}Th as dominating the dose. As noted previously, the daughter products, such as ^{229}Th and ^{226}Ra, are computed differently in the two transport codes, which explain the differences.

Summary of Corroboration—For most of the modeling cases, the performance projections for two separate models compare reasonably well both in terms of the mean annual dose levels and the radionuclides important to the dose. The few differences noted are explainable and attributed to use of different approaches for calculating decay chain transport (i.e., differential transport of precursor and daughter product).

A more detailed discussion of the corroboration of the TSPA-LA Model results using the Simplified TSPA Analysis is presented Section 7.7.2.

8.4.4.2 Comparison with Electric Power Research Institute TSPA Analysis

The EPRI developed its own TSPA Analysis, which is implemented in the Integrated Multiple Assumptions and Release Code (IMARC) (EPRI 2005 [DIRS 178580]). EPRI developed IMARC to provide an independent assessment of key technical and scientific issues associated with the proposed repository at Yucca Mountain. Like the TSPA-LA Model, the EPRI TSPA Analysis uses coupled component models to simulate the response of the repository to changing conditions and disruptive events. With regard to treatment of uncertainty, the EPRI TSPA Analysis accounts for epistemic uncertainties in the model parameters but does not consider aleatory uncertainties associated with occurrence of disruptive events. At present, the EPRI TSPA Analysis only considers four scenarios consisting of nominal, igneous, seismic, and human intrusion. In contrast to the TSPA-LA Model, the EPRI TSPA Analysis for the nominal scenario includes early failure of one WP and one DS. The available EPRI documentation presents a simulation of postclosure performance for the combined nominal and early failure modeling case for a 1,000,000-year time period.

Combined Nominal and Early Failure Modeling Case Results—The TSPA-LA Model projections for this case are shown on Figure 7.7.3-3 and for IMARC on Figure 5-10 of *Program on Technology Innovation: Evaluation of a Spent Fuel Repository at Yucca Mountain, Nevada, 2005 Progress Report* (EPRI 2005 [DIRS 182229]). The mean annual dose history curves for

TSPA-LA Model and IMARC show a similar trend in the dose histories, with a significant increase in dose to the RMEI after about 100,000 years. The TSPA-LA Model projections indicate a peak mean annual dose of 0.4 mrem at 1,000,000 years, whereas the IMARC result shows a peak of about 0.02 mrem. In both the TSPA-LA Model and IMARC model results, the peak mean annual dose is dominated by a single radionuclide, ^{129}I. In addition to peak dose, the other notable difference between the two performance results is the initial breakthrough; the TSPA-LA Model results indicate dose exposure starting at about 400 to 500 years, whereas the IMARC results occur at about 7,000 years.

The main differences in the two independent projections are largely attributed to a distinct technical basis for the EBS and release rate calculation. For example, the EPRI TSPA Analysis only accounts for CSNF waste and considers failure of DS, WP, and cladding, whereas the TSPA-LA Model accounts for CSNF, DSNF, and HLW, but does not take credit for cladding in CSNF WPs. In addition, seepage rates used in the EPRI TSPA Analysis are significantly lower than the corresponding rates used in the TSPA-LA Model, which appear to cause a delay in radionuclide release from the EBS. There are other differences related to the abstraction of features and processes. It is important to keep in mind that the performance projections published by EPRI were intended to status the development of their independent capability and not to present a performance demonstration in accordance with NRC regulation.

Summary of Corroboration—The comparisons of performance projections generally corroborate the TSPA-LA results and therefore provide additional confidence in the validity and defensibility of the performance demonstration. A more detailed discussion of the comparison of the EPRI TSPA Analysis and TSPA-LA Model results is presented in Section 7.7.3

Performance Margin Analysis

A Performance Margin Analysis (PMA) was conducted to quantitatively evaluate the differences in repository performance due to significant explicit and implicit conservatisms embedded in the TSPA-LA Model subcomponents. The conservatisms were evaluated to (1) confirm that they are conservative with respect to the mean annual dose of the TSPA-LA Model; (2) quantify the extent to which they, individually and collectively, overestimate the projected annual dose; and (3) assess that the evaluated conservatisms did not introduce any inappropriate risk dilution in the TSPA-LA results presented in support of the LA. The PMA was conducted by first modifying selected submodels and parameters of the TSPA-LA Model, including the additional submodels and parameters for the PMA and then repeating the sequence of calculation for a select set of modeling cases that were run for the TSPA-LA. PMA was conducted for both 10,000-year and 1,000,000-year time periods and on the same set of modeling cases as the TSPA-LA Model. The details of approach and results of the PMA are presented in Section 7.7.4 with additional supporting material in Appendix C. Summarizing here, the results show that the conservatism evaluated in the PMA are indeed conservative with respect to the total system performance measures (e.g., peak mean annual dose), as the largest doses calculated in the PMA for the 10,000 year and 1,000,000 year are significantly lower than the doses used in compliance demonstration. The largest calculated PMA mean annual doses are lower by over an order of magnitude and a factor of two over the largest mean annual dose relative to the TSPA-LA Model (Section 8.1) for the time periods of 10,000 years and 1,000,000 years, respectively. Further, the PMA analysis demonstrated that the significant conservatisms did not introduce risk dilution in

the TSPA-LA results presented (Section 8.1.1 in Volume III) in support of compliance with the regulatory dose requirement, as demonstrated by the absence of higher peak doses in the PMA results for both the probabilistic projections of the expected annual dose and the comparison of the projected total mean annual dose for the PMA relative to the TSPA-LA. The PMA results also have different significant modeling cases than the TSPA-LA Model due primarily to the items selected for modification in PMA.

8.4.5 Reviews of YMP TSPA Methodology

Independent reviews have played an important role in the development and advancement of the TSPA-LA methodology, as well as in improving its overall conceptual framework. Peer reviews conducted by teams of external experts were commissioned by the YMP in order to ensure that the TSPA methodology would be based on well-established principles, evidence supported, and be technically defensible for the licensing review. Various national and international expert groups have participated in formal reviews of the TSPA methodology and its supporting technical basis. Moreover, various federal oversight and regulatory agencies have regularly reviewed the TSPA methodology. These agencies have included the Nuclear Waste Technical Review Board (NWTRB), NRC's Advisory Committee on Nuclear Waste, and NRC's Division of Nuclear Materials, Safety, and Safeguards staff.

In the subsequent text, three of the comprehensive reviews that were conducted by groups independent of the TSPA-LA Model development are summarized.

8.4.5.1 TSPA-Viability Assessment Peer Review

The first independent and formal evaluation of the TSPA methodology was conducted in support of the DOE Viability Assessment of the Yucca Mountain site (DOE 1998 [DIRS 101779]). The six member peer review group, designated as the TSPA-Viability Assessment (VA) Review Panel, conducted a phased review of the YMP's TSPA methodology over a two-year period. The TSPA-VA peer review was conducted in accordance with the Management and Operating Contractor's QA procedure, QAP-3-3, *Peer Review*, which was in effect at that time of the review.

With regard to the TSPA-VA methodology, the review panel concluded that the "overall performance assessment framework and the approach used to developing the TSPA-VA were sound and followed accepted methods" (Budnitz et al. 1999 [DIRS 102726], p. 2). However, the panel identified deficiencies in some of the component models; these aspects were judged deficient because they, in the view of the panel, lacked an adequate theoretical basis. Some of the review panel's major comments included: (1) TSPA component models and their adequacy to capture relevant phenomena, (2) proper coupling between TSPA component models and submodels, (3) testing and evaluation of the modeled behavior, (4) adequacy and completeness of the supporting database, (5) treatment of model and parameter uncertainties, and (6) potential non-conservative approaches.

Some of the panel's specific recommendations for improving the YMP's TSPA methodology included:

- Make the TSPA submodels more realistic, where supported by data
- Reduce uncertainty (i.e., epistemic) through additional data collection
- Perform additional auxiliary analyses and sensitivity analyses to better understand complex system behavior
- Perform qualitative and quantitative comparisons of the TSPA model components with several man-made and natural analogues
- Conduct follow-on peer reviews of the TSPA methodology.

The YMP implemented the review panel's recommendations for improving the TSPA methodology, as well as those for additional field and laboratory data collection. The review panel's final report is entitled *Peer Review of the Total System Performance Assessment-Viability Assessment Final Report* (Budnitz et al. 1999 [DIRS 102726]). The YMP staff responses to the review panel's comments and recommendations are documented in *Comment Response on the Final Report: Peer Review of the Total System Performance Assessment-Viability Assessment (TSPA-VA)* (CRWMS M&O 1999 [DIRS 153111]).

Additional information on the TSPA-VA review panel comments is presented in Section 7.9.1 of Volume II.

8.4.5.2 Joint Nuclear Energy/International Atomic Energy Agency Peer Review

At the request of DOE, the Organization for Economic Cooperation and Development's (OECD's) Nuclear Energy Agency (NEA) and the International Atomic Energy Agency (IAEA) assembled a team of experts to peer review the TSPA Model for Yucca Mountain. That version of the TSPA Model was to be used for the assessment conducted to support the DOE site recommendation (SR) process. The 10-member international review group, designated as the International Review Team (IRT), reviewed the following aspects of the TSPA-SR model:

- Technical basis for the performance assessment, including identification and justification of the conditions and characteristics modeled at the system level
- Development of the key conceptual models, including the assumptions made with respect to the representations of relevant FEPs
- Adequacy of the treatment of the undisturbed and disturbed system performance
- Adequacy of the methods used, and the cases considered, in sensitivity and uncertainty evaluations
- Overall clarity and completeness of the technical report describing this system-level performance evaluation.

The IRT review was conducted during June 2001 through December 2001. As indicated in their final report, the IRT concluded that "the TSPA-SR methodology is soundly based and has been implemented in a competent manner" (OECD and IAEA 2002 [DIRS 158098], p. 10). In their final report, the IRT made a total of 27 major recommendations for future improvements of the TSPA methodology. Some of the general recommendations for improvements included:

1. A more systematic treatment of uncertainties
2. An investigation of potential risk dilution
3. Improved characterization of the waste forms
4. Use of natural analogues.

The YMP addressed all of the IRT recommendations in developing the TSPA-LA model and in preparing the postclosure demonstration for the LA. The improved systematic treatment of aleatory and epistemic uncertainties is reflected in Section 6.1.2 (Volume I) and Appendix J (Volume III). The investigation of potential risk dilution was largely accomplished through a critical review of the TSPA parameter uncertainty characterizations, which is discussed in Section 8.4.3. Improved characterization of the waste forms is discussed in Section 6.3.7. The use of natural analogs is described in Section 7.8.

A more detailed summary of the IRT review comments and recommendations is presented in Section 7.9.2.

8.4.5.3 Independent Validation Review Team Technical Review

In early preparations for the LA, the YMP commissioned an independent and comprehensive review of the TSPA methodology with the objectives of: (1) examining the defensibility of the TSPA methodology, (2) implementing a model validation strategy, and (3) making a determination of model validity based on a technical review. The critical review of the technical basis was to be based on reviews of the supporting analysis and/or model reports. Implementation of the model validation strategy would follow the applicable process steps outlined in the NRC/SKI white paper on model validation (Eisenberg et al. 1999 [DIRS 155354], pp. 21 to 26). A determination of TSPA Model validity was to be based on conformance with detailed technical criteria. An independent group, designated as the Independent Validation Review Team (IVRT), was formed and chartered to accomplish the review objectives. This team was independent of the TSPA-LA Model development.

The in-depth critical reviews of the TSPA methodology were largely conducted in 2004, while the implementation of a model validation strategy and determination of model validity was performed in 2005. The technical review was conducted in accordance with the then effective QA procedure, LP-SIII.10Q-BSC, *Models*. The IVRT issued their final report in February 2006 (Booth 2006 [DIRS 176638]).

The following is a summary of the IVRT's major recommendations and findings that lead to further improvements of the TSPA-LA methodology.

Review TSPA Methodology and Technical Basis—The IVRT critical reviews of the TSPA technical basis were largely conducted in parallel with the preparation of the supporting analysis and/or model reports and the TSPA component models. The concurrent review and development

efforts had the advantage that the IVRT comments and recommendations could be addressed and incorporated in the final analysis and/or model reports and in the updated version of the TSPA Model. With regard to the TSPA methodology, the IVRT critique and recommendations lead to significant improvements (Booth 2006 [DIRS 176638]) in the defensibility of:

- Conceptual framework and mathematical formulation of the seismic ground motion and igneous intrusion component models
- Formulation and coupling of in-package chemistry and the radionuclide transport abstraction
- Biosphere dose conversion factors and number of key radionuclides considered in the calculation of organ dose
- Uncertainty characterizations for the igneous and seismic events.

The IVRT thoroughly reviewed all the draft analysis and/or model reports and provided nearly 400 technical comments; addressing those comments improved the defensibility of the technical basis as well as the transparency of analysis and/or model reports. One of the more important benefits of this part of the IVRT review was the careful scrutiny of the plausible conservatisms, identification of potential optimisms, and inconsistencies in draft component models. As a result of these comments, the TSPA staff corrected the inconsistencies and conducted impact analyses to evaluate the significance of the conservatisms and potential optimisms in terms of the relative movement of the mean dose curve.

Model Validation Process and Determination of Model Validity—As directed by the YMP, the IVRT critically reviewed the TSPA methodology against 20 technical criteria grouped into three categories (BSC 2005 [DIRS 173309], pp. 18 to 20), namely: (1) general criteria for the TSPA Model framework, (2) specific criteria for the component models and submodels, and (3) specific criteria for the total system model. A total of five general criteria were specified for the model framework that focused on examining the appropriateness and reasonableness of the overall conceptual model, identification of FEPs and inclusion in the models, consistency of the process models and derived abstractions, and confidence-building analyses. The specific criteria for submodels, which consisted of five criteria, focused on the mathematical basis of the models (e.g., assumptions and technical bases, time step and spatial discretization, and consistency of simulation outputs and model abstraction). The 10 specific criteria for the total system model covered such aspects as statistical sampling of uncertain parameters, initial and boundary conditions, parameter distributions, number of realizations, and verification of the TSPA-LA Model software.

The IVRT findings with respect to the general and specific review criteria are presented in the attachment to the memo containing reference to the TSPA-LA (Booth 2006 [DIRS 176638], Attachment draft Rev 01E, Sections C.5.1 through C.5.3, pp. C-39 through C-116). The IVRT determinations regarding the 20 criteria being met, or not met, were used to make a peer group judgment with respect to conformance with two key model validation goals (BSC 2005 [DIRS 173309], Section 2.10.1), namely:

1. To describe the postclosure performance of the repository system for the nominal, igneous, and seismic scenario classes

2. To produce an estimate of mean dose (and other performance measures, as appropriate) that is consistent with the degree of conservatism representative of the component abstraction models and parameters (and their uncertainty) that are input to the TSPA-LA Model.

The IVRT interpreted the first goal as to "require an approach to TSPA Model development that produced estimates of the performance measures of interest with neither pessimistic nor optimistic bias" (Booth 2006 [DIRS 176638], Attachment draft REV 01E, Section C.5.0.2, p. C-37). The second goal was interpreted by the IVRT to "require an approach to model development that did not underestimate the performance measures because the component [model] abstraction and parameter probability density functions were developed with a conservative bias" (Booth 2006 [DIRS 176638], Attachment draft REV 01E, Section C.5.0.2, p. C-37).

The IVRT finding for these two model validation goals was that they had not been met by the 2005 version of the TSPA Model. The rationale for their finding centered on their views that:

- Uncertainty was not characterized as realistically as available information and data allowed

- Inconsistent treatment of uncertainty among the barrier components

- Model appeared to contain potentially significant optimisms and conservatisms.

For the most part, the IVRT views were attributed to deficiencies in the component models for the DS and WP, which were not sufficiently mature at the time of the review. The optimisms referred to by the IVRT were attributed to the: (1) DS component model not accounting for degradation and failure mechanisms, and (2) DS and WP component models not accounting for early failures. With regard to conservatisms, the IVRT noted that the representation of the natural barriers was underestimated to the extent of being extremely conservative (Booth 2006 [DIRS 176638], Attachment draft REV 01E, Section C.5.1.1.2.1, p. C-42).

The IVRT's findings on the two model validation goals prompted additional work to improve the uncertainty treatment, remove the excessive model conservatisms and optimisms. Moreover, the IVRT's finding altered the TSPA compliance strategy from one that relied heavily on conservatism to one that used more realistic models and more rigorous representation of uncertainties.

Additional information on the IVRT review comments and recommendations are presented in Section 7.9.3.

9. INPUTS AND REFERENCES

9.1 DOCUMENTS CITED

159915 Abraham, S. 2002. Recommendation for Approval of the Yucca Mountain Site for the Development of a Nuclear Waste Repository, Along with a Comprehensive Statement of the Basis of Recommendation. Letter from S. Abraham (DOE) to The President, February 14, 2002, with attachment. ACC: HQO.20020325.0001; HQO.20020325.0002.

109715 Ahlers, C.F.; Finsterle, S.; and Bodvarsson, G.S. 1999. "Characterization and Prediction of Subsurface Pneumatic Response at Yucca Mountain, Nevada." *Journal of Contaminant Hydrology, 38,* (1-3), 47-68. New York, New York: Elsevier. TIC: 244160.

180383 Alekseenko, S.V.; Markovich, D.M.; Nakoryakov, V.E.; and Shtork, S.I. 1998. "Rivulet Flow of Liquid on the Outer Surface of an Inclined Cylinder." *Journal of Applied Mechanics and Technical Physics, 38,* (4), 649-653. [New York, New York]: Plenum Publishing. TIC: 259289.

103597 Altman, W.D.; Donnelly, J.P.; and Kennedy, J.E. 1988. *Peer Review for High-Level Nuclear Waste Repositories: Generic Technical Position.* NUREG-1297. Washington, D.C.: U.S. Nuclear Regulatory Commission. TIC: 200651.

169668 Anderson, T.W. 1984. *An Introduction to Multivariate Statistical Analysis.* 2nd Edition. New York, New York: John Wiley & Sons. TIC: 244809.

180487 Anovitz, L.M.; Riciputi, L.R.; Cole, D.R.; Gruszkiewicz, M.S.; and Elam, J.M. 2006. "The Effect of Changes in Relative Humidity on the Hydration Rate of Pachuca Obsidian." *Journal of Non-Crystalline Solids, 352,* 5652-5662. [New York, New York]: Elsevier. TIC: 259330.

169793 Anspaugh, L.R.; Simon, S.L.; Gordeev, K.I.; Likhtarev, I.A.; Maxwell, R.M.; and Shinkarev, S.M. 2002. "Movement of Radionuclides in Terrestrial Ecosystems by Physical Processes." *Health Physics, 82,* (5), 669-679. [Baltimore, Maryland: Lippincott Williams & Wilkins]. TIC: 256136.

107506 Apostolakis, G. 1990. "The Concept of Probability in Safety Assessments of Technological Systems." *Science, 250,* 1359-1364. Washington, D.C.: American Association for the Advancement of Science. TIC: 212560.

107710 Apostolakis, G.E. 1989. "Uncertainty in Probabilistic Safety Assessment." *Nuclear Engineering and Design, 115,* (1), 173-179. Amsterdam, The Netherlands: Elsevier. TIC: 245806.

182227 Apted, M. 2006. *Program on Technology Innovation: Effects of Multiple Seismic Events and Rockfall on Long-Term Performance of the Yucca Mountain Repository.* EPRI TR 1013444. Palo Alto, California: Electric Power Research Institute. TIC: 259559.

182327 Apted, M. and Kessler, J. 2005. *Program on Technology Innovation: Potential Igneous Processes Relevant to the Yucca Mountain Repository: Intrusive-Release Scenario, Analysis and Implications.* EPRI TR 1011165. Palo Alto, California: Electric Power Research Institute. TIC: 259646.

182228 Apted, M. and Kessler, M. 2005. *Program on Technology Innovation: Effects of Seismicity and Rockfall on Long-Term Performance of the Yucca Mountain Repository, 2005 Progress Report.* EPRI TR 1011812. Palo Alto, California: Electric Power Research Institute. TIC: 259560.

182229 Apted, M. and Ross, A. 2005. *Program on Technology Innovation: Evaluation of a Spent Fuel Repository at Yucca Mountain, Nevada, 2005 Progress Report.* EPRI TR 1010074. Palo Alto, California: Electric Power Research Institute. TIC: 259561.

182231 Apted, M.; Ross, A.; and Kessler, J. 2006. *Program on Technology Innovation: EPRI Yucca Mountain Spent Fuel Repository Evaluation, 2006 Progress Report.* EPRI TR 1013445. Palo Alto, California: Electric Power Research Institute. TIC: 259562.

141615 ASM International 1990. *Properties and Selection: Nonferrous Alloys and Special-Purpose Materials.* Volume 2 of *ASM Handbook.* Formerly Tenth Edition, Metals Handbook. 5th Printing 1998. [Materials Park, Ohio]: ASM International. TIC: 241059.

133378 ASM International. 1987. *Corrosion.* Volume 13 of *ASM Handbook.* Formerly 9th Edition, Metals Handbook. [Materials Park, Ohio]: ASM International. TIC: 240704.

145103 ASME (American Society of Mechanical Engineers) 1998. *1998 ASME Boiler and Pressure Vessel Code.* 1998 Edition with 1999 and 2000 Addenda. New York, New York: American Society of Mechanical Engineers. TIC: 247429.

105725 ASTM C 1174-97. 1998. *Standard Practice for Prediction of the Long-Term Behavior of Materials, Including Waste Forms, Used in Engineered Barrier Systems (EBS) for Geological Disposal of High-Level Radioactive Waste.* West Conshohocken, Pennsylvania: American Society for Testing and Materials. TIC: 246015.

103508 Avallone, E.A. and Baumeister, T., III, eds. 1987. *Marks' Standard Handbook for Mechanical Engineers.* 9th Edition. New York, New York: McGraw-Hill. TIC: 206891.

159379 Aziz, P.M. 1956. "Application of the Statistical Theory of Extreme Values to the Analysis of Maximum Pit Depth Data for Aluminum." *Corrosion, 12,* (10), 35-46. Houston, Texas: National Association of Corrosion Engineers. TIC: 241560.

100309 Barnard, R.W.; Wilson, M.L.; Dockery, H.A.; Gauthier, J.H.; Kaplan, P.G.; Eaton, R.R.; Bingham, F.W.; and Robey, T.H. 1992. *TSPA 1991: An Initial Total-System Performance Assessment for Yucca Mountain.* SAND91-2795. Albuquerque, New Mexico: Sandia National Laboratories. ACC: NNA.19920630.0033.

156269 Bear, J. 1972. *Dynamics of Fluids in Porous Media.* Environmental Science Series. Biswas, A.K., ed. New York, New York: Elsevier. TIC: 217356.

166708 Beer, F.P. and Johnston, E.R., Jr. 1981. *Mechanics of Materials.* New York, New York: McGraw-Hill. TIC: 255414.

180397 Belton, J.W. 1935. "The Surface Tensions of Ternary Solutions. Part I. The Surface Tensions of Aqueous Solutions of (a) Sodium and Potassium Chlorides, (b) Sodium Chloride and Hydrochloric Acid.." *Transactions of the Faraday Society, XXXI,* 1413-1419. Edinburgh, Scotland: Gurney and Jackson. TIC: 259689.

105742 Bernstein, P.L. 1996. *Against the Gods: The Remarkable Story of Risk.* New York, New York: John Wiley & Sons. TIC: 245429.

179825 Beven, K.; Freer, J.; Hankin, B.; and Schulz, K. 2000. "The Use of Generalised Likelihood Measures for Uncertainty Estimation in High-Order Models of Environmental Systems." *Nonlinear and Nonstationary Signal Processing.* Fitzgerald, W.J.; Smith, R.L.; Walden, A.T.; and Young, P.C.; eds. Pages 115-151. New York, New York: Cambridge University Press. TIC: 259258.

154522 BIOMASS (Biosphere Modelling and Assessment) 2000. *Example Reference Biosphere 2A: Agricultural Well, Constant Biosphere.* Draft TECDOC. BIOMASS/T1/WD08. Vienna, Austria: International Atomic Energy Agency, Division of Radiation and Waste Safety. TIC: 249456.

168563 BIOMASS (Biosphere Modelling and Assessment) 2003. *"Reference Biospheres" for Solid Radioactive Waste Disposal, Report of BIOMASS Theme 1 of the BIOsphere Modelling and ASSessment (BIOMASS) Programme, Part of the IAEA Co-ordinated Research Project on Biosphere Modelling and Assessment (BIOMASS).* IAEA-BIOMASS-6. Vienna, Austria: International Atomic Energy Agency, Waste Safety Section. TIC: 255411.

180470 Blake, C.A.; Coleman, C.F.; Brown, K.B.; Hill, D.G.; Lowrie, R.S.; and Schmitt, J.M. 1956. "Studies in the Carbonate-Uranium System." *Journal of the American Chemical Society, 78,* 5978-5983. [Washington, D.C.: American Chemical Society]. TIC: 219100.

162477 Bodvarsson, G.S.; Kwicklis, E.; Shan, C.; and Wu, Y.S. 2003. "Estimation of Percolation Flux from Borehole Temperature Data at Yucca Mountain, Nevada." *Journal of Contaminant Hydrology, 62-63,* 3-22. New York, New York: Elsevier. TIC: 254205.

159041 Bonano, E.J. and Apostolakis, G.E. 1991. "Theoretical Foundations and Practical Issues for Using Expert Judgements in Uncertainty Analysis of High-Level Radioactive Waste Disposal." *Radioactive Waste Management and the Nuclear Fuel Cycle, 16,* (2), 137-158. [New York, New York]: Harwood Academic Publishers. TIC: 252826.

176638 Booth, T.C. 2006. "Independent Validation Review Team (IVRT) Issues, Bechtel-SAIC Responses, and IVRT Assessment of Responses Related to Review of the TSPA Model and Supporting Analyses and Model Reports (AMRs)." Interoffice memorandum from T.C. Booth (BSC) to File, March 16, 2006, 0315068011, with enclosures. ACC: MOL.20060320.0115.

155233 Bourgoyne, A.T., Jr.; Millheim, K.K.; Chenevert, M.E.; and Young, F.S., Jr. 1986. "Rotary Drilling Bits." *Applied Drilling Engineering.* [SPE Textbook Series Volume 2]. Pages 190-245. Richardson, Texas: Society of Petroleum Engineers. TIC: 250085.

155318 Boyer, H.E. and Gall, T.L., eds. [1984]. *Metals Handbook.* Desk Edition. 10th Printing 1997. Metals Park, Ohio: American Society for Metals. TIC: 250192.

107727 Breeding, R.J.; Helton, J.C.; Gorham, E.D.; and Harper, F.T. 1992. "Summary Description of the Methods Used in the Probabilistic Risk Assessments for NUREG-1150." *Nuclear Engineering and Design, 135,* 1-27. New York, New York: Elsevier. TIC: 246312.

159576 Brocoum, S. 2001. "Transmittal of Report Addressing Key Technical Issues (KTI) Structural Deformation and Seismicity (SDS)." Letter from S. Brocoum (DOE/YMSCO) to C.W. Reamer (NRC), October 25, 2001, OL&RC:TCG-0140, with enclosure. ACC: MOL.20020304.0297; MOL.20030714.0094.

162420 Brossia, C.S. and Cragnolino, G.A. 2001. "Effects of Environmental and Metallurgical Conditions on the Passive and Localized Dissolution of Ti-0.15%Pd." *Corrosion, 57,* (9), 768-776. Houston, Texas: National Association of Corrosion Engineers. TIC: 254028.

180832 Brossia, C.S. and Cragnolino, G.A. 2004. "Effect of Palladium on the Corrosion Behavior of Titanium." *Corrosion Science, 46,* 1693-1711. [New York, New York]: Elsevier. TIC: 259423.

154657 BSC (Bechtel SAIC Company) 2001. *FY01 Supplemental Science and Performance Analyses, Volume 1: Scientific Bases and Analyses.* TDR-MGR-MD-000007 REV 00. Las Vegas, Nevada: Bechtel SAIC Company. ACC: MOL.20010712.0062.

167572 BSC (Bechtel SAIC Company) 2001. *MKTABLE Software Management Report.* SDN: 10505-SMR-1.00-00. Las Vegas, Nevada: Bechtel SAIC Company. ACC: MOL.20010712.0055.

161068 BSC (Bechtel SAIC Company) 2002. *Design Document (DD) for iTOUGH2 V5.0.* DI: 10003-DD-5.0-00. Las Vegas, Nevada: Bechtel SAIC Company. ACC: MOL.20020923.0144.

167547 BSC (Bechtel SAIC Company) 2002. *Design Document for WAPDEG 4.07.* SDN: 10000-DD-04.07-00. Las Vegas, Nevada: Bechtel SAIC Company. ACC: MOL.20030409.0229; MOL.20040427.0343.

158794 BSC (Bechtel SAIC Company) 2002. *Guidelines for Developing and Documenting Alternative Conceptual Models, Model Abstractions, and Parameter Uncertainty in the Total System Performance Assessment for the License Application.* TDR-WIS-PA-000008 REV 00 ICN 01. Las Vegas, Nevada: Bechtel SAIC Company. ACC: MOL.20020904.0002.

167548 BSC (Bechtel SAIC Company) 2002. *Installation Test Plan for WAPDEG 4.07.* SDN: 10000-ITP-4.07-01. Las Vegas, Nevada: Bechtel SAIC Company. ACC: MOL.20030409.0231; MOL.20040427.0343.

161067 BSC (Bechtel SAIC Company) 2002. *Requirements Document (RD) for iTOUGH2 V5.0-00.* DI: 10003-RD-5.0-0. Las Vegas, Nevada: Bechtel SAIC Company. ACC: MOL.20020923.0143.

167545 BSC (Bechtel SAIC Company) 2002. *Requirements Document for WAPDEG 4.07.* SDN: 10000-RD-4.07-00. Las Vegas, Nevada: Bechtel SAIC Company. ACC: MOL.20030409.0228; MOL.20040427.0343.

161066 BSC (Bechtel SAIC Company) 2002. *User's Manual (UM) for iTOUGH2 V5.0.* DI: 10003-UM-5.0-00. Las Vegas, Nevada: Bechtel SAIC Company. ACC: MOL.20020923.0147.

162606 BSC (Bechtel SAIC Company) 2002. *Users' Manual for WAPDEG 4.07.* SDN: 10000-UM-4.07-00. Las Vegas, Nevada: Bechtel SAIC Company. ACC: MOL.20030409.0233; MOL.20040427.0343.

167542 BSC (Bechtel SAIC Company) 2002. *Validation Test Plan for WAPDEG 4.07.* SDN: 10000-VTP-4.07-00. Las Vegas, Nevada: Bechtel SAIC Company. ACC: MOL.20030409.0232; MOL.20040427.0343.

160437 BSC (Bechtel SAIC Company) 2002. *Validation Test Report (VTR) for iTOUGH2 V5.0.* 10003-VTR-5.0-00. Las Vegas, Nevada: Bechtel SAIC Company. ACC: MOL.20020923.0148.

167554 BSC (Bechtel SAIC Company) 2002. *Validation Test Report for WAPDEG 4.07.* SDN: 10000-VTR-4.07-00. Las Vegas, Nevada: Bechtel SAIC Company. ACC: MOL.20030409.0234; MOL.20040427.0343.

163152 BSC (Bechtel SAIC Company) 2003. *Dissolved Concentration Limits of Radioactive Elements.* ANL-WIS-MD-000010 REV 02. Las Vegas, Nevada: Bechtel SAIC Company. ACC: DOC.20030624.0003.

161962 BSC (Bechtel SAIC Company) 2003. *In-Package Chemistry Abstraction.* ANL-EBS-MD-000037 REV 02. Las Vegas, Nevada: Bechtel SAIC Company. ACC: DOC.20030723.0003.

161727 BSC (Bechtel SAIC Company) 2003. *Repository Design, Repository/PA IED Subsurface Facilities.* 800-IED-EBS0-00402-000-00B. Las Vegas, Nevada: Bechtel SAIC Company. ACC: MOL.20030109.0146.

161317 BSC (Bechtel SAIC Company) 2003. *WAPDEG Analysis of Waste Package and Drip Shield Degradation.* ANL-EBS-PA-000001 REV 01. Las Vegas, Nevada: Bechtel SAIC Company. ACC: DOC.20031208.0004.

170038 BSC (Bechtel SAIC Company) 2004. *Analysis of Hydrologic Properties Data.* ANL-NBS-HS-000042 REV 00. Las Vegas, Nevada: Bechtel SAIC Company. ACC: DOC.20041005.0004; DOC.20050815.0003.

170024 BSC (Bechtel SAIC Company) 2004. *Analysis of Mechanisms for Early Waste Package/Drip Shield Failure.* CAL-EBS-MD-000030 REV 00C. Las Vegas, Nevada: Bechtel SAIC Company. ACC: DOC.20040913.0006; DOC.20050606.0005; DOC.20050830.0002.

169857 BSC (Bechtel SAIC Company) 2004. *Calibrated Properties Model.* MDL-NBS-HS-000003 REV 02. Las Vegas, Nevada: Bechtel SAIC Company. ACC: DOC.20041006.0004.

169989 BSC (Bechtel SAIC Company) 2004. *Characterize Framework for Igneous Activity at Yucca Mountain, Nevada.* ANL-MGR-GS-000001 REV 02. Las Vegas, Nevada: Bechtel SAIC Company. ACC: DOC.20041015.0002; DOC.20050718.0007.

170035 BSC (Bechtel SAIC Company) 2004. *Conceptual Model and Numerical Approaches for Unsaturated Zone Flow and Transport.* MDL-NBS-HS-000005 REV 01. Las Vegas, Nevada: Bechtel SAIC Company. ACC: DOC.20040922.0006; DOC.20050307.0009.

169987 BSC (Bechtel SAIC Company) 2004. *CSNF Waste Form Degradation: Summary Abstraction.* ANL-EBS-MD-000015 REV 02. Las Vegas, Nevada: Bechtel SAIC Company. ACC: DOC.20040908.0001; DOC.20050620.0004.

169988 BSC (Bechtel SAIC Company) 2004. *Defense HLW Glass Degradation Model.* ANL-EBS-MD-000016 REV 02. Las Vegas, Nevada: Bechtel SAIC Company. ACC: DOC.20041020.0015; DOC.20050922.0002.

169855 BSC (Bechtel SAIC Company) 2004. *Development of Numerical Grids for UZ Flow and Transport Modeling.* ANL-NBS-HS-000015 REV 02. Las Vegas, Nevada: Bechtel SAIC Company. ACC: DOC.20040901.0001.

169425 BSC (Bechtel SAIC Company) 2004. *Dissolved Concentration Limits of Radioactive Elements.* ANL-WIS-MD-000010 REV 03. Las Vegas, Nevada: Bechtel SAIC Company. ACC: DOC.20041109.0006.

166107 BSC (Bechtel SAIC Company) 2004. *Drift Degradation Analysis.* ANL-EBS-MD-000027 REV 03. Las Vegas, Nevada: Bechtel SAIC Company. ACC: DOC.20040915.0010; DOC.20050419.0001; DOC.20051130.0002; DOC.20060731.0005.

170040 BSC (Bechtel SAIC Company) 2004. *Drift-Scale Radionuclide Transport.* MDL-NBS-HS-000016 REV 01. Las Vegas, Nevada: Bechtel SAIC Company. ACC: DOC.20040927.0031; DOC.20050927.0003.

172453 BSC (Bechtel SAIC Company) 2004. *DSNF and Other Waste Form Degradation Abstraction.* ANL-WIS-MD-000004 REV 04. Las Vegas, Nevada: Bechtel SAIC Company. ACC: DOC.20041201.0007.

170002 BSC (Bechtel SAIC Company) 2004. *Future Climate Analysis.* ANL-NBS-GS-000008 REV 01. Las Vegas, Nevada: Bechtel SAIC Company. ACC: DOC.20040908.0005.

169218 BSC (Bechtel SAIC Company) 2004. *Natural Analogue Synthesis Report.* TDR-NBS-GS-000027 REV 01. Las Vegas, Nevada: Bechtel SAIC Company. ACC: DOC.20040524.0008.

172452 BSC (Bechtel SAIC Company) 2004. *Performance Confirmation Plan.* TDR-PCS-SE-000001 REV 05. Las Vegas, Nevada: Bechtel SAIC Company. ACC: DOC.20041122.0002.

170006 BSC (Bechtel SAIC Company) 2004. *Saturated Zone Colloid Transport.* ANL-NBS-HS-000031 REV 02. Las Vegas, Nevada: Bechtel SAIC Company. ACC: DOC.20041008.0007; DOC.20051215.0005.

167652 BSC (Bechtel SAIC Company) 2004. *Seepage Model for PA Including Drift Collapse.* MDL-NBS-HS-000002 REV 03. Las Vegas, Nevada: Bechtel SAIC Company. ACC: DOC.20040922.0008; DOC.20051205.0001.

170950 BSC (Bechtel SAIC Company) 2004. *Technical Work Plan for: Near-Field Environment and Transport In-Drift Heat and Mass Transfer Model and Analysis Reports Integration.* TWP-MGR-PA-000018 REV 01. Las Vegas, Nevada: Bechtel SAIC Company. ACC: DOC.20040729.0006.

167969 BSC (Bechtel SAIC Company) 2004. *Technical Work Plan for: Performance Assessment Unsaturated Zone.* TWP-NBS-HS-000003 REV 02 [Errata 001]. Las Vegas, Nevada: Bechtel SAIC Company. ACC: MOL.20030102.0108; DOC.20040121.0001.

168449 BSC (Bechtel SAIC Company) 2004. *Technical Work Plan for: TSPA-LA Model Development, Initial Use, and Documentation.* TWP-MGR-PA-000012 REV 00. Las Vegas, Nevada: Bechtel SAIC Company. ACC: DOC.20040322.0003.

169861 BSC (Bechtel SAIC Company) 2004. *UZ Flow Models and Submodels.* MDL-NBS-HS-000006 REV 02. Las Vegas, Nevada: Bechtel SAIC Company. ACC: DOC.20041101.0004; DOC.20050629.0003.

169996 BSC (Bechtel SAIC Company) 2004. *WAPDEG Analysis of Waste Package and Drip Shield Degradation.* ANL-EBS-PA-000001 REV 02. Las Vegas, Nevada: Bechtel SAIC Company. ACC: DOC.20041004.0005.

169734 BSC (Bechtel SAIC Company) 2004. *Yucca Mountain Site Description.* TDR-CRW-GS-000001 REV 02 ICN 01. Two volumes. Las Vegas, Nevada: Bechtel SAIC Company. ACC: DOC.20040504.0008.

174067 BSC (Bechtel SAIC Company) 2005. *Atmospheric Dispersal and Deposition of Tephra from a Potential Volcanic Eruption at Yucca Mountain, Nevada.* MDL-MGR-GS-000002 REV 02. Las Vegas, Nevada: Bechtel SAIC Company. ACC: DOC.20050825.0001; DOC.20050908.0001; DOC.20060306.0008.

172827 BSC (Bechtel SAIC Company) 2005. *Characteristics of the Receptor for the Biosphere Model.* ANL-MGR-MD-000005 REV 04. Las Vegas, Nevada: Bechtel SAIC Company. ACC: DOC.20050405.0005.

173800 BSC (Bechtel SAIC Company) 2005. *Development of the Total System Performance Assessment-License Application Features, Events, and Processes.* TDR-WIS-MD-000003 REV 02. Las Vegas, Nevada: Bechtel SAIC Company. ACC: DOC.20050829.0004.

172232 BSC (Bechtel SAIC Company) 2005. *Drift-Scale Coupled Processes (DST and TH Seepage) Models.* MDL-NBS-HS-000015 REV 02. Las Vegas, Nevada: Bechtel SAIC Company. ACC: DOC.20050114.0004; DOC.20051115.0002.

173981 BSC (Bechtel SAIC Company) 2005. *Features, Events, and Processes: Disruptive Events.* ANL-WIS-MD-000005 REV 03. Las Vegas, Nevada: Bechtel SAIC Company. ACC: DOC.20050830.0008.

173303 BSC (Bechtel SAIC Company) 2005. *IED Interlocking Drip Shield and Emplacement Pallet [Sheet 1 of 1].* 800-IED-WIS0-00401-000-00E. Las Vegas, Nevada: Bechtel SAIC Company. ACC: ENG.20050301.0007.

174101 BSC (Bechtel SAIC Company) 2005. *Mountain-Scale Coupled Processes (TH/THC/THM) Models.* MDL-NBS-HS-000007 REV 03. Las Vegas, Nevada: Bechtel SAIC Company. ACC: DOC.20050825.0007.

173309 BSC (Bechtel SAIC Company) 2005. *Technical Work Plan for: TSPA-LA FY 05-06 Activities.* TWP-MGR-PA-000031 REV 00. Las Vegas, Nevada: Bechtel SAIC Company. ACC: DOC.20050401.0006.

178275 BSC (Bechtel SAIC Company) 2006. *Analysis of Alcove 8/Niche 3 Flow and Transport Tests.* ANL-NBS-HS-000056 REV 00. Las Vegas, Nevada: Bechtel SAIC Company. ACC: DOC.20060901.0003.

178672 BSC (Bechtel SAIC Company) 2006. *Impacts of Solubility and Other Geochemical Processes on Radionuclide Retardation in the Natural System – Rev 01.* Las Vegas, Nevada: Bechtel SAIC Company. ACC: MOL.20060105.0022.

177101 BSC (Bechtel SAIC Company) 2006. *Inhalation Exposure Input Parameters for the Biosphere Model.* ANL-MGR-MD-000001 REV 04. Las Vegas, Nevada: Bechtel SAIC Company. ACC: DOC.20060605.0011.

177375 BSC (Bechtel SAIC Company) 2006. *Technical Work Plan for Saturated Zone Flow and Transport Modeling.* TWP-NBS-MD-000006 REV 02. Las Vegas, Nevada: Bechtel SAIC Company. ACC: DOC.20060519.0002.

177389 BSC (Bechtel SAIC Company) 2006. *Technical Work Plan for Waste Form Testing and Modeling.* TWP-WIS-MD-000018 REV 01. Las Vegas, Nevada: Bechtel SAIC Company. ACC: DOC.20060817.0001.

178448 BSC (Bechtel SAIC Company) 2006. *Technical Work Plan for: Igneous Activity Assessment for Disruptive Events.* TWP-WIS-MD-000007 REV 09 ICN 01. Las Vegas, Nevada: Bechtel SAIC Company. ACC: DOC.20060814.0018.

177739 BSC (Bechtel SAIC Company) 2006. *Technical Work Plan for: Near-Field Environment: Engineered Barrier System: Radionuclide Transport Abstraction Model Report.* TWP-MGR-PA-000020 REV 03. Las Vegas, Nevada: Bechtel SAIC Company. ACC: DOC.20060915.0005.

177465 BSC (Bechtel SAIC Company) 2006. *Technical Work Plan for: Unsaturated Zone Flow, Drift Seepage and Unsaturated Zone Transport Modeling.* TWP-MGR-HS-000004 REV 04. Las Vegas, Nevada: Bechtel SAIC Company. ACC: DOC.20060824.0001.

178693 BSC (Bechtel SAIC Company) 2007. *Subsurface Geotechnical Parameters Report.* ANL-SSD-GE-000001 REV 00. Las Vegas, Nevada: Bechtel SAIC Company. ACC: ENG.20070115.0006.

102726 Budnitz, B.; Ewing, R.C.; Moeller, D.W.; Payer, J.; Whipple, C.; and Witherspoon, P.A. 1999. *Peer Review of the Total System Performance Assessment-Viability Assessment Final Report.* Las Vegas, Nevada: Total System Performance Assessment Peer Review Panel. ACC: MOL.19990317.0328.

103635 Budnitz, R.J.; Apostolakis, G.; Boore, D.M.; Cluff, L.S.; Coppersmith, K.J.; Cornell, C.A.; and Morris, P.A. 1997. *Recommendations for Probabilistic Seismic Hazard Analysis: Guidance on the Uncertainty and Use of Experts.* NUREG/CR-6372. Two volumes. Washington, D.C.: U.S. Nuclear Regulatory Commission. TIC: 235076; 235074.

159728 Bureau of the Census. 2002. "2000 Summary File 3 (SF 3) Sample Data, Amargosa Valley CCD, Nye County, Nevada." Washington, D.C.: U.S. Department of Commerce, Bureau of the Census. Accessed August 28, 2002. TIC: 253098. URL: http://factfinder.census.gov/servlet/DTTable?_ts=48597952130

163209 Byers, C.D.; Jercinovic, M.J.; Ewing, R.C.; and Keil, K. 1985. "Basalt Glass: An Analogue for the Evaluation of the Long-Term Stability of Nuclear Waste Form Borosilicate Glasses." *Scientific Basis for Nuclear Waste Management VIII, Symposium held November 26-29, 1984, Boston, Massachusetts.* Jantzen, C.M.; Stone, J.A.; and Ewing, R.C., eds. *44,* 583-590. Pittsburgh, Pennsylvania: Materials Research Society. TIC: 203665.

179405 Campbell, G.S. 1974. "A Simple Method for Determining Unsaturated Conductivity from Moisture Retention Data." *Soil Science, 117,* (6), 311-314. Baltimore, Maryland: Williams & Wilkins]. TIC: 259680.

180398 Campbell, G.S. and Shiozawa, Sho 1992. "Prediction of Hydraulic Properties of Soils Using Particle-Size Distribution and Bulk Density Data." *Indirect Methods for Estimating the Hydraulic Properties of Unsaturated Soils, Proceedings of the International Workshop on Indirect Methods for Estimating the Hydraulic Properties of Unsaturated Soils, Riverside, Californaia, October 11-13, 1989.* van Genuchten, M.Th.; Leij, F.J.; and Lund, L.J., eds. Pages 317-328. Riverside, California: U.S. Department of Agriculture, Agricultural Research Service. TIC: 259691.

106346 Chen, F.; Ewing R.C.; and Clark S.B. 1999. "The Gibbs Free Energies and Enthalpies of Formation of U6+ Phases: An Empirical Method of Prediction." *American Mineralogist, 84,* (4), 650-664. Washington, D.C.: American Mineralogist. TIC: 245800.

103714 Codell, R.; Eisenberg, N.; Fehringer, D.; Ford, W.; Margulies, T.; McCartin, T.; Park, J.; and Randall, J. 1992. *Initial Demonstration of the NRC's Capability to Conduct a Performance Assessment for a High-Level Waste Repository.* NUREG-1327. Washington, D.C.: U.S. Nuclear Regulatory Commission. TIC: 204809.

102646 Connor, C.B. and Hill, B.E. 1995. "Three Nonhomogeneous Poisson Models for the Probability of Basaltic Volcanism: Application to the Yucca Mountain Region, Nevada." *Journal of Geophysical Research, 100,* (B6), 10,107-10,125. Washington, D.C.: American Geophysical Union. TIC: 237682.

158968 Cooke, R.M. 1991. *Experts in Uncertainty, Opinion and Subjective Probability in Science.* Oxford, New York: Oxford University Press. TIC: 252710.

101234 Cranwell, R.M.; Guzowski, R.V.; Campbell, J.E.; and Ortiz, N.R. 1990. *Risk Methodology for Geologic Disposal of Radioactive Waste, Scenario Selection Procedure.* NUREG/CR-1667. Washington, D.C.: U.S. Nuclear Regulatory Commission. ACC: NNA.19900611.0073.

100720 Criscenti, L.J.; Laniak, G.F.; and Erikson, R.L. 1996. "Propagation of Uncertainty through Geochemical Code Calculations." *Geochimica et Cosmochimica Acta, 60,* (19), 3551-3568. New York, New York: Pergamon Press. TIC: 239507.

163211 Crovisier, J.L.; Fritz, B.; Grambow, B.; and Eberhart, J.P. 1986. "Dissolution of Basaltic Glass in Seawater: Experiments and Thermodynamic Modelling." *Scientific Basis for Nuclear Waste Management IX, Symposium held September 9-11, 1985, Stockholm, Sweden.* Werme, L.O., ed. *50,* 273-280. Pittsburgh, Pennsylvania: Materials Research Society. TIC: 203664.

180488 Crovisier, J-L.; Advocat, T.; and Dussossoy, J-L. 2003. "Nature and Role of Natural Alteration Gels Formed on the Surface of Ancient Volcanic Glasses (Natural Analogs of Waste Containment Glasses)." *Journal of Nuclear Materials, 321,* 91-109. [New York, New York]: Elsevier. TIC: 259328.

100198 CRWMS M&O 1995. *Total System Performance Assessment - 1995: An Evaluation of the Potential Yucca Mountain Repository.* B00000000-01717-2200-00136 REV 01. Las Vegas, Nevada: CRWMS M&O. ACC: MOL.19960724.0188.

100116 CRWMS M&O 1996. *Probabilistic Volcanic Hazard Analysis for Yucca Mountain, Nevada.* BA0000000-01717-2200-00082 REV 0. Las Vegas, Nevada: CRWMS M&O. ACC: MOL.19971201.0221.

101111 CRWMS M&O 1997. *Saturated Zone Flow and Transport Expert Elicitation Project.* Las Vegas, Nevada: CRWMS M&O. ACC: MOL.19980224.0353.

123196 CRWMS M&O 1998. "Geology and Geochronology of Basaltic Volcanism in the Yucca Mountain Region." Chapter 2 of *Synthesis of Volcanism Studies for the Yucca Mountain Site Characterization Project.* Deliverable 3781MR1. Las Vegas, Nevada: CRWMS M&O. ACC: MOL.19990511.0400.

100356 CRWMS M&O 1998. "Unsaturated Zone Hydrology Model." Chapter 2 of *Total System Performance Assessment-Viability Assessment (TSPA-VA) Analyses Technical Basis Document.* B00000000-01717-4301-00002 REV 01. Las Vegas, Nevada: CRWMS M&O. ACC: MOL.19981008.0002.

103731 CRWMS M&O 1998. *Probabilistic Seismic Hazard Analyses for Fault Displacement and Vibratory Ground Motion at Yucca Mountain, Nevada.* Milestone SP32IM3, September 23, 1998. Three volumes. Las Vegas, Nevada: CRWMS M&O. ACC: MOL.19981207.0393.

100353 CRWMS M&O 1998. *Saturated Zone Flow and Transport Expert Elicitation Project.* Deliverable SL5X4AM3. Las Vegas, Nevada: CRWMS M&O. ACC: MOL.19980825.0008.

105347 CRWMS M&O 1998. *Synthesis of Volcanism Studies for the Yucca Mountain Site Characterization Project.* Deliverable 3781MR1. Las Vegas, Nevada: CRWMS M&O. ACC: MOL.19990511.0400.

100349 CRWMS M&O 1998. *Waste Package Degradation Expert Elicitation Project.* Rev. 1. Las Vegas, Nevada: CRWMS M&O. ACC: MOL.19980727.0002.

153111 CRWMS M&O 1999. *Comment Response on the Final Report: Peer Review of the Total System Performance Assessment-Viability Assessment (TSPA-VA).* B00000000-01717-5700-00037 REV 01. Las Vegas, Nevada: CRWMS M&O. ACC: MOL.19990920.0197.

152499 CRWMS M&O 2000. *SCCD Software Routine Report.* SDN: 10343-SRR-2.01-00. Las Vegas, Nevada: CRWMS M&O. ACC: MOL.20010205.0113.

143665 CRWMS M&O 2000. *Total System Performance Assessment for the Site Recommendation.* TDR-WIS-PA-000001 REV 00. Las Vegas, Nevada: CRWMS M&O. ACC: MOL.20001005.0282.

153246 CRWMS M&O 2000. *Total System Performance Assessment for the Site Recommendation.* TDR-WIS-PA-000001 REV 00 ICN 01. Las Vegas, Nevada: CRWMS M&O. ACC: MOL.20001220.0045.

154291 CRWMS M&O 2001. *Abstraction of Drift Seepage.* ANL-NBS-MD-000005 REV 01. Las Vegas, Nevada: CRWMS M&O. ACC: MOL.20010309.0019.

153263 CRWMS M&O 2001. *EQ6 Calculations for Chemical Degradation of N Reactor (U-metal) Spent Nuclear Fuel Waste Packages.* CAL-EDC-MD-000010 REV 00. Las Vegas, Nevada: CRWMS M&O. ACC: MOL.20010227.0017.

160149 Czarnecki, J.B. 1985. *Simulated Effects of Increased Recharge on the Ground-Water Flow System of Yucca Mountain and Vicinity, Nevada-California.* Water-Resources Investigations Report 84-4344. Denver, Colorado: U.S. Geological Survey. TIC: 203222.

100131 D'Agnese, F.A.; Faunt, C.C.; Turner, A.K.; and Hill, M.C. 1997. *Hydrogeologic Evaluation and Numerical Simulation of the Death Valley Regional Ground-Water Flow System, Nevada and California.* Water-Resources Investigations Report 96-4300. Denver, Colorado: U.S. Geological Survey. ACC: MOL.19980306.0253.

120425 D'Agnese, F.A.; O'Brien, G.M.; Faunt, C.C.; and San Juan, C.A. 1999. *Simulated Effects of Climate Change on the Death Valley Regional Ground-Water Flow System, Nevada and California.* Water-Resources Investigations Report 98-4041. Denver, Colorado: U.S. Geological Survey. TIC: 243555.

182090 Dartevelle, S. and Valentine, G. A. 2007. *Interaction of Multiphase Magmatic Flows with Underground Openings at the Proposed Yucca Mountain Radioactive Waste Repository (Southern Nevada, USA).* LA-UR-07-3579. Los Alamos, New Mexico: Los Alamos National Laboratory. ACC: LLR.20070807.0153.

100027 Day, W.C.; Dickerson, R.P.; Potter, C.J.; Sweetkind, D.S.; San Juan, C.A.; Drake, R.M., II; and Fridrich, C.J. 1998. *Bedrock Geologic Map of the Yucca Mountain Area, Nye County, Nevada.* Geologic Investigations Series I-2627. Denver, Colorado: U.S. Geological Survey. ACC: MOL.19981014.0301.

182065 De Windt, L.; Schneider, H.; Ferry, C.; Catalette, H.; Lagneau, V.; Poinssot, C.; Poulesquen, A.; and Jegou, C. 2006. "Modeling Spent Nuclear Fuel Alteration and Radionuclide Migration in Disposal Conditions." *Radiochimica Acta, 94,* 787-794. München, Germany: Oldenbourg Wissenschaftsverlag. TIC: 259598.

171480 Dillmann, Ph.; Mazaudier, F.; and Hœrlé, S. 2004. "Advances in Understanding Atmospheric Corrosion of Iron. I. Rust Characterisation of Ancient Ferrous Artefacts Exposed to Indoor Atmospheric Corrosion." *Corrosion Science, 46,* 1401 - 1429. [New York, New York]: Elsevier. TIC: 256483.

100550 DOE (U.S. Department of Energy) 1998. *Total System Performance Assessment.* Volume 3 of *Viability Assessment of a Repository at Yucca Mountain.* DOE/RW-0508. Washington, D.C.: U.S. Department of Energy, Office of Civilian Radioactive Waste Management. ACC: MOL.19981007.0030.

101779 DOE (U.S. Department of Energy) 1998. *Viability Assessment of a Repository at Yucca Mountain.* DOE/RW-0508. Overview and five volumes. Washington, D.C.: U.S. Department of Energy, Office of Civilian Radioactive Waste Management. ACC: MOL.19981007.0027; MOL.19981007.0028; MOL.19981007.0029; MOL.19981007.0030; MOL.19981007.0031; MOL.19981007.0032.

118968 DOE (U.S. Department of Energy) 2000. *DOE Spent Nuclear Fuel Grouping in Support of Criticality, DBE, TSPA-LA.* DOE/SNF/REP-046, Rev. 0. Idaho Falls, Idaho: U.S. Department of Energy, Idaho Operations Office. ACC: DOC.20030905.0021.

155970 DOE (U.S. Department of Energy) 2002. *Final Environmental Impact Statement for a Geologic Repository for the Disposal of Spent Nuclear Fuel and High-Level Radioactive Waste at Yucca Mountain, Nye County, Nevada.* DOE/EIS-0250. Washington, D.C.: U.S. Department of Energy, Office of Civilian Radioactive Waste Management. ACC: MOL.20020524.0314; MOL.20020524.0315; MOL.20020524.0316; MOL.20020524.0317; MOL.20020524.0318; MOL.20020524.0319; MOL.20020524.0320.

167603 DOE (U.S. Department of Energy) 2003. *Design Document for: ASHPLUME_DLL_LA Version 2.0, Rev. No. 00.* Document ID: 11117-DD-2.0-00. Las Vegas, Nevada: U.S. Department of Energy, Office of Repository Development. ACC: MOL.20031212.0439.

167588 DOE (U.S. Department of Energy) 2003. *Design Document for: SZ_CONVOLUTE Version 3.0.* 10207-DD-3.0-00. Las Vegas, Nevada: U.S. Department of Energy, Office of Repository Development. ACC: MOL.20030717.0479.

167590 DOE (U.S. Department of Energy) 2003. *Installation Test Process for: SZ_CONVOLUTE Version 3.0.* 10207-ITP-3.0-00. Las Vegas, Nevada: U.S. Department of Energy, Office of Repository Development. ACC: MOL.20030717.0480.

167606 DOE (U.S. Department of Energy) 2003. *Installation Test Process for: ASHPLUME_DLL_LA Version 2.0.* Document ID: 11117-ITP-2.0-00. Las Vegas, Nevada: U.S. Department of Energy, Office of Repository Development. ACC: MOL.20031212.0440.

167587 DOE (U.S. Department of Energy) 2003. *Requirements Document for: SZ_CONVOLUTE Version 3.0.* 10207-RD-3.0-00. Las Vegas, Nevada: U.S. Department of Energy, Office of Repository Development. ACC: MOL.20030717.0478.

167601 DOE (U.S. Department of Energy) 2003. *Requirements Document for: ASHPLUME_DLL_LA, V2.0, Rev. No. 00.* Document ID: 11117-RD-2.0-00. Las Vegas, Nevada: U.S. Department of Energy, Office of Repository Development. ACC: MOL.20031212.0438.

167597 DOE (U.S. Department of Energy) 2003. *Software Management Report, MFCP_LA, V1.0.* DI: 11071-SMR-1.0-00. Las Vegas, Nevada: U.S. Department of Energy, Office of Repository Development. ACC: MOL.20030529.0258.

167564 DOE (U.S. Department of Energy) 2003. *Software Management Report: CWD Version Number 2.0.* Document ID: 10363-SMR-2.0-00. Las Vegas, Nevada: U.S. Department of Energy, Office of Repository Development. ACC: MOL.20030501.0182.

163377 DOE (U.S. Department of Energy) 2003. Source Term Estimates for DOE Spent Nuclear Fuels. DOE/SNF/REP-078, Rev. 0. Idaho Falls, Idaho: U.S. Department of Energy, Idaho Operations Office. TIC: 254275.

167607 DOE (U.S. Department of Energy) 2003. *User's Manual for: ASHPLUME_DLL_LA Version 2.0, UM Rev. No.: 00.* Document ID: 11117-UM-2.0-00. Las Vegas, Nevada: U.S. Department of Energy, Office of Repository Development. ACC: MOL.20031212.0444.

167591 DOE (U.S. Department of Energy) 2003. *Users Manual, SZ_CONVOLUTE Version 3.0.* 10207-UM-3.0-00. Las Vegas, Nevada: U.S. Department of Energy, Office of Repository Development. ACC: MOL.20030717.0483.

167589 DOE (U.S. Department of Energy) 2003. *Validation Test Process for: SZ_CONVOLUTE Version 3.0.* 10207-VTP-3.0-00. Las Vegas, Nevada: U.S. Department of Energy, Office of Repository Development. ACC: MOL.20030717.0481.

167604 DOE (U.S. Department of Energy) 2003. *Validation Test Process for: ASHPLUME_DLL_LA Version 2.0.* Document ID: 11117-VTP-2.0-01. Las Vegas, Nevada: U.S. Department of Energy, Office of Repository Development. ACC: MOL.20031212.0441.

166506 DOE (U.S. Department of Energy) 2003. *Validation Test Report for: ASHPLUME_DLL_LA Version 2.0.* 11117-VTR-2.0-00. Las Vegas, Nevada: U.S. Department of Energy, Office of Repository Development. ACC: MOL.20031212.0443.

167593 DOE (U.S. Department of Energy) 2003. *Validation Test Report for: SZ_CONVOLUTE.* 10207-VTR-3.0-0.0. Las Vegas, Nevada: U.S. Department of Energy, Office of Repository Development. ACC: MOL.20030717.0484.

168977 DOE (U.S. Department of Energy) 2004. *Software Management Report for: SOILEXP_LA, V1.0, SMR REV. NO.: 00.* Document ID: 10933-SMR-1.0-00. Las Vegas, Nevada: U.S. Department of Energy, Office of Repository Development. ACC: MOL.20040227.0046.

168978 DOE (U.S. Department of Energy) 2004. *Software Management Report for: PassTable1D_LA, V1.0.* Document ID: 11142-SMR-1.0-00. Las Vegas, Nevada: U.S. Department of Energy, Office of Repository Development. ACC: MOL.20040310.0105.

168981 DOE (U.S. Department of Energy) 2004. *Software Management Report for: PassTable3D_LA, V1.0, SMR Rev. No.: 00.* Document ID: 11143-SMR-1.0-00. Las Vegas, Nevada: U.S. Department of Energy, Office of Repository Development. ACC: MOL.20040317.0127.

168988 DOE (U.S. Department of Energy) 2004. *Software Management Report, INTERPZDLL_LA, V1.0, STN: 11107-1.0-00, Rev. 00.* Document ID: 11107-SMR-1.0-00. Las Vegas, Nevada: U.S. Department of Energy, Office of Repository Development. ACC: MOL.20040130.0403.

169354 DOE (U.S. Department of Energy) 2004. *Source Term Estimates for DOE Spent Nuclear Fuels.* DOE/SNF/REP-078, Rev. 1. Three volumes. Idaho Falls, Idaho: U.S. Department of Energy, Idaho Operations Office. ACC: MOL.20040524.0451.

173440 DOE (U.S. Department of Energy) 2005. *Design Document for: FEHM V2.23.* Document ID: 10086-DD-2.23-00. Las Vegas, Nevada: U.S. Department of Energy, Office of Repository Development. ACC: MOL.20050301.0043.

174594 DOE (U.S. Department of Energy) 2005. *Design Document for: MVIEW V4.0.* Document ID: 10072-DD-4.0-00. Las Vegas, Nevada: U.S. Department of Energy, Office of Repository Development. ACC: MOL.20050712.0025.

173464 DOE (U.S. Department of Energy) 2005. *Design Document for: SEEPAGEDLL_LA V1.2.* Document ID: 11076-DD-1.2-00. Las Vegas, Nevada: U.S. Department of Energy, Office of Repository Development. ACC: MOL.20050406.0440.

173450 DOE (U.S. Department of Energy) 2005. *Design Document for: TSPA_Input_DB Version 2.0.* Document ID: 10931-DD-2.0-00. Las Vegas, Nevada: U.S. Department of Energy, Office of Repository Development. ACC: MOL.20050131.0430.

173449 DOE (U.S. Department of Energy) 2005. *Requirements Document for: TSPA_Input_DB Version 2.0.* Document ID: 10931-RD-2.0-00. Las Vegas, Nevada: U.S. Department of Energy, Office of Repository Development. ACC: MOL.20050131.0427.

173465 DOE (U.S. Department of Energy) 2005. *Requirements Document for: SEEPAGEDLL_LA V1.2.* Document ID: 11076-RD-1.2-00. Las Vegas, Nevada: U.S. Department of Energy, Office of Repository Development. ACC: MOL.20050406.0437.

174593 DOE (U.S. Department of Energy) 2005. *Requirements Document for: MVIEW V4.0.* Document ID: 10072-RD-4.0-01. Las Vegas, Nevada: U.S. Department of Energy, Office of Repository Development. ACC: MOL.20050712.0023.

174616 DOE (U.S. Department of Energy) 2005. *Requirements Document for: FEHM V2.23.* Document ID: 10086-RD-2.23-00. Las Vegas, Nevada: U.S. Department of Energy, Office of Repository Development. ACC: MOL.20050301.0040.

173442 DOE (U.S. Department of Energy) 2005. *Software Validation Report for: FEHM V2.23.* Document ID: 10086-SVR-2.23-00-Win2000. Las Vegas, Nevada: U.S. Department of Energy, Office of Repository Development. ACC: MOL.20050301.0049.

173462 DOE (U.S. Department of Energy) 2005. *Software Validation Report for: SEEPAGEDLL_LA V1.2.* Document ID: 11076-SVR-1.2-00. Las Vegas, Nevada: U.S. Department of Energy, Office of Repository Development. ACC: MOL.20050406.0429.

173463 DOE (U.S. Department of Energy) 2005. *User Information Document for: SEEPAGEDLL_LA V1.2.* Document ID: 11076-UID-1.2-00. Las Vegas, Nevada: U.S. Department of Energy, Office of Repository Development. ACC: MOL.20050406.0425.

173441 DOE (U.S. Department of Energy) 2005. *User Information for: FEHM V2.23.* Document ID: 10086-UID-2.23-00. Las Vegas, Nevada: U.S. Department of Energy, Office of Repository Development. ACC: MOL.20050301.0046.

174595 DOE (U.S. Department of Energy) 2005. *User Information for: MVIEW 4.0.* Document ID: 10072-UID-4.0-00. Las Vegas, Nevada: U.S. Department of Energy, Office of Repository Development. ACC: MOL.20050712.0027.

181286 DOE (U.S. Department of Energy) 2006. *Design Document for SZ_CONVOLUTE Version 3.10.* Document ID: 10207-DD-3.10-00. Las Vegas, Nevada: U.S. Department of Energy, Office of Repository Development. ACC: MOL.20061106.0219.

181075 DOE (U.S. Department of Energy) 2006. *Design Document for: ASHPLUME_DLL_LA V2.1.* Document ID: 11117-DD-2.1-00. Las Vegas, Nevada: U.S. Department of Energy, Office of Repository Development. ACC: MOL.20061106.0387.

181101 DOE (U.S. Department of Energy) 2006. *Design Document for: GetThk_LA v1.0.* Document ID: 11229-DD-1.0-00. Las Vegas, Nevada: U.S. Department of Energy, Office of Repository Development. ACC: MOL.20060915.0165.

181115 DOE (U.S. Department of Energy) 2006. *Design Document for: MkTable_LA v1.0.* Document ID: 11217-DD-1.0-00. Las Vegas, Nevada: U.S. Department of Energy, Office of Repository Development. ACC: MOL.20060413.0351.

181128 DOE (U.S. Department of Energy) 2006. *Design Document for: PREWAP_LA v1.1.* Document ID: 10939-DD-1.1-00. Las Vegas, Nevada: U.S. Department of Energy, Office of Repository Development. ACC: MOL.20060418.0165.

181132 DOE (U.S. Department of Energy) 2006. *Design Document for: SEEPAGEDLL_LA V1.3.* Document ID: 11076-DD-1.3-00. Las Vegas, Nevada: U.S. Department of Energy, Office of Repository Development. ACC: MOL.20060525.0296.

181284 DOE (U.S. Department of Energy) 2006. *Requirements Document for SZ_CONVOLUTE V. 3.10.* Document ID: 10207-RD-3.10-00. Las Vegas, Nevada: U.S. Department of Energy, Office of Repository Development. ACC: MOL.20061106.0218.

181073 DOE (U.S. Department of Energy) 2006. *Requirements Document for: ASHPLUME_DLL_LA V2.1.* Document ID: 11117-RD-2.1-00. Las Vegas, Nevada: U.S. Department of Energy, Office of Repository Development. ACC: MOL.20061106.0385.

181094 DOE (U.S. Department of Energy) 2006. *Requirements Document for: FEHM V2.24.* Document ID: 10086-RD-2.24-00. Las Vegas, Nevada: U.S. Department of Energy, Office of Repository Development. ACC: MOL.20061127.0272.

181100 DOE (U.S. Department of Energy) 2006. *Requirements Document for: GetThk_LA v1.0.* Document ID: 11229-RD-1.0-00. Las Vegas, Nevada: U.S. Department of Energy, Office of Repository Development. ACC: MOL.20060915.0163.

181114 DOE (U.S. Department of Energy) 2006. *Requirements Document for: MkTable_LA v1.0.* Document ID: 11217-RD-1.0-00. Las Vegas, Nevada: U.S. Department of Energy, Office of Repository Development. ACC: MOL.20060413.0349.

181127 DOE (U.S. Department of Energy) 2006. *Requirements Document for: PREWAP_LA v1.1.* Document ID: 10939-RD-1.1-00. Las Vegas, Nevada: U.S. Department of Energy, Office of Repository Development. ACC: MOL.20060418.0163.

181131 DOE (U.S. Department of Energy) 2006. *Requirements Document for: SEEPAGEDLL_LA V1.3.* Document ID: 11076-RD-1.3-00. Las Vegas, Nevada: U.S. Department of Energy, Office of Repository Development. ACC: MOL.20060525.0294.

181077 DOE (U.S. Department of Energy) 2006. *Software Validation Report for: ASHPLUME_DLL_LA Version 2.1 Operating in GoldSim under the Windows 2000 Environment.* Document ID: 11117-SVR-2.1-00-Win2000. Las Vegas, Nevada: U.S. Department of Energy, Office of Repository Development. ACC: MOL.20070102.0246.

181104 DOE (U.S. Department of Energy) 2006. *Software Validation Report for: GetThk_LA v1.0.* Document ID: 11229-SVR-1.0-00-WIN2000. Las Vegas, Nevada: U.S. Department of Energy, Office of Repository Development. ACC: MOL.20060915.0173.

181105 DOE (U.S. Department of Energy) 2006. *Software Validation Report for: GetThk_LA v1.0.* Document ID: 11229-SVR-1.0-00-WIN2003. Las Vegas, Nevada: U.S. Department of Energy, Office of Repository Development. ACC: MOL.20060915.0171.

181113 DOE (U.S. Department of Energy) 2006. *Software Validation Report for: MFCP_LA v1.0.* Document ID: 11071-SVR-1.0-01-WIN2003. Las Vegas, Nevada: U.S. Department of Energy, Office of Repository Development. ACC: MOL.20061218.0126.

181117 DOE (U.S. Department of Energy) 2006. *Software Validation Report for: MkTable_LA v1.0.* Document ID: 11217-SVR-1.0-00-WIN2000. Las Vegas, Nevada: U.S. Department of Energy, Office of Repository Development. ACC: MOL.20060413.0357.

181120 DOE (U.S. Department of Energy) 2006. *Software Validation Report for: PASSTABLE1D_LA v1.0.* Document ID: 11142-SVR-1.0-01-WIN2003. Las Vegas, Nevada: U.S. Department of Energy, Office of Repository Development. ACC: MOL.20061218.0107.

181130 DOE (U.S. Department of Energy) 2006. *Software Validation Report for: PREWAP_LA v1.1.* Document ID: 10939-SVR-1.1-00-WIN2000. Las Vegas, Nevada: U.S. Department of Energy, Office of Repository Development. ACC: MOL.20060418.0171.

181134 DOE (U.S. Department of Energy) 2006. *Software Validation Report for: SEEPAGEDLL_LA V1.3.* Document ID: 11076-SVR-1.3-00-WIN2000. Las Vegas, Nevada: U.S. Department of Energy, Office of Repository Development. ACC: MOL.20060525.0302.

181139 DOE (U.S. Department of Energy) 2006. *Software Validation Report for: TSPA_Input_DB v2.2.* Document ID: 10931-SVR-2.2-00-WIN2000. Las Vegas, Nevada: U.S. Department of Energy, Office of Repository Development. ACC: MOL.20060222.0422.

181140 DOE (U.S. Department of Energy) 2006. *Software Validation Report for: TSPA_Input_DB v2.2.* Document ID: 10931-SVR-2.2-01-WIN2003. Las Vegas, Nevada: U.S. Department of Energy, Office of Repository Development. ACC: MOL.20061011.0198.

181076 DOE (U.S. Department of Energy) 2006. *User Information Document for: ASHPLUME_DLL_LA Version 2.1.* Document ID: 11117-UID-2.1-00. Las Vegas, Nevada: U.S. Department of Energy, Office of Repository Development. ACC: MOL.20070102.0242.

181102 DOE (U.S. Department of Energy) 2006. *User Information Document for: GetThk_LA v1.0.* Document ID: 11229-UID-1.0-00. Las Vegas, Nevada: U.S. Department of Energy, Office of Repository Development. ACC: MOL.20060915.0169.

181116 DOE (U.S. Department of Energy) 2006. *User Information Document for: MkTable_LA v1.0.* Document ID: 11217-UID-1.0-00. Las Vegas, Nevada: U.S. Department of Energy, Office of Repository Development. ACC: MOL.20060413.0354.

181129 DOE (U.S. Department of Energy) 2006. *User Information Document for: PREWAP_LA v1.1.* Document ID: 10939-UID-1.1-00. Las Vegas, Nevada: U.S. Department of Energy, Office of Repository Development. ACC: MOL.20060418.0169.

181133 DOE (U.S. Department of Energy) 2006. *User Information Document for: SEEPAGEDLL_LA V1.3.* Document ID: 11076-UID-1.3-00. Las Vegas, Nevada: U.S. Department of Energy, Office of Repository Development. ACC: MOL.20060525.0300.

181137 DOE (U.S. Department of Energy) 2006. *User Information Document for: TSPA_Input_DB Version 2.2.* Document ID: 10931-UID-2.2-00. Las Vegas, Nevada: U.S. Department of Energy, Office of Repository Development. ACC: MOL.20060222.0419.

182907 DOE (U.S. Department of Energy) 2007. *Design Document for: EXDOC_LA Version 2.0.* Document ID: 11193-DD-2.0-01. Las Vegas, Nevada: U. S. Department of Energy, Office of Repository Development. ACC: MOL.20070723.0262.

181081 DOE (U.S. Department of Energy) 2007. *Design Document for: FAR Version 1.1.* Document ID: 11190-DD-1.1-00. Las Vegas, Nevada: U.S. Department of Energy, Office of Repository Development. ACC: MOL.20070323.0328.

183118 DOE (U.S. Department of Energy) 2007. *Design Document for: FAR Version 1.2.* Document ID: 11190-DD-1.2-00. Las Vegas, Nevada: U.S. Department of Energy, Office of Repository Development. ACC: MOL.20070919.0327.

181095 DOE (U.S. Department of Energy) 2007. *Design Document for: FEHM V2.24-01.* Document ID: 10086-DD-2.24-01-00. Las Vegas, Nevada: U.S. Department of Energy, Office of Repository Development. ACC: MOL.20070309.0032.

182562 DOE (U.S. Department of Energy) 2007. *Design Document for: FEHM V2.25.* Document ID: 10086-DD-2.25-01. Las Vegas, Nevada: U. S. Department of Energy, Office of Repository Development. ACC: MOL.20070712.0363.

181107 DOE (U.S. Department of Energy) 2007. *Design Document for: GoldSim v9.60.* Document ID: 10344-DD-9.60-01. Las Vegas, Nevada: U.S. Department of Energy, Office of Repository Development. ACC: MOL.20070416.0338.

181122 DOE (U.S. Department of Energy) 2007. *Design Document for: PassTable1D_LA version 2.0.* Document ID: 11142-DD-2.0-01. Las Vegas, Nevada: U.S. Department of Energy, Office of Repository Development. ACC: MOL.20070420.0359.

182917 DOE (U.S. Department of Energy) 2007. *Design Document for: PassTable3D_LA Version 2.0.* Document ID: 11143-DD-2.0-00. Las Vegas, Nevada: U. S. Department of Energy, Office of Repository Development. ACC: MOL.20070816.0247.

182051 DOE (U.S. Department of Energy) 2007. *Quality Assurance Requirements and Description.* DOE/RW-0333P, Rev. 19. Washington, D. C.: U.S. Department of Energy, Office of Civilian Radioactive Waste Management. ACC: DOC.20070717.0006.

181080 DOE (U.S. Department of Energy) 2007. *Requirements Document for: FAR Version 1.1.* Document ID: 11190-RD-1.1-00. Las Vegas, Nevada: U.S. Department of Energy, Office of Repository Development. ACC: MOL.20070323.0326.

181106 DOE (U.S. Department of Energy) 2007. *Requirements Document for: GoldSim v9.60.* Document ID: 10344-RD-9.60-00. Las Vegas, Nevada: U.S. Department of Energy, Office of Repository Development. ACC: MOL.20070416.0330.

181121 DOE (U.S. Department of Energy) 2007. *Requirements Document for: PassTable1D_LA Version 2.0.* Document ID: 11142-RD-2.0-01. Las Vegas, Nevada: U.S. Department of Energy, Office of Repository Development. ACC: MOL.20070420.0357.

182561 DOE (U.S. Department of Energy) 2007. *Requirements Document for: FEHM V2.25.* Document ID: 10086-RD-2.25-01. Las Vegas, Nevada: U. S. Department of Energy, Office of Repository Development. ACC: MOL.20070712.0361.

182906 DOE (U.S. Department of Energy) 2007. *Requirements Document for: EXDOC_LA Version 2.0.* Document ID: 11193-RD-2.0-01. Las Vegas, Nevada: U. S. Department of Energy, Office of Repository Development. ACC: MOL.20070723.0260.

182916 DOE (U.S. Department of Energy) 2007. *Requirements Document for: PassTable3D_LA Version 2.0.* Document ID: 11143-RD-2.0-00. Las Vegas, Nevada: U.S. Department of Energy, Office of Repository Development. ACC: MOL.20070816.0245.

183117 DOE (U.S. Department of Energy) 2007. *Requirements Document for: FAR Version 1.2.* Document ID: 11190-RD-1.2-00. Las Vegas, Nevada: U. S. Department of Energy, Office of Repository Development. ACC: MOL.20070919.0325.

181079 DOE (U.S. Department of Energy) 2007. *Software Validation Report for: CWD v2.0.* Document ID: 10363-SVR-2.0-01-WIN2003. Las Vegas, Nevada: U.S. Department of Energy, Office of Repository Development. ACC: MOL.20070209.0021.

181085 DOE (U.S. Department of Energy) 2007. *Software Validation Report for: FAR Version 1.1.* Document ID: 11190-SVR-1.1-00-Win2000. Las Vegas, Nevada: U.S. Department of Energy, Office of Repository Development. ACC: MOL.20070417.0338.

181087 DOE (U.S. Department of Energy) 2007. *Software Validation Report for: FAR Version 1.1.* Document ID: 11190-SVR-1.1-00-Win2003. Las Vegas, Nevada: U.S. Department of Energy, Office of Repository Development. ACC: MOL.20070417.0340.

181092 DOE (U.S. Department of Energy) 2007. *Software Validation Report for: INTERPZDLL_LA v1.0.* Document ID: 11107-SVR-1.0-01-WIN2003. Las Vegas, Nevada: U.S. Department of Energy, Office of Repository Development. ACC: MOL.20070220.0471.

181097 DOE (U.S. Department of Energy) 2007. *Software Validation Report for: FEHM V2.24-01.* Document ID: 10086-SVR-2.24-01-00-Win2000. Las Vegas, Nevada: U.S. Department of Energy, Office of Repository Development. ACC: MOL.20070309.0047.

181098 DOE (U.S. Department of Energy) 2007. *Software Validation Report for: FEHM V2.24-01.* Document ID: 10086-SVR-2.24-01-00-Win2003. Las Vegas, Nevada: U.S. Department of Energy, Office of Repository Development. ACC: MOL.20070309.0045.

181109 DOE (U.S. Department of Energy) 2007. *Software Validation Report for: GoldSim v9.60 on Windows 2000.* Document ID: 10344-SVR-9.60-00-WIN2000. Las Vegas, Nevada: U.S. Department of Energy, Office of Repository Development. ACC: MOL.20070416.0341.

181110 DOE (U.S. Department of Energy) 2007. *Software Validation Report for: GoldSim v9.60 on Windows Server 2003.* Document ID: 10344-SVR-9.60-00-WIN2003. Las Vegas, Nevada: U.S. Department of Energy, Office of Repository Development. ACC: MOL.20070416.0343.

181111 DOE (U.S. Department of Energy) 2007. *Software Validation Report for: GoldSim v9.60 on Window XP.* Document ID: 10344-SVR-9.60-00-WINXP. Las Vegas, Nevada: U.S. Department of Energy, Office of Repository Development. ACC: MOL.20070416.0345.

181118 DOE (U.S. Department of Energy) 2007. *Software Validation Report for: MkTable_LA v1.0.* Document ID: 11217-SVR-1.0-01-WIN2003. Las Vegas, Nevada: U.S. Department of Energy, Office of Repository Development. ACC: MOL.20070208.0274.

181119 DOE (U.S. Department of Energy) 2007. *Software Validation Report for: MView 4.0.* Document ID: 10072-SVR-4.0-01-WinXP. Las Vegas, Nevada: U.S. Department of Energy, Office of Repository Development. ACC: MOL.20070417.0382.

181124 DOE (U.S. Department of Energy) 2007. *Software Validation Report for: PassTable1D_LA v2.0.* Document ID: 11142-SVR-2.0-00-WIN2000. Las Vegas, Nevada: U.S. Department of Energy, Office of Repository Development. ACC: MOL.20070420.0363.

181125 DOE (U.S. Department of Energy) 2007. *Software Validation Report for: PassTable1D_LA Version 2.0.* Document ID: 11142-SVR-2.0-00-WIN2003. Las Vegas, Nevada: U.S. Department of Energy, Office of Repository Development. ACC: MOL.20070420.0365.

181126 DOE (U.S. Department of Energy) 2007. *Software Validation Report for: PassTable3D_LA v1.0.* Document ID: 11143-SVR-1.0-01-WIN2003. Las Vegas, Nevada: U.S. Department of Energy, Office of Repository Development. ACC: MOL.20070208.0286.

181135 DOE (U.S. Department of Energy) 2007. *Software Validation Report for: SEEPAGEDLL_LA V1.3.* Document ID: 11076-SVR-1.3-01-WIN2003. Las Vegas, Nevada: U.S. Department of Energy, Office of Repository Development. ACC: MOL.20070223.0249.

181141 DOE (U.S. Department of Energy) 2007. *Software Validation Report for: WAPDEG v4.07.* Document ID: 10000-SVR-4.07-01-WIN2003. Las Vegas, Nevada: U.S. Department of Energy, Office of Repository Development. ACC: MOL.20070417.0371.

181275 DOE (U.S. Department of Energy) 2007. *Software Validation Report for: ASHPLUME_DLL_LA Version 2.1 Operating in GoldSim under the Windows Server 2003 Environment.* Document ID: 11117-SVR-2.1-01-Win2003. Las Vegas, Nevada: U.S. Department of Energy, Office of Repository Development. ACC: MOL.20070223.0261.

181277 DOE (U.S. Department of Energy) 2007. *Software Validation Report for: SCCD v2.01.* Document ID: 10343-SVR-2.01-01-WIN2003. Las Vegas, Nevada: U.S. Department of Energy, Office of Repository Development. ACC: MOL.20070209.0013.

182566 DOE (U.S. Department of Energy) 2007. *Software Validation Report for: FEHM V2.25 for Windows 2000.* Document ID: 10086-SVR-2.25-00- Win2000. Las Vegas, Nevada: U.S. Department of Energy, Office of Repository Development. ACC: MOL.20070712.0371.

182567 DOE (U.S. Department of Energy) 2007. *Software Validation Report for: FEHM V2.25 for Windows 2003.* Document ID: 10086-SVR-2.25-00- Win2003. Las Vegas, Nevada: U.S. Department of Energy, Office of Repository Development. ACC: MOL.20070712.0373.

182568 DOE (U.S. Department of Energy) 2007. *Software Validation Report for: FEHM Version 2.25 for Windows XP.* Document ID: 10086-SVR-2.25-00-WinXP. Las Vegas, Nevada: U.S. Department of Energy, Office of Repository Development. ACC: MOL.20070712.0375.

182909 DOE (U.S. Department of Energy) 2007. *Software Validation Report for: EXDOC_LA Version 2.0.* Document ID: 11193-SVR-2.0-00-WIN2000. Las Vegas, Nevada: U. S. Department of Energy, Office of Repository Development. ACC: MOL.20070723.0266.

182910 DOE (U.S. Department of Energy) 2007. *Software Validation Report for: EXDOC_LA Version 2.0.* Document ID: 11193-SVR-2.0-00-WIN2003. Las Vegas, Nevada: U.S. Department of Energy, Office of Repository Development. ACC: MOL.20070723.0268.

182911 DOE (U.S. Department of Energy) 2007. *Software Validation Report for: EXDOC_LA Version 2.0.* Document ID: 11193-SVR-2.0-00-WINXP. Las Vegas, Nevada: U. S. Department of Energy, Office of Repository Development. ACC: MOL.20070723.0270.

182913 DOE (U.S. Department of Energy) 2007. *Software Validation Report for: GoldSim Version 9.60.100 on Windows 2000.* Document ID: 10344-SVR-9.60-01-WIN2000. Las Vegas, Nevada: U.S. Department of Energy, Office of Repository Development. ACC: MOL.20070711.0250.

182914 DOE (U.S. Department of Energy) 2007. *Software Validation Report for: GoldSim Version 9.60.100 Windows Server 2003.* Document ID: 10344-SVR-9.60-01-WIN2003. Las Vegas, Nevada: U.S. Department of Energy, Office of Repository Development. ACC: MOL.20070711.0252.

182915 DOE (U.S. Department of Energy) 2007. *Software Validation Report for: GoldSim Version 9.60.100 on Windows XP.* Document ID: 10344-SVR-9.60-01-WINXP. Las Vegas, Nevada: U. S. Department of Energy, Office of Repository Development. ACC: MOL.20070711.0254.

182919 DOE (U.S. Department of Energy) 2007. *Software Validation Report for: PassTable3D_LA Version 2.0.* Document ID: 11143-SVR-2.0-00-WIN2000. Las Vegas, Nevada: U.S. Department of Energy, Office of Repository Development. ACC: MOL.20070816.0254.

182920 DOE (U.S. Department of Energy) 2007. *Software Validation Report for: PassTable3D_LA Version 2.0.* Document ID: 11143-SVR-2.0-00-WIN2003. Las Vegas, Nevada: U. S. Department of Energy, Office of Repository Development. ACC: MOL.20070816.0256.

183120 DOE (U.S. Department of Energy) 2007. *Software Validation Report for: FAR Version 1.2.* Document ID: 11190-SVR-1.2-00-Win2000. Las Vegas, Nevada: U.S. Department of Energy, Office of Repository Development. ACC: MOL.20070919.0334.

183121 DOE (U.S. Department of Energy) 2007. *Software Validation Report for: FAR Version 1.2.* Document ID: 11190-SVR-1.2-00-Win2003. Las Vegas, Nevada: U.S. Department of Energy, Office of Repository Development. ACC: MOL.20070919.0336.

181289 DOE (U.S. Department of Energy) 2007. *Software Validation Report, SZ_CONVOLUTE Version 3.10.01.* Document ID: 10207-SVR-3.10.01-00-Win2000. Las Vegas, Nevada: U.S. Department of Energy, Office of Repository Development. ACC: MOL.20070501.0392.

181290 DOE (U.S. Department of Energy) 2007. *Software Validation Report, SZ_Convolute Version 3.10.01.* Document ID: 10207-3.10.01-00-Win2003. Las Vegas, Nevada: U.S. Department of Energy, Office of Repository Development. ACC: MOL.20070501.0394.

181084 DOE (U.S. Department of Energy) 2007. *User Information Document for: FAR Version 1.1.* Document ID: 11190-UID-1.1-00. Las Vegas, Nevada: U.S. Department of Energy, Office of Repository Development. ACC: MOL.20070417.0336.

181096 DOE (U.S. Department of Energy) 2007. *User Information Document for: FEHM V2.24-01.* Document ID: 10086-UID-2.24-01-00. Las Vegas, Nevada: U.S. Department of Energy, Office of Repository Development. ACC: MOL.20070309.0037.

181108 DOE (U.S. Department of Energy) 2007. *User Information Document for: GoldSim Version 9.60.* Document ID: 10344-UID-9.60-00. Las Vegas, Nevada: U.S. Department of Energy, Office of Repository Development. ACC: MOL.20070416.0339.

181123 DOE (U.S. Department of Energy) 2007. *User Information Document for: PassTable1D_LA Version 2.0.* Document ID: 11142-UID-2.0-00. Las Vegas, Nevada: U.S. Department of Energy, Office of Repository Development. ACC: MOL.20070420.0361.

181288 DOE (U.S. Department of Energy) 2007. *User Information Document for: SZ_Convolute V. 3.10.* Document ID: 10207-UID-3.10-00. Las Vegas, Nevada: U.S. Department of Energy, Office of Repository Development. ACC: MOL.20070223.0313.

182565 DOE (U.S. Department of Energy) 2007. *User Information Document for: FEHM Version 2.25.* Document ID: 10086-UID-2.25-00. Las Vegas, Nevada: U.S. Department of Energy, Office of Repository Development. ACC: MOL.20070712.0365.

182908 DOE (U.S. Department of Energy) 2007. *User Information Document for: EXDOC_LA Version 2.0.* Document ID: 11193-UID-2.0-00. Las Vegas, Nevada: U. S. Department of Energy, Office of Repository Development. ACC: MOL.20070723.0264.

182918 DOE (U.S. Department of Energy) 2007. *User Information Document for: PassTable3D_LA Version 2.0.* Document ID: 11143-UID-2.0-00. Las Vegas, Nevada: U. S. Department of Energy, Office of Repository Development. ACC: MOL.20070816.0252.

183116 DOE (U.S. Department of Energy) 2007. *User Information Document for: FAR Version 1.2.* Document ID: 11190-UID-1.2-00. Las Vegas, Nevada: U.S. Department of Energy, Office of Repository Development. ACC: MOL.20070919.0332.

116801 Driscoll, F.G. 1986. *Groundwater and Wells.* 2nd Edition. St. Paul, Minnesota: Johnson Filtration Systems. TIC: 217555.

162466 Duan, N. 1982. "Models for Human Exposure to Air Pollution." *Environment International, 8,* 305-309. [New York, New York]: Pergamon Press. TIC: 250558.

179404 Dullien, F.A.L. 1979. *Porous Media: Fluid Transport and Pore Structure.* New York, New York: Academic Press. TIC: 259702.

105483 Dzombak, D.A. and Morel, F.M.M. 1990. *Surface Complexation Modeling, Hydrous Ferric Oxide*. New York, New York: John Wiley & Sons. TIC: 224089.

173071 Ebert, W.L.; Fortner, J.A.; Finch, R.J.; Jerden, J.L., Jr.; and Cunnane, J.C. 2005. *FY 2004 Annual Report for Waste Form Testing Activities.* ANL-05/08. Argonne, Illinois: Argonne National Laboratory. ACC: MOL.20050502.0239.

108015 Efurd, D.W.; Runde, W.; Banar, J.C.; Janecky, D.R.; Kaszuba, J.P.; Palmer, P.D.; Roensch, F.R.; and Tait, C.D. 1998. "Neptunium and Plutonium Solubilities in a Yucca Mountain Groundwater." *Environmental Science & Technology, 32,* (24), 3893-3900. [Easton, Pennsylvania]: American Chemical Society. TIC: 243857.

180746 Ehrenberg, H.; Svoboda, G.; Wltschek, G.; Wiesmann, M.; Trouw, F.; Weitzel, H.; and Fuess, H. 1995. "Crystal and Magnetic Structure of {alpha}-NiMoO{subscript 4}." *Journal of Magetism and Magnetic Materials, 150,* 371-376. [New York, New York]: Elsevier. TIC: 259369.

155354 Eisenberg, N.A.; Lee, M.P.; Federline, M.V.; Wingefors, S.; Andersson, J.; Norrby, S.; Sagar, B.; and Wittmeyer, G.W. 1999. *Regulatory Perspectives on Model Validation in High-Level Radioactive Waste Management Programs: A Joint NRC/SKI White Paper.* NUREG-1636. Washington, D.C.: U.S. Nuclear Regulatory Commission. TIC: 246310.

154149 EPRI (Electric Power Research Institute) 2000. *Evaluation of the Candidate High-Level Radioactive Waste Repository at Yucca Mountain Using Total System Performance Assessment, Phase 5.* 1000802. Palo Alto, California: Electric Power Research Institute. TIC: 249555.

158069 EPRI (Electric Power Research Institute) 2002. *Evaluation of the Proposed High-Level Radioactive Waste Repository at Yucca Mountain Using Total System Performance Assessment, Phase 6.* EPRI TR-1003031. Palo Alto, California: Electric Power Research Institute. TIC: 252239.

171915 EPRI (Electric Power Research Institute) 2004. *Potential Igneous Processes Relevant to the Yucca Mountain Repository: Extrusive-Release Scenario.* EPRI TR-1008169. Palo Alto, California: Electric Power Research Institute. TIC: 256654.

112115 Evans, M.; Hastings, N.; and Peacock, B. 1993. *Statistical Distributions.* 2nd Edition. New York, New York: John Wiley & Sons. TIC: 246114.

146355 Fabryka-Martin, J.T.; Wolfsberg, A.V.; Roach, J.L.; Winters, S.T.; and Wolfsberg, L.E. 1998. "Using Chloride to Trace Water Movement in the Unsaturated Zone at Yucca Mountain." *High-Level Radioactive Waste Management, Proceedings of the Eighth International Conference, Las Vegas, Nevada, May 11-14, 1998.* Pages 264-268. La Grange Park, Illinois: American Nuclear Society. TIC: 237082.

181367 Fayek, M.; Ren, M.; Goodell, P.; Dobson, P.; Saucedo, A.; Kelts, A.; Utsunomiya, S.; Ewing, R.C.; Riciputi, L.R.; and Reyes, I. 2006. "Paragenesis and Geochronology of the Nopal I Uranium Deposit, Mexico." *Proceedings of the 11th International High-Level Radioactive Waste Management Conference (IHLRWM), April 30-May 4, 2006, Las Vegas, Nevada.* Pages 55-62. La Grange Park, Illinois: American Nuclear Society. TIC: 258345.

107822 Feller, W. 1971. *An Introduction to Probability Theory and Its Applications.* 2nd Edition. Volume II. New York, New York: John Wiley & Sons. TIC: 235188.

104385 Fillmore, D.L. 1998. *Parameter Selection for Department of Energy Spent Nuclear Fuel to be Used in the Yucca Mountain Viability Assessment.* INEEL/EXT-98-00666. Idaho Falls, Idaho: Idaho National Engineering and Environmental Laboratory. ACC: MOL.19990511.0296.

127332 Finch, R.J.; Buck, E.C.; Finn, P.A.; and Bates, J.K. 1999. "Oxidative Corrosion of Spent UO2 Fuel in Vapor and Dripping Groundwater at 90°C." *Scientific Basis for Nuclear Waste Management XXII, Symposium held November 30-December 4, 1998, Boston, Massachusetts, U.S.A.* Wronkiewicz, D.J. and Lee, J.H., eds. *556,* 431-438. Warrendale, Pennsylvania: Materials Research Society. TIC: 246426.

109425 Forester, R.M.; Bradbury, J.P.; Carter, C.; Elvidge-Tuma, A.B.; Hemphill, M.L.; Lundstrom, S.C.; Mahan, S.A.; Marshall, B.D.; Neymark, L.A.; Paces, J.B.; Sharpe, S.E.; Whelan, J.F.; and Wigand, P.E. 1999. *The Climatic and Hydrologic History of Southern Nevada During the Late Quaternary.* Open-File Report 98-635. Denver, Colorado: U.S. Geological Survey. TIC: 245717.

168717 Frankel, J.J. 1967. "Forms and Structures of Intrusive Basaltic Rocks." *Basalts, the Poldervaart Treatise on Rocks of Basaltic Composition.* Volume 1. Hess, H.H. and Poldervaart, A., eds. Pages 63-102. New York, New York: Interscience Publishers. TIC: 254505.

101173 Freeze, R.A. and Cherry, J.A. 1979. *Groundwater.* Englewood Cliffs, New Jersey: Prentice-Hall. TIC: 217571.

181362 French, D.; Anthony, E.; and Goodell, P. 2006. "U-Series Disequilibria in Soils, Peña Blanca Natural Analog, Chihuahua, Mexico." *Proceedings of the 11th International High-Level Radioactive Waste Management Conference (IHLRWM), April 30-May 4, 2006, Las Vegas, Nevada.* Pages 63-69. La Grange Park, Illinois: American Nuclear Society. TIC: 258345.

180468 Fujiwara, K.; Yamana, H.; Fujii, T.; and Moriyama, H. 2002. "Solubility Product of Plutonium Hydros Oxide and Its Ionic Strength Dependence." *Radiochim Acta, 90,* (12), 857-861. München, Germany: Oldenbourg Wissenschaftsverlag. TIC: 252601.

105636 George-Aniel, B.; Leroy, J.L.; and Poty, B. 1991. "Volcanogenic Uranium Mineralizations in the Sierra Pena Blanca District, Chihuahua, Mexico: Three Genetic Models." *Economic Geology, 86,* (2), 233-248. El Paso, Texas: Economic Geology Publishing. TIC: 237050.

179134 Ghezzehei, T.A.; Dobson, P.F.; Rodriguez, J.A.; and Cook, P.J. 2006. "Infiltration and Seepage through Fractured Welded Tuff." *Proceedings of the 11th International High-Level Radioactive Waste Management Conference (IHLRWM), April 30 - May 4, 2006, Las Vegas, Nevada.* Pages 105-110. La Grange Park, Illinois: American Nuclear Society. TIC: 258345.

181099 Gibson, P. 2007. "Re: Memo Containing Reference to Draft TSPA-LA REV 01E." E-mail from P. Gibson to B. Mukhopadhyay, May 17, 2007, with attachment. ACC: LLR.20070518.0132; MOL.20060519.0089.

171782 Gisch, R.G. 2004. Postclosure Source Term Information for Naval Spent Fuel with Attachment Entitled "NNPP Postclosure Source Term Discussion for Seismic Disruptive Event Scenario". Letter from R.G. Gisch (DOE) to W.J. Arthur, III (DOE/ORD), September 2, 2004, 09130043151, NA:FA:KAKenney U#04-02635, with attachment. ACC: MOL.20040922.0363.

184807 GoldSim Technology Group 2007. *Radioactive and Hazardous Waste Management Applications Using GoldSim.* White Paper. [Issaquah, Washington]: GoldSim Technology Group. TIC: 260020.

183214 GoldSim Technology Group 2007. *GoldSim Contaminant Transport Module.* Version 4.20. Issaquah, Washington: GoldSim Technology Group. TIC: 259223.

181727 GoldSim Technology Group 2007. *User's Guide, GoldSim Probabilistic Simulation Environment.* Version 9.60. Two volumes. Issaquah, Washington: GoldSim Technology Group. TIC: 259221.

181364 Goldstein, S.J.; Luo, S.; Ku, T.L.; and Murrell, M.T. 2006. "Uranium-Series Constraints on Radionuclide Transport and Groundwater Flow at the Nopal I Uranium Deposit, Sierra Peña Blanca, Mexico." *International High-Level Radioactive Waste Management Conference (IHLRWM), April 30-May 4, 2006, Las Vegas, Nevada.* Pages 215-222. La Grange Park, Illinois: American Nuclear Society. TIC: 258345.

168528 Goldstein, S.J.; Murrell, M.T.; Simmons, A.M.; Oliver, R.D.; Dobson, P.F.; Reyes, I.A.; and de la Garza, R. 2003. "Evidence for Radium Mobility at the Nopal I Uranium Deposit, Peña Blanca, Mexico." *Abstracts with Programs - Geological Society of America, 35,* (6), 436. Boulder, Colorado: Geological Society of America. TIC: 254862.

149484 Goodell, P.C. 1981. "Geology of the Peña Blanca Uranium Deposits, Chihuahua, Mexico." *Uranium in Volcanic and Volcaniclastic Rocks, [Symposium held in El Paso, Texas, February 25-27, 1980]*. Goodell, P.C. and Waters, A.C., eds. AAPG Studies in Geology No. 13. Pages 275-291. [Tulsa, Oklahoma]: American Association of Petroleum Geologists. TIC: 247861.

176673 Gordon, S.J. and Brady, P.V. 2002. "In Situ Determination of Long-Term Basaltic Glass Dissolution in the Unsaturated Zone." *Chemical Geology, 190,* ([1-4]), 113-122. [New York, New York]: Elsevier. TIC: 258314.

163257 Grambow, B. 1985. "A General Rate Equation for Nuclear Waste Glass Corrosion." *Scientific Basis for Nuclear Waste Management VIII, Symposium held November 26-29, 1984, Boston, Massachusetts.* Jantzen, C.M.; Stone, J.A.; and Ewing, R.C., eds. *44,* 15-27. Pittsburgh, Pennsylvania: Materials Research Society. TIC: 203665.

181381 Grambow, B. 2006. "Nuclear Waste Glasses - How Durable?" *Elements, 2,* (6), 357-364. Québec, Canada: Mineralogical Society of America. TIC: 259580.

171412 Grambow, B. and Müller, R. 2001. "First-Order Dissolution Rate Law and the Role of Surface Layers in Glass Performance Assessment." *Journal of Nuclear Materials, 298,* 112-124. [New York, New York]: Elsevier. TIC: 256444.

163258 Grambow, B.; Jercinovic, M.J.; Ewing, R.C.; and Byers, C.D. 1986. "Weathered Basalt Glass: A Natural Analogue for the Effects of Reaction Progress on Nuclear Waste Glass Alteration." *Scientific Basis for Nuclear Waste Management IX, Symposium held September 9-11, 1985, Stockholm, Sweden.* Werme, L.O., ed. *50,* 263-272. Pittsburgh, Pennsylvania: Materials Research Society. TIC: 203664.

113255 Grandstaff, D.E. 1976. "A Kinetic Study of the Dissolution of Uraninite." *Economic Geology and the Bulletin of The Society of Economic Geologists, 71,* (8), 1493-1506. El Paso, Texas: Economic Geology Publishing. TIC: 246339.

183165 Grant Prideco 2003. Drill Collars. Pages 97-108. [Houston, Texas]: Grant Prideco. TIC: 259728.

149485 Green, R.T. and Rice, G. 1995. "Numerical Analysis of a Proposed Percolation Experiment at the Pena Blanca Natural Analog Site." *High Level Radioactive Waste Management, Proceedings of the Sixth Annual International Conference, Las Vegas, Nevada, April 30-May 5, 1995.* Pages 226-228. La Grange Park, Illinois: American Nuclear Society. TIC: 215781.

149528 Green, R.T.; Meyer-James, K.A.; and Rice, G. 1995. *Hydraulic Characterization of Hydrothermally Altered Nopal Tuff.* NUREG/CR-6356. San Antonio, Texas: Center for Nuclear Regulatory Analyses. TIC: 247869.

101671 Grenthe, I.; Fuger, J.; Konings, R.J.M.; Lemire, R.J.; Muller, A.B.; Nguyen-Trung, C.; and Wanner, H. 1992. *Chemical Thermodynamics of Uranium.* Volume 1 of *Chemical Thermodynamics.* Wanner, H. and Forest, I., eds. Amsterdam, The Netherlands: North-Holland Publishing Company. TIC: 224074.

168382 Guillaumont, R.; Fanghänel, T.; Fuger, J.; Grenthe, I.; Neck, V.; Palmer, D.A.; and Rand, M.H. 2003. *Update on the Chemical Thermodynamics of Uranium, Neptunium, Plutonium, Americium and Technetium.* Mompean, F.J.; Illemassene, M.; Domenech-Orti, C.; and Ben Said, K., eds. Chemical Thermodynamics 5. Amsterdam, The Netherlands: Elsevier. TIC: 255230.

156830 Guimerà, J. and Carrera, J. 2000. "A Comparison of Hydraulic and Transport Parameters Measured in Low-Permeability Fractured Media." *Journal of Contaminant Hydrology, 41,* ([3-4]), 261-281. [New York, New York]: Elsevier. TIC: 251013.

107512 Hacking, I. 1975. *The Emergence of Probability: A Philosophical Study of Early Ideas About Probability, Induction and Statistical Inference.* New York, New York: Cambridge University Press. TIC: 245428.

146529 Hahn, G.J. and Shapiro, S.S. 1967. *Statistical Models in Engineering.* New York, New York: John Wiley & Sons. TIC: 247729.

158798 Hamby, D.M. 1994. "A Review of Techniques for Parameter Sensitivity Analysis of Environmental Models." *Environmental Monitoring and Assessment, 32,* (2), 135-154. Dordrecht, The Netherlands: Kluwer Academic. TIC: 251324.

182008 Hanson, B.D.; Friese, J.I.; and Soderquist, C.Z. 2004. "Initial Results from Dissolution Testing of Spent Fuel Under Acidic Conditions." *Scientific Basis for Nuclear Waste Mangement XXVIII, Symposium, April 13-16, 2004, San Francisco, California, U.S.A.* Hanchar, J.M.; Stroes-Gascoyne, S.; and Browning, L., eds. *824,* 113-118. Warrendale, Pennsylvania: Materials Research Society. TIC: 256855.

179403 Harris, R.F. 1985. "Effect of Water Potential on Microbial Growth and Activity." Chapter 2 of *Water Potential Relations in Soil Microbiology.* SSSA Special Publication Number 9. Kral, D.M. and M.K. Cousin, eds. Madison, Wisconsin: Soil Science Society of America. TIC: 259690.

117826 Haukwa, C.; Wu, Y.S.; Hinds, J.J.; Zhang, W.; Ritcey, A.C.; Pan, L.H.; Simmons, A.M.; and Bodvarsson, G.S. 1998. *Results of Sensitivity Studies of Thermo-Hydrologic Behavior Conducted on Hydrologic Parameter Sets.* Milestone SP3CK5M4. Berkeley, California: Lawrence Berkeley National Laboratory. ACC: MOL.19980918.0001.

101995 Haynes International 1988. Hastelloy Alloy C-22. Kokomo, Indiana: Haynes International. TIC: 239938.

100452 Helton, J.C. 1993. "Uncertainty and Sensitivity Analysis Techniques for Use in Performance Assessment for Radioactive Waste Disposal." *Reliability Engineering and System Safety, 42,* (2-3), 327-367. Barking, Essex, England: Elsevier. TIC: 237878.

107739 Helton, J.C. 1994. "Treatment of Uncertainty in Performance Assessments for Complex Systems." *Risk Analysis, 14,* (4), 483-511. New York, New York: Plenum Press. TIC: 245848.

107823 Helton, J.C. 1996. "Probability, Conditional Probability and Complementary Cumulative Distribution Functions in Performance Assessment for Radioactive Waste Disposal." *Reliability Engineering and System Safety, 54,* 145-163. Oxford, United Kingdom: Elsevier. TIC: 246183.

107496 Helton, J.C. 1997. "Uncertainty and Sensitivity Analysis in the Presence of Stochastic and Subjective Uncertainty." *Journal of Statistical Computation and Simulation, 57,* (1-4), 3-76. New York, New York: Gordon and Breach Science Publishers. TIC: 245958.

159042 Helton, J.C. 1999. "Uncertainty and Sensitivity Analysis in Performance Assessment for the Waste Isolation Pilot Plant." *Computer Physics Communications, 117,* ([1-2]), 156-180. New York, New York: Elsevier. TIC: 253133.

170558 Helton, J.C. 2003. "Mathematical and Numerical Approaches in Performance Assessment for Radioactive Waste Disposal: Dealing with Uncertainty." Chapter 12 of *Modelling Radioactivity in the Environment.* Scott, E.M., ed. Radioactivity in the Environment. New York, New York: Elsevier. TIC: 256241.

107498 Helton, J.C. and Burmaster, D.E. 1996. "Guest Editorial: Treatment of Aleatory and Epistemic Uncertainty in Performance Assessments for Complex Systems." *Reliability Engineering and System Safety, 54,* 91-94. New York, New York: Elsevier. TIC: 245900.

156572 Helton, J.C. and Davis, F.J. 2000. *Sampling-Based Methods for Uncertainty and Sensitivity Analysis.* SAND99-2240. Albuquerque, New Mexico: Sandia National Laboratories. TIC: 251256.

183872 Helton, J.C. and Davis, F.J. 2002. "Illustration of Sampling-Based Methods for Uncertainty and Sensitivity Analysis." *Risk Analysis, 22,* (3), 591-622. [Malden, Massachusetts: Blackwell Publishing]. TIC: 259830.

163475 Helton, J.C. and Davis, F.J. 2002. *Latin Hypercube Sampling and the Propagation of Uncertainty in Analyses of Complex Systems.* SAND2001-0417. Albuquerque, New Mexico: Sandia National Laboratories. TIC: 254367.

170518 Helton, J.C. and Davis, F.J. 2003. "Latin Hypercube Sampling and the Propagation of Uncertainty in Analyses of Complex Systems." *Reliability Engineering & System Safety, 81,* ([1]), 23-69. [New York, New York]: Elsevier. TIC: 256239.

171759 Helton, J.C. and Marietta, M.G. 2000. "The 1996 Performance Assessment for the Waste Isolation Pilot Plant." *Reliability Engineering and System Safety, 69,* 1-3. [New York, New York]: Elsevier. TIC: 256585.

159560 Helton, J.C.; Johnson, J.D.; McKay, M.D.; Shiver, A.W.; and Sprung, J.L. 1995. "Robustness of an Uncertainty and Sensitivity Analysis of Early Exposure Results with the MACCS Reactor Accident Consequence Model." *Reliability Engineering & System Safety, 48,* ([2]), 129-148. [New York, New York]: Elsevier. TIC: 253092.

183873 Helton, J.C.; Johnson, J.D.; Sallaberry, C.J.; and Storlie, C.B. 2006. "Survey of Sampling-Based Methods for Uncertainty and Sensitivity Analysis." *Reliability Engineering and System Safety, 91,* 1175-1209. [New York, New York]: Elsevier. TIC: 259831.

151040 Hill, B.E.; Connor, C.B.; Jarzemba, M.S.; La Femina, P.C.; Navarro, M.; and Strauch, W. 1998. "1995 Eruptions of Cerro Negro Volcano, Nicaragua, and Risk Assessment for Future Eruptions." *Geological Society of America Bulletin, 110,* (10), 1231-1241. Boulder, Colorado: Geological Society of America. TIC: 245102.

107502 Hoffman, F.O. and Hammonds, J.S. 1994. "Propagation of Uncertainty in Risk Assessments: The Need to Distinguish Between Uncertainty Due to Lack of Knowledge and Uncertainty Due to Variability." *Risk Analysis, 14,* (5), 707-712. New York, New York: Plenum. TIC: 246313.

100902 Hora, S.C. and Iman, R.L. 1989. "Expert Opinion in Risk Analysis: The NUREG-1150 Methodology." *Nuclear Science and Engineering, 102,* 323-331. La Grange Park, Illinois: American Nuclear Society. TIC: 236031.

167022 Hua, F.; Mon, K.; Pasupathi, V.; Gordon, G.; and Shoesmith, D. 2004. "Corrosion of Ti Grade 7 and Other Ti Alloys in Nuclear Waste Repository Environments - A Review." *Corrosion/2004, 59th Annual Conference & Exposition, March 28-April 1, 2004, New Orleans.* Paper No. 04689. Houston, Texas: NACE International. TIC: 255943.

155232 IADC (International Association of Drilling Contractors) 1992. *Drilling Manual.* 11th Edition. [Houston, Texas]: International Association of Drilling Contractors. TIC: 232344.

153705 ICRP (International Commission on Radiological Protection) 1994. *Human Respiratory Tract Model for Radiological Protection.* Volume 24, Nos. 1-3 of *Annals of the ICRP.* Smith, H., ed. ICRP Publication 66. [New York, New York]: Pergamon. TIC: 249223.

178810 Ilton, E.S.; Liu, C.; Yantasee, W.; Wang, Z.; Moore, D.A.; Felmy, A.R.; and Zachara, J.M. 2006. "The Dissolution of Synthetic Na-Boltwoodite in Sodium Carbonate Solutions." *Geochimica et Cosmochimica Acta, 70,* 4836-4849. [New York, New York]: Elsevier. TIC: 259016.

146012 Iman, R.L. 1982. "Statistical Methods for Including Uncertainties Associated with the Geologic Isolation of Radioactive Waste Which Allow for a Comparison with Licensing Criteria." *Proceedings of the Symposium on Uncertainties Associated with the Regulation of the Geologic Disposal of High-Level Radioactive Waste, Gatlinburg, Tennessee, March 9-13, 1981.* Kocher, D.C., ed. NUREG/CP-0022. Pages145-157. Washington, D.C.: U.S. Nuclear Regulatory Commission. TIC: 213069.

158984 Iman, R.L. 1992. "Uncertainty and Sensitivity Analysis for Computer Modeling Applications." *Reliability Technology, 1992, Presented at the Winter Annual Meeting of the American Society of Mechanical Engineers, Anaheim, California, November 8-13, 1992.* Cruse, T.A., ed. AD-Vol. 28. Pages 153-168. New York, New York: American Society of Mechanical Engineers. TIC: 252828.

124158 Iman, R.L. and Conover, W.J. 1982. "A Distribution-Free Approach to Inducing Rank Correlation Among Input Variables." *Communications in Statistics, Simulation and Computation, 11,* (3), 311-334. New York, New York: Marcel Dekker. TIC: 243311.

159050 Iman, R.L. and Davenport, J.M. 1982. "Rank Correlation Plots for Use with Correlated Input Variables." *Communications in Statistics, Simulation and Computation, 11,* (3), 335-360. New York, New York: Marcel Dekker. TIC: 252829.

159052 Iman, R.L. and Helton, J.C. 1988. "An Investigation of Uncertainty and Sensitivity Analysis Techniques for Computer Models." *Risk Analysis, 8,* (1), 71-90. [New York, New York: Plenum Press]. TIC: 252831.

159039 Iman, R.L. and Helton, J.C. 1991. "The Repeatability of Uncertainty and Sensitivity Analyses for Complex Probabilistic Risk Assessments." *Risk Analysis, 11,* (4), 591-606. [New York, New York: Plenum Press]. TIC: 252830.

163337 Incropera, F.P. and DeWitt, D.P. 2002. *Fundamentals of Heat and Mass Transfer.* 5th Edition. [New York, New York]: John Wiley & Sons. TIC: 254280.

100987 Jarzemba, M.S.; LaPlante, P.A.; and Poor, K.J. 1997. *ASHPLUME Version 1.0—A Code for Contaminated Ash Dispersal and Deposition, Technical Description and User's Guide.* CNWRA 97-004, Rev. 1. San Antonio, Texas: Center for Nuclear Waste Regulatory Analyses. ACC: MOL.20010727.0162.

182066 Jégou, C.; Peuget, S.; Broudic, V.; Roudil, D.; Deschanels, X.; and Bart, J.M. 2004. "Identification of the Mechanism Limiting the Alteration of Clad Spent Fuel Segments in Aerated Carbonated Groundwater." *Journal of Nuclear Materials, 326,* 144-155. [New York, New York]: Elsevier. TIC: 259605.

125291 Johnson, A.B., Jr. and Francis, B. 1980. *Durability of Metals from Archaeological Objects, Metal Meteorites, and Native Metals.* PNL-3198. Richland, Washington: Pacific Northwest Laboratory. TIC: 229619.

167761 Kahraman, S.; Balci, C.; Yazici, S.; and Bilgin, N. 2000. "Prediction of the Penetration Rate of Rotary Blast Hole Drills Using a New Drillability Index." *International Journal of Rock Mechanics and Mining Sciences, 37,* ([5]), 729-743. [New York, New York]: Pergamon. TIC: 255709.

107741 Kaplan, S. 1993. "Formalisms for Handling Phenomenological Uncertainties: The Concepts of Probability, Frequency, Variability, and Probability of Frequency." *Nuclear Technology, 102,* (1), 137-142. La Grange Park, Illinois: American Nuclear Society. TIC: 245866.

100557 Kaplan, S. and Garrick, B.J. 1981. "On the Quantitative Definition of Risk." *Risk Analysis, 1,* (1), 11-27. New York, New York: Plenum Press. TIC: 241205.

180396 Katz, D.M.; Watts, F.J.; and Burroughs, E.R. 1995. "Effects of Surface Roughness and Rainfall Impact on Overland Flow." *Journal of Hydraulic Engineering, 121,* (7), 546-553. [Reston, Virginia]: American Society of Civil Engineers. TIC: 259291.

159053 Keeney, R.L. and von Winterfeldt, D. 1991. "Eliciting Probabilities from Experts in Complex Technical Problems." *IEEE Transactions on Engineering Management, 38,* (3), 191-201. [New York, New York: Institute of Electrical and Electronics Engineers]. TIC: 253205.

103282 Kersting, A.B.; Efurd, D.W.; Finnegan, D.L.; Rokop, D.J.; Smith, D.K.; and Thompson, J.L. 1999. "Migration of Plutonium in Ground Water at the Nevada Test Site." *Nature, 397,* ([6714]), 56-59. [London, England: Macmillan Journals]. TIC: 243597.

179402 Kimball, B.A.; Jackson, R.D.; Reginato, R.J.; Nakayama, F.S.; and Idso, S.B. 1976. "Comparison of Field-Measured and Calculated Soil–Heat Fluxes." *Soil Science Society of America Journal, 40,* (1), 18-28. [Madison, Wisconsin]: Soil Science Society of America. TIC: 259679.

159054 Kleijnen, J.P.C. and Helton, J.C. 1999. "Statistical Analyses of Scatterplots to Identify Important Factors in Large-Scale Simulations, 1: Review and Comparison of Techniques." *Reliability Engineering & System Safety, 65,* ([2]), 147-185. [New York, New York]: Elsevier. TIC: 253203.

160094 Klepeis, N.E. 1999. "An Introduction to the Indirect Exposure Assessment Approach: Modeling Human Exposure Using Microenvironmental Measurements and the Recent National Human Activity Pattern Survey." *Environmental Health Perspectives, 107,* (Supplement 2), 365-374. [Research Park Triangle, North Carolina: National Institute of Environmental Health Sciences, National Institutes of Health]. TIC: 250567.

100909 Kotra, J.P.; Lee, M.P.; Eisenberg, N.A.; and DeWispelare, A.R. 1996. *Branch Technical Position on the Use of Expert Elicitation in the High-Level Radioactive Waste Program.* NUREG-1563. Washington, D.C.: U.S. Nuclear Regulatory Commission. TIC: 226832.

178580 Kozak, M. and Kessler, J. 2005. *Program on Technology Innovation: EPRI Yucca Mountain Total System Performance Assessment Code (IMARC) Version 8, Model Description.* 1011813. Palo Alto, California: Electric Power Research Institute. TIC: 259558.

182054 Kuechler, R. and Noack, K. 2007. "Comparison of the Solution Behaviour of a Pyrite-Calcite Mixture in Batch and Unsaturated Sand Column." *Journal of Contaminant Hydrology, 90,* 203-220. [New York, New York]: Elsevier. TIC: 259604.

100051 Langmuir, D. 1997. *Aqueous Environmental Geochemistry.* Upper Saddle River, New Jersey: Prentice Hall. TIC: 237107.

167579 LANL (Los Alamos National Laboratory) 2003. *Software Users Manual (UM) for the FEHM Application Version 2.21.* Document ID: 10086-UM-2.21-00. Los Alamos, [New Mexico]: Los Alamos National Laboratory. ACC: MOL.20031031.0266.

160187 Lasaga, A.C. 1981. "Transition State Theory." Chapter 4 of *Kinetics of Geochemical Processes.* Lasaga, A.C., and Kirkpatrick, R.J., eds. Reviews in Mineralogy Volume 8. Washington, D.C.: Mineralogical Society of America. TIC: 239318.

100913 Lee, J.H.; Chambre, P.L.; and Andrews, R.W. 1996. "Mathematical Models for Diffusive Mass Transfer from Waste Package Container with Multiple Perforations." *Proceedings of the 1996 International Conference on Deep Geological Disposal of Radioactive Waste, September 16-19, 1996, Winnipeg, Manitoba, Canada.* Pages 5-61–5-72. Toronto, Ontario, Canada: Canadian Nuclear Society. TIC: 233923.

100464 Leigh, C.D.; Thompson, B.M.; Campbell, J.E.; Longsine, D.E.; Kennedy, R.A.; and Napier, B.A. 1993. *User's Guide for GENII-S: A Code for Statistical and Deterministic Simulations of Radiation Doses to Humans from Radionuclides in the Environment.* SAND91-0561. Albuquerque, New Mexico: Sandia National Laboratories. ACC: MOL.20010721.0031.

101714 Leslie, B.W.; Pearcy, E.C.; and Prikryl, J.D. 1993. "Oxidative Alteration of Uraninite at the Nopal I Deposit, Mexico: Possible Contaminant Transport and Source Term Constraints for the Proposed Repository at Yucca Mountain." *Scientific Basis for Nuclear Waste Management XVI, Symposium held November 30-December 4, 1992, Boston, Massachusetts.* Interrante, C.G. and Pabalan, R.T., eds. *294,* 505-512. Pittsburgh, Pennsylvania: Materials Research Society. TIC: 208880.

109967 Leslie, B.W.; Pickett, D.A.; and Pearcy, E.C. 1999. "Vegetation-Derived Insights on the Mobilization and Potential Transport of Radionuclides from the Nopal I Natural Analog Site, Mexico." *Scientific Basis for Nuclear Waste Management XXII, Symposium held November 30-December 4, 1998, Boston, Massachusetts, U.S.A.* Wronkiewicz, D.J. and Lee, J.H., eds. *556,* 833-842. Warrendale, Pennsylvania: Materials Research Society. TIC: 246426.

100053 Levy, S.S. 1991. "Mineralogic Alteration History and Paleohydrology at Yucca Mountain, Nevada." *High Level Radioactive Waste Management, Proceedings of the Second Annual International Conference, Las Vegas, Nevada, April 28-May 3, 1991. 1,* 477-485. La Grange Park, Illinois: American Nuclear Society. TIC: 204272.

121006 Lichtner, P.C.; Keating, G.; and Carey, B. 1999. *A Natural Analogue for Thermal-Hydrological-Chemical Coupled Processes at the Proposed Nuclear Waste Repository at Yucca Mountain, Nevada.* LA-13610-MS. Los Alamos, New Mexico: Los Alamos National Laboratory. TIC: 246032.

178081 Lide, D.R., ed. 2006. *CRC Handbook of Chemistry and Physics.* 87th Edition. Boca Raton, Florida: CRC Press. TIC: 258634.

172722 Lieser, K.H. and Bauscher, C. 1987. "Technetium in the Hydrosphere and in the Geosphere. I. Chemistry of Technetium and Iron in Natural Waters and Influence of the Redox Potential on the Sorption of Technetium." *Radiochimica Acta, 42,* (4), 205-213. München, Germany: R. Oldenbourg Verlag. TIC: 256859.

106684 Lieser, K.H. and Muhlenweg, U. 1988. "Neptunium in the Hydrosphere and in the Geosphere, I. Chemistry of Neptunium in the Hydrosphere and Sorption of Neptunium from Groundwaters on Sediments Under Aerobic and Anaerobic Conditions." *Radiochimica Acta, 43,* 27-35. München, Germany: R. Oldenbourg Verlag. TIC: 236783.

180748 Lin, C.; Leslie, B.; Codell, R.; Arlt, H.; and Ahn, T. 2003. "Potential Importance of Fluoride to Performance of the Drip Shield." *Proceedings of the 10th International High-Level Radioactive Waste Management Conference (IHLRWM), March 30-April 2, 2003, Las Vegas, Nevada.* Pages 646-652. La Grange Park, Illinois: American Nuclear Society. TIC: 254559.

109440 Litwin, R.J.; Smoot, J.P.; Durika, N.J.; and Smith, G.I. 1999. "Calibrating Late Quaternary Terrestrial Climate Signals: Radiometrically Dated Pollen Evidence from the Southern Sierra Nevada, USA." *Quaternary Science Reviews, 18,* 1151-1171. New York, New York: Pergamon Press. TIC: 245700.

169948 Liu, H.H.; Bodvarsson, G.S.; and Zhang, G. 2004. "Scale Dependency of the Effective Matrix Diffusion Coefficient." *Vadose Zone Journal, 3,* ([1]), 312-315. Madison, Wisconsin: Soil Science Society of America. TIC: 256150.

105729 Liu, H.H.; Doughty, C.; and Bodvarsson, G.S. 1998. "An Active Fracture Model for Unsaturated Flow and Transport in Fractured Rocks." *Water Resources Research, 34,* (10), 2633-2646. Washington, D.C.: American Geophysical Union. TIC: 243012.

162470 Liu, H-H.; Haukwa, C.B.; Ahlers, C.F.; Bodvarsson, G.S.; Flint, A.L.; and Guertal, W.B. 2003. "Modeling Flow and Transport in Unsaturated Fractured Rock: An Evaluation of the Continuum Approach." *Journal of Contaminant Hydrology, 62-63,* 173-188. New York, New York: Elsevier. TIC: 254205.

162478 Liu, J.; Sonnenthal, E.L.; and Bodvarsson, G.S. 2003. "Calibration of Yucca Mountain Unsaturated Zone Flow and Transport Model Using Porewater Chloride Data." *Journal of Contaminant Hydrology, 62-63,* 213-235. New York, New York: Elsevier. TIC: 254205.

170258 LLNL (Lawrence Livermore National Laboratory) 2000. *Validation Test Plan, The Prediction of Thermohydrologic Behavior—NUFT 3.0.1s.* Document Number: 10130-VTP-3.0.1s-00. North Las Vegas, Nevada: U.S. Department of Energy, Yucca Mountain Site Characterization Office. ACC: MOL.20010905.0180.

170259 LLNL (Lawrence Livermore National Laboratory) 2002. *Validation Test Plan, The Prediction of Thermohydrologic Behavior—NUFT 3.0s, Rev 02.* Software Document Number: 10088-VTP-3.0s-02. North Las Vegas, Nevada: U.S. Department of Energy, Yucca Mountain Site Characterization Office. ACC: MOL.20031024.0397.

168999 Loo, H.H.; MacKay, N.S.; and Wheatley, P.D. 2004. *Additional DOE Spent Nuclear Fuel Information in Support of TSPA-LA Analysis.* DOE/SNF/REP-081, Rev. 0. Idaho Falls, Idaho: U.S. Department of Energy, DOE Idaho Operations Office. ACC: DOC.20040202.0007.

166315 Lu, N.; Conca, J.; Parker, G.R.; Leonard, P.A.; Moore, B.; Strietelmeier, B.; and Triay, I.R. 2000. *Adsorption of Actinides onto Colloids as a Function of Time, Temperature, Ionic Strength, and Colloid Concentration, Waste Form Colloids Report for Yucca Mountain Program (Colloid Data Summary from 1999 to 2000 Research).* LA-UR-00-5121. Los Alamos, New Mexico: Los Alamos National Laboratory. ACC: MOL.20031204.0108.

125923 Lutze, W.; Grambow, B.; Ewing, R.C.; and Jercinovic, M.J. 1987. "The Use of Natural Analogues in the Long-Term Extrapolation of Glass Corrosion Processes." *Natural Analogues in Radioactive Waste Disposal, Symposium held in Brussels on 28-30 April 1987.* Côme, B. and Chapman, N.A., eds. EUR 11037 EN. Pages 142-152. Norwell, Massachusetts: Graham & Trotman. TIC: 247254.

162465 Mage, D.T. 1985. "Concepts of Human Exposure Assessment for Airborne Particulate Matter." *Environment International, 11,* 407-412. [New York, New York]: Pergamon Press. TIC: 250582.

182155 Manepally, C.; Bradbury, K.; Colton, S.; Dinwiddle, C.; Green, R.; McGinnis, R.; Sims, D.; Smart, K.; and Walter, G. 2007. *The Nature of Flow in the Faulted and Fractured Paintbrush Nonwelded Hydrogeologic Unit.* San Antonio, Texas: Center for Nuclear Waste Regulatory Analyses. ACC: LLR.20070725.0014.

159031 Martinez, L.J.; Meertens, C.M.; and Smith, R.B. 1998. "Rapid Deformation Rates Along the Wasatch Fault Zone, Utah, from First GPS Measurements with Implications for Earthquake Hazard." *Geophysical Research Letters, 25,* (4), 567-570. [Washington, D.C.]: American Geophysical Union. TIC: 246585.

111885 Mattsson, H. and Olefjord, I. 1990. "Analysis of Oxide Formed on Ti During Exposure in Bentonite Clay-I. The Oxide Growth." *Werkstoffe und Corrosion, 41,* (7), 383-390. Weinheim, Germany: VCH Verlagsgesellschaft mbH. TIC: 246290.

179401 Matubayasi, N.; Matsuo, H.; Yamamoto, K.; Yamaguchi, S.; and Matuzawa, A. 1999. "Thermodynamic Quantities of Surface Formation of Aqueous Electrolyte Solutions I. Aqueous Solutions of NaCl, MgCl{subscript 2} and LaCl{subscript 3}." *Journal of Colloid and Interface Science, 209,* 398-402. [New York, New York]: Academic Press. TIC: 259292.

127905 McKay, M.D.; Beckman, R.J.; and Conover, W.J. 1979. "A Comparison of Three Methods for Selecting Values of Input Variables in the Analysis of Output from a Computer Code." *Technometrics, 21,* (2), 239-245. Alexandria, Virginia: American Statistical Association. TIC: 221741.

182657 McKenzie, J.M. 2007. Postclosure Radionuclide Release Source Term for Representative Naval SNF Waste Package - Igneous Intrusive and Nominal/Early Failure Scenarios. Letter from J.M. McKenzie to E.F. Sproat, III, August 22, 2007, NR:RA:GFHOLDEN U#07-03303, with enclosure. ACC: LLR.20070823.0027.

162827 McKnight, S.B. and Williams, S.W. 1997. "Old Cinder Cone or Young Composite Volcano?: The Nature of Cerro Negro, Nicaragua." *Geology, 25,* (4), 339–342. [Boulder, Colorado: Geological Society of America]. TIC: 254104.

181382 McLoughlin, S.D.; Hyatt, N.C.; Hand, R.J.; and Lee, W.E. 2006. "Corrosion of Archaeological Model Glasses After 32 Years of Burial at Ballidon." *Scientific Basis for Nuclear Waste Management XXIX, Symposime held September 12-16, 2005, Ghent, Belgium.* Iseghem, P.V.; ed. *932,* 1065-1072. Warrendale, Pennsylvania: Materials Research Society. TIC: 259526.

180862 Meinrath, G. 2001. "Measurement Uncertainty of Thermodynamic Data." *Fresenius Journal of Analytical Chemistry,* (369), 690-697. [New York, New York]: Springer-Verlag. TIC: 259386.

180861 Meinrath, G.; Ekberg, C.; Landgren, A.; and Liljenzin, J.O 2000. "Assessment of Uncertainty in Parameter Evaluation and Prediction." *Talanta, 51,* 231-246. [New York, New York]: Elsevier. TIC: 259387.

110460 Meyer, M.A. and Booker, J.M. 1991. *Eliciting and Analyzing Expert Judgement, A Practical Guide.* Volume 5 of *Knowledge-Based Systems.* Boose, J. and Gaines, B., eds. San Diego, California: Academic Press. TIC: 235911.

105462 Miller, G.A. 1977. *Appraisal of the Water Resources of Death Valley, California-Nevada.* Open-File Report 77-728. Menlo Park, California: U.S. Geological Survey. ACC: HQS.19880517.1934.

161678 Molecke, M.A.; Ruppen, J.A.; and Diegle, R.B. 1982. *Materials for High-Level Waste Caister/Overpacks in Salt Formations.* SAND82-0429. Albuquerque, New Mexico: Sandia National Laboratories. TIC: 231459.

159055 Mosleh, A.; Bier, V.M.; and Apostolakis, G. 1988. "A Critique of Current Practice for the Use of Expert Opinions in Probabilistic Risk Assessment." *Reliability Engineering and System Safety, 20,* 63-85. [New York, New York]: Elsevier. TIC: 253204.

121310 Murphy, W.M. 1995. "Contributions of Thermodynamic and Mass Transport Modeling to Evaluation of Groundwater Flow and Groundwater Travel Time at Yucca Mountain, Nevada." *Scientific Basis for Nuclear Waste Management XVIII, Symposium held October 23-27, 1994, Kyoto, Japan.* Murakami, T. and Ewing, R.C., eds. *353,* 419-426. Pittsburgh, Pennsylvania: Materials Research Society. TIC: 216341.

149529 Murphy, W.M. and Codell, R.B. 1999. "Alternate Source Term Models for Yucca Mountain Performance Assessment Based on Natural Analog Data and Secondary Mineral Solubility." *Scientific Basis for Nuclear Waste Management XXII, Symposium held November 30-December 4, 1998, Boston, Massachusetts.* Wronkiewicz, D.J. and Lee, J.H., eds. *556,* 551-558. Warrendale, Pennsylvania: Materials Research Society. TIC: 246426.

151773 Murphy, W.M. and Pearcy, E.C. 1992. "Source-Term Constraints for the Proposed Repository at Yucca Mountain, Nevada, Derived from the Natural Analog at Pena Blanca, Mexico." *Scientific Basis for Nuclear Waste Management XV, Symposium held November 4-7, 1991, Strasbourg, France.* Sombret, C.G., ed. *257,* 521-527. Pittsburgh, Pennsylvania: Materials Research Society. TIC: 204618.

151772 Murphy, W.M.; Pearcy, E.C.; and Goodell, P.C. 1991. "Possible Analog Research Sites for the Proposed High-Level Nuclear Waste Repository in Hydrologically Unsaturated Tuff at Yucca Mountain, Nevada." *Nuclear Science and Technology, Fourth Natural Analogue Working Group Meeting and Pocos de Caldas Project Final Workshop, Pitlochry, 18 to 22 June 1990, Scotland, Final Report.* Come, B. and Chapman N.A., eds. EUR 13014 EN. Pages 267-276. Brussels, [Belgium]: Commission of European Communities. TIC: 248757.

181017 Myers, T.G. 2002. "Modeling Laminar Sheet Flow Over Rough Surfaces." *Water Resources Research, 38,* (11), 12-1 - 12-12. Washington, D.C.: American Geophysical Union. TIC: 259426.

157927 Napier, B.A.; Peloquin, R.A.; Strenge, D.L.; and Ramsdell, J.V. 1988. *Conceptual Representation.* Volume 1 of *GENII - The Hanford Environmental Radiation Dosimetry Software System.* PNL-6584. Richland, Washington: Pacific Northwest Laboratory. TIC: 252237.

177331 Napier, B.A.; Strenge, D.L.; Ramsdell, J.V., Jr.; Eslinger, P.W.; and Fosmire, C. 2006. *GENII Version 2 Software Design Document.* PNNL-14584, Rev. 1. [Richland, Washington]: Pacific Northwest National Laboratory. ACC: MOL.20060815.0035.

179400 Nassar, I.N. and Horton, R. 1989. "Water Transport in Unsaturated Nonisothermal Salty Soil: II. Theoretical Development." *Soil Science Society of America Journal, 53,* 1330-1337. [Madison, Wisconsin]: Soil Science Society of America. TIC: 259678.

152309 NEA (Nuclear Energy Agency) 1999. *An International Database of Features, Events and Processes.* Paris, France: Organisation for Economic Co-operation and Development. TIC: 248820.

180924 Neymark, L.A.; Paces, J.B.; Marshall, B.D.; Peterman, Z.E.; and Whelan, J.F. 2005. "Geochemical and C, O, Sr, and U-series Isotopic Evidence for the Meteoric Origin of Calcrete at Solitario Wash, Crater Flat, Nevada, USA." *Environmental Geology, 48,* 450-465. [New York, New York]: Springer-Verlag. TIC: 258003.

100809 Nguyen, S.N.; Silva, R.J.; Weed, H.C.; and Andrews, J.E., Jr. 1992. "Standard Gibbs Free Energies of Formation at the Temperature 303.15 K of Four Uranyl Silicates: Soddyite, Uranophane, Sodium Boltwoodite, and Sodium Weeksite." *Journal of Chemical Thermodynamics, 24,* (1-6), 359-376. New York, New York: Academic Press. TIC: 238507.

155218 Nitsche, H.; Gatti, R.C.; Standifer, E.M.; Lee, S.C.; Müller, A.; Prussin, T.; Deinhammer, R.S.; Maurer, H.; Becraft, K.; Leung, S.; and Carpenter, S.A. 1993. *Measured Solubilities and Speciations of Neptunium, Plutonium, and Americium in a Typical Groundwater (J-13) from the Yucca Mountain Region.* LA-12562-MS. Los Alamos, New Mexico: Los Alamos National Laboratory. ACC: NNA.19930507.0136.

144515 Nitsche, H.; Roberts, K.; Prussin, T.; Muller, A.; Becraft, K.; Keeney, D.; Carpenter, S.A.; and Gatti, R.C. 1994. *Measured Solubilities and Speciations from Oversaturation Experiments of Neptunium, Plutonium, and Americium in UE-25P #1 Well Water from the Yucca Mountain Region Milestone Report 3329-WBS1.2.3.4.1.3.1.* LA-12563-MS. Los Alamos, New Mexico: Los Alamos National Laboratory. TIC: 210589.

160556 Ogden, H.R. 1960. "Titanium and Its Alloys." In *Materials,* Volume I, Chapter 30 of *Reactor Handbook.* 2nd Edition. New York, New York: Interscience Publishers. TIC: 245052.

180494 Ojovan, M.I.; Hand, R.J.; Ojovan, N.V.; and Lee, W.E. 2005. "Corrosion of Alkali-Borosilicate Waste Glass K-26 in Non-Saturated Conditions." *Journal of Nuclear Materials, 340,* 12-24. [New York, New York]: Elsevier. TIC: 259324.

101280 Ortiz, T.S.; Williams, R.L.; Nimick, F.B.; Whittet, B.C.; and South, D.L. 1985. *A Three-Dimensional Model of Reference Thermal/Mechanical and Hydrological Stratigraphy at Yucca Mountain, Southern Nevada.* SAND84-1076. Albuquerque, New Mexico: Sandia National Laboratories. ACC: MOL.19980602.0331.

159057 Owen, A.B. 1992. "A Central Limit Theorem for Latin Hypercube Sampling." *Journal of the Royal Statistical Society: Series B, Statistical Methodology, 54,* (2), 541-551. London, England: Royal Statistical Society. TIC: 253131.

174513 Paces, J.B. and Neymark, L.A. 2004. "U-Series Evidence of Water-Rock Interaction at Yucca Mountain, Nevada, USA." *Proceedings of the Eleventh International Symposium on Water-Rock Interaction, WRI-11, 27 June-2 July 2004.* Wanty, R.B. and Seal, R.R., II, eds. *1,* 475-479. New York, New York: A.A. Balkema Publishers. TIC: 257516.

174071 Painter, S.; Cvetkovic, V.; Pickett, D.; and Turner, D.R. 2002. "Significance of Kinetics for Sorption of Inorganic Colloids: Modeling and Experiment Interpretation Issues." *Environmental Science & Technology, 36,* (24), 5369-5375. [Washington, D.C.]: American Chemical Society. TIC: 257438.

164181 Pan, L.; Warrick, A.W.; and Wierenga, P.J. 1997. "Downward Water Flow Through Sloping Layers in the Vadose Zone: Time-Dependence and Effect of Slope Length." *Journal of Hydrology, 199,* ([1-2]), 36-52. [New York, New York]: Elsevier. TIC: 254555.

180455 Pan, P. and Campbell, A.B. 1998. "The Characterization of Np{subscript 2}O{subscript 5}(c) and Its Dissolution in CO{subscript 2}-Free Aqueous Solutions at pH 6 to 13 and 25ºC." *Radiochimica Acta, 81,* (2), . München, Germany: R. Oldenbourg Verlag. TIC: 259301.

179398 Papendick, R.I. and Campbell, G.S. 1981. "Theory and Measurement of Water Potential." Chapter 1 of *Water Potential Relations in Soil Microbiology.* SSSA Special Publication Number 9. Pages 1-22. Madison, Wisconsin: Soil Science Society of America. TIC: 218386.

103896 Parrington, J.R.; Knox, H.D.; Breneman, S.L.; Baum, E.M.; and Feiner, F. 1996. *Nuclides and Isotopes, Chart of the Nuclides.* 15th Edition. San Jose, California: General Electric Company and KAPL, Inc. TIC: 233705.

159059 Parry, G.W. and Winter, P.W. 1981. "Characterization and Evaluation of Uncertainty in Probabilistic Risk Analysis." *Nuclear Safety, 22,* (1), 28-41. Washington, D.C.: U.S. Department of Energy, Technical Information Center. TIC: 252834.

170519 Paté-Cornell, M.E. 1986. "Probability and Uncertainty in Nuclear Safety Decisions." *Nuclear Engineering and Design, 93,* ([2-3]), 319-327. Amsterdam, The Netherlands: North-Holland. TIC: 256240.

107499 Paté-Cornell, M.E. 1996. "Uncertainties in Risk Analysis: Six Levels of Treatment." *Reliability Engineering and System Safety, 54,* 95-111. New York, New York: Elsevier. TIC: 245961.

149523 Pearcy, E.C. 1994. *Fracture Transport of Uranium at the Nopal I Natural Analog Site.* CNWRA 94-011. San Antonio, Texas: Center for Nuclear Waste Regulatory Analyses. TIC: 247808.

110223 Pearcy, E.C.; Prikryl, J.D.; and Leslie, B.W. 1995. "Uranium Transport Through Fractured Silicic Tuff and Relative Retention in Areas with Distinct Fracture Characteristics." *Applied Geochemistry, 10,* 685-704. Oxford, United Kingdom: Elsevier. TIC: 246848.

151774 Pearcy, E.C.; Prikryl, J.D.; Murphy, W.M.; and Leslie, B.W. 1993. *Uranium Mineralogy of the Nopal I Natural Analog Site, Chihuahua, Mexico.* CNWRA 93-012. San Antonio, Texas: Center for Nuclear Waste Regulatory Analyses. TIC: 246628.

100486 Pearcy, E.C.; Prikryl, J.D.; Murphy, W.M.; and Leslie, B.W. 1994. "Alteration of Uraninite from the Nopal I Deposit, Pena Blanca District, Chihuahua, Mexico, Compared to Degradation of Spent Nuclear Fuel in the Proposed U.S. High-Level Nuclear Waste Repository at Yucca Mountain, Nevada." *Applied Geochemistry, 9,* 713-732. New York, New York: Elsevier. TIC: 236934.

109989 Pickett, D.A. and Murphy, W.M. 1997. "Isotopic Constraints on Radionuclide Transport at Pena Blanca." *Seventh EC Natural Analogue Working Group Meeting: Proceedings of an International Workshop held in Stein am Rhein, Switzerland from 28 to 30 October 1996.* von Maravic, H. and Smellie, J., eds. EUR 17851 EN. Pages 113-122. Luxembourg, Luxembourg: Office for Official Publications of the European Communities. TIC: 247461.

110009 Pickett, D.A. and Murphy, W.M. 1999. "Unsaturated Zone Waters from the Nopal I Natural Analog, Chihuahua, Mexico - Implications for Radionuclide Mobility at Yucca Mountain." *Scientific Basis for Nuclear Waste Management XXII, Symposium held November 30-December 4, 1998, Boston, Massachusetts.* Wronkiewicz, D.J. and Lee, J.H., eds. *556,* 809-816. Warrendale, Pennsylvania: Materials Research Society. TIC: 246426.

182055 Pierce, E.M.; Icenhower, J.P.; Serne, R.J.; and Catalano, J.G. 2005. "Experimental Determination of UO{subscript 2}(cr) Dissolution Kinetics: Effects of Solution Saturation State and pH." *Journal of Nuclear Materials, 345,* 206-218. [New York, New York]: Elsevier. TIC: 259597.

107812 PLG (Pickard, Lowe, and Garrick) 1982. *Indian Point Probabilistic Safety Study.* Irvine, California: Pickard, Lowe, and Garrick. TIC: 247144.

107813 PLG (Pickard, Lowe, and Garrick) 1983. *Seabrook Station Probabilistic Safety Assessment.* PLG-0300, Rev. 2. Sections 4-13. Irvine, California: Pickard, Lowe and Garrick. TIC: 247143.

148063 PLG (Pickard, Lowe, and Garrick) 1983. *Seabrook Station Probabilistic Safety Assessment, Main Report.* PLG-0300, Rev. 2. Sections 1-3. Irvine, California: Pickard, Lowe and Garrick. TIC: 247420.

103316 Press, W.H.; Teukolsky, S.A.; Vetterling, W.T.; and Flannery, B.P. 1992. *Numerical Recipes in Fortran 77, The Art of Scientific Computing.* Volume 1 of *Fortran Numerical Recipes.* 2nd Edition. Cambridge, United Kingdom: Cambridge University Press. TIC: 243606.

104250 Pruess, K. 1999. "A Mechanistic Model for Water Seepage Through Thick Unsaturated Zones in Fractured Rocks of Low Matrix Permeability." *Water Resources Research, 35,* (4), 1039-1051. Washington, D.C.: American Geophysical Union. TIC: 244913.

167791 Putot, C.J.M.; Guesnon, J.; Perreau, P.J.; and Constantinescu, A. 2000. "Quantifying Drilling Efficiency and Disruption: Field Data vs. Theoretical Model." *SPE Drilling & Completion, 15,* (2), 118-125. [Richardson, Texas]: Society of Petroleum Engineers. TIC: 255897.

122768 Rai, D. 1984. "Solubility Product of Pu(IV) Hydrous Oxide and Equilibrium Constants of Pu (IV)/Pu (V), Pu (IV)/Pu (VI), and Pu (V)/Pu (VI) Couples." *Radiochimica Acta, 35,* 97-106. München, Germany: R. Oldenbourg Verlag. TIC: 219109.

137138 Rai, D. and Ryan, J.L. 1985. "Neptunium (IV) Hydrous Oxide Solubility under Reducing and Carbonate Conditions." *Inorganic Chemistry, 24,* (3), 247-251. Washington, D.C.: American Chemical Society. TIC: 246852.

168392 Rai, D.; Moore, D.A.; Felmy, A.R.; Choppin, G.R.; and Moore, R.C. 2001. "Thermodynamics of the PuO{subscript 2}{superscript +}-Na{superscript +}-OH{superscript -}-Cl{superscript -}-ClO{subscript 4}{superscript -}-H{subscript 2}O System: Use of NpO{subscript 2}{superscript +} Pitzer Parameters for PuO{subscript 2}{superscript +}." *Radiochimica Acta, 89,* ([8]), 491-498. München, Germany: Oldenbourg Wissenschaftsverlag. TIC: 255398.

158380 Reamer, C.W. 2001. "U.S. Nuclear Regulatory Commission/U.S. Department of Energy Technical Exchange and Management Meeting on Total System Performance Assessment and Integration (August 6 through 10, 2001)." Letter from C.W. Reamer (NRC) to S. Brocoum (DOE/YMSCO), August 23, 2001, with enclosure. ACC: MOL.20011029.0281.

145383 Rechard, R.P. 1999. "Historical Relationship Between Performance Assessment for Radioactive Waste Disposal and Other Types of Risk Assessment." *Risk Analysis, 19,* (5), 763-807. New York, New York: Kluwer Academic / Plenum Publishers. TIC: 246972.

147343 Rechard, R.P., ed. 1993. *Initial Performance Assessment of the Disposal of Spent Nuclear Fuel and High Level Waste Stored at Idaho National Engineering Laboratory.* SAND93-2330. Volumes 1 and 2. Albuquerque, New Mexico: Sandia National Laboratories. TIC: 247212.

179246 Reimus, P.W.; Callahan, T.J.; Ware, S.D.; Haga, M.J.; and Counce, D.A. 2007. "Matrix Diffusion Coefficients in Volcanic Rocks at the Nevada Test Site: Influence of Matrix Porosity, Matrix Permeability, and Fracture Coating Minerals." *Journal of Contaminant Hydrology, 93,* 85-95. [New York, New York]: Elsevier. TIC: 259673.

149533 Reyes-Cortes, I.A. 1997. *Geologic Studies in the Sierra de Peña Blanca, Chihuahua, Mexico.* Ph.D. dissertation. El Paso, Texas: University of Texas at El Paso. TIC: 247866.

180698 Robinson, B.A.; Wolfsberg, A.V.; Viswanathan, H.S.; and Reimus, P.W. 2007. "A Colloid-Facilitated Transport Model with Variable Colloid Transport Properties." *Geophysical Research Letters, 34,* 1-5. [Washington, D.C.]: American Geophysical Union. TIC: 259346.

108567 Robinson, R.A. and Stokes, R.H. 1965. *Electrolyte Solutions, The Measurement and Interpretation of Conductance, Chemical Potential and Diffusion in Solutions of Simple Electrolytes.* 2nd Edition (Revised). Washington, D.C.: Butterworth. TIC: 242575.

181366 Rodríguez-Pineda, J.A.; Goodell, P.; Dobson, P.F.; Walton, J.; Oliver, R.D.; De La Garza, R.; and Harder, S. 2005. "Regional Hydrology of the Nopal I Site, Sierra de Peña Blanca, Chihuahua, Mexico." *Abstracts with Programs - Geological Society of America, 37,* (7), 196. Boulder, Colorado: Geological Society of America. TIC: 258167.

172064 Ross, S.M. 1993. *Introduction to Probability Models.* 5th Edition. San Diego, California: Academic Press. TIC: 245879.

182190 Runde, W.; Neu, M.P.; Conradson, S.D.; Clark, D.L.; Palmer, P.D.; Reilly, S.D.; Scott, B.L.; and Tait, C.D. 1997. "Spectroscopic Investigation of Actinide Speciation in Concentrated Chloride Solution." *Scientific Basis for Nuclear Waste Management XX, Symposium held December 2-6 1996, Boston Massachusetts.* Gray, W.J. and Triay, I.R., eds. *465,* 693-703. Pittsburgh, Pennsylvania: Materials Research Society. TIC: 238884.

180747 Ruschak, K.J.; Weinstein, S.J.; and Ng, K. 2001. "Developing Film Flow on an Inclined Plane with a Critical Point." *Journal of Fluids Engineering, 123,* 698-703. [New York, New York]: American Society of Mechanical Engineers. TIC: 259356.

182015 Santos, B.G.; Noël, J.J.; and Shoesmith, D.W. 2006. "The Influence of Calcium Ions on the Development of Acidity in Corrosion Product Deposits on SIMFUEL, UO{subscript 2}." *Journal of Nuclear Materials, 350,* 320-331. [New York, New York]: Elsevier. TIC: 259603.

182052 Santos, B.G.; Noël, J.J.; and Shoesmith, D.W. 2006. "The Influence of Silicate on the Development of Acidity in Corrosion Product Deposits on SIMFUEL (UO{subscript 2})." *Corrosion Science, 48,* 3852-3868. [New York, New York]: Elsevier. TIC: 259602.

100075 Sawyer, D.A.; Fleck, R.J.; Lanphere, M.A.; Warren, R.G.; Broxton, D.E.; and Hudson, M.R. 1994. "Episodic Caldera Volcanism in the Miocene Southwestern Nevada Volcanic Field: Revised Stratigraphic Framework, {superscript 40}Ar/{superscript 39}Ar Geochronology, and Implications for Magmatism and Extension." *Geological Society of America Bulletin, 106,* (10), 1304-1318. Boulder, Colorado: Geological Society of America. TIC: 222523.

162423 Schijven, J.F.; Hoogenboezem, W.; Hassanizadeh, S.M.; and Peters, J.H. 1999. "Modeling Removal of Bacteriophages MS2 and PRD1 by Dune Recharge at Castricum, Netherlands." *Water Resources Research, 35,* (4), 1101-1111. Washington, D.C.: American Geophysical Union. TIC: 252295.

112147 Schutz, R.W. and Thomas, D.E. 1987. "Corrosion of Titanium and Titanium Alloys." In *Corrosion,* Volume 13, Pages 669-706 of *ASM Handbook.* Formerly 9th Edition, Metals Handbook. [Materials Park, Ohio]: ASM International. TIC: 240704.

159070 Shafer, G. 1978. "Non-Additive Probabilities in the Work of Bernoulli and Lambert." *Archive for History of Exact Sciences, 19,* (4), 309-370. New York, New York: Springer-Verlag. TIC: 253047.

161591 Sharpe, S. 2003. *Future Climate Analysis—10,000 Years to 1,000,000 Years After Present.* MOD-01-001 REV 01. [Reno, Nevada: Desert Research Institute]. ACC: MOL.20030407.0055.

159545 Sheppard, M.I.; Sheppard, S.C.; and Amiro, B.D. 1991. "Mobility and Plant Uptake of Inorganic {superscript 14}C and {superscript 14}C-Labelled PCB in Soils of High and Low Retention." *Health Physics, 61,* (4), 481-492. New York, New York: Pergamon Press. TIC: 252687.

119589 Shibata, T. 1996. "Statistical and Stochastic Approaches to Localized Corrosion." *Corrosion, 52,* (11), 813-830. Houston, Texas: National Association of Corrosion Engineers. TIC: 236691.

114445 Shoesmith, D.W. 1999. *Fuel Corrosion Processes Under Waste Disposal Conditions.* AECL-12034. Pinawa, Manitoba, Canada: Whiteshell Laboratories. TIC: 246006.

113368 Shoesmith, D.W. and Sunder, S. 1992. "The Prediction of Nuclear Fuel (UO2) Dissolution Rates Under Waste Disposal Conditions." *Journal of Nuclear Materials, 190,* 20-35. Amsterdam, The Netherlands: Elsevier. TIC: 246431.

164741 Singh, B. 2002. "Nuclear Data Sheets for A = 79." *Nuclear Data Sheets, 96,* (1), 1-240. San Diego, California: Elsevier. TIC: 254728.

109480 Smith, G.I. and Bischoff, J.L., eds. 1997. *An 800,000-Year Paleoclimatic Record from Core OL-92, Owens Lake, Southeast California.* Geological Society of America, Special Paper 317. Boulder, Colorado: Geological Society of America. TIC: 236857.

119483 Smyth, J.R. 1982. "Zeolite Stability Constraints on Radioactive Waste Isolation in Zeolite-Bearing Volcanic Rocks." *Journal of Geology, 90,* (2), 195-201. Chicago, Illinois: University of Chicago Press. TIC: 221104.

177081 SNL (Sandia National Laboratories) 2006. *Data Analysis for Infiltration Modeling: Extracted Weather Station Data Used to Represent Present-Day and Potential Future Climate Conditions in the Vicinity of Yucca Mountain.* ANL-MGR-MD-000015 REV 00. Las Vegas, Nevada: Sandia National Laboratories. ACC: DOC.20070109.0002.

181244 SNL (Sandia National Laboratories) 2007. *Abstraction of Drift Seepage.* MDL-NBS-HS-000019 REV 01 ADD 01. Las Vegas, Nevada: Sandia National Laboratories. ACC: DOC.20070807.0001.

181267 SNL (Sandia National Laboratories) 2007. *Analysis of Dust Deliquescence for FEP Screening.* ANL-EBS-MD-000074 REV 01 AD 01. Las Vegas, Nevada: Sandia National Laboratories. ACC: DOC.20070911.0004; DOC.20070824.0001.

178765 SNL (Sandia National Laboratories) 2007. *Analysis of Mechanisms for Early Waste Package/Drip Shield Failure.* ANL-EBS-MD-000076 REV 00. Las Vegas, Nevada: Sandia National Laboratories. ACC: DOC.20070629.0002; DOC.20071003.0015.

177431 SNL (Sandia National Laboratories) 2007. *Atmospheric Dispersal and Deposition of Tephra from a Potential Volcanic Eruption at Yucca Mountain, Nevada.* MDL-MGR-GS-000002 REV 03. Las Vegas, Nevada: Sandia National Laboratories. ACC: DOC.20071010.0003.

177399 SNL (Sandia National Laboratories) 2007. *Biosphere Model Report.* MDL-MGR-MD-000001 REV 02. Las Vegas, Nevada: Sandia National Laboratories. ACC: DOC.20070830.0007.

179545 SNL (Sandia National Laboratories) 2007. *Calibrated Unsaturated Zone Properties.* ANL-NBS-HS-000058 REV 00. Las Vegas, Nevada: Sandia National Laboratories. ACC: DOC.20070530.0013.

174260 SNL (Sandia National Laboratories) 2007. *Characterize Eruptive Processes at Yucca Mountain, Nevada.* ANL-MGR-GS-000002 REV 03. Las Vegas, Nevada: Sandia National Laboratories. ACC: DOC.20070301.0001.

180616 SNL (Sandia National Laboratories) 2007. *Cladding Degradation Summary for LA.* ANL-WIS-MD-000021 REV 03 ADD 01. Las Vegas, Nevada: Sandia National Laboratories. ACC: DOC.20050815.0002; DOC.20070614.0002.

184077 SNL (Sandia National Laboratories) 2007. *Data Qualification Report for the Qualification of the Preliminary Output from MDL-NBS-HS-000023, REV 01.* TDR-NBS-HS-000020 REV 00. Las Vegas, Nevada: Sandia National Laboratories.

177430 SNL (Sandia National Laboratories) 2007. *Dike/Drift Interactions.* MDL-MGR-GS-000005 REV 02. Las Vegas, Nevada: Sandia National Laboratories. ACC: DOC.20071009.0015.

177418 SNL (Sandia National Laboratories) 2007. *Dissolved Concentration Limits of Elements with Radioactive Isotopes.* ANL-WIS-MD-000010 REV 06. Las Vegas, Nevada: Sandia National Laboratory. ACC: DOC.20070918.0010.

177404 SNL (Sandia National Laboratories) 2007. *Drift-Scale THC Seepage Model.* MDL-NBS-HS-000001 REV 05. Las Vegas, Nevada: Sandia National Laboratories. ACC: DOC.20071010.0004.

177407 SNL (Sandia National Laboratories) 2007. *EBS Radionuclide Transport Abstraction.* ANL-WIS-PA-000001 REV 03. Las Vegas, Nevada: Sandia National Laboratories. ACC: DOC.20071004.0001.

177412 SNL (Sandia National Laboratories) 2007. *Engineered Barrier System: Physical and Chemical Environment.* ANL-EBS-MD-000033 REV 06. Las Vegas, Nevada: Sandia National Laboratories. ACC: DOC.20070907.0003.

179476 SNL (Sandia National Laboratories) 2008. *Features, Events, and Processes for the Total System Performance Assessment: Methods.* ANL-WIS-MD-000026 REV 00. Las Vegas, Nevada: Sandia National Laboratories.

183041 SNL (Sandia National Laboratories) 2008. *Features, Events, and Processes for the Total System Performance Assessment: Analyses.* ANL-WIS-MD-000027 REV 00. Las Vegas, Nevada: Sandia National Laboratories.

178519 SNL (Sandia National Laboratories) 2007. *General Corrosion and Localized Corrosion of Waste Package Outer Barrier.* ANL-EBS-MD-000003 REV 03. Las Vegas, Nevada: Sandia National Laboratories. ACC: DOC.20070730.0003; DOC.20070807.0007.

180778 SNL (Sandia National Laboratories) 2007. *General Corrosion and Localized Corrosion of the Drip Shield.* ANL-EBS-MD-000004 REV 02 ADD 01. Las Vegas, Nevada: Sandia National Laboratories. ACC: DOC.20060427.0002; DOC.20070807.0004; DOC.20071003.0019.

181648 SNL (Sandia National Laboratories) 2007. *In-Drift Natural Convection and Condensation.* MDL-EBS-MD-000001 REV 00 AD 01. Las Vegas, Nevada: Sandia National Laboratories. ACC: DOC.20050330.0001; DOC.20051122.0005; DOC.20070907.0004.

177411 SNL (Sandia National Laboratories) 2007. *In-Drift Precipitates/Salts Model.* ANL-EBS-MD-000045 REV 03. Las Vegas, Nevada: Sandia National Laboratories. ACC: DOC.20070306.0037.

180472 SNL (Sandia National Laboratories) 2007. *Initial Radionuclide Inventories.* ANL-WIS-MD-000020 REV 01 ADD 01. Las Vegas, Nevada: Sandia National Laboratories. ACC: DOC.20050927.0005; DOC.20070801.0001.

180506 SNL (Sandia National Laboratories) 2007. *In-Package Chemistry Abstraction.* ANL-EBS-MD-000037 REV 04 ADD 01. Las Vegas, Nevada: Sandia National Laboratories. ACC: DOC.20070816.0004.

178851 SNL (Sandia National Laboratories) 2007. *Mechanical Assessment of Degraded Waste Packages and Drip Shields Subject to Vibratory Ground Motion.* MDL-WIS-AC-000001 REV 00. Las Vegas, Nevada: Sandia National Laboratories. ACC: DOC.20070917.0006.

177422 SNL (Sandia National Laboratories) 2007. *MOX Spent Nuclear Fuel and LaBS Glass for TSPA-LA.* ANL-WIS-MD-000022 REV 01. Las Vegas, Nevada: Sandia National Laboratories. ACC: DOC.20070220.0007.

181383 SNL (Sandia National Laboratories) 2007. *Multiscale Thermohydrologic Model.* ANL-EBS-MD-000049 REV 03 ADD 01. Las Vegas, Nevada: Sandia National Laboratories. ACC: DOC.20070831.0003.

177432 SNL (Sandia National Laboratories) 2007. *Number of Waste Packages Hit by Igneous Events.* ANL-MGR-GS-000003 REV 03. Las Vegas, Nevada: Sandia National Laboratories. ACC: DOC.20071002.0001.

184748 SNL (Sandia National Laboratories) 2008. *Particle Tracking Model and Abstraction of Transport Processes.* MDL-NBS-HS-000020 REV 02 AD 02. Las Vegas, Nevada: Sandia National Laboratories.

177424 SNL (Sandia National Laboratories) 2007. *Radionuclide Screening.* ANL-WIS-MD-000006 REV 02. Las Vegas, Nevada: Sandia National Laboratories. ACC: DOC.20070326.0003.

177396 SNL (Sandia National Laboratories) 2007. *Radionuclide Transport Models Under Ambient Conditions.* MDL-NBS-HS-000008 REV 02 ADD 01. Las Vegas, Nevada: Sandia National Laboratories. ACC: DOC.20050823.0003; DOC.20070718.0003.

179347 SNL (Sandia National Laboratories) 2007. *Redistribution of Tephra and Waste by Geomorphic Processes Following a Potential Volcanic Eruption at Yucca Mountain, Nevada.* MDL-MGR-GS-000006 REV 00. Las Vegas, Nevada: Sandia National Laboratories. ACC: DOC.20071220.0004.

183750 SNL (Sandia National Laboratories) 2008. *Saturated Zone Flow and Transport Model Abstraction.* MDL-NBS-HS-000021 REV 03 AD 02. Las Vegas, Nevada: Sandia National Laboratories. ACC: DOC.20080107.0006.

177394 SNL (Sandia National Laboratories) 2007. *Saturated Zone In-Situ Testing.* ANL-NBS-HS-000039 REV 02. Las Vegas, Nevada: Sandia National Laboratories. ACC: DOC.20070608.0004.

177391 SNL (Sandia National Laboratories) 2007. *Saturated Zone Site-Scale Flow Model.* MDL-NBS-HS-000011 REV 03. Las Vegas, Nevada: Sandia National Laboratories. ACC: DOC.20070626.0004; DOC.20071001.0013.

176828 SNL (Sandia National Laboratories) 2007. *Seismic Consequence Abstraction.* MDL-WIS-PA-000003 REV 03. Las Vegas, Nevada: Sandia National Laboratories. ACC: DOC.20070928.0011.

182145 SNL (Sandia National Laboratories) 2007. *Simulation of Net Infiltration for Present-Day and Potential Future Climates.* MDL-NBS-HS-000023 REV 01 AD 01. Las Vegas, Nevada: Sandia National Laboratories.

177392 SNL (Sandia National Laboratories) 2007. *Site-Scale Saturated Zone Transport.* MDL-NBS-HS-000010 REV 03. Las Vegas, Nevada: Sandia National Laboratories. ACC: DOC.20070822.0003, DOC.20080117.0002.

181953 SNL (Sandia National Laboratories) 2007. *Stress Corrosion Cracking of Waste Package Outer Barrier and Drip Shield Materials.* ANL-EBS-MD-000005 REV 04. Las Vegas, Nevada: Sandia National Laboratories. ACC: DOC.20070913.0001.

179287 SNL (Sandia National Laboratories) 2007. *Technical Work Plan for: Revision of Model Reports for Near-Field and In-Drift Water Chemistry.* TWP-MGR-PA-000038 REV 02. Las Vegas, Nevada: Sandia National Laboratories. ACC: DOC.20070110.0004.

182219 SNL (Sandia National Laboratories) 2007. *Technical Work Plan for: Igneous Activity Assessment for Disruptive Events.* TWP-WIS-MD-000007 REV 10. Las Vegas, Nevada: Sandia National Laboratories. ACC: DOC.20070830.0002.

184920 SNL (Sandia National Laboratories) 2008. *Technical Work Plan for: Total System Performance Assessment FY 07-08 Activities.* TWP-MGR-PA-000045 REV 01 ICN 02. Las Vegas, Nevada: Sandia National Laboratories. ACC: DOC.20080131.0048.

179354 SNL (Sandia National Laboratories) 2007. *Total System Performance Assessment Data Input Package for Requirements Analysis for Engineered Barrier System In-Drift Configuration.* TDR-TDIP-ES-000010 REV 00. Las Vegas, Nevada: Sandia National Laboratories. ACC: DOC.20070921.0008.

179394 SNL (Sandia National Laboratories) 2007. *Total System Performance Assessment Data Input Package for Requirements Analysis for Transportation Aging and Disposal Canister and Related Waste Package Physical Attributes Basis for Performance Assessment.* TDR-TDIP-ES-000006 REV 00. Las Vegas, Nevada: Sandia National Laboratories. ACC: DOC.20070918.0005.

179412 SNL (Sandia National Laboratories) 2007. *Total System Performance Assessment Data Input Package for Site-Scale Saturated Zone Breakthrough Curves.* TDR-TDIP-NS-000005 REV 00. Las Vegas, Nevada: Sandia National Laboratories. ACC: DOC.20070423.0004.

179466 SNL (Sandia National Laboratories) 2007. *Total System Performance Assessment Data Input Package for Requirements Analysis for Subsurface Facilities.* TDR-TDIP-PA-000001 REV 00. Las Vegas, Nevada: Sandia National Laboratories. ACC: DOC.20070921.0007.

179567 SNL (Sandia National Laboratories) 2007. *Total System Performance Assessment Data Input Package for Requirements Analysis for DOE SNF/HLW and Naval SNF Waste Package Physical Attributes Basis for Performance Assessment.* TDR-TDIP-ES-000009 REV 00. Las Vegas, Nevada: Sandia National Laboratories. ACC: DOC.20070921.0009.

180677 SNL (Sandia National Laboratories) 2007. *Total System Performance Assessment (TSPA) Data Input Package for Saturated Zone 1-D Transport Model.* TDR-TDIP-NS-000006 REV 00. Las Vegas, Nevada: Sandia National Laboratories. ACC: DOC.20070503.0008.

181031 SNL (Sandia National Laboratories) 2007. *Total System Performance Assessment (TSPA) Data Input Package for General Corrosion and Localized Corrosion of Waste Package Outer Barrier.* TDR-TDIP-ES-000001 REV 01. Las Vegas, Nevada: Sandia National Laboratories. ACC: DOC.20070510.0001.

184614 SNL (Sandia National Laboratories) 2007. *UZ Flow Models and Submodels.* MDL-NBS-HS-000006 REV 03 AD 01. Las Vegas, Nevada: Sandia National Laboratories. ACC: DOC.20080108.0003

177423 SNL (Sandia National Laboratories) 2007. *Waste Form and In-Drift Colloids-Associated Radionuclide Concentrations: Abstraction and Summary.* MDL-EBS-PA-000004 REV 03. Las Vegas, Nevada: Sandia National Laboratories. ACC: DOC.20071018.0019.

159400 Snow, J.K. and Wernicke, B.P. 2000. "Cenozoic Tectonism in the Central Basin and Range: Magnitude, Rate, and Distribution of Upper Crustal Strain." *American Journal of Science, 300,* (9), 659-719. New Haven, Connecticut: Yale University, Kline Geology Laboratory. TIC: 253039.

117127 Sonnenthal, E.L. and Bodvarsson, G.S. 1999. "Constraints on the Hydrology of the Unsaturated Zone at Yucca Mountain, NV from Three-Dimensional Models of Chloride and Strontium Geochemistry." *Journal of Contaminant Hydrology, 38,* (1-3), 107-156. New York, New York: Elsevier. TIC: 244160.

159060 Stein, M. 1987. "Large Sample Properties of Simulations Using Latin Hypercube Sampling." *Technometrics, 29,* (2), 143-151. [Alexandria, Virginia]: American Statistical Association. TIC: 253129.

151957 Stuckless, J.S. 2000. *Archaeological Analogues for Assessing the Long-Term Performance of a Mined Geologic Repository for High-Level Radioactive Waste.* Open-File Report 00-181. Denver, Colorado: U.S. Geological Survey. ACC: MOL.20000822.0366.

125332 Stumm, W. and Morgan, J.J. 1996. *Aquatic Chemistry, Chemical Equilibria and Rates in Natural Waters.* 3rd Edition. New York, New York: John Wiley & Sons. TIC: 246296.

100489 Suzuki, T. 1983. "A Theoretical Model for Dispersion of Tephra." *Arc Volcanism: Physics and Tectonics, Proceedings of a 1981 IAVCEI Symposium, August-September, 1981, Tokyo and Hakone.* Shimozuru, D. and Yokoyama, I., eds. Pages 95-113. Tokyo, Japan: Terra Scientific Publishing Company. TIC: 238307.

182056 Sverdrup, H. and Warfvinge, P. 1988. "Weathering of Primary Silicate Minerals in the Natural Soil Environment in Relation to a Chemical Weathering Model." *Water, Air, and Soil Pollution, 38,* 387-408. [Boston, Massachusetts]: Kluwer Academic Publishers. TIC: 259601.

119053 Thatcher, W.; Foulger, G.R.; Julian, B.R.; Svarc, J.; Quilty, E.; and Bawden, G.W. 1999. "Present-Day Deformation Across the Basin and Range Province, Western United States." *Science, 283,* (5408), 1714-1718. Washington, D.C.: American Association for the Advancement of Science. TIC: 246227.

159061 Thorne, M.C. 1993. "The Use of Expert Opinion in Formulating Conceptual Models of Underground Disposal Systems and the Treatment of Associated Bias." *Reliability Engineering and System Safety, 42,* 161-180. [New York, New York]: Elsevier. TIC: 252832.

180513 Tokunaga, T.K.; Olson, K.R.; and Wan, J. 2005. "Infiltration Flux Distributions in Unsaturated Rock Deposits and Their Potential Implications for Fractured Rock Formations." *Geophysical Research Letters, 32,* (L05405), 1-4. [Washington, D.C.]: American Geophysical Union. TIC: 259312.

170136 Truesdell, A.H. and Jones, B.F. 1974. "WATEQ, A Computer Program for Calculating Chemical Equilibria of Natural Waters." *Journal of Research of the U.S. Geological Survey, 3,* (2), 233-248. Menlo Park, California: U.S. Geological Survey. TIC: 224163.

183166 Varel International 2006. Roller Cone Bits, Oil & Gas Products 2006. Carrollton, Texas: Varel International. TIC: 259758.

128494 Vesely, W.E.; Goldberg, F.F.; Roberts, N.H.; and Haasl, D.F. 1981. *Fault Tree Handbook.* NUREG - 0492. Washington, D.C.: U.S. Nuclear Regulatory Commission. TIC: 208328.

164449 Waiting, D.J.; Stamatakos, J.A.; Ferrill, D.A.; Sims, D.W.; Morris, A.P.; Justus, P.S.; and Ibrahim, A.K. 2003. "Methodologies for the Evaluation of Faulting at Yucca Mountain, Nevada." *Proceedings of the 10th International High-Level Radioactive Waste Management Conference (IHLRWM), March 30-April 2, 2003, Las Vegas, Nevada.* Pages 377-387. La Grange Park, Illinois: American Nuclear Society. TIC: 254559.

127454 Walton, J.C. 1994. "Influence of Evaporation on Waste Package Environment and Radionuclide Release from a Tuff Repository." *Water Resources Research, 30,* (12), 3479-3487. Washington, D.C.: American Geophysical Union. TIC: 246921.

108835 Wang, J.S.Y. and Narasimhan, T.N. 1985. "Hydrologic Mechanisms Governing Fluid Flow in a Partially Saturated, Fractured, Porous Medium." *Water Resources Research, 21,* (12), 1861-1874. Washington, D.C.: American Geophysical Union. TIC: 225290.

106793 Wang, J.S.Y. and Narasimhan, T.N. 1993. "Unsaturated Flow in Fractured Porous Media." Chapter 7 of *Flow and Contaminant Transport in Fractured Rock.* Bear, J.; Tsang, C-F.; and de Marsily, G., eds. San Diego, California: Academic Press. TIC: 235461.

155234 Warren, T.M. 1987. "Penetration-Rate Performance of Roller-Cone Bits." *Drilling.* SPE Reprint Series No. 22. Richardson, Texas: Society of Petroleum Engineers. TIC: 250084.

180902 Weber, C.L.; Vanbriesen, J.M.; and Small, M.S. 2006. "A Stochastic Regression Approach to Analyzing Thermodynamic Uncertainty in Chemical Speciation Modeling." *Environmental Science & Technology, 40,* (12), 3872-3878. [Washington, D.C.]: American Chemical Society. TIC: 259389.

100476 Wescott, R.G.; Lee, M.P.; Eisenberg, N.A.; McCartin, T.J.; and Baca, R.G., eds. 1995. *NRC Iterative Performance Assessment Phase 2, Development of Capabilities for Review of a Performance Assessment for a High-Level Waste Repository.* NUREG-1464. Washington, D.C.: U.S. Nuclear Regulatory Commission. ACC: MOL.19960710.0075.

182943 Wheatley, P.D. 2007. "Transmittal of Document EDF-NSNF-035, Radionuclide Inventory Calculation Checkes, SFD Version 5.0.1, Rev. 1." Letter from P.D. Wheatley (INL) to K. Knowles (SNL) and R.M. Kacich (BSC), August, 23, 2007, CCN 210849, with enclosure. ACC: RPM.20070828.0160.

168088 White, A.F. and Brantley, S.L. 2003. "The Effect of Time on the Weathering of Silicate Minerals: Why Do Weathering Rates Differ in the Laboratory and Field?" *Chemical Geology, 202,* ([3-4]), 479-506. [New York, New York]: Elsevier. TIC: 255730.

157307 Williams, N.H. 2001. "Contract No. DE-AC08-01RW12101 – Total System Performance Assessment – Analyses for Disposal of Commercial and DOE Waste Inventories at Yucca Mountain – Input to Final Environmental Impact Statement and Site Suitability Evaluation REV 00 ICN 02." Letter from N.H. Williams (BSC) to J.R. Summerson (DOE/YMSCO), December 11, 2001, RWA:cs-1204010670, with enclosure. ACC: MOL.20011213.0056.

157389 Williams, N.H. 2001. "Contract No. DE-AC08-01RW12101 – Uncertainty Analyses and Strategy Letter Report, REV 00, Activity #SA011481M4." Letter from N.H. Williams (BSC) to S.J. Brocoum (DOE/YMSCO), November 19, 2001, JM:cs-1116010483, with enclosure. ACC: MOL.20020109.0064.

115085 Wilson, C.N. and Gray, W. J. 1990. "Measurement of Soluble Nuclide Dissolution Rates from Spent Fuel." *Scientific Basis for Nuclear Waste Management XIII, Symposium held November 27-30, 1989, Boston, Massachusetts.* Oversby, V.M. and Brown, P.W., eds. *176,* 489-498. Pittsburgh, Pennsylvania: Materials Research Society. TIC: 203658.

100191 Wilson, M.L.; Gauthier, J.H.; Barnard, R.W.; Barr, G.E.; Dockery, H.A.; Dunn, E.; Eaton, R.R.; Guerin, D.C.; Lu, N.; Martinez, M.J.; Nilson, R.; Rautman, C.A.; Robey, T.H.; Ross, B.; Ryder, E.E.; Schenker, A.R.; Shannon, S.A.; Skinner, L.H.; Halsey, W.G.; Gansemer, J.D.; Lewis, L.C.; Lamont, A.D.; Triay, I.R.; Meijer, A.; and Morris, D.E. 1994. *Total-System Performance Assessment for Yucca Mountain – SNL Second Iteration (TSPA-1993).* SAND93-2675. Executive Summary and two volumes. Albuquerque, New Mexico: Sandia National Laboratories. ACC: NNA.19940112.0123.

174895 Wittman, R.S.; Buck, E.C.; and Hanson, B.D. 2005. *Data Analysis of Plutonium Sorption on Colloids in a Minimal Kinetics Model.* PNNL-15285. Richland, Washington: Pacific Northwest National Laboratory. ACC: MOL.20050811.0087.

174800 Wong, L.L.; Lian, T.; Fix, D.V.; Sutton, M.; and Rebak, R.B. 2004. "Surface Analysis of Alloy 22 Coupons Exposed for Five Years to Concentrated Ground Waters." *Corrosion/2004, 59th Annual Conference & Exposition, March 28 - April 1, 2004, New Orleans.* Paper No. 04701. Houston, Texas: NACE International. TIC: 255943.

163662 Woods, A.W.; Sparks, S.; Bokhove, O.; LeJeune, A-M.; Conner, C.B.; and Hill, B.E. 2002. "Modeling Magma-Drift Interaction at the Proposed High-Level Radioactive Waste Repository at Yucca Mountain, Nevada, USA." *Geophysical Research Letters, 29,* (13), 19-1 through 19-4. [Washington, D.C.]: American Geophysical Union. TIC: 254467.

102047 Wronkiewicz, D.J.; Bates, J.K.; Wolf, S.F.; and Buck, E.C. 1996. "Ten-Year Results from Unsaturated Drip Tests with UO{subscript 2} at 90°C: Implications for the Corrosion of Spent Nuclear Fuel." *Journal of Nuclear Materials, 238,* (1), 78-95. Amsterdam, The Netherlands: North-Holland. TIC: 243361.

117161 Wu, Y.S.; Haukwa, C.; and Bodvarsson, G.S. 1999. "A Site-Scale Model for Fluid and Heat Flow in the Unsaturated Zone of Yucca Mountain, Nevada." *Journal of Contaminant Hydrology, 38,* (1-3), 185-215. New York, New York: Elsevier. TIC: 244160.

156399 Wu, Y.S.; Liu, H.H.; Bodvarsson, G.S.; and Zellmer, K.E. 2001. *A Triple-Continuum Approach for Modeling Flow and Transport Processes in Fractured Rock.* LBNL-48875. Berkeley, California: Lawrence Berkeley National Laboratory. TIC: 251297.

117167 Wu, Y.S.; Ritcey, A.C.; and Bodvarsson, G.S. 1999. "A Modeling Study of Perched Water Phenomena in the Unsaturated Zone at Yucca Mountain." *Journal of Contaminant Hydrology, 38,* (1-3), 157-184. New York, New York: Elsevier. TIC: 244160.

160195 Wu, Y-S.; Pan, L.; Zhang, W.; and Bodvarsson, G.S. 2002. "Characterization of Flow and Transport Processes within the Unsaturated Zone of Yucca Mountain, Nevada, Under Current and Future Climates." *Journal of Contaminant Hydrology, 54,* ([3-4]), 215-247. [New York, New York]: Elsevier. TIC: 253316.

154918 Wu, Y-S.; Zhang, W.; Pan, L.; Hinds, J.; and Bodvarsson, G.S. 2000. *Capillary Barriers in Unsaturated Fractured Rocks of Yucca Mountain, Nevada.* LBNL-46876. Berkeley, California: Lawrence Berkeley National Laboratory. TIC: 249912.

161058 Wu, Y-S.; Zhang, W.; Pan, L.; Hinds, J.; and Bodvarsson, G.S. 2002. "Modeling Capillary Barriers in Unsaturated Fractured Rock." *Water Resources Research, 38,* (11), 35-1 through 35-12. [Washington, D.C.]: American Geophysical Union. TIC: 253854.

159465 Yu, C.; Zielen, A.J.; Cheng, J.-J.; LePoire, D.J.; Gnanapragasam, E.; Kamboj, S.; Arnish, J.; Wallo, A., III; Williams, W.A.; and Peterson, H. 2001. *User's Manual for RESRAD Version 6.* ANL/EAD-4. Argonne, Illinois: Argonne National Laboratory. TIC: 252702.

180273 Zhang, K.; Wu, Y-S.; and Pan, L. 2006. "Temporal Damping Effect of the Yucca Mountain Fractured Unsaturated Rock on Transient Infiltration Pulses." *Journal of Hydrology, 327,* 235-248. [New York, New York]: Elsevier. TIC: 259283.

154702 Zheng, C. and Bennett, G.D. 1995. *Applied Contaminant Transport Modeling, Theory and Practice.* New York, New York: Van Nostrand Reinhold. TIC: 249865.

100615 Zyvoloski, G.A.; Robinson, B.A.; Dash, Z.V.; and Trease, L.L. 1997. *User's Manual for the FEHM Application–A Finite-Element Heat- and Mass-Transfer Code.* LA-13306-M. Los Alamos, New Mexico: Los Alamos National Laboratory. TIC: 235999.

9.2 CODES, STANDARDS, REGULATIONS, AND PROCEDURES

180319 10 CFR 63. 2007. Energy: Disposal of High-Level Radioactive Wastes in a Geologic Repository at Yucca Mountain, Nevada. Internet Accessible.

173176 40 CFR 197. 2004. Protection of Environment: Public Health and Environmental Radiation Protection Standards for Yucca Mountain, Nevada: ACC: MOL.20050324.0101.

175755 40 CFR 197. 2005. Protection of Environment: Public Health and Environmental Radiation Protection Standards for Yucca Mountain, Nevada. ACC: MOL.20051121.0084.

155216 66 FR 32074. 40 CFR Part 197, Public Health and Environmental Radiation Protection Standards for Yucca Mountain, NV; Final Rule. ACC: MOL.20050418.0113.

156671 66 FR 55732. Disposal of High-Level Radioactive Wastes in a Proposed Geologic Repository at Yucca Mountain, NV, Final Rule. 10 CFR Parts 2, 19, 20, 21, 30, 40, 51, 60, 61, 63, 70, 72, 73, and 75. ACC: MOL.20050324.0102; MOL.20050418.0124.

177357 70 FR 49014. Public Health and Environmental Radiation Protection Standards for Yucca Mountain, NV. Internet Accessible.

178394 70 FR 53313. Implementation of a Dose Standard After 10,000 Years. Internet Accessible.

122137 DOE (U.S. Department of Energy) 1995. *The Nuclear Waste Policy Act, as Amended, with Appropriations Acts Appended.* DOE/RW-0438, Rev. 1. Washington, D.C.: U.S. Department of Energy, Office of Civilian Radioactive Waste Management. ACC: HQO.19950124.0001.

100975 DOE 1996. *Title 40 CFR Part 191 Compliance Certification Application for the Waste Isolation Pilot Plant.* DOE/CAO-1996-2184. Twenty-one volumes. Carlsbad, New Mexico: U.S. Department of Energy, Carlsbad Area Office. TIC: 240511.

100017 Energy Policy Act of 1992. Public Law No. 102-486, 106 Stat. 2776. TIC: 233191.

116135 EPA (U.S. Environmental Protection Agency) 1997. *Activity Factors.* Volume III of *Exposure Factors Handbook.* EPA/600/P-95/002Fc. Washington, D.C.: U.S. Environmental Protection Agency. TIC: 241062.

175544 EPA (U.S. Environmental Protection Agency) 2002. *Federal Guidance Report 13, CD Supplement, Cancer Risk Coefficients for Environmental Exposure to Radionuclides, EPA.* EPA-402-C-99-001, Rev. 1. [Washington, D.C.]: U.S. Environmental Protection Agency. ACC: MOL.20051013.0016.

100061 National Research Council. 1990. *Rethinking High-Level Radioactive Waste Disposal, A Position Statement of the Board on Radioactive Waste Management.* Washington, D.C.: National Academy Press. TIC: 205153.

100018 National Research Council. 1995. *Technical Bases for Yucca Mountain Standards.* Washington, D.C.: National Academy Press. TIC: 217588.

107799 NRC (U.S. Nuclear Regulatory Commission) 1975. *Reactor Safety Study: An Assessment of Accident Risks in U.S. Commercial Nuclear Power Plants.* WASH-1400. Washington, D.C.: U.S. Nuclear Regulatory Commission. TIC: 236923.

107798 NRC (U.S. Nuclear Regulatory Commission) 1990. *Severe Accident Risks: An Assessment for Five U.S. Nuclear Power Plants.* NUREG-1150. Washington, D.C.: U.S. Nuclear Regulatory Commission. TIC: 214826.

163274 NRC (U.S. Nuclear Regulatory Commission) 2003. *Yucca Mountain Review Plan, Final Report.* NUREG-1804, Rev. 2. Washington, D.C.: U.S. Nuclear Regulatory Commission, Office of Nuclear Material Safety and Safeguards. TIC: 254568.

182132 NRC (U.S. Nuclear Regulatory Commission) 2007. *Igneous Activity at Yucca Mountain: Technical Basis for Decisionmaking.* [Washington, D.C.]: U.S. Nuclear Regulatory Commission, Advisory Committee on Nuclear Waste and Materials. ACC: LLR.20070725.0023.

176542 *Nuclear Energy Institute, Inc., Petitioner v. U.S. Environmental Protection Agency, Respondent,* No. 01-1258 (U.S. Court of Appeals for the District of Columbia Circuit). Argued January 14, 2004 and Decided July 9, 2004. Internet Accessible.

131951 Nuclear Waste Policy Act of 1982. 42 U.S.C. 10101-10133. (1988). Internet Accessible.

100016 Nuclear Waste Policy Amendments Act of 1987. Public Law No. 100-203, 101 Stat. 1330. TIC: 223717.

103445 OECD (Organization for Economic Co-operation and Development) 1997. *Lessons Learnt From Ten Performance Assessment Studies.* Paris, France: Organization for Economic Co-operation and Development. TIC: 243964.

158098 OECD (Organization for Economic Co-operation and Development) and IAEA (International Atomic Energy Agency) 2002. *An International Peer Review of the Yucca Mountain Project TSPA-SR, Total System Performance Assessment for the Site Recommendation (TSPA-SR).* Paris, France: Organization for Economic Co-operation and Development, Nuclear Energy Agency. TIC: 252385.

159027 OECD (Organization for Economic Co-operation and Development, Nuclear Energy Agency) 2001. *Chemical Thermodynamics of Neptunium and Plutonium.* Volume 4 of *Chemical Thermodynamics.* New York, New York: Elsevier. TIC: 209037.

154158 USDA (U.S. Department of Agriculture) 2000. *Food and Nutrient Intakes by Individuals in the United States, 1994-1996.* Nationwide Food Surveys Report No. 96-3. Two volumes. [Washington, D.C.: U.S. Department of Agriculture]. TIC: 249498.

9.3 SOFTWARE CODES

181034 ASHPLUME_DLL_LA V. 2.0. 2003. WINDOWS 2000. STN: 11117-2.0-00.

181035 ASHPLUME_DLL_LA V. 2.1. 2006. WinDOWS 2000/XP. STN: 11117-2.1-00.

180147 ASHPLUME_DLL_LA V. 2.1. 2007. WINDOWS 2003. STN: 11117-2.1-01.

162809 CWD V. 2.0. 2003. WINDOWS 2000. STN: 10363-2.0-00.

181037 CWD V. 2.0. 2007. WINDOWS 2003. STN: 10363-2.0-01.

162228 EQ3/6 V. 8.0. 2003. WINDOWS 2000, WIN NT 4.0, WIN 98, WIN 95. STN: 10813-8.0-00.

176889 EQ3/6 V. 8.1. 2005. WINDOWS 2000. STN: 10813-8.1-00.

159731 EQ6 V. 7.2bLV. 2002. WINDOWS 2000, NT. STN: 10075-7.2bLV-02.

182102 EXDOC_LA V. 2.0. 2007. WINDOWS XP, WINDOWS 2000 & WINDOWS 2003. STN: 11193-2.0-00.

180002 FAR V. 1.1. 2007. WINDOWS 2000 & 2003. STN: 11190-1.1-00.

182225 FAR V. 1.2. 2007. WINDOWS 2000 & WINDOWS 2003. STN: 11190-1.2-00.

173139 FEHM V. 2.23. 2005. WINDOWS 2000. STN: 10086-2.23-00.

179419 FEHM V. 2.24-01. 2007. WIN2003, 2000, & XP, Red Hat Linux 2.4.21, OS 5.9. STN: 10086-2.24-01-00.

182477 FEHM V. 2.25. 2007. Win2000, WinXP, Win2003, SunOS5.9, Linux2.4.21. STN: 10086-2.25-00.

159684 FEPS Database Software Program V. .2. 2002. WINDOWS 2000. STN: 10418-.2-00.

181089 FEPS Viewer V. 1.0. 2007. Windows 2000/XP. STN: 611664-1.0-00.

164315 FLUENT V. 6.0.12. 2003. Redhat Linux V7.3. STN: 10550-6.0.12-01.

181040 GetThk_LA V. 1.0. 2006. WINDOWS 2000 & WINDOWS 2003. STN: 11229-1.0-00.

173352 GOLDSIM V. 8.02.400. 2005. WINDOWS 2000. STN: 10344-8.02-04.

174650 GoldSim V. 8.02.500. 2005. WINDOWS 2000. STN: 10344-8.02-05.

180224 GoldSim V. 9.60. 2007. WINDOWS 2000, WINDOWS XP, WINDOWS 2003. STN: 10344-9.60-00.

181903 Goldsim V. 9.60.100. 2007. WIN 2000, 2003, XP. STN: 10344-9.60-01.

167885 InterpZdll_LA V. 1.0. 2004. WINDOWS 2000. STN: 11107-1.0-00.

181043 InterpZdll_LA V. 1.0. 2007. WINDOWS 2003. STN: 11107-1.0-01.

160106 iTOUGH2 V. 5.0. 2002. SunOS 5.5.1, OSF1 V5.1, RedHat V7.2 and V7.3. STN: 10003-5.0-00.

167884 MFCP_LA V. 1.0. 2003. WINDOWS 2000. STN: 11071-1.0-00.

181045 MFCP_LA V. 1.0. 2006. WINDOWS 2003. STN: 11071-1.0-01.

174528 MkTable V. 1.00. 2003. WINDOWS 2000. STN: 10505-1.00-00.

181047 MkTable_LA V. 1.0. 2006. WINDOWS 2000. STN: 11217-1.0-00.

181048 MkTable_LA V. 1.0. 2007. WINDOWS 2003. STN: 11217-1.0-01.

164274 MSTHAC V. 7.0. 2002. SUN O.S. 5.8. STN: 10419-7.0-00.

181049 MView V. 4.0. 2007. WINDOWS XP. STN: 10072-4.0-01.

169130 PassTable1D_LA V. 1.0. 2004. WINDOWS 2000. STN: 11142-1.0-00.

181050 PassTable1D_LA V. 1.0. 2006. WINDOWS 2003. STN: 11142-1.0-01.

181051 PassTable1D_LA V. 2.0. 2007. WINDOWS 2000 & WINDOWS 2003. STN: 11142-2.0-00.

168980 PassTable3D_LA V. 1.0. 2004. WINDOWS 2000. STN: 11143-1.0-00.

181052 PassTable3D_LA V. 1.0. 2007. WINDOWS 2003. STN: 11143-1.0-01.

182556 PassTable3D_LA V. 2.0. 2007. WINDOWS 2000 & WINDOWS 2003. STN: 11143-2.0-00.

181053 PREWAP_LA V. 1.1. 2006. WINDOWS 2000. STN: 10939-1.1-00.

181157 SCCD V. 2.01. 2003. WINDOWS 2000. STN: 10343-2.01-00.

181054 SCCD V. 2.01. 2007. WINDOWS 2003. STN: 10343-2.01-01.

173435 SEEPAGEDLL_LA V. 1.2. 2005. WINDOWS 2000. STN: 11076-1.2-00.

180318 SEEPAGEDLL_LA V. 1.3. 2006. WINDOWS 2000. STN: 11076-1.3-00.

181058 SEEPAGEDLL_LA V. 1.3. 2007. WINDOWS 2003. STN: 11076-1.3-01.

152844 Software Code: ASHPLUME V. 2.0. 2001. PC. STN: 10022-2.0-00.

161296 Software Code: ASHPLUME V1.4LV. 2002. PC, Windows 2000/NT/98. STN: 10022-1.4LV-02.

153964 Software Code: EQ3/6 V. 7.2b. 1999. UCRL-MA-110662 (LSCR198).

167883 Soilexp_LA V. 1.0. 2004. WINDOWS 2000. STN: 10933-1.0-00.

164180 Software Code: SZ_Convolute V. 3.0. 2003. PC, Windows 2000. 10207-3.0-00.

181060 SZ_CONVOLUTE V. 3.10.01. 2007. WINDOWS 2000 & WINDOWS 2003. STN: 10207-3.10.01-00.

146654 T2R3D V. 1.4. 1999. UNIX, WINDOWS 95/98NT 4.0. STN: 10006-1.4-00.

161491 TOUGH2 V. 1.6. 2003. DOS Emulation (win95/98), SUN OS 5.5.1., OSF1 V4.0. STN: 10007-1.6-01.

181061 TSPA_Input_DB V. 2.2. 2006. WINDOWS 2000. STN: 10931-2.2-00.

181062 TSPA_Input_DB V. 2.2. 2006. WINDOWS 2003. STN: 10931-2.2-01.

161240 WAPDEG V. 4.07. 2002. WINDOWS NT 4.0. STN: 10000-4.07-00.

181774 WAPDEG V. 4.07. 2003. Windows 2000. STN: 10000-4.07-00.

181064 WAPDEG V. 4.07. 2007. WINDOWS SERVER 2003. STN: 10000-4.07-01.

9.4 SOURCE DATA LISTED BY DATA TRACKING NUMBER

151139 GS000308315121.003. Meteorological Stations Selected to Represent Future Climate States at Yucca Mountain, Nevada. Submittal date: 03/14/2000.

165226 GS030408312272.002. Analysis of Water-Quality Samples for the Period from July 2002 to November 2002. Submittal date: 05/07/2003.

165624 LA0303HV831352.003. Fraction of Colloids that Travel Unretarded. Submittal date: 03/31/2003.

164362 LA0306SK831231.001. SZ Site-Scale Transport Model, FEHM Files for Base Case. Submittal date: 06/25/2003.

164713 LA0307BY831811.001. Characterize Igneous Framework Additional Output. Submittal date: 07/29/2003.

171584 LA0408AM831341.001. Unsaturated Zone Distribution Coefficients (Kds) for U, Np, Pu, Am, Pa, Cs, Sr, Ra, and Th. Submittal date: 08/24/2004.

179987 LA0612DK831811.001. Magma and Eruption Properties for Potential Volcano at Yucca Mountain. Submittal date: 03/23/2007.

180497 LA0701PANS02BR.003. UZ Transport Parameters. Submittal date: 04/23/2007.

184763 LA0702AM150304.001. Probability Distribution Functions and Correlations for Sampling of Sorption Coefficient Probability Distributions of Radionuclides in the SZ at the YM. Submittal date: 01/17/2008.

179495 LA0702PADE01EG.001. Igneous Temperatures. Submittal date: 02/01/2007.

179496 LA0702PADE01EG.002. EBS Failure Fractions. Submittal date: 02/02/2007.

179980 LA0702PADE03GK.002. Input Parameter Values for the ASHPLUME V2.1_DLL_LA Model for TSPA. Submittal date: 03/23/2007.

180322 LA0702PANS02BR.001. Repository and Water Table Bins. Submittal date: 04/16/2007.

159525 LB0205REVUZPRP.001. Fracture Properties for UZ Model Layers Developed from Field Data. Submittal date: 05/14/2002.

159526 LB0207REVUZPRP.001. Revised UZ Fault Zone Fracture Properties. Submittal date: 07/03/2002.

159672 LB0207REVUZPRP.002. Matrix Properties for UZ Model Layers Developed from Field and Laboratory Data. Submittal date: 07/15/2002.

163047 LB03033DSSFF9I.001. 3-D Site Scale UZ Flow Fields for 9 Infiltration Scenarios: Simulations Using Alternative Hydraulic Properties. Submittal date: 03/28/2003.

163687 LB0304SMDCREV2.002. Seepage Modeling for Performance Assessment, Including Drift Collapse: Summary Plot Files and Tables. Submittal date: 04/11/2003.

180511 LB0307SEEPDRCL.001. Seepage into Collapsed Drift: Simulations. Submittal date: 07/21/2003.

166116 LB0310AMRU0120.002. Mathcad 11 Spreadsheets for Probabilistic Seepage Evaluation. Submittal date: 10/23/2003.

173280 LB0407AMRU0120.001. Supporting Calculations and Analysis for Seepage Abstraction and Summary of Abstraction Results. Submittal date: 07/29/2004.

180502 LB0610UZDSCP10.001. Drift-Scale Calibrated Property Set for the 10-Percentile Infiltration Map. Submittal date: 11/02/2006.

179180 LB0610UZDSCP30.001. Drift-Scale Calibrated Property Set for the 30-Percentile Infiltration Map. Submittal date: 11/02/2006.

178586 LB0611MTSCHP10.001. Mountain Scale Calibrated Property Set for the 10-Percentile Infiltration Map. Submittal date: 11/28/2006.

180293 LB0611MTSCHP30.001. Mountain Scale Calibrated Property Set for the 30-Percentile Infiltration Map. Submittal date: 11/28/2006.

183948 LB0611UZDSCP50.001. Drift-Scale Calibrated Property Set for the 50-Percentile Infiltration Map. Submittal date: 11/28/2006.

180294 LB0612MTSCHP50.001. Mountain Scale Calibrated Property Set for the 50-Percentile Infiltration Map. Submittal date: 12/19/2006.

180295 LB0612MTSCHP90.001. Mountain Scale Calibrated Property Set for the 90-Percentile Infiltration Map. Submittal date: 12/20/2006.

180296 LB0612MTSCHPFT.001. Calibrated UZ Fault Property Sets. Submittal date: 12/07/2006.

179296 LB0612PDFEHMFF.001. Flow-Field Conversions from TOUGH2 to FEHM Format for Present Day 10-, 30-, 50-, and 90-Percentile Infiltration Maps. Submittal date: 12/19/2006.

183949 LB0612UZDSCP90.001. Drift-Scale Calibrated Property Set for the 90-Percentile Infiltration Map. Submittal date: 12/20/2006.

179160 LB0701GTFEHMFF.001. Flow-Field Conversions from TOUGH2 to FEHM Format for Glacial Transition Climate 10th-, 30th-, 50th-, and 90th-Percentile Infiltration Maps. Submittal date: 01/05/2007.

179297 LB0701MOFEHMFF.001. Flow-Field Conversions from TOUGH2 to FEHM Format for Monsoon Climate 10th-, 30th-, 50th-, and 90th-Percentile Infiltration Maps. Submittal date: 01/05/2007.

179299 LB0701PAKDSESN.001. Unsaturated Zone Sorption Coefficients for Selenium and Tin. Submittal date: 01/31/2007.

179283 LB0701PAWFINFM.001. Weighting Factors for Infiltration Maps. Submittal date: 01/25/2007.

179507 LB0702PAFEM10K.002. Flow Field Conversions to FEHM Format for Post 10,000 Year Peak Dose Fluxes in the Unsaturated Zone for Four Selected Infiltration Rates. Submittal date: 02/15/2007.

179511 LB0702PASEEP01.001. New Extended-Range Seepage Look-Up Tables for Intact and Collapsed Drifts Plus Supporting Files. Submittal date: 02/20/2007.

181635 LB0702PASEEP02.001. Seepage Abstraction for Degraded Drifts. Submittal date: 06/29/2007.

180776 LB0702PAUZMTDF.001. Unsaturated Zone Matrix Diffusion Coefficients. Submittal date: 05/10/2007.

163712 LL030412512251.057. LTCTF Corrosion Rate Calculations for Five-Year Exposed Alloy C22 Specimens Cleaned Under TIP-CM-51. Submittal date: 05/28/2003.

179590 LL0702PA027MST.082. Output for ANL-EBS-MD-000049 Multiscale Thermohydrologic Model for the Mean Host-Rock Thermal Conductivity, 10-Percentile Percolation Flux, Collapsed-Drift, High and Low Rubble Thermal Conductivity Cases. Submittal date: 02/15/2007.

179853 LL0703PA011MST.006. Output for ANL-EBS-MD-000049 REV 04 Multiscale Thermohydrologic Model for the Mean Host-Rock Thermal Conductivity, 10-Percentile Percolation Flux Case. Submittal date: 03/07/2007.

179854 LL0703PA012MST.007. Output for ANL-EBS-MD-000049 REV 04 Multiscale Thermohydrologic Model for the Mean Host-Rock Thermal Conductivity, 30-Percentile Percolation Flux Case. Submittal date: 03/13/2007.

179855 LL0703PA013MST.008. Output for ANL-EBS-MD-000049 REV 04 Multiscale Thermohydrologic Model for the Mean Host-Rock Thermal Conductivity, 50-Percentile Percolation Flux Case. Submittal date: 03/13/2007.

179856 LL0703PA014MST.009. Output for ANL-EBS-MD-000049 REV 04 Multiscale Thermohydrologic Model for the Mean Host-Rock Thermal Conductivity, 90-Percentile Percolation Flux Case. Submittal date: 03/13/2007.

179857 LL0703PA015MST.010. Output for ANL-EBS-MD-000049 REV 04 Multiscale Thermohydrologic Model for the Low Host-Rock Thermal Conductivity, 10-Percentile Percolation Flux Case. Submittal date: 03/13/2007.

179858 LL0703PA016MST.011. Output for ANL-EBS-MD-000049 REV 04 Multiscale Thermohydrologic Model for the High Host-Rock Thermal Conductivity, 90-Percentile Percolation Flux Case. Submittal date: 03/13/2007.

179859 LL0703PA017MST.012. Output for ANL-EBS-MD-000049 REV 04 Multiscale Thermohydrologic Model for the High Host-Rock Thermal Conductivity, 10-Percentile Percolation Flux Case. Submittal date: 03/13/2007.

179981 LL0703PA026MST.013. Weighting Factors for Low (10-Percentile), Mean, and High (90-Percentile) Host-Rock Thermal Conductivity Cases for ANL-EBS-MD-000049 Multiscale Thermohydrologic Model. Submittal date: 03/28/2007.

179982 LL0703PA034MST.016. Output for ANL-EBS-MD-000049 Multiscale Thermohydrologic Model for the Low Host-Rock Thermal Conductivity, 30-Percentile Percolation Flux (P30L) Case. Submittal date: 03/22/2007.

179985 LL0703PA035MST.017. Output for ANL-EBS-MD-000049 Multiscale Thermohydrologic Model for the High Host-Rock Thermal Conductivity, 30-Percentile Percolation Flux (P30H) Case. Submittal date: 03/22/2007.

179986 LL0703PA036MST.018. Output for ANL-EBS-MD-000049 Multiscale Thermohydrologic Model for the Low Host-Rock Thermal Conductivity, 50-Percentile Percolation Flux (P50L) Case. Submittal date: 03/22/2007.

179989 LL0703PA037MST.019. Output for ANL-EBS-MD-000049 Multiscale Thermohydrologic Model for the High Host-Rock Thermal Conductivity, 50-Percentile Percolation Flux (P50H) Case. Submittal date: 03/22/2007.

179992 LL0703PA038MST.020. Output for ANL-EBS-MD-000049 Multiscale Thermohydrologic Model for the Low Host-Rock Thermal Conductivity, 90-Percentile Percolation Flux (P90L) Case. Submittal date: 03/22/2007.

148850 MO0003RIB00071.000. Physical and Chemical Characteristics of Alloy 22. Submittal date: 03/13/2000.

152926 MO0003RIB00073.000. Physical and Chemical Characteristics of Ti Grades 7 and 16. Submittal date: 03/13/2000.

153044 MO0003RIB00076.000. Physical and Chemical Characteristics of Type 316N Grade. Submittal date: 03/14/2000.

148744 MO0003SZFWTEEP.000. Data Resulting from the Saturated Zone Flow and Transport Expert Elicitation Project. Submittal date: 03/06/2000.

165800 MO0310MWDWAPAN.002. WAPDEG Analysis of Waste Package and Drip Shield Degradation. Submittal date: 10/16/2003.

169007 MO0404ANLSF001.001. CSNF Radionuclide Release Model. Submittal date: 04/09/2004.

171483 MO0408MWDDDMIO.002. Drift Degradation Model Inputs and Outputs. Submittal date: 08/31/2004.

171751 MO0408SPADRWSD.002. Desert Rock Wind Speed and Wind Direction Analyses for Years 1978 - 2003. Submittal date: 08/19/2004.

180755 MO0411SPACLDDG.003. Updated TSPA-LA Parameters from Clad Degradation-Summary and Abstraction for LA, ANL-WIS-MD-000021 REV 03. Submittal date: 05/10/2007.

172682 MO0501BPVELEMP.001. Bounded Horizontal Peak Ground Velocity Hazard at the Repository Waste Emplacement Level. Submittal date: 01/11/2005.

172830 MO0502ANLGAMR1.016. HLW Glass Degradation Model. Submittal date: 02/08/2005.

172893 MO0502SPAINPCA.000. In-Package Chemistry Abstraction. Submittal date: 02/25/2005.

173893 MO0505SPAROCKM.000. Rock Mass and Invert Properties for TSPA-LA. Submittal date: 05/23/2005.

174806 MO0506MWDPPMSV.000. PREWAP Processing of MSTHM Files for Spatial Variability Analyses. Submittal date: 06/27/2005.

174809 MO0506MWDTLMV3.000. TSPA-LA Model V3. Submittal date: 06/15/2005.

173958 MO0506SPAROCKU.000. Rock Unit, Radionuclide, and Colloid Parameters for Particle Tracking. Submittal date: 06/03/2005.

175064 MO0508SEPFEPLA.002. LA FEP List and Screening. Submittal date: 08/22/2005.

182281 MO0605SPAFORTY.000. Fortymile Wash Drainage Basin Dem. Submittal date: 08/02/2007.

182035 MO0612WPOUTERB.000. Output from General and Localized Corrosion of Waste Package Outer Barrier Report. Submittal date: 07/18/2007.

180439 MO0701PACSNFCP.000. CSNF Colloid Parameters. Submittal date: 04/17/2007.

180393 MO0701PAGLASWF.000. Glass Waste Form Colloid Parameters. Submittal date: 04/17/2007.

179310 MO0701PAGROUND.000. Groundwater Colloid Concentration Parameters. Submittal date: 01/18/2007.

180440 MO0701PAIRONCO.000. Colloidal Iron Corrosion Products Parameters. Submittal date: 04/17/2007.

180392 MO0701PAKDSUNP.000. Colloidal KDS for U, NP, RA and SN. Submittal date: 04/17/2007.

180508 MO0701PASHIELD.000. Waste Package/Drip Shield Early Failure Probabilities. Submittal date: 04/24/2007.

180391 MO0701PASORPTN.000. Colloidal Sorption Coefficients for PU, AM, TH, CS, and PA. Submittal date: 04/17/2007.

179334 MO0701RLTSCRNA.000. Results of Screening Analysis. Submittal date: 01/30/2007.

179358 MO0702PADISCON.001. Dissolved Concentration Limits of Elements with Radioactive Isotopes. Submittal date: 02/15/2007.

182578 MO0702PAFARDAT.001. FAR Data. Submittal date: 08/21/2007.

181219 MO0702PAFLUORI.000. Fluoride Uncertainty Associated with Dissolved Concentration Limits. Submittal date: 06/01/2007.

181588 MO0702PAFRACSS.000. FRAC_CSNF_PKGS_SS. Submittal date: 06/28/2007.

179327 MO0702PAGBDCFS.001. Groundwater Biosphere Dose Conversion Factors. Submittal date: 02/09/2007.

179328 MO0702PAGWPROS.001. Groundwater Protection Standards Conversion Factors. Submittal date: 02/06/2007.

179329 MO0702PAINHALA.001. Inhalation Dose Factors. Submittal date: 02/15/2007.

180377 MO0702PALOVERT.000. Condensation Abstraction: Well-Ventilated Drip Shield; Low Invert Transport, (0-10,000 Years). Submittal date: 04/16/2007.

180376 MO0702PALV010K.000. Condensation Abstraction: Unventilated Drip Shield; Low Invert Transport, (0-10,000 Years). Submittal date: 04/16/2007.

179925 MO0702PASTREAM.001. Waste Stream Composition and Thermal Decay Histories for LA. Submittal date: 02/15/2007.

180514 MO0702PASTRESS.002. Output DTN of Model Report, “Stress Corrosion Cracking of Waste Package Outer Barrier and Drip Shield Materials,” ANL-EBS-MD-000005. Submittal date: 04/24/2007.

179330 MO0702PAVBPDCF.000. Volcanic Biosphere Dose Conversion Factors. Submittal date: 02/21/2007.

181990 MO0703PAEVSIIC.000. Evaluation of Stage II Condensation. Submittal date: 07/16/2007.

182029 MO0703PAGENCOR.001. Output from General Corrosion and Localized Corrosion of Waste Package Outer Barrier 2007 Second Version. Submittal date: 07/18/2007.

182093 MO0703PAHYTHRM.000. Hydrological and Thermal Properties of the Invert. Submittal date: 07/19/2007.

183148 MO0703PASDSTAT.001. Statistical Analyses for Seismic Damage Abstractions. Submittal date: 09/21/2007.

183156 MO0703PASEISDA.002. Seismic Damage Abstractions for TSPA Compliance Case. Submittal date: 09/21/2007.

184647 MO0704PAFEHMBR.001. FEHM Model and Input. Submittal date: 01/10/2008.

180442 MO0704PAPTTFBR.002. Particle Tracking Transfer Functions. Submittal date: 04/12/2007.

182149 MO0704PASCOURD.000. Scour Depth. Submittal date: 07/25/2007.

180389 MO0704PASOLCAP.000. In-Package Solubility "Caps" for Pu, Np, U, Th, Am, and Pa. Submittal date: 04/06/2007.

181281 MO0705GOLDSIMB.000. Goldsim Biosphere Model Files for Calculating Groundwater and Volcanic Biosphere Dose Conversion Factors. Submittal date: 05/08/2007.

181613 MO0706SPAFEPLA.001. FY 2007 LA FEP List and Screening. Submittal date: 06/20/2007.

184664 MO0712PBANLNWP.000. Probabilistic Analysis of Navy Waste Packages. Submittal date: 12/13/2007.

163563 SN0302T0502203.001. Saturated Zone Anisotropy Distribution Near the C-Wells. Submittal date: 02/26/2003.

165640 SN0308T0503100.008. Revised Frequency Distributions for Net Infiltrations and Weighting Factors Applied to Lower, Mean, and Upper Climates. Submittal date: 08/28/2003.

168763 SN0310T0502103.009. Revised Saturated Zone Transport Abstraction Model Uncertain Inputs. Submittal date: 10/09/2003.

168761 SN0310T0505503.004. Initial Radionuclide Inventories for TSPA-LA. Submittal date: 10/27/2003.

178850 SN0612T0502404.014. Thermodynamic Database Input File for EQ3/6 - DATA0.YMP.R5. Submittal date: 12/15/2006.

180523 SN0701PAEBSPCE.001. PCE TDIP Potential Seepage Water Chemistry Lookup Tables. Submittal date: 04/25/2007.

179425 SN0701PAEBSPCE.002. PCE TDIP PCO2 and Total Carbon Lookup Tables. Submittal date: 01/30/2007.

182961 SN0701PAWPHIT1.001. Number of Waste Packages Hit by Igneous Events. Submittal date: 09/13/2007.

180451 SN0702PAIPC1CA.001. In-Package Chemistry Calculations and Abstractions. Submittal date: 04/19/2007.

179504 SN0702PASZFTMA.001. Saturated Zone Flow and Transport Model Abstraction. Submittal date: 02/06/2007.

183471 SN0702PASZFTMA.002. Saturated Zone 1-D Transport Model. Submittal date: 10/15/2007.

181571 SN0703PAEBSPCE.006. Physical and Chemical Environment (PCE) TDIP Water-Rock Interaction Parameter Table and Salt Separation Tables with Supporting Files. Submittal date: 06/27/2007.

184141 SN0703PAEBSPCE.007. Physical and Chemical Environment (PCE) TDIP Uncertainty Evaluations and Supporting Files. Submittal date: 11/30/2007.

183217 SN0703PAEBSRTA.001. Inputs Used in the Engineered Barrier System (EBS) Radionuclide Transport Abstraction. Submittal date: 09/28/2007.

182122 SN0704PADSGCMT.001. Drip Shield General Corrosion Models Based on 2.5-Year Titanium Grade 7 Corrosion Rates. Submittal date: 07/24/2007.

182188 SN0704PADSGCMT.002. Drip Shield General Corrosion Rate Multiplier for Titanium Grade 29. Submittal date: 07/27/2007.

181837 SN0706PAEBSPCE.016. P&CE Invert Relative Humidity (RH) Boundary Table. Submittal date: 06/28/2007.

183485 SN0710PASZFTMA.003. Updated Saturated Zone 1-D Transport Model. Submittal date: 10/10/2007.